t No. FHWA-RD-79-115

TE
662
.A3
no.
FHWA-
RD-
79-
115

UCTURAL EVALUATION OF NEW CONCEPTS FOR IG-SPAN CULVERTS AND CULVERT INSTALLATIONS

December 1979
Interim Report

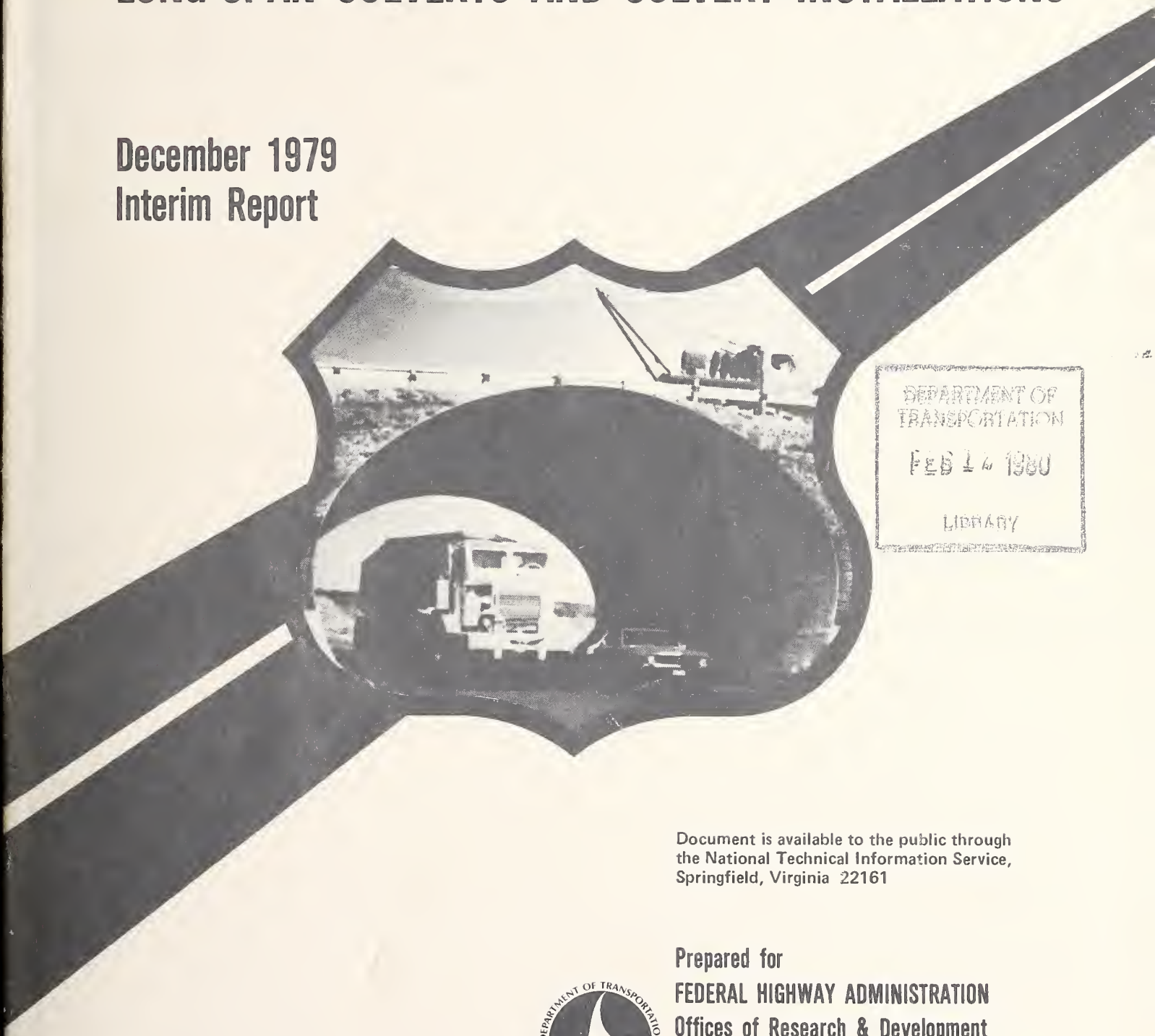

DEPARTMENT OF TRANSPORTATION
FEB 14 1980
LIBRARY

Document is available to the public through the National Technical Information Service, Springfield, Virginia 22161

Prepared for
FEDERAL HIGHWAY ADMINISTRATION
Offices of Research & Development
Structures & Applied Mechanics Division
Washington, D.C. 20590

FOREWORD

Finite element analyses are used to evaluate the relative merits of conventional and new concepts of soil-structure design parameters for long-span culverts, including soil quality and compaction, footing width (for arches), metal liner thickness, metal liner shape, scale of structure, special features such as thrust beams, rib stiffeners and soil bin, reinforced earth, stabilized soil zones, placement of soft materials to promote soil arching, and joint slippage to reduce thrust. The effectiveness of concrete slabs for limiting deflections of culverts is also determined. In a similar manner to the study for long-span culverts, old and new concepts for smaller traditional culverts are analytically analyzed to determine the relative merits of bedding configurations, imperfect trench configurations, selective placement of soft backpacking, selective placement of stabilized soils, V-notch bedding, and fluid jackets for concrete pipe.

This report is the second interim report from research contract FH-11-9408 awarded the University of Notre Dame as one segment of the Federal Highway Administration's Federally Coordinated Program for Research and Development Project 5I "Improved Structural Design and Construction Techniques for Culverts." The first interim report, FHWA-RD-77-131, is entitled "Review of the Design and Construction of Long Span, Corrugated-Metal, Buried Conduits." A final report on the work under this contract is expected in late 1980.

Copies of the report are being distributed by memorandum to researchers and other interested engineers.

Charles F. Scheffey
Director, Office of Research
Federal Highway Administration

NOTICE

This document is disseminated under the sponsorship of the Department of Transportation in the interest of information exchange. The United States Government assumes no liability for its contents or use thereof.

The contents of this report reflect the views of the authors who are responsible for the facts and the accuracy of the data presented herein. The contents do not necessarily reflect the official views or policy of the Department of Transportation.

This report does not constitute a standard, specification, or regulation.

The United States Government does not endorse products or manufacturers. Trademarks or manufacturers' names appear herein only because they are considered essential to the object of this document.

TE
662
.A3
no. FHWA-RD-
9-
15

Technical Report Documentation Page

1. Report No.	2. Government Accession No.	3. Recipient's Catalog No.
FHWA-RD-79-115		

4. Title and Subtitle	5. Report Date
Structural Evaluation of New Concepts for Long-Span Culverts and Culvert Installations	December 1979
	6. Performing Organization Code
	8. Performing Organization Report No.
7. Author(s) M.G. Katona, D.F. Meinhert, R. Orillac, C.H. Lee	
9. Performing Organization Name and Address University of Notre Dame Notre Dame, Indiana 46556	10. Work Unit No. (TRAIS) FCP 35I3-241
	11. Contract or Grant No. DOT-FH-11-9408
12. Sponsoring Agency Name and Address Federal Highway Administration Office of Research, HRS-14 Washington, D.C. 20590	13. Type of Report and Period Covered Interim Report May 1976 - July 1979
	14. Sponsoring Agency Code 80925

15. Supplementary Notes

Contract Manager: G. W. Ring

16. Abstract

Analytical structural evaluations of long-span and conventional culvert installations are made using a finite element soil-structure model. Included in the evaluation are the relative merits of conventional soil-structure design parameters of soil quality and compaction, footing width (for arches), metal liner thickness, metal liner shape, scale of structure, and special manufacturing features, such as thrust beam, rib stiffeners, and soil bin. Results indicate that soil stiffness is the most significant parameter related to deformations in the structure. Maximum thrust force is generally insensitive to all conventional design parameters. Further analytical evaluations are made of new concepts, including reinforced earth, stabilized soil zones, selective placement of soft inclusions, and controlled joint slippage. Results suggest that soil reinforcement used in conjunction with long-span culverts may be a cost-effective technique to limit structural deformations and enhance structural capacity. It also appears that controlled joint slippage may be the most cost-effective method to reduce thrust.

Other parameters investigated included selective placement of stabilized soil, V-notch void, and fluid jackets for concrete pipe, all of which appeared to improve the structural performance of culverts.

DEPARTMENT OF TRANSPORTATION
FEB 12 1980
LIBRARY

17. Key Words	18. Distribution Statement
Culverts, Long-Span Culvert, Reinforced Earth, Soil-Structure Interaction, Culvert Joint Slippage	This document is available to the public through the National Technical Information Service, Springfield, Virginia 22161.

19. Security Classif. (of this report)	20. Security Classif. (of this page)	21. No. of Pages	22. Price
Unclassified	Unclassified	294	

Form DOT F 1700.7 (8-72)

ABSTRACT

STRUCTURAL EVALUATION OF NEW CONCEPTS FOR
LONG-SPAN CULVERTS AND CULVERT INSTALLATIONS

In this study the main emphasis is on structural evaluation of long-span corrugated metal culverts commonly used as substitutes for small bridges with span lengths in the range of 15 to 50 ft (5 to 16 m). Also investigated are smaller traditional culverts (reinforced concrete and corrugated metal) with nominal diameters on the order of 6 ft (2 m). For both systems the final goal is to evaluate new and/or improved concepts to enhance the structural performance and capacity, leading to the safe and economical design of buried culverts.

Structural evaluation of long-span culverts is presented in a step-by-step manner. First, available experimental data is collected and presented in graphs illustrating key structural trends and behavior characteristics, thereby providing a data base as well as guidelines for subsequent analytical development. Next a finite element soil-structure model of a typical long-span system is established and examined in detail with regard to fundamental modeling parameters. These include loading techniques (e.g., incremental construction, temporary compaction loads, and traveling vehicles) and nonlinear effects of geometry, soil, metal liner, and soil-structure interface.

Having established a reasonable finite element model, the next step considers the analytical evaluation and relative merits of conventional soil-structure design parameters currently used in practice. These include; soil quality and compaction, footing width (for arches), metal liner thickness, metal liner shape, scale of structure, and special manufacturing features, such as, thrust beam, rib stiffeners, and soil bin. Results indicate that soil quality (i.e., stiffness) is generally the most significant parameter with regard to minimizing deformations in the structure. However, maximum thrust force in the liner is generally insensitive to all conventional design parameters.

For the final phase of the long-span study new concepts to enhance the long-span structural performance are analytically evaluated. Concepts considered include modifications to the soil, such as, reinforced earth, stabilized soil zones, and selective placement of soft materials to promote soil arching. Modifications to metal liner include controlled joint slippage to reduce thrust, and increased bending stiffness to limit early-stage deformations. Results suggest that soil reinforcement laid in horizontal rows between the footing and crown may be the most cost-effective technique to limit structural deformations and enhance structural capacity.

Based on limited analytical analyses, it appears that controlled joint slippage may be the most effective method to reduce thrust, however this needs to be confirmed by further field experiments and more rigorous analysis.

In a similar manner, old and new concepts for smaller traditional culverts are analytically evaluated to determine the relative merits of the concepts for deeply buried installations. Parameters and concepts investigated include; bedding configurations, imperfect trench configurations, selective placement of soft backpacking, selective placement of stabilized soil, V-notch void beneath culvert, and fluid jackets for concrete pipe.

Overall recommendations based on structural evaluation and economic considerations are to pursue the concepts of reinforced earth and controlled joint slippage to improve the capacity and performance of long-span culverts. For traditional pipe culverts, new concepts that appear most fruitful are soft backpacking, V-notch trench, and fluid jacket concept.

It is recommended to investigate these concepts with combined experimental and analytical programs with the ultimate goal of providing design guidelines and recommendations for field applications.

ACKNOWLEDGMENTS

Representatives of industry, state highway departments, universities, and research groups have been very helpful in providing information and constructive comments for this research effort. Specifically, Mr. Robert Odello of the Naval Civil Engineering Laboratory contributed the background information on materials costs and properties presented in Appendix A.

A special thank you is extended to Professor Sydney Kelsey of the University of Notre Dame for his technical support and guidance and to Mr. Jay Allgood, formally of the Naval Civil Engineering Laboratory for his unwavering encouragement of this work.

Most of all, a deep appreciation is extended to the Federal Highway Administration and to Mr. George W. Ring, III., Project Technical Manager, for the opportunity to work on this challenging problem. Mr. Ring provided direction, numerous technical papers and reports, and helpful comments throughout this study.

CONTENTS

	Page
CHAPTER 1 - Introduction	
1.1 Background	1
1.2 Objective	5
1.3 Scope and Approach	5
CHAPTER 2 - Experimental Data	9
2.1 Statement of Purpose	9
2.2 Existing Experimental Studies	10
2.3 Dead Load Results	11
2.4 Live Load Results	21
2.5 Time Dependent Effects	23
2.6 Commentary on Existing Data	24
2.7 Findings and Conclusions	25
2.8 Recommendations for Future Experimental Studies	27
2.9 Figures 2-1 through 2-16	29
CHAPTER 3 - Basic Model, Definition and Results	46
3.1 Statement of Purpose	46
3.2 Basic Model Description	46
3.3 Basic Model Performance	50
3.4 Figures 3-1 through 3-24	54
CHAPTER 4 - Analysis of Dead and Live Loading	77
4.1 Statement of Purpose	77
4.2 Incremental Gravity vs. Connection Loads	77
4.3 Nonsymmetric Gravity Loads	78
4.4 Traveling Live Loads	81
4.5 Figures 4-1 through 4-31	86

Page

CHAPTER 5 - Nonlinear Studies of Long-Span Behavior 119
5.1 Statement of Purpose 119
5.2 Geometric Nonlinearity 119
5.3 Soil-Structure Interface Friction 120
5.4 Material Nonlinearity 122
5.5 Summary of Nonlinear Effects 126
5.6 Figures 5-1 through 5-5 127

CHAPTER 6 - Parameter Studies of Conventional Long-Spans 133
6.1 Statement of Purpose 133
6.2 Soil Stiffness 133
6.3 Footing Width 135
6.4 Liner Thickness 136
6.5 Liner Shape 137
6.6 Liner Scale 138
6.7 Special Features 140
6.8 Summary of Conventional Parameters 141
6.9 Figures 6-1 through 6-11 143

CHAPTER 7 - Parameter Studies of New Concepts for Long Spans 155
7.1 Statement of Purpose 155
7.2 Reinforced Earth 155
7.3 Soil Stabilization 161
7.4 Soft Inclusions 164
7.5 Improvements to Metal Liner 167
7.6 Figures 7-1 through 7-27 170

CHAPTER 8 - Parameter Studies of New Concepts for Traditional Culverts 199
8.1 Statement of Purpose 199
8.2 Effect of Bedding Material 199

Page

8.3 Effect of Imperfect Trench Parameters 202
8.4 Effect of Backpacking Parameters 203
8.5 Effect of Soil Stabilization 204
8.6 Effect of V-Notch Under Pipe 206
8.7 Fluid-Like Jacket for Reinforced Concrete 207
8.8 Figures 8-1 through 8-13 210

CHAPTER 9 - Summary and Recommendations 224
9.1 Summary of Findings and Long Spans 224
9.2 Summary of Findings for Traditional Culverts 232
9.3 Recommendations 233

APPENDIXES
A - Materials for New Structural Concepts 235
B - Reinforced Earth 262

REFERENCES 280

METRIC CONVERSION FACTORS

Approximate Conversions to Metric Measures

Symbol	When You Know	Multiply by	To Find	Symbol
	LENGTH			
in	inches	*2.5	centimeters	cm
ft	feet	30	centimeters	cm
yd	yards	0.9	meters	m
mi	miles	1.6	kilometers	km
	AREA			
in^2	square inches	6.5	square centimeters	cm^2
ft^2	square feet	0.09	square meters	m^2
yd^2	square yards	0.8	square meters	m^2
mi^2	square miles	2.5	square kilometers	km^2
	acres	0.4	hectares	ha
	MASS (weight)			
oz	ounces	28	grams	g
lb	pounds	0.45	kilograms	kg
	short tons (2000 lb)	0.9	tonnes	t
	VOLUME			
tsp	teaspoons	5	milliliters	ml
Tbsp	tablespoons	15	milliliters	ml
fl oz	fluid ounces	30	milliliters	ml
c	cups	0.24	liters	l
pt	pints	0.47	liters	l
qt	quarts	0.95	liters	l
gal	gallons	3.8	liters	l
ft^3	cubic feet	0.03	cubic meters	m^3
yd^3	cubic yards	0.76	cubic meters	m^3
	TEMPERATURE (exact)			
°F	Fahrenheit temperature	5/9 (after subtracting 32)	Celsius temperature	°C

*1 in = 2.54 (exactly). For other exact conversions and more detailed tables, see NBS Misc. Publ. 286, Units of Weights and Measures, Price $2.25, SD Catalog No. C13.10:286.

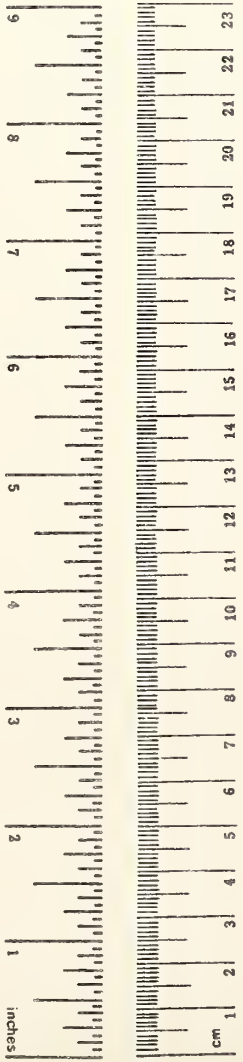

Approximate Conversions from Metric Measures

Symbol	When You Know	Multiply by	To Find	Symbol
	LENGTH			
mm	millimeters	0.04	inches	in
cm	centimeters	0.4	inches	in
m	meters	3.3	feet	ft
m	meters	1.1	yards	yd
km	kilometers	0.6	miles	mi
	AREA			
cm^2	square centimeters	0.16	square inches	in^2
m^2	square meters	1.2	square yards	yd^2
km^2	square kilometers	0.4	square miles	mi^2
ha	hectares (10,000 m^2)	2.5	acres	
	MASS (weight)			
g	grams	0.035	ounces	oz
kg	kilograms	2.2	pounds	lb
t	tonnes (1000 kg)	1.1	short tons	
	VOLUME			
ml	milliliters	0.03	fluid ounces	fl oz
l	liters	2.1	pints	pt
l	liters	1.06	quarts	qt
l	liters	0.26	gallons	gal
m^3	cubic meters	35	cubic feet	ft^3
m^3	cubic meters	1.3	cubic yards	yd^3
	TEMPERATURE (exact)			
°C	Celsius temperature	9/5 (then add 32)	Fahrenheit temperature	°F

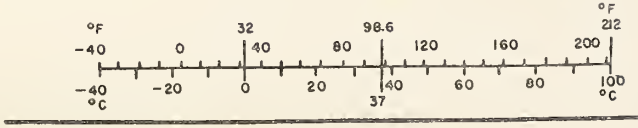

CHAPTER 1

INTRODUCTION

1.1 BACKGROUND

Over the years buried pipe culverts have been increasing in size and scope of application. In particular, the so-called "long-span culvert", introduced in about 1964, has been used in more than 600 installations as substitutes for small bridges, including grade separations for waterways, roadways, railways and pedestrian traffic. Typical span lengths range from 15 to 50 ft (5 to 16 m). Manufacturers of long-span culverts estimate cost savings ranging from 30% and more over comparable conventionable bridge structures. Thus, in view of the current bridge repair and replacement program in the United States (Federal Highway Administration estimates nearly 18% of all U.S. bridges on the Federal-Aid System of Highways are in disrepair or functionally obsolete), usage of long-span structure will probably increase markedly. Accordingly, analytical and experimental investigations of long spans are timely and can lead to improved design methods, greater span lengths, and increased structural capacity.

Reference (1-1) provides an excellent state-of-the-art survey on long spans including; manufacturers, design concepts, construction practices, economics, failures, and experimental investigations. The above survey sponsored by the Federal Highway Administration and conducted by Selig, Abel, Kulhawy and Falby, is part of the current work project and provides a comprehensive background to this report. Here a brief summary of long-span concepts pertinent to this report is given.

Long spans are usually constructed by bolting together curved, structural plates of corrugated metal into an arch shape with the ends anchored into concrete footings. Alternatively, closed shapes such as ellipses and inverted pear-shaped sections are also commonly used. Figure 1-1 illustrates some typical shapes along with nomenclature popularly used with long-span structures.

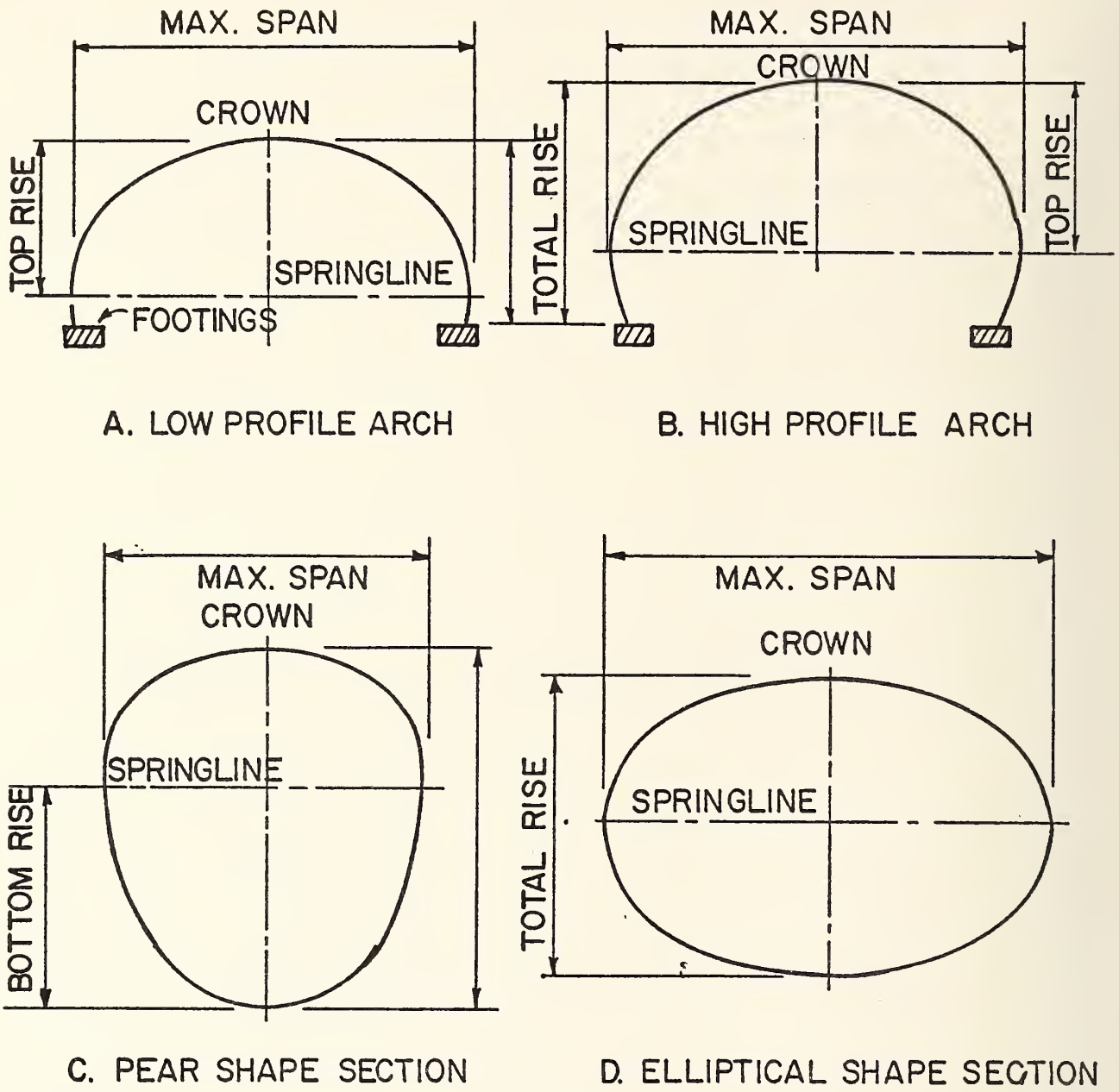

Figure 1.1 Typical Long-Span Liner Shapes and Nomenclature

The most important step in the construction process is placing soil (backfilling) around the corrugated metal liner. It is imperative that the soil be of good structural quality and properly compacted one lift at a time, symmetrically on both sides of the metal liner. During this process, the lateral soil pressure moves the sides of the liner inward and the crown upward ... called "peaking". Once the backfill soil is level with crown, subsequent soil lifts reverse this trend pushing the crown downward and sides outward. Outward movement mobilizes lateral soil resistance limiting both lateral and vertical movement.

The interaction of soil and liner working in tandem provides the remarkable structural integrity of the long-span system. Indeed, the soil must be viewed as the primary stiffness component in limiting liner movement as opposed to the compartively small liner bending stiffness. Nonlinear characteristics of soil stiffness is such that increased confining pressure increases stiffness. Thus, as outward liner movement occurs, the soil is compressed and its stiffness is enhanced.

Soil, however, plays a dual role. On the one hand, it serves as the primary stiffness component of the system. On the other hand, it transmits loads from its own body weight and surface loads to the liner through normal pressure and shear traction on the circumference. Thus the liner must be designed to withstand these loads which in turn must be determined from soil-structure interaction principles.

With regard to the liner, the basic structural responses of concern are excessive deflections which can lead to elastic or inelastic buckling, and excessive thrust stress (average stress through liner wall) which can cause local seam failure or wall failure as well as promote buckling. Unlike surface structures, excessive bending stress is of secondary concern for buried culverts. That is, outer fiber yielding due to bending can be tolerated (and expected) to some degree because movement of the liner is controlled by the soil stiffness. Thus, even if a plastic-hinge collapse mechanism develops in the liner, the soil stiffness would prevent collapse unless the primary considerations , excessive inward deflections coupled with large thrusts, enduced buckling .

The concept of "soil arching" is a useful measure for assessing portions of soil load carried by the culvert. Qualitatively, positive soil arching is a favorable condition where some of the column soil weight above the culvert is diverted around the culvert in a compression soil arch. Such a condition can occur for very flexible culverts buried in stiff soils. Negative soil arching is unfavorable and implies the culvert is "drawing" in more soil load than the column weight of soil above it. Most culverts experience this condition to some degree.

The net thrust force at the culvert springlines is the best quantitative measure of arching. If the net thrust force is less than column soil weight, positive arching is implied. Otherwise, if net thrust force exceeds column soil weight, negative arching is implied.

Some investigators consider soil pressure acting on the crown as a measure of soil arching. Here it is said, positive arching occurs if crown pressure is less than free field overburden pressure, and negative arching occurs if the reverse is true. This viewpoint is generally not valid because crown pressure may be substantially below overburden pressure, yet the distribution of normal pressure and shear traction is such that the net springline thrust exceeds soil column weight. This is demonstrated both experimentally and analytically in this report.

For the most part, current design methods for long spans are based on experience rather than a viable analytical model (1-1). This is because a reasonable analytical model is complicated eventhough the long span is conceptually a simple system. Complications are due to soil-structure interaction phenomena requiring both soil and culvert to be considered as structural components ... one cannot simply assume the loads acting on the liner. Analytical modeling difficulties include; incremental construction (i.e., modeling the soil placement in a series of construction increments), temporary compaction loads, interface slippage between culvert and soil, material nonlinearties of soil and culvert, as well as a large variety of geometrical configurations and special features.

The finite element method (FEM) appears to be the best method for formulating and solving this complicated boundary value problem. Indeed this is a singular point of common agreement among many investigators in the field of soil-structure interaction (1-2 through 1-8). In particular, recent applications of FEM to long-span systems show great promise for understanding long-span behavior and evaluating design concepts (1-9, 1-10, 1-11, 1-12).

1.2 OBJECTIVE

The overall goal of this study is to propose and analytically evaluate new and/or improved concepts for the safe and economical design of buried culverts. Emphasis is on long-span systems with the ultimate objective of enhancing structural capacity and/or span lengths. In addition, improved techniques for conventional pipe culverts are also proposed and evaluated.

In order to achieve the above goal, many preliminary objectives are required. To begin with, experimental data must be collected and collated to identify behavioral characteristics and key structural trends. Concurrently, a viable analytical model (FEM) must be developed and evaluated with experimental trends to establish proper analytical modeling techniques. Once a viable analytical model is established, conventional design concepts can be evaluated to ascertain the relative merits of current design concepts as well as provide insight into improved methods. Armed with this information, new and innovative concepts can be proposed and analytically evaluated.

Those new techniques which appear most cost-effective will be recommended for full experimental and analytical investigation, and ultimately, can be introduced into practice.

1.3 SCOPE AND APPROACH

To meet the above objectives, the following step-by-step approach is systematically undertaken and is reported herein.

1. State-Of-The-Art Survey: Current concepts of long-span design and construction practices are reviewed including economic considerations and documented failures. This work is reported in Reference (1-1).

2. Collect and Collate Experimental Data: All available experimental data on long spans including displacements, thrusts, soil pressures, and time effects is collected and displayed on reference graphs for the purpose of identifying key structural trends and the effect of system parameters. Both dead and live loading responses are reported (Chapter 2).

3. Introduction of "Basic" Finite Element Model: A typical high profile arch (long-span system) is defined and modeled with a finite element idealization. The basic model is used as a reference to assess how subsequent changes in system parameters influence key structural responses and how these responses conform to experimental findings (Chapter 3).

4. Analysis of Loading Conditions: Incremental construction gravity loads, temporary compaction loads, and traveling live loads are analysed by varying parameters of the basic model for both symmetric and nonsymmetric load conditions. Comparisons between analytical results and experimental observations are noted including the effects of a concrete relieving slab for live loads (Chapter 4).

5. Analysis of Nonlinear Behavior: Linear assumptions in the basic model are systematically removed one at a time to ascertain the relative importance of various nonlinear effects. This includes geometric nonlinearity, material nonlinearity in culvert and soil, and frictional slippage between culvert and soil (Chapter 5).

6. Parameter Studies of Conventional Long Spans: By selectively altering the properties and configurations of the basic model, the relative merits of conventional long span concepts and parameters are evaluated. These studies include; soil quality, footing width, liner gage, liner configuration (high profile, low profile, and ellipse), liner scale, and special features (thrust beam, rib-stiffeners, and soil bin)(Chapter 6).

7. Evaluation of New Concepts for Long Spans: Proposed concepts to improve structural integrity of long-span include; incorporation of reinforced earth, selective soil stabilization, and soft inclusions to promote positive soil arching (see Appendices A and B for background information and relative costs). With regard to the metal liner, potential improvements are slotted bolt connections at seams and enhanced bending stiffness. Most of these concepts are individually evaluated by modifying the basic model to simulate the new concept and then compared to the unmodified model (Chapter 7).

8. Evaluation of New Concepts for Traditional Pipe Culverts:

   The last investigation is concerned with traditional round pipe culverts including reinforced concrete and corrugated metal. Analytical investigation includes evaluating bedding and imperfect trench designs as well as new concepts such as soft backpacking, stabilized soil, v-notch trench, and fluid-like jackets for concrete pipe culverts (Chapter 8).

9. Summary and Recommendations: Major findings and highlights are summarized along with a recommendation for future studies based on the new concepts that appear most cost-effective (Chapter 9).

Throughout this study, the CANDE finite element program (1-13, 1-14) is the primary tool for analysis and evaluation. All problems are restricted to plane strain geometry and small deformations except in Chapter 5.

CHAPTER 2

EXPERIMENTAL DATA

2.1 STATEMENT OF PURPOSE

Prior to this study, no concentrated effort has been undertaken to collate the information on existing experimental studies of long-span systems. Identifying and interpreting existing experimental results is of prime importance in both the evaluation of existing designs and in developing new design approaches and concepts.

Objective and Purpose. The objective of this chapter is to present existing published and unpublished field test data with the intent of identifying key structural trends of long-span systems. Results of this study are intended for the following purposes; (1) To provide an informative data base on the behavior of long-span systems, (2) To establish key structural trends useful as "benchmark" comparisons with analytical studies, and (3) To identify areas where additional experimental work is required.

Scope and Limitations. Available experimental data is presented separately for two fundamental loading situations; (1) incremented dead weight of soil only (including whatever temporary compaction loads employed), and (2) live loads of trucks transversing shallow cover heights. For dead load cases, the data includes deflections and thrusts at the crown and springline of the metal liner along with soil pressures at a few key locations. For live loading cases, only crown deflections are presented. In addition to the above, time dependent effects are presented for long-term dead loading.

As discussed in the next section, available experimental data is scanty and often subject to interpretation. These points will be addressed as they arise in subsequent sections.

2.2 EXISTING EXPERIMENTAL STUDIES

It is common to classify experimental data in two catagories; controlled laboratories studies (usually scale models) and prototype field studies. Both catagories of experiments provide a better understanding on the structural behavior of long-span systems. Laboratory studies permit isolating and investigating the effects of various system parameters, whereas field studies, lacking quality control (e.g., temperature, moisture, soil conditions, etc.), reflect a more realistic environment.

At this writing there are, however, no known published or unpublished laboratory experimental studies on long-span corrugated metal culverts. Quite contrary to a traditional engineering development of a new product, testing of long spans began with full scale field installations. Consequently, data reported herein is strictly from field studies.

Sources of Field Data. Manufacturers of long-span culverts are the principle source of field data. Some fabricators (e.g., Armco, Inc.) have made a practice of taking field measurements on almost all their long-span installations. The measurements usually consist of only crown deflection and are used to monitor liner deformation during the backfilling operation. The fabricator generally keeps these records for construction control until construction is completed and they are not intended for publication in a technical report.

Only a few installations have been extensively instrumented. Even fewer of the extensively instrumented installations exist as formally published technical information. Most current research information exists in the form of internal reports by or for the manufacturer. References 2-1 and 2-2, and personal communications with industry and state highway departments provided the foundation of the data base presented next.

The significant field studies available and examined for this report are listed in Table 2-1a and are in reverse

chronological order by year reported. The table lists the major geometrical characteristics of a particular long-span system in columns 3 through 7. Also summarized in column 8 is a check list of the type of measurements made for each of the field studies listed. Column 10 cites the associated reference. Table 2-1b provides a brief narrative summary of the field studies list in Table 2-1a.

Processing Field Data. Upon inspecting the parameters in Table 2-1a, it is evident that the long-span systems differ in shape (ellipse, low arch, high arch, pipe arch), dimensions, and material. Clearly, these differences make it difficult to isolate the effect of any particular parameter and establish meaningful trends. To complicate matters, the characteristics of the soil (e.g., type, compaction, stiffness, etc.) are for the most part unknown (or not reported) in the corresponding references.

In order to provide a common bases of comparison for deflections, thrusts, and pressures, non-dimensional response ratios are employed as defined in Table 2-2. (Also shown in box-score fashion is the available data for the dead, live, and time effect studies.) The non-dimensional definitions are arbitrary but insights into their selection will be presented subsequently.

Moments are not included in the following results because data is highly erratic and appear to be very sensitive to backfilling operations (2-3). Moreover, moments are considered of secondary importance in design considerations.

2.3 DEAD LOAD RESULTS

In this section the soil and structure responses due to incremental soil construction are presented and discussed.

Crown Deflection. A load-history plot of the crown deflection,

Table2-1a; Principal Field Studies and Data Type Collected

	Installation	Fabricator	Culvert Description*	Span (ft)	Total Rise (ft)	Top Rise (ft)	Depth of Cover Above Crown (ft)	Measurements Reported (8)							Data Used in Study	Reference Number
								Liner Deflection	Liner Strains	Soil Strains	Soil Stresses	Long Term	Tension Rods	Dead Load Rdg	Live Load Rdg	
	(1)	(2)	(3)	(4)	(5)	(6)	(7)									(9)	(10)
1.	Bucks County, Pennsylvania, 1978	Armco	High Profile Arch Plates 0.215 in.	25.8	15.0	9.0	23.0	x	x	x	x	x		x		yes	2-3, 2-4 2-5, 2-6
2.	Penrose, Colorado, 1977	Armco	High Profile Arch Plates 0.184 in.	45.	23.	15.5	9.5	x	x					x		yes	2-7
3.	Stenner Creek, California, 1977	Armco	High Profile Arch Plates 0.313 in.	35.3	20.0	10.5	4.0	x							x	yes	2-8
4.	Greenbrier County, West Virginia, 1976	Kaiser Aluminum	Pipe Arch Plates -----	35.	21.	13.	3.	x					x	x		no	2-9
5.	Los Angeles, California, 1976	Armco	High Profile Arch Plates 0.215 in.	24.	15.	8.5	24	x	x		x	x		x		yes	2-10
6.	James Bay, Quebec, 1975	Armco	Low Profile Arch Arch Ribs & Squeeze Blocks Plates 0.276	51.	26.	21.	44.	x	x		x			x		yes	2-11
7.	Santa Clara County, California, 1975	Kaiser Aluminum	Horizontal Ellipse Plates 0.20 to 0.25 in.	24.2	19.4	9.7	8	x						x		yes	2-12
8.	Thunder Bay, Ontario, 1975	Westeel-Rosco	Horizontal Ellipse 1 ft. releiving slab Plates 0.215 in.	29.	16.	8	3.5	x		x	x			x	x	yes	2-13
9.	Zimmer Power Plant, Cincinnati, Ohio, 1974	Armco	Horizontal Ellipse Plates 0.215 to 0.245 in.	24.5	17.7	8.9	24.3	x	x					x		yes	2-14
10.	Port Dover, Ontario, 1973	Armco	Low Profile Arch Ribs Plates 0.245 in.	50.	18.		5			x	x	x		x		no	2-15
11.	Kettle Creek, St. Thomas Ontario, 1971	Armco	Horizontal Ellipse Plates 0.245 to 0.276 in.	37.	27.	13.5	26.			x				x		no	2-15
12.	Germany 1963	Armco	Pipe Arch Plates 0.184 in.	21.	13.	9.5	3 & 6	x	x		x	x		x	x	no	2-16
13.	British Columbia	Armco	Horizontal Ellipse	30.				x	x		x			x		no	-
14.	Mica Dam, British Columbia	Armco														no	-
15.	Washington County, New York	Republic	Plates .164 in.	22.	15.		6.							x	x	no	-

Table 2-1b: Commentary of Table 2-1a

1. Bucks County, Pennsylvania - a well conceived, well documented experimental study measuring the effects of dead load. (2-3, 2-4, 2-5, 2-6)

2. Penrose, Colorado - installation instrumented by the Colorado Highway Department. Measured crown deflections and liner strains. Many of the strain gages failed and therefore, the investigation does not provide valuable information except for fairly complete history of crown deflection. (2-7)

3. Stenner Creek, California - measures the vertical deflections of the liner for the exclusive effects of moving live load (HS-20 truck). (2-8)

4. Greenbrier County, East Virginia - aluminum liner plates. Measurements of liner deformation complicated by using tension rods during construction. (2-9)

5. Los Angeles (Limekilm Creek), California - well conceived study. Strain gage liner data good. Liner deflections difficult to use in analysis. Long term data available. (2-10)

6. James Bay, Quebec - liner strain gage information incomplete. Some difficulty in assessing the behavior during the initial backfilling operations. Reports the behavior of the soil-structures system when squeeze blocks exist at the foundation. (2-11)

7. Santa Clara County, California - basically an anlytical F.E.M. study of installation. Liner deflections are the only measurements reported. (2-12)

8. Thunder Bay, Ontario - instrumentation for liner placed after backfilling complete. Best results pertain to the soil characteristics. (2-13)

9. Zimmer Power Plant, Cincinnati, Ohio - reasonably complete information on the liner deflection characteristics. Liner strains available for selected portion of backfilling. Well conceived study but not completely implemented. (2-14)

10. Port Dover, Ontario - soil behavior study exclusively, including some long term effects. (2-15)

(continued)

Table 2-1b - continued

11. St. Thomas (Kettle Creek), Ontario - similar to Port Dover soil study. (2-15)

12. Germany - well conceived test. Thoroughly instrumented but data somewhat difficult to use because paper was originally in German and translated to English. Figure legends poorly identified. (2-16)

13, 14, 15. British Columbia, Mica Dam, Washington County - information is in unpublished state and difficult to access.

Table 2-2: Non-dimensional Form and Presented Data

	Relative Crown Deflection ΔY	Relative Springline Deflection ΔX	Liner Thrust N	Vertical Soil Pressure σ_y	Horizontal Soil Pressure σ_x
Non-dimensional form	$\frac{\Delta Y}{T_R}$	$\frac{\Delta X}{L}$	$\frac{N}{W^*}$	$\frac{\sigma_y}{\sigma_f}$	$\frac{\sigma_x}{K_o \sigma_f}$
Dead Load Study	✓	✓	✓	✓	✓
Live Load Study	✓				
Time Effect Study	✓	✓	✓	✓	✓

T_R = total rise (invert to crown or footing to crown).

L = span length (springline-to-springline).

W^* = (L/2)*(top-rise)*(soil density).

σ_f = free field soil pressure due to soil weight.

K_o = lateral soil pressure coefficient.

in non-dimensional form, for the complete backfilling operation from footing elevation to top of fill is shown in Figure 2-1 for seven different long-span systems. The crown deflection relative to the footing (or invert) is non-dimensionalized by dividing it by the total culvert rise. Thus, it may be regarded as a percentage of culvert height. Likewise, the fill height is non-dimensionalized by factoring it by the total culvert rise. In most cases, engineering judgement was required in assessing the fill-height origin used as reference in the reported data. Consequently, relative comparisons between the displacement magnitudes must be done with caution.

Upon inspecting Figure 2.1 the following general trends are observed. When the fill height ratio is about 1.0, fill height at the elevation of the crown, the crown deflection peaks so that the deflection curve slopes change from positive to negative. Prior to peaking the deflection slopes appear steeper than the deflection slopes beyond the point of peaking. For the data plotted, the crown does not experience a net downward deflection due to dead load. However, if overburden loading continued, the deflection slopes indicate a net downward deflection would occur and continue to increase in a linear fashion.

A different perspective of the same data can be achieved by referencing the crown deflections to fill-soil-height beginning at the springline (i.e., assume deflections are zero with fill at springline). The motivation for this is that the data can be compared with analytical results in subsequent chapters which is also referenced to soil fill at springline.

The crown deflections resulting from fill soil referenced at the springline is shown in Figure 2-2 wherein the fill-height-ratio is redefined as fill height above springline-to-top rise of liner. Thus, as before, a fill-height-ratio of 1.0 implies fill soil is level with the crown. Again, it is observed that

crown peaking occurs when fill soil is at the crown level. However, the magnitude of peaking is decreased and the magnitude of flattening is increased due to the shift of fill height reference.

An interesting comparison can be made between the horizontal ellipse installation (Zimmer Power Plant) and the arch installations (Bucks County, Penrose, Stenner Creek, James Bay). In the post-peaking range, the crown deflections (and slopes) of the ellipse demonstrate a greater rate of flattening (downward crown movement) than the arch installations. This behavior is consistant with subsequent analytical studies wherein it is surmized that arches are better suited to resist flattening because the nearly verticle sidewalls provide a larger area for passive soil resistance than in the case of a horizontal ellipse.

The crown deflection characteristics of a high profile arch (Bucks County) and a low profile arch (James Bay) demonstrate similar behavior.

Crown deflection response for data for Bucks County high profile arch and James Bay low profile arch indicate that the high and low profile arch have a similar crown deflection behavior. Since the top arches of the two types are nearly identical, one could reasonably expect similar deflection response. The only major differences in these two installations is that the low profile arch had squeeze blocks at the footing level. Assuming the squeeze blocks were used to promote soil arching, the blocks have no apparent influence on the crown deflection.

Springline Deflection. Springline deflection results plotted with the fill height referenced at the footing elevation are shown in Figure 2-3. The initial part of this figure shows springline deflection moving inward. As the fill height approaches the springline elevation, a fill height ratio of 0.5 to 0.7 on Figure 2-3, the springline deflects inward at a reduced rate. When the fill is near the crown, the springline

deflection begins to reverse direction and move outward. However, the passive resistance of the soil resists outward motion so that very little change is seen in the springline dimension.

Liner Thrust. Very few culvert installations have been sufficiently instrumented with either mechanical or electrical resistance strain gages to measure the thrust force on the cross-section of the liner. Three experimental studies, Bucks County, Los Angeles, and Zimmer Power Plant have reported data on liner thrust and are sufficiently complete to define the thrust characteristics of the liner due to dead load alone.

The thrust at the springline elevation is generally higher than the thrust at the crown by virtue of traction shear between the liner and the soil and distribution of normal soil pressure. Springline thrust, therefore, will be used as the basis for discussing liner thrust behavior. Figure 2-4 is a plot of springline thrust for the Bucks County installation as the fill height is raised from the footing level to full fill height. The plot does not include the thrust caused by self-weight of the liner, only the dead load effect of the fill is shown. The magnitude of springline thrust is observed to increase in a non-linear fashion prior to fill being placed above the crown. As the fill is placed above the crown, the thrust magnitude appears to increase in a linear fashion. The discontinuity shown on Figure 2-4, between the springline and crown elevations, may be a result of liner joint slippage at one or several longitudinal bolt seams.

Thrust measurements for the Los Angeles and Zimmer Power Plant installations were recorded beginning at a fill height reference approximately one meter above the crown. By also referencing the Bucks County data to this location, thrust data from all three installations are shown in non-dimensional form in Figure 2-5. Thrust is non-dimensionalized by dividing it by a block of soil weight having dimensions, one unit thick,

one-half span wide, and a height equal to top rise. Thus, a thrust ratio of 1.0 infers that the springline thrust is equal to soil weight in the square region bounded by a lower horizontal line at the fill height reference (one meter above crown), an upper horizontal line raised a top-rise distance, a vertical line tangent to springline, and the verticle centerline.

In Figure 2.5 fill height is plotted in reference to the springline and non-dimensionalized by dividing it by top rise height. The dashed line shown in the figure has a slope of 1.0 so that data points above the dashed line infer springline thrust is greater than column soil weight (negative arching), and data points below the line are less (positive arching).

Although the thrust data points are somewhat scattered, the general trend suggests that thrust increases linearly with fill height with a slope of approximately 1.0 indicating neutral arching. However, it must be remembered that this data does not include the additional thrust from initial backfilling of fill soil from footing (or invert) to crown. Thus, the total springline thrust may slightly exceed soil column weight implying a slight negative arching. For shallow buried installations the initial backfilling thrust is relatively more significant than for the deeply buried installation. In the instrumented case of the deeply buried Bucks County installation (Figure 2-4), initial backfilling thrust is 14% of the total thrust at full fill height.

The relative thrust response of the crown and the springline are shown in Figure 2-6 for data from the Los Angeles installation. Observe that the right and left springline thrusts are not identical because of relative footing settlement. According to the liner fabricator, the right footing was founded on insitu soil whereas the left footing was placed on structural fill material. The thrust in the left side of the liner is less because of the larger soil deformation (settlement/consolidation)

of the structural fill at the footing level.

Comparing the average springline thrust to the crown thrust, shown in Figure 3-7, the crown thrust is about 25% less than that of the springline.

Soil Pressure Distribution. Several field investigation programs (2-2, 2-4, 2-5, 2-6, 2-10, 2-11, 2-13, 2-15, 2-16) have studied the soil deformations and stress distributions in the vicinity of the buried culvert. The most comprehensive of these is Reference 2-3 to 2-6 (Bucks County) whose data will be subsequently discussed.

Because of soil stress redistribution around the culvert liner, the vertical soil pressure immediately above the crown is usually less than the free field soil pressure. This redistribution phenomena is shown by the plot of the vertical stress distribution of the experimental data on the left hand side of Figure 2-7. Immediately over the crown, the soil stress is significantly less than the free field soil stress. At distances farther away from the crown the soil stress approaches the free field stress. Data plotted in Figure 2-7 represents the soil stresses measured at the completion of the backfilling operation.

The soil stress distribution at the springline for both the horizontal and the vertical soil stresses are opposite the trend observed from the crown, shown on right side of Figure 2-7. In the immediate vicinity of the liner at the springline, the vertical and horizontal stresses are higher than the free field stress. As expected, the horizontal stress at the springline is larger than the free field stress because the soil is laterally compressed due to outward liner deformation. Horizontal and vertical stresses are normalized by free field stresses where the coefficient of passive earth pressure which was taken as about 0.5 from Reference 2-3.

The high horizontal and higher vertical soil stresses in

the immediate vicinity of the liner are seen to dissipate rapidly. However, to maintain equilibrium, it is likely the stresses dip below free field values before they approach free field values at some distance from the culvert.

Fill height load histories for vertical stresses near the crown and the springline are shown respectively in Figures 2-8 and 2-9. Horizontal stress histories near the springline are shown in Figure 2-10. With exception to the experimental data collected immediately after installation of the stress gages, the trends recorded during the "short time" backfilling history indicate that the stress increases in an approximate linear fashion as the fill height increases. Deviations from the calculated free field stress are apparent by comparing the distance between the solid curves representing measured data and the dashed curve representing the free field stress.

2.4 LIVE LOAD RESULTS

Availability. Two experimental field investigations have collected some information on the live load response of the corrugated metal arch culvert. The best and most comprehensively gathered information is found in a Federal Highway Administration internal report (2-8) discussing the testing of a culvert installed in California. Additional, but minimal, data was also collected and published on a shallow buried installation in Canada (2-13). Data reported in Reference 2-8 (Stenner Creek) is on a high profile arch whereas Reference 2-13 (Thunder Bay) data is on a horizontal ellipse with a shallow depth of burial and a relieving slab 2.7 feet (.8m) above the crown elevation.

These two studies have reported data on the behavior of the crown deflection only as the culvert was acted upon by a moving vehicular live load. No definitive information on thrust, springline deflection or soil stresses are reported. In both of

these studies the live load consisted of a loaded two axle truck. Data reported for Stenner Creek is for the structural response to a standard H20 (M18) truck while the data for Thunder Bay uses a vehicle loaded to slightly less than the H20 (M18) standard.

Crown Deflection. Figure 2-11 is an experimental influence line of vertical crown deflection as a function of the position of the truck's middle axis for the Senner Creek installation. Two plots are shown representing the crown deflections as the vehicle passes transversely over the culvert in each direction. Data points in the two plots are not mirror symmetric and, therefore, are presented separately rather than averaged. Unsymmetrical behavior is possibly a result of the introduction of residual deflections of the crown and/or experimental error.

The different curves in Figure 2-11a and 2-11b represent the crown deflection response as the fill height ratio (ratio of the fill height above the springline to top rise distance) increases. The deeper the culvert is buried in soil, the smaller the total amplitude (peaking and flattening) of crown deflection.

For each of the fill height ratios plotted, note that the crown first deflects upward (peaking) as the moving live load first comes on the culvert span. As the live load approaches the crown, the crown deflects downward (flattening) as the live load gets closer to the crown position. Both Figures 2-11a and b show that when the moving live load is in the vicinity of 1/8 the culvert span on either side of the crown position (distance ratio on Figure 2-11 of 0.00 to 0.40), the crown deflection changes from peaking to flattening. In general, the load location producing zero crown deflection moves away from the centerline as fill height increases.

By selecting one position of the live load vehicle a new curve can be derived from the data shown in Figures 2-11a and b. With the vehicle middle axis at the crown position a plot

of the crown deflection as a function of the fill height ratio is shown in Figure 2-12. This figure clearly indicates how the crown deflection rapidly decreases as the depth of culvert burial increases. Also shown is the slight difference in the experimental behavior for the two traffic flow directions.

An additional data point is also shown in Figure 2-12 from the Thundery Bay installation. This one result is of low magnitude and does not appear to be consistant with the result of Stenner Creek. However, part of the difference may be attributed to a lighter live load vehicle and more importantly the presence of a concrete relieving slab placed 2.7 feet (.8m) above the crown.

At present, these are the only live load results available in the technical literature.

2.5 TIME DEPENDENT EFFECTS

Table 2-1 indicates that most of the field investigations have been conducted since 1970. Frequently, the instrumentation for measuring long term effects has not been included in the experimental study. Four of the studies listed in Table 2-1 (Bucks County, Los Angeles, Port Dover, and Kettle Creek) have been monitored over a sufficient period of time to examine the time dependent data trend. Two of these four have time dependent measurements exclusively on the soil (Port Dover and Kettle Creek) and two have time measurements on the structural liner and some on the soil characteristics (Bucks County and Los Angeles). The following discussion will concentrate on the latter two investigations.

The crown deflection history over a period of about one year is shown in Figure 2-13 for the Los Angeles installation. This data shows that the crown has continued to deflect downward (flattening) without an additional dead load from backfilling. Shortly after completing the backfilling operation,

about 2 months, the crown flattening appears to have stabilized and appears to be creeping back upward at the end of the recording period.

Figure 2-14 illustrates the time effect for thrust at the crown and springline for the same installation. The measured data, however, seem to indicate that the thrust responses did not stabilize in the same fashion as the crown deflection. Specifically, the crown thrust first decreases but then after about six months the trend reverses. The springline thrust appears to increase slightly in the first months after backfilling is completed and then begins decreasing. It appears that the thrust at the springline and the crown are approaching a common value.

Time dependent thrust data from Bucks County are shown in Figure 2-15. For the time interval selected, four months after construction, the crown thrust, with exception of one data point, remained the same and the springline thrust increases about 14%. The magnitude of the thrust changes with time are considerably different for the Bucks County and Los Angeles installations.

In an earlier figure, Figure 2-7, the soil stress distribution around the liner at the completion of construction indicated high vertical and horizontal stresses at the springline and low vertical stresses at the crown. Figure 2-16 superimposes on that data the measured soil stresses four months after the end of construction. All soil stress were observed to increase in magnitude although no additional dead load was applied. The soil stresses increases in Figure 2-16 show approximately the same (15 percent) increase observed in Figure 2-15.

2.6 COMMENTARY ON EXISTING DATA

During the data evaluation phase of this study, the authors found numerous shortcomings, inconsistances and deletions in

the data available for comparative purposes. The most severe drawback is that there are too few test data available to develop confident trends. In many cases it was found that even with the available data comparisons between experimental investigations could not be made.

In the majority of the references used, there is a complete void in reporting the soil characteristics. The essential soil characteristics are considered to be unit weight, water content, gradation and stress-strain-stiffness parameters including triaxial tests.

For the data measurements reported in the references, inconsistancies in zero referencing and incomplete results made it very difficult to construct meaningful trends of behavior. The most frustrating aspect of the data evaluation has been the lack of a consistant reference point for fill height. It is suggested that conditions at a backfill height at the footing level be used in future investigations because all intermediate reference origins can then be analytically determined. In several studies the conditions at the footing level were not recorded, necessitating either the elimination of that data from consideration or introducing an error by attempting to approximate the needed information at the footing level.

Data pertinent to the electrical resistant strain gages on the liner were also particularly difficult to use in evaluation because of failure of key gages (no redundancy) and the complicated or unclear methods of data presentation.

2.7 FINDINGS AND CONCLUSIONS

In spite of the shortcomings of the experimental data discussed in the previous section, the following general trends of long-span structural behavior appear valid.

Dead Load of Soil Backfilling. During backfilling operations from the footing (or invert), the crown deflection increases

rapidly to a maximum peaking position when the fill height is level with crown. Subsequent increases in fill height reverses the direction of crown deflection but downward crown deflection proceeds at a slower rate. High and low profile arches exhibit similar crown deflection patterns, however, horizontal ellipse installations appear to flatten at a significantly higher rate (with respect to fill height) than arch installations.

Springline deflection reaches its maximum inward movement when the fill height is at crown level and then reverses direction as fill height further increases. However, the rate of return movement is significantly reduced due to mobilization of lateral soil pressure.

Maximum thrust in liner occurs in the region between the footing and the springline. As soil is backfilled from the footing to crown, thrust increases at an increasing rate. As fill soil is placed above the crown, thrust increases at a constant rate equivalent to the column weight of soil above the crown. Thus, the total accumulated thrust at full fill height is greater than column weight of soil.

Thrust at the crown is consistantly less than thrust at the springline by about 25%.

Vertical soil pressure in the vicinity of the crown is significantly less than free field overburden pressure. Contrarily, vertical and horizontal soil pressure are greater than free field stresses in the vicinity of the springline.

Vehicle Live Loads. As a traveling load transverses a shallowly buried long span installation, the crown initially moves upward (peaking). However, as the load approaches the long-span central portion the crown begins to flatten and is maximum when the load is at the centerline. The magnitude of peaking and flattening is extremely sensitive to cover height. For example, increasing the cover height from 10% of top-rise to 20% of top-rise decreased the maximum live-load crown

deflection by 60%.

Time Effects. The lack of consistant time-dependent data and the relatively short recording periods makes it difficult to draw definite conclusions with regards to long-term time effects. As a general trend, downward crown deflection and maximum thrust increase after the end of construction but not consistantly. The influence of factors such as seasonal changes, moisture, and temperature are not known.

2.8 RECOMMENDATIONS FOR FUTURE EXPERIMENTAL STUDIES

As evidenced by the small amount of experimental data on long-span systems, much additional experimental investigation is required to validate existing data and, more importantly, to obtain information in areas where there is a complete lack of data. In particular, no viable data exists on tests-to-failure, and consequently, the mechanisms of failure are not understood. Clearly, a rational design procedure cannot be devised until failure mechanisms are understood and proper design criterions have been established.

Other aspects requiring additional experimental investigation include the following catagories for both shallow and deeply buried systems:

1. Liner Parameters

   (a) Effect of liner dimensions and shape, e.g., span-to-rise ratio for common shapes such as ellipses, open-arches, pipe-arches, etc.

   (b) Effect of liner stiffness in bending and thrust, e.g., liner corrugation, thickness, and material properties.

   (c) Influence of joint slippage at bolted seam connections and squeeze block footings to reduce thrust.

2. Soil Parameters

   (a) Effect of soil type and compaction for structural quality backfill.

(b) Measurements of soil-structure interface traction (both normal and shear pressures).

(c) Environmental effects such as moisture and temperature including long-term loading.

Both laboratory and field experimental studies are necessary for a comprehensive investigation. In particular, it is suggested and highly recommended that laboratory studies be conducted first. Models of large scale structures can be economically investigated with the purpose of studying new construction concepts, parametric investigations, verification of design recommendations. The controlled environment of the laboratory can be an effective means of providing information currently not reported in the field investigations as well as adding to the data existing in the literature.

Laboratory investigations provide a viable alternative for long term studies because of the better probability of continued electrical instrumentation operation, better control of soil properties, more accurate control of foundation settlements, thermal variations, and moisture.

In conjunction with experimental studies, an analytical model should be developed and/or further improved (e.g., CANDE), so that, the analytical model reflects the basic experimental results. Once this is achieved a rational design/analysis procedure can be devised for long-span systems and new concepts can be confidently tested.

2.9 Figures 2-1 through 2-16

		Page
Fig. 2-1	Crown deflection as a function of total culvert rise vs. fill height (w/r footing) ratio.	30
Fig. 2-2	Crown deflection as a function of total culvert rise vs. fill height (relative to springline) ratio.	31
Fig. 2-3	Springline deflection as a function of culvert span vs. fill height (w/r footing) ratio.	32
Fig. 2-4	General thrust behavior of culvert liner at the springline.	33
Fig. 2-5	Thrust in liner from a consistent reference above crown.	34
Fig. 2-6	Thrust response of springline and crown.	35
Fig. 2-7	Soil stress distribution around culvert (Bucks County).	36
Fig. 2-8	Vertical stresses above the crown (Bucks County).	37
Fig. 2-9	Vertical soil stress along springline (Bucks County).	38
Fig. 2-10	Horizontal stresses along springline (Bucks County).	39
Fig. 2-11	Crown deflection as a function of load position.	40
Fig. 2-12	Crown deflection as a function of fill height.	41
Fig. 2-13	Time dependent characteristics of crown deflection.	42
Fig. 2-14	Time dependent characteristics of springline and crown thrust.	43
Fig. 2-15	Thrust stress distribution in culvert liner showing dependent effect.	44
Fig. 2-16	Time dependent characteristics of soil stresses near crown and springline (Bucks County).	45

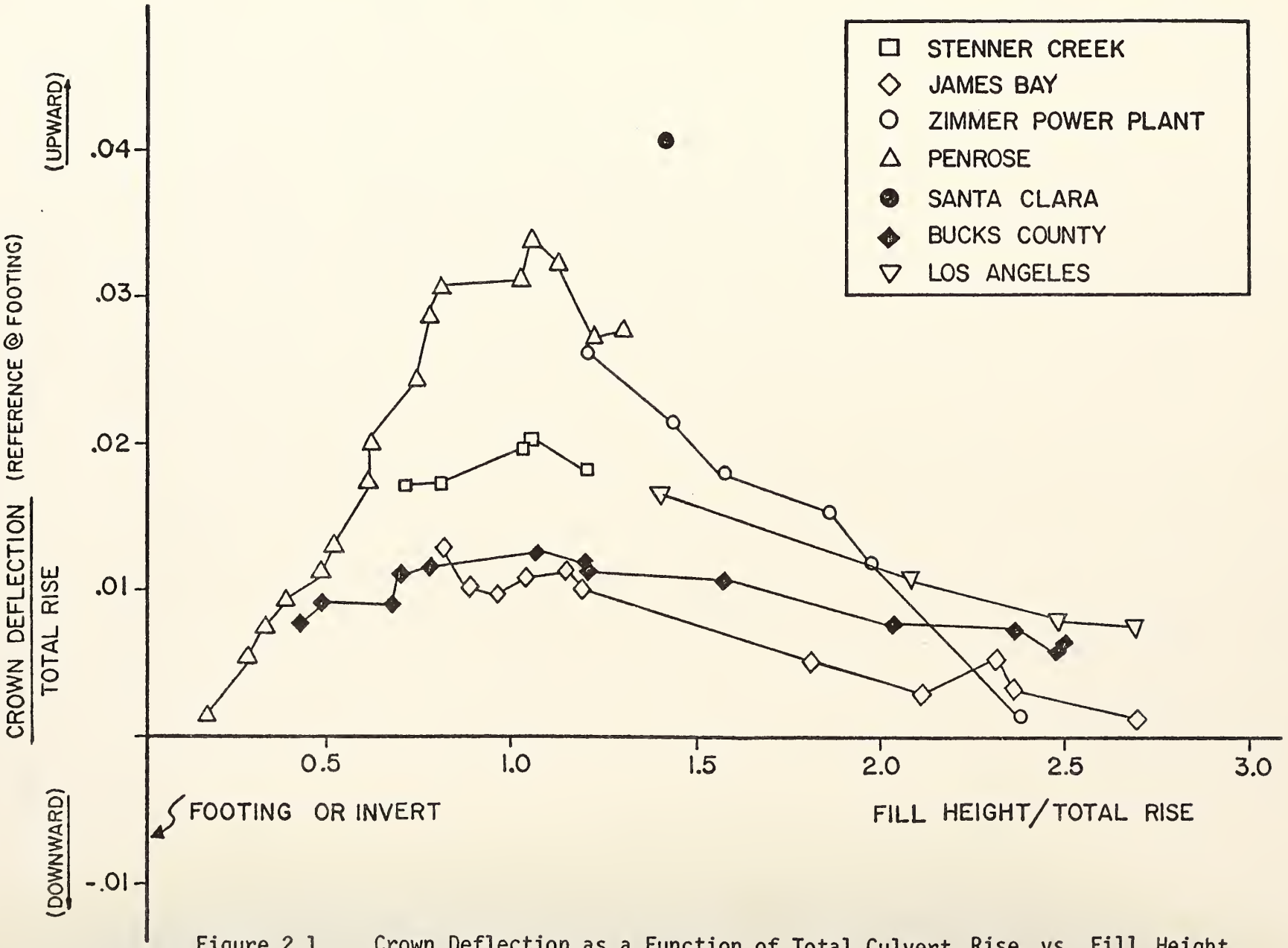

Figure 2.1 . Crown Deflection as a Function of Total Culvert Rise vs. Fill Height (w/r Footing) Ratio

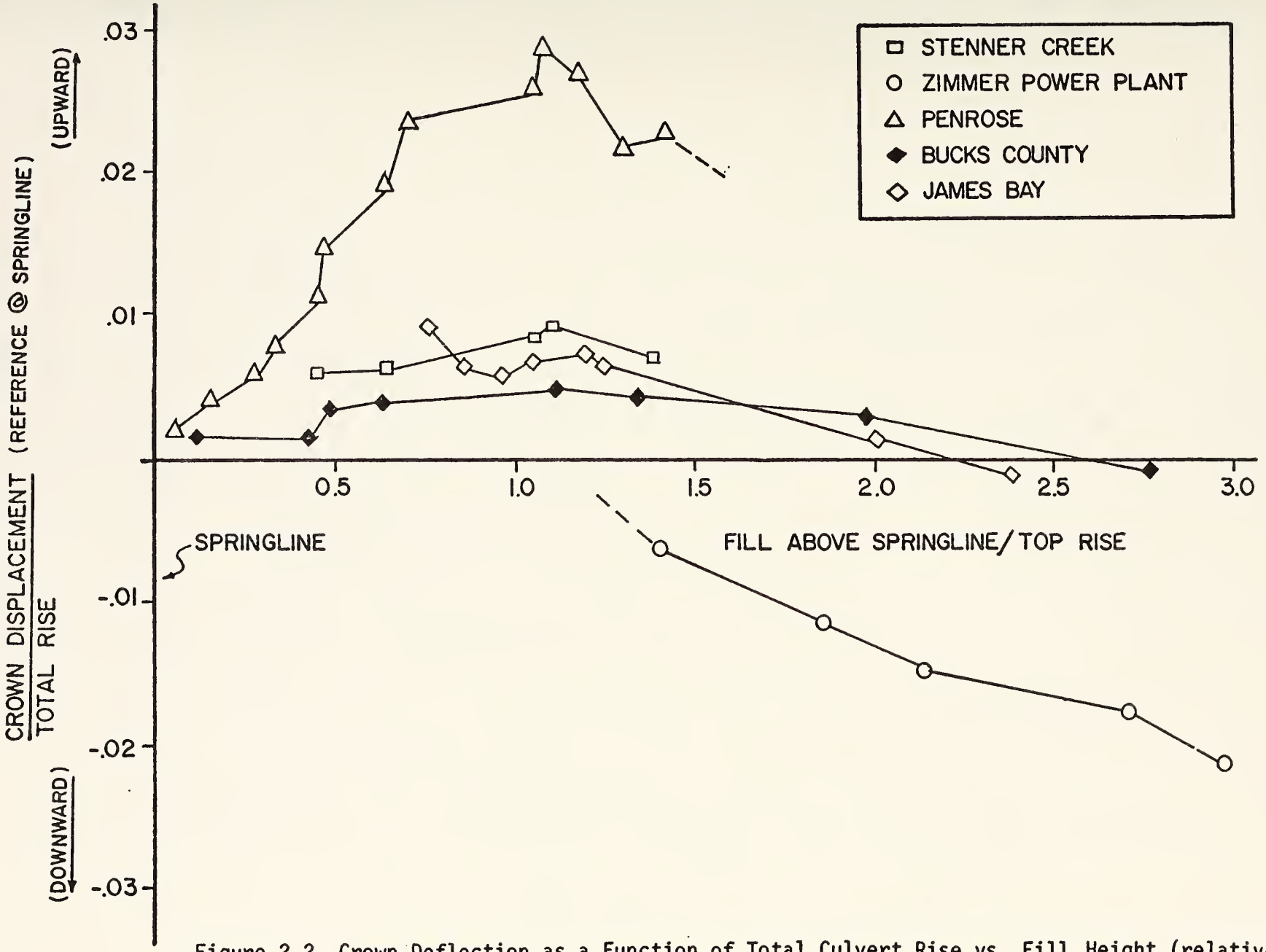

Figure 2.2 Crown Deflection as a Function of Total Culvert Rise vs. Fill Height (relative to Springline) Ratio

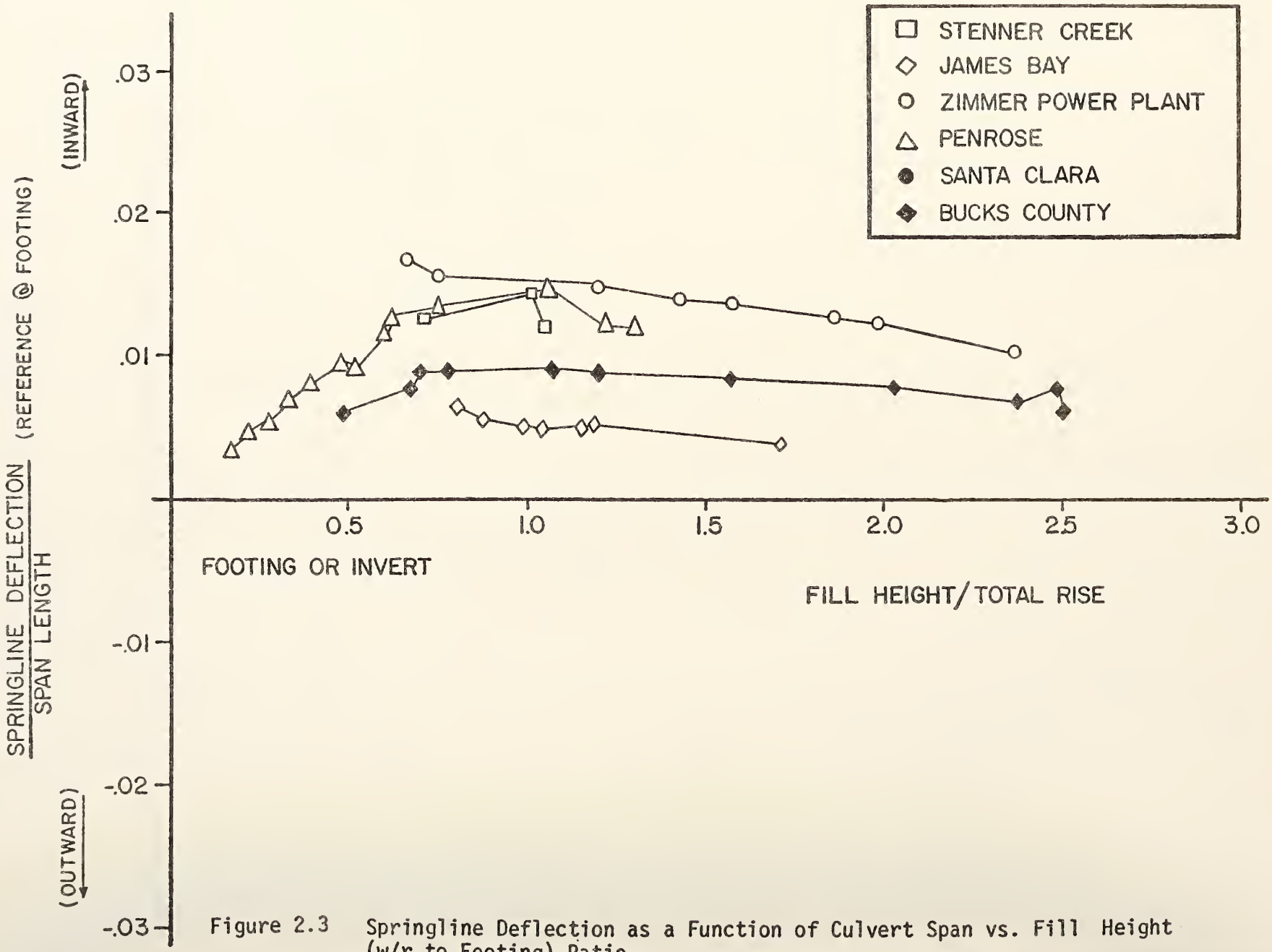

Figure 2.3 Springline Deflection as a Function of Culvert Span vs. Fill Height (w/r to Footing) Ratio

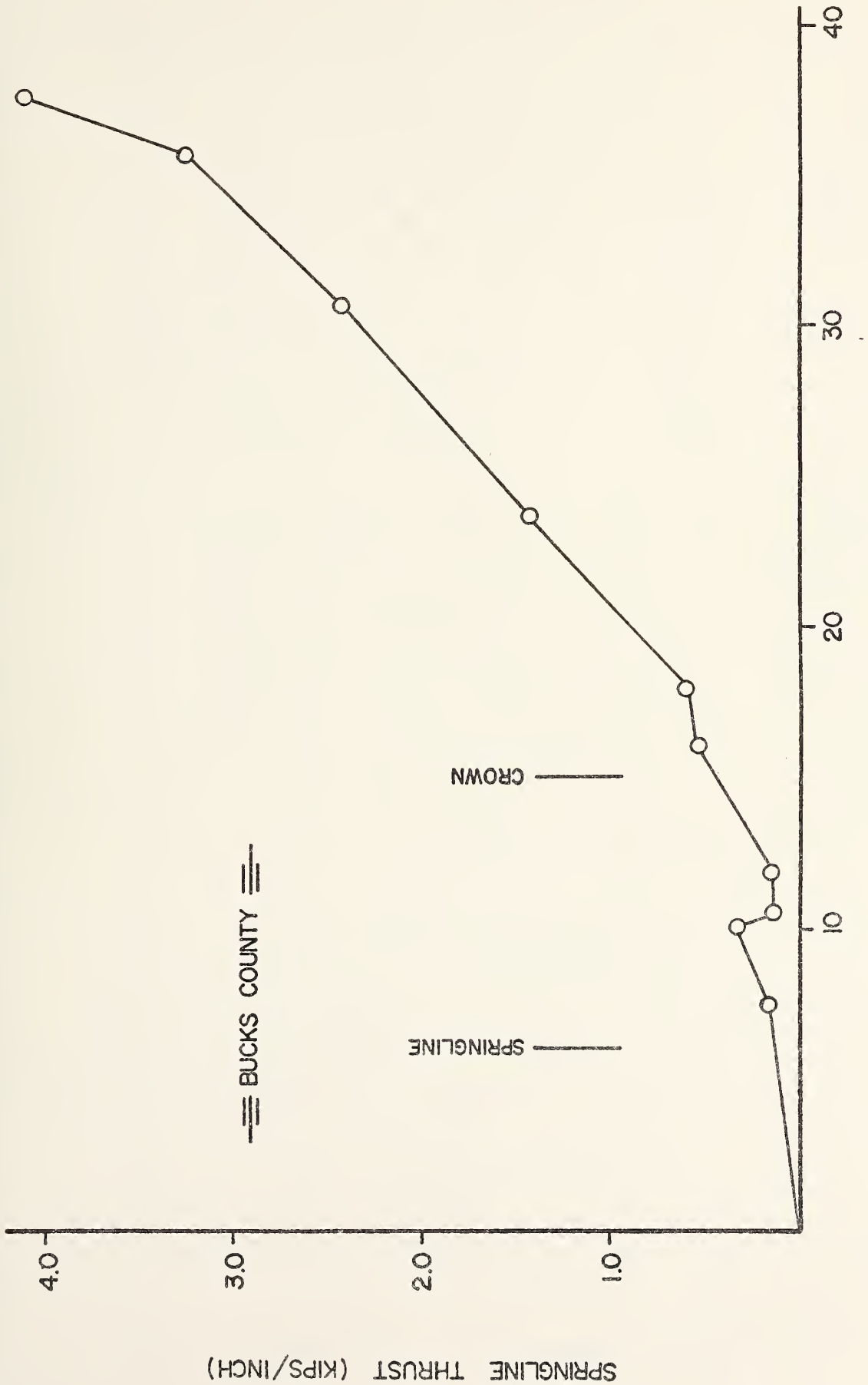

Figure 2.4 General Thrust Behavior of Culvert Liner at the Springline

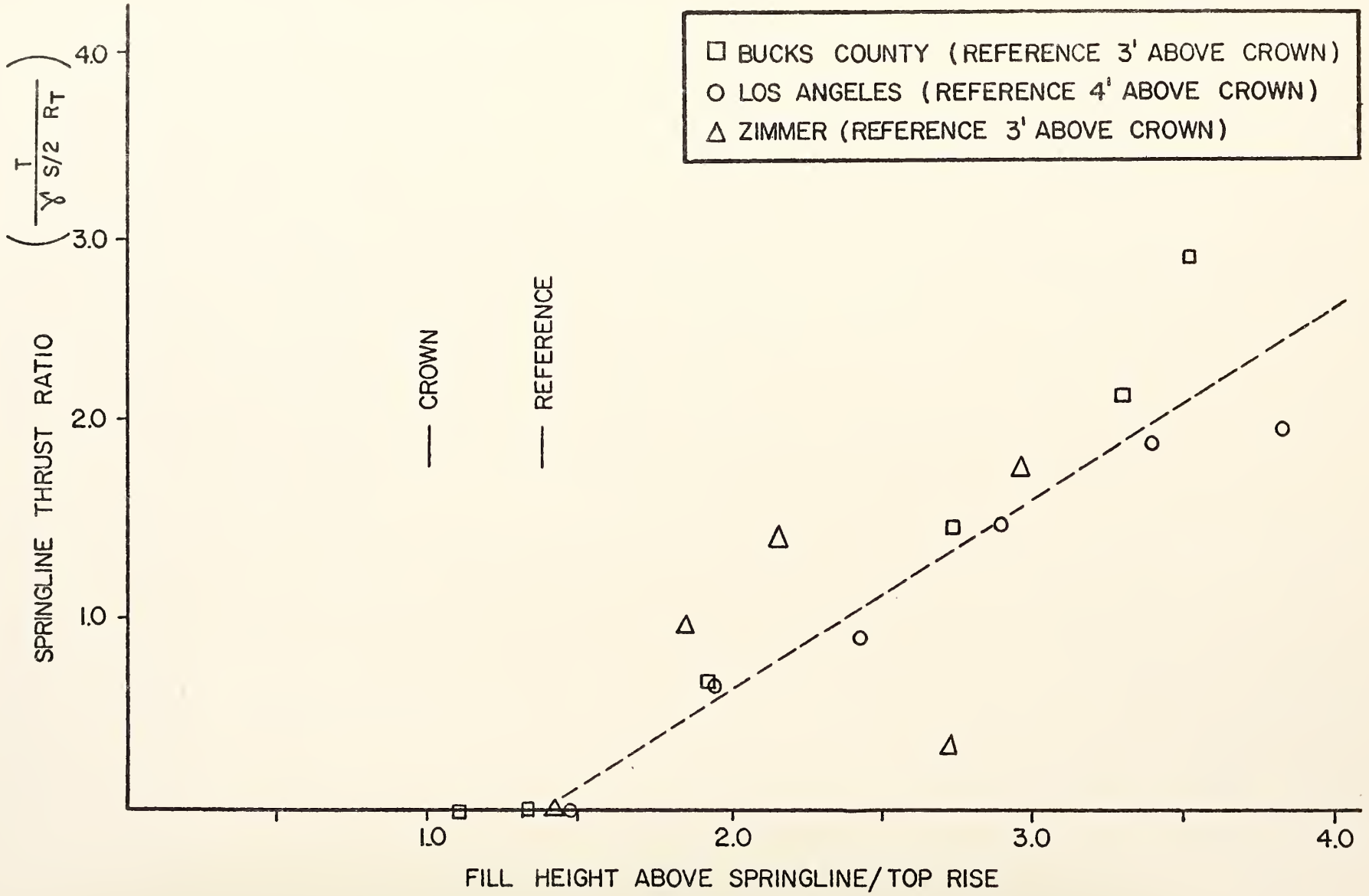

Figure 2.5 Thrust in Liner from a Consistent Reference above Crown

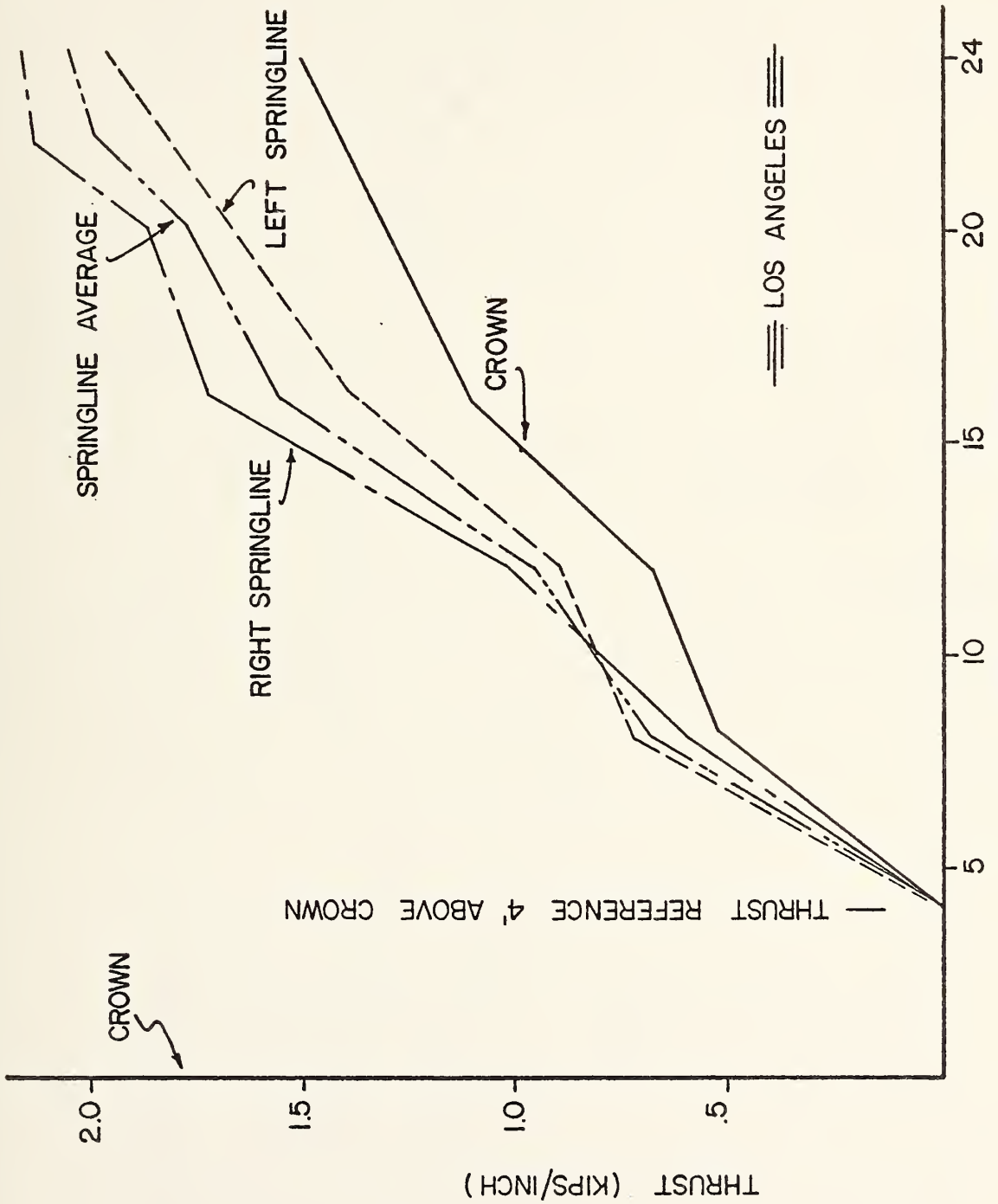

Figure 2.6 Thrust Response of Springline and Crown

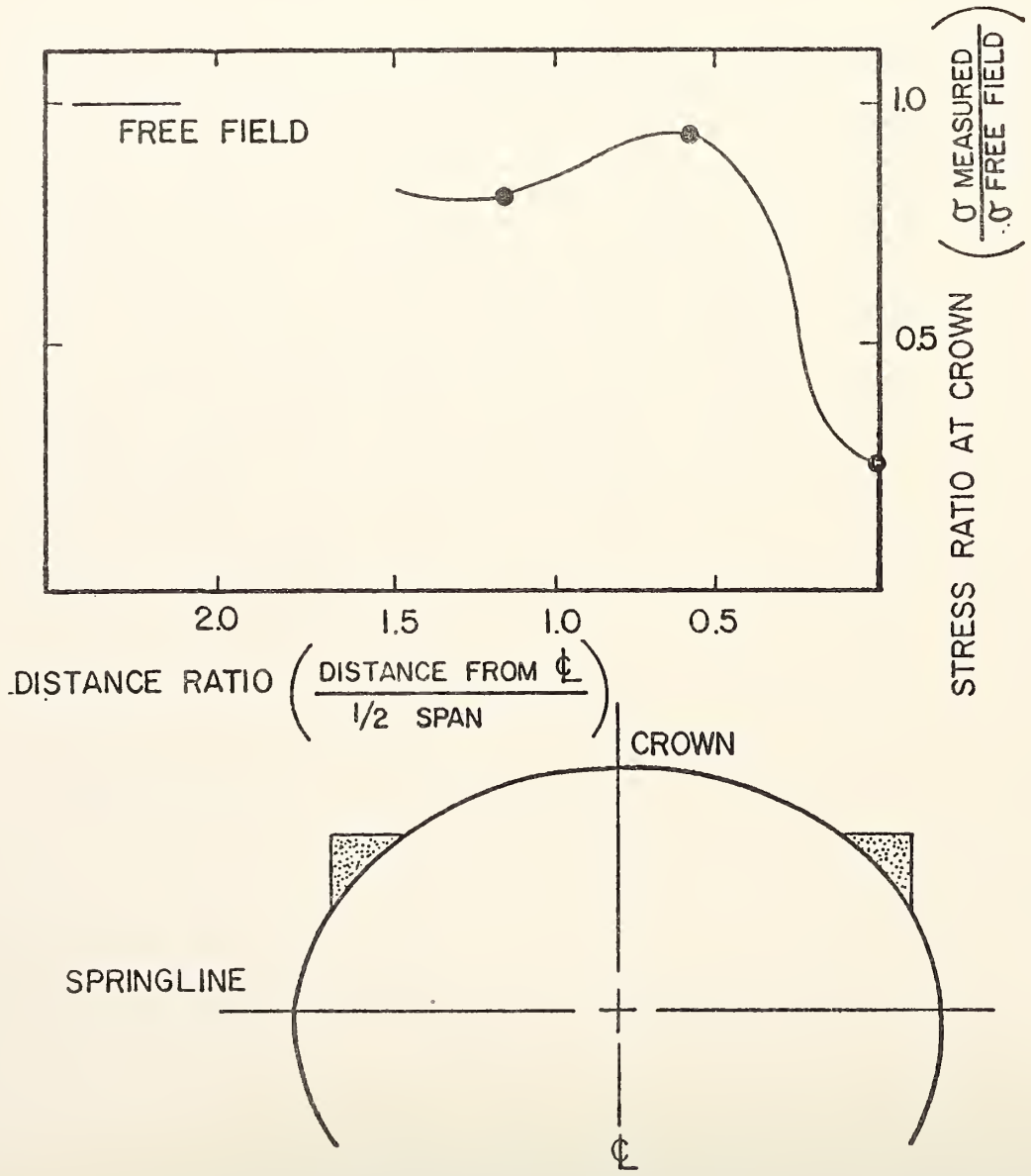

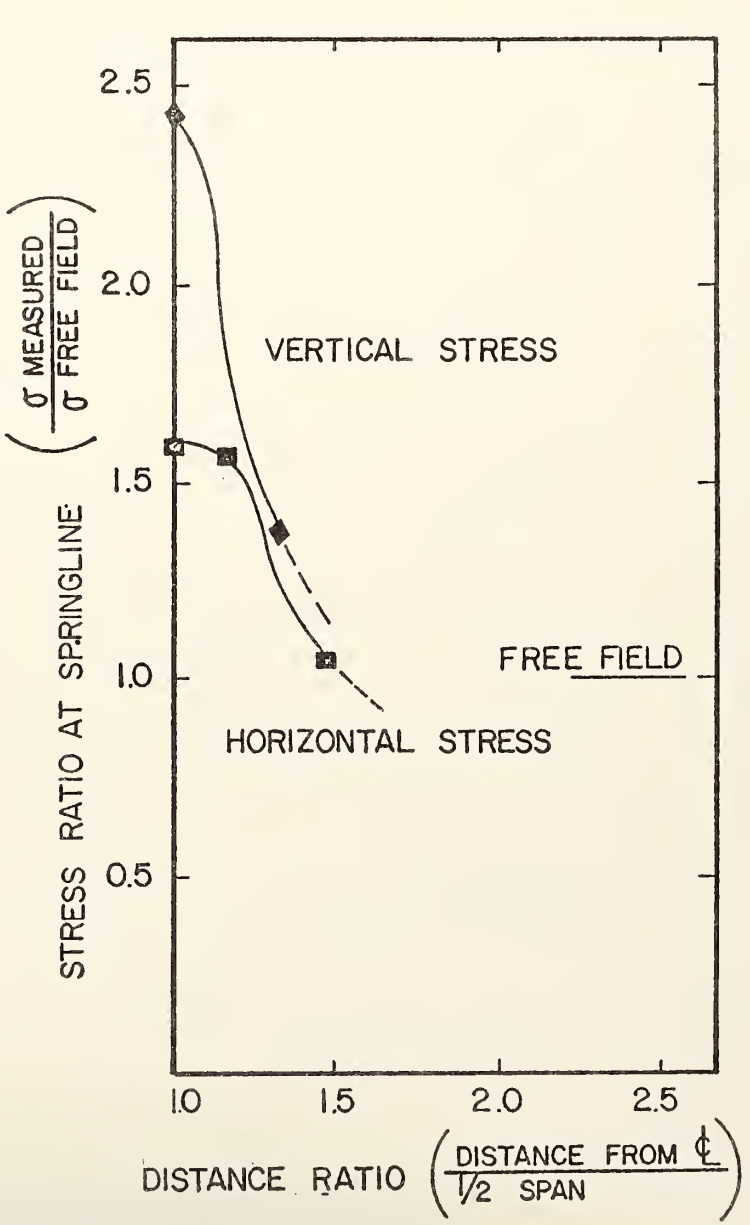

Figure 2.7 Soil Stress Distribution Around Culvert (Bucks County)

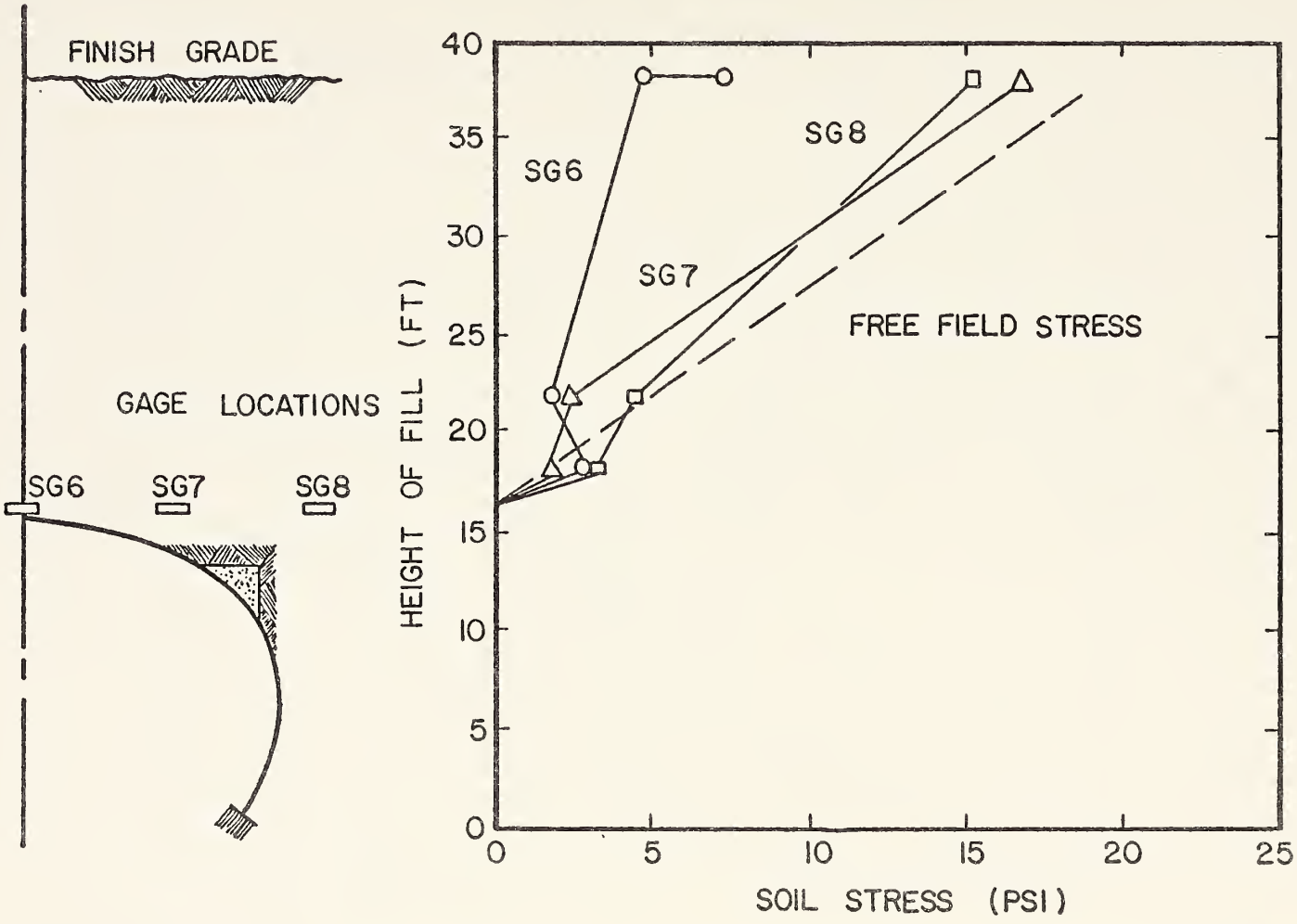

Figure 2.8 Vertical Stresses Above the Crown (Bucks County)

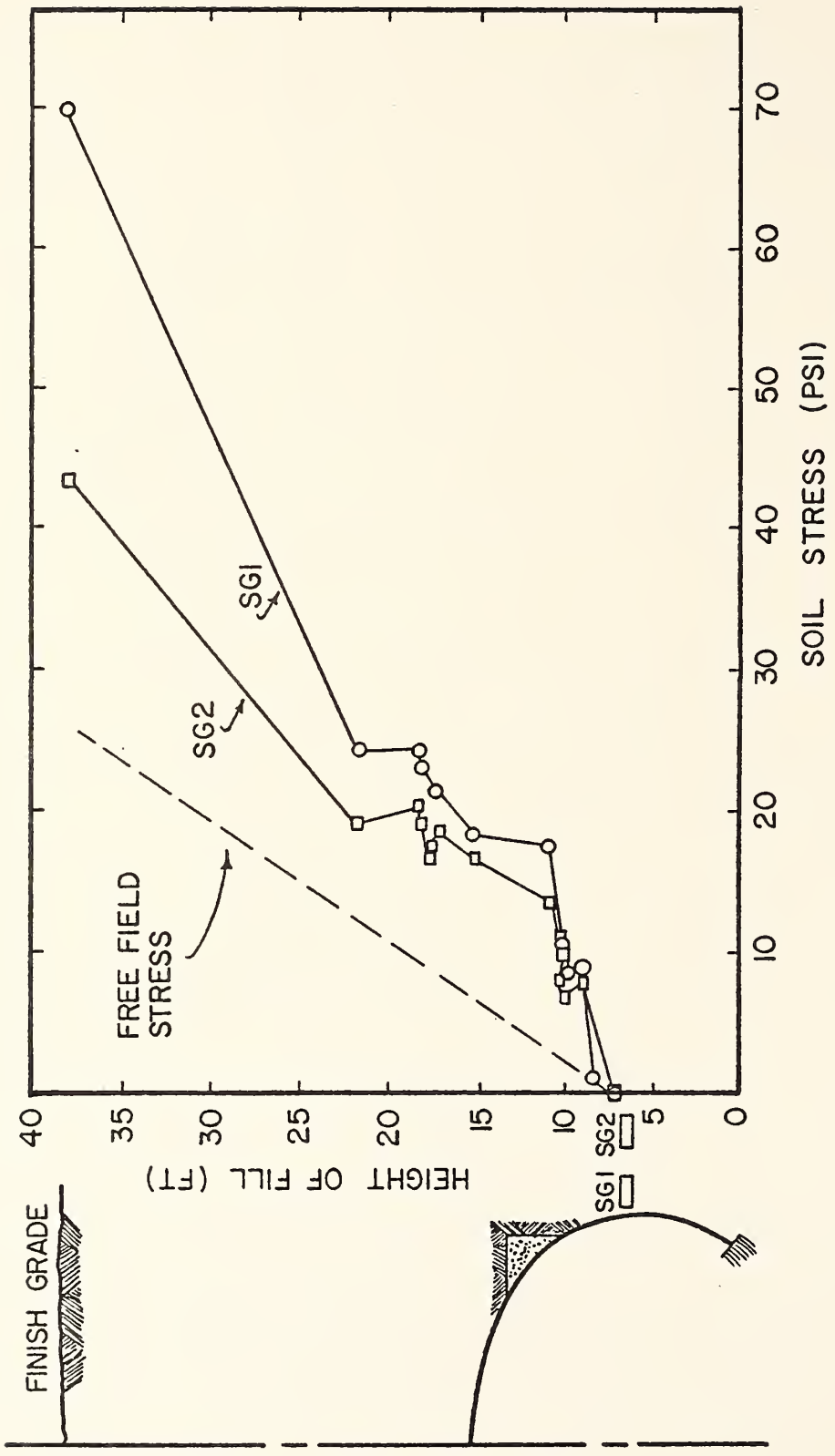

Figure 2.9 Vertical Soil Stress Along Springline (Bucks County)

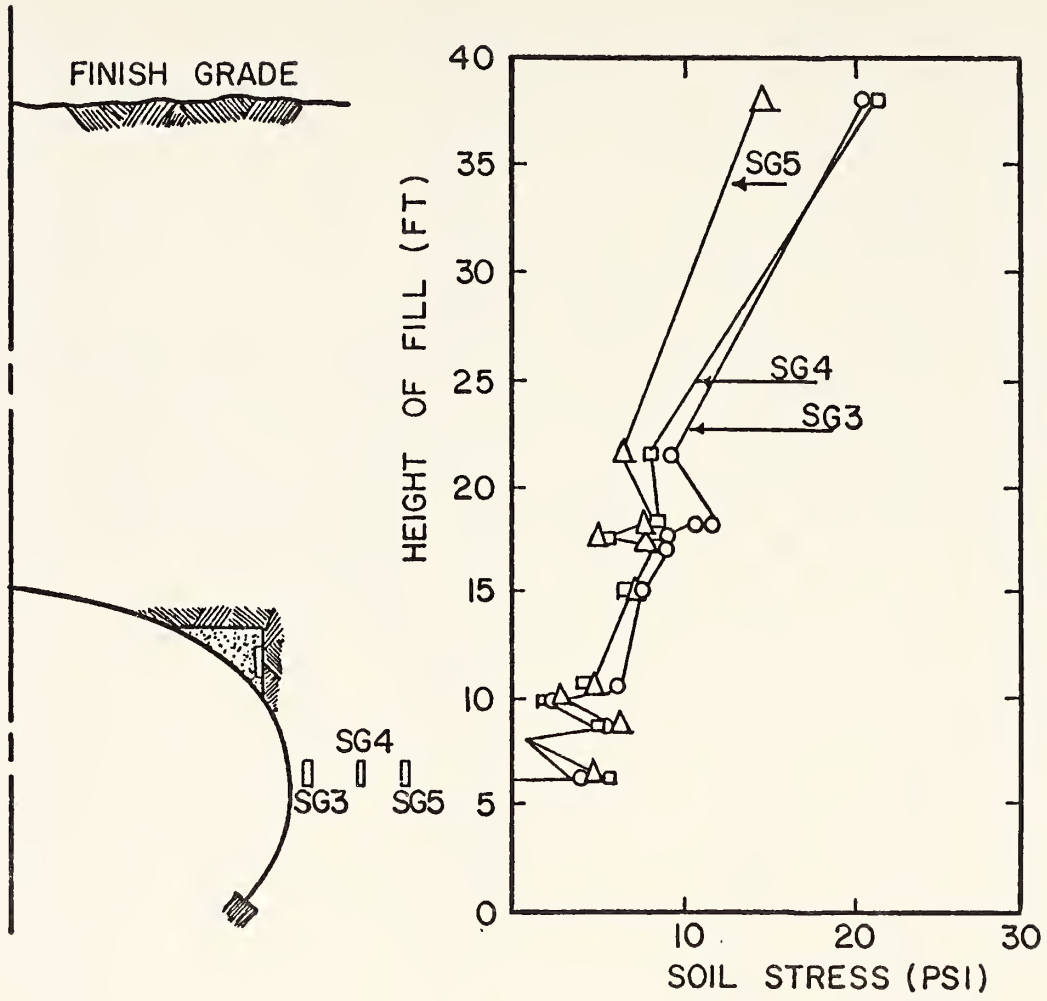

Figure 2.10 Horizontal Stresses Along Springline (Bucks County)

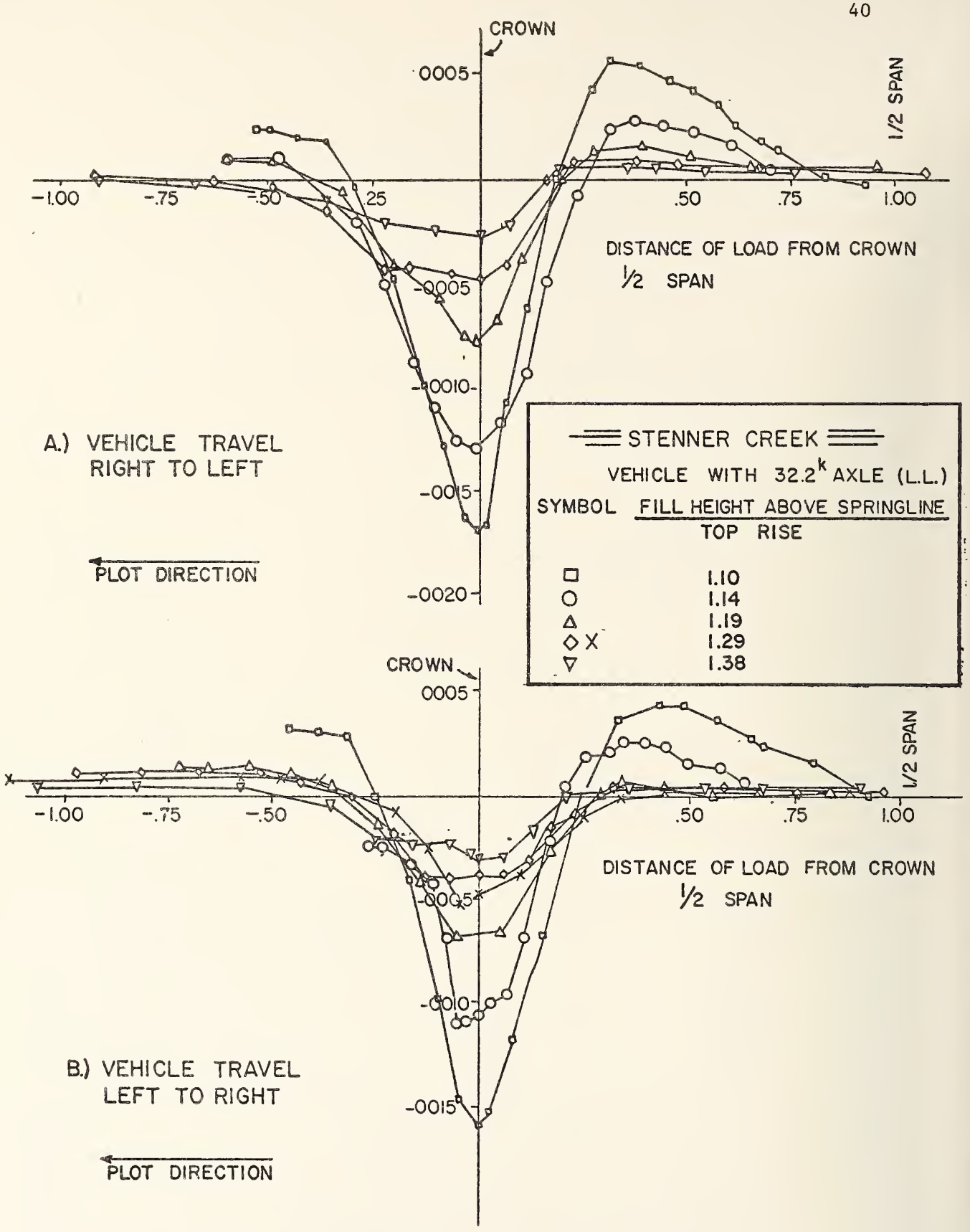

Figure 2.11 Crown Deflection as a Function of Load Position.

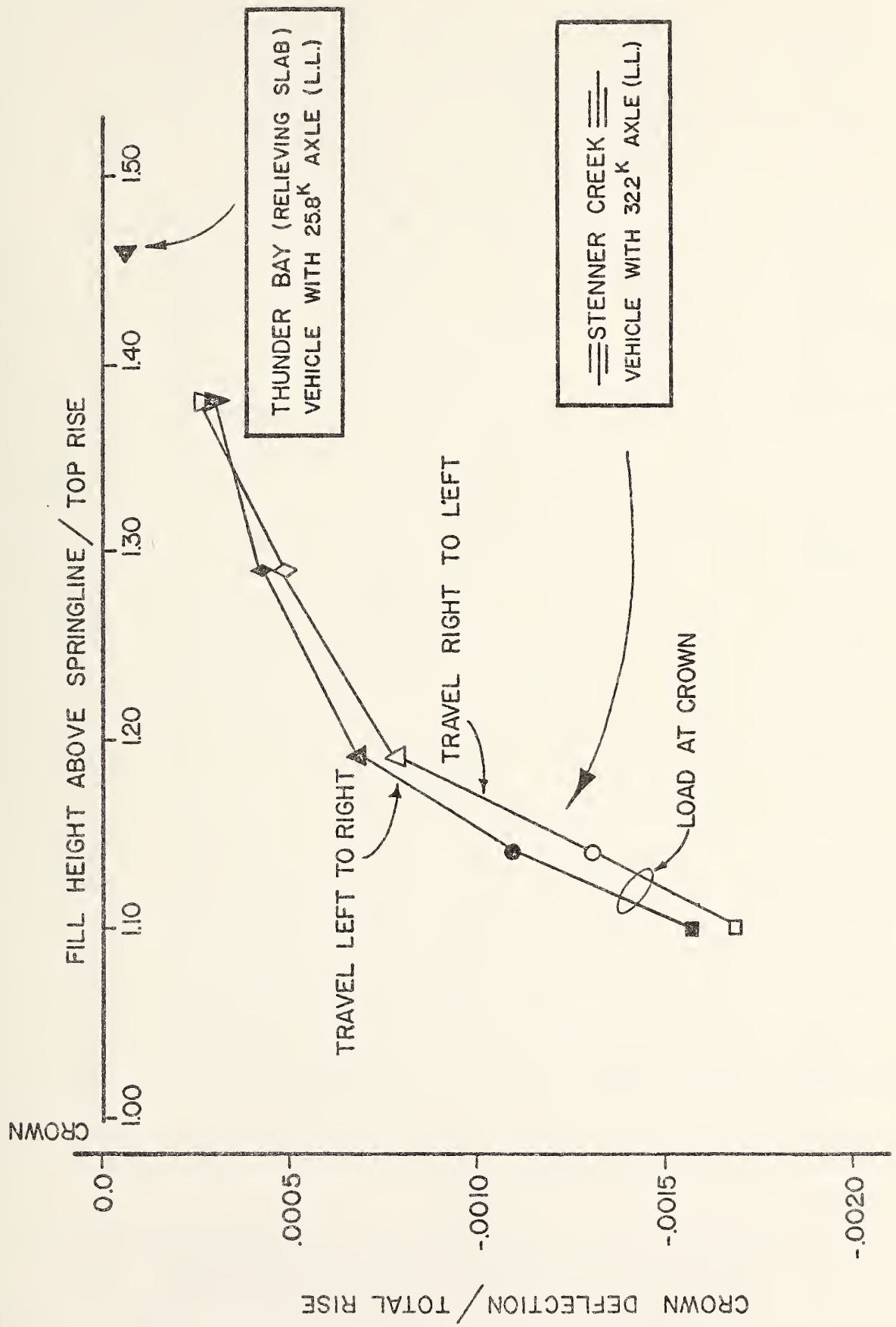

Figure 2.12 Crown Deflection as a Function of Fill Height

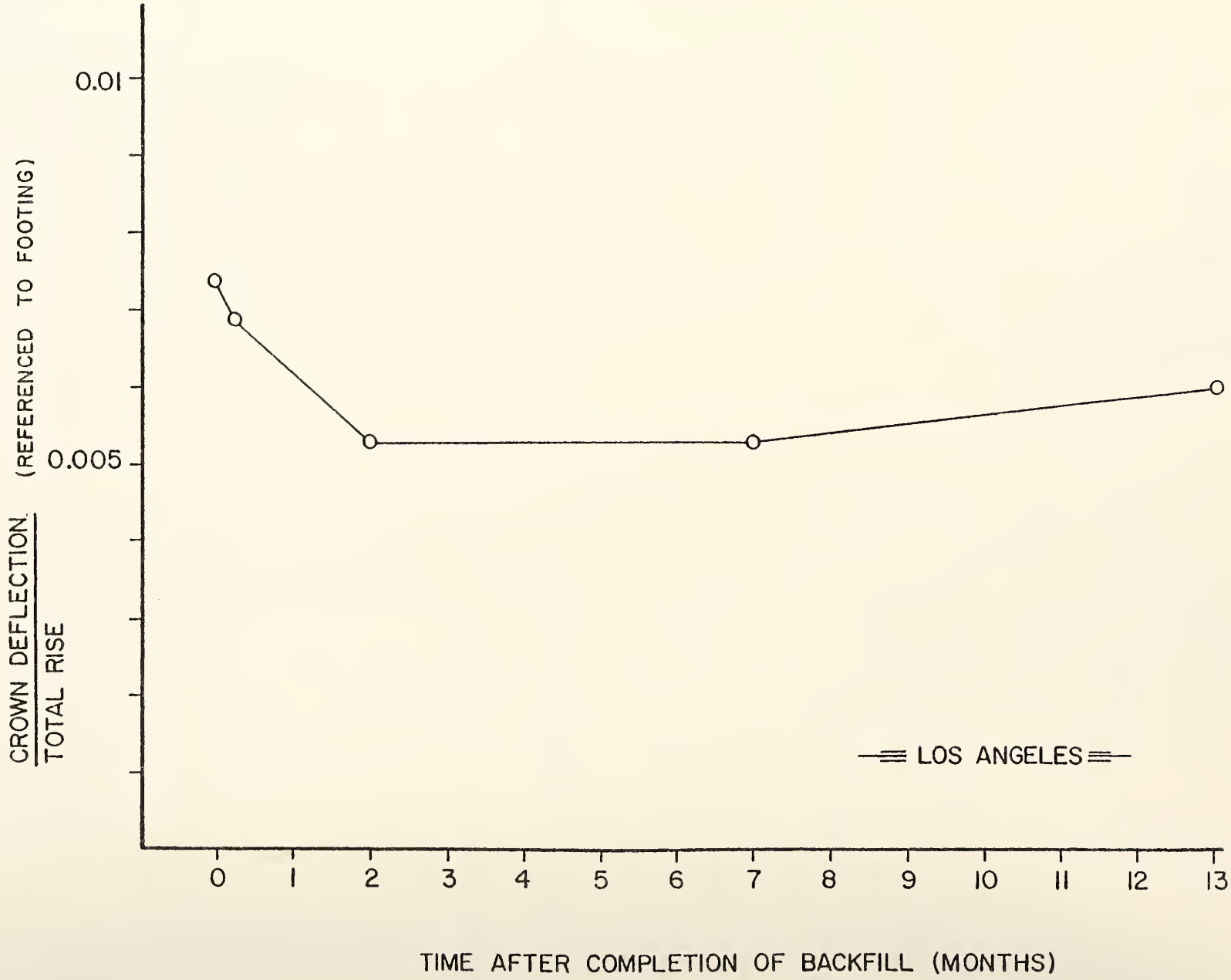

Figure 2.13 Time Dependent Characteristics of Crown Deflection

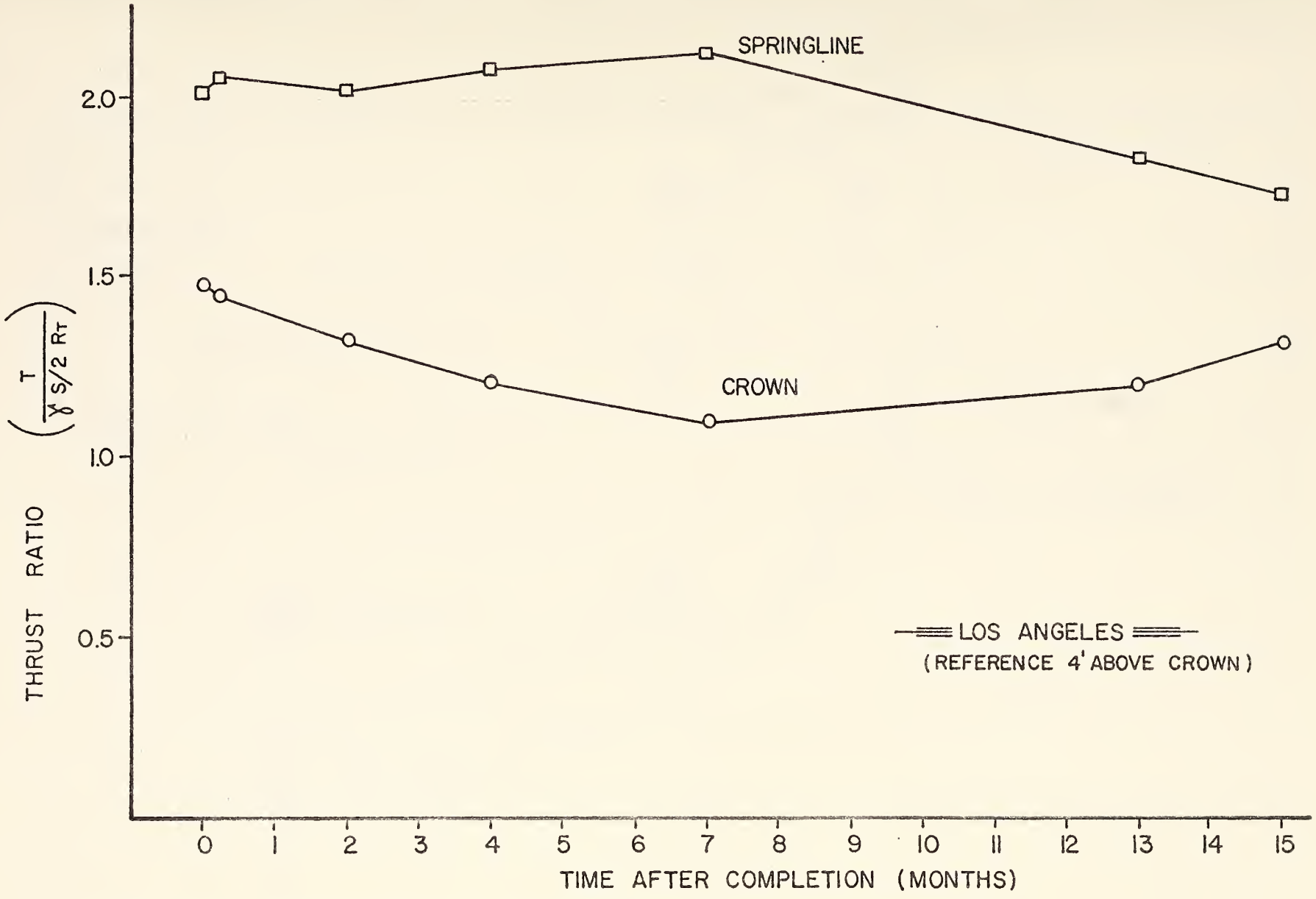

Figure 2.14 Time Dependent Characteristics of Springline and Crown Thrust

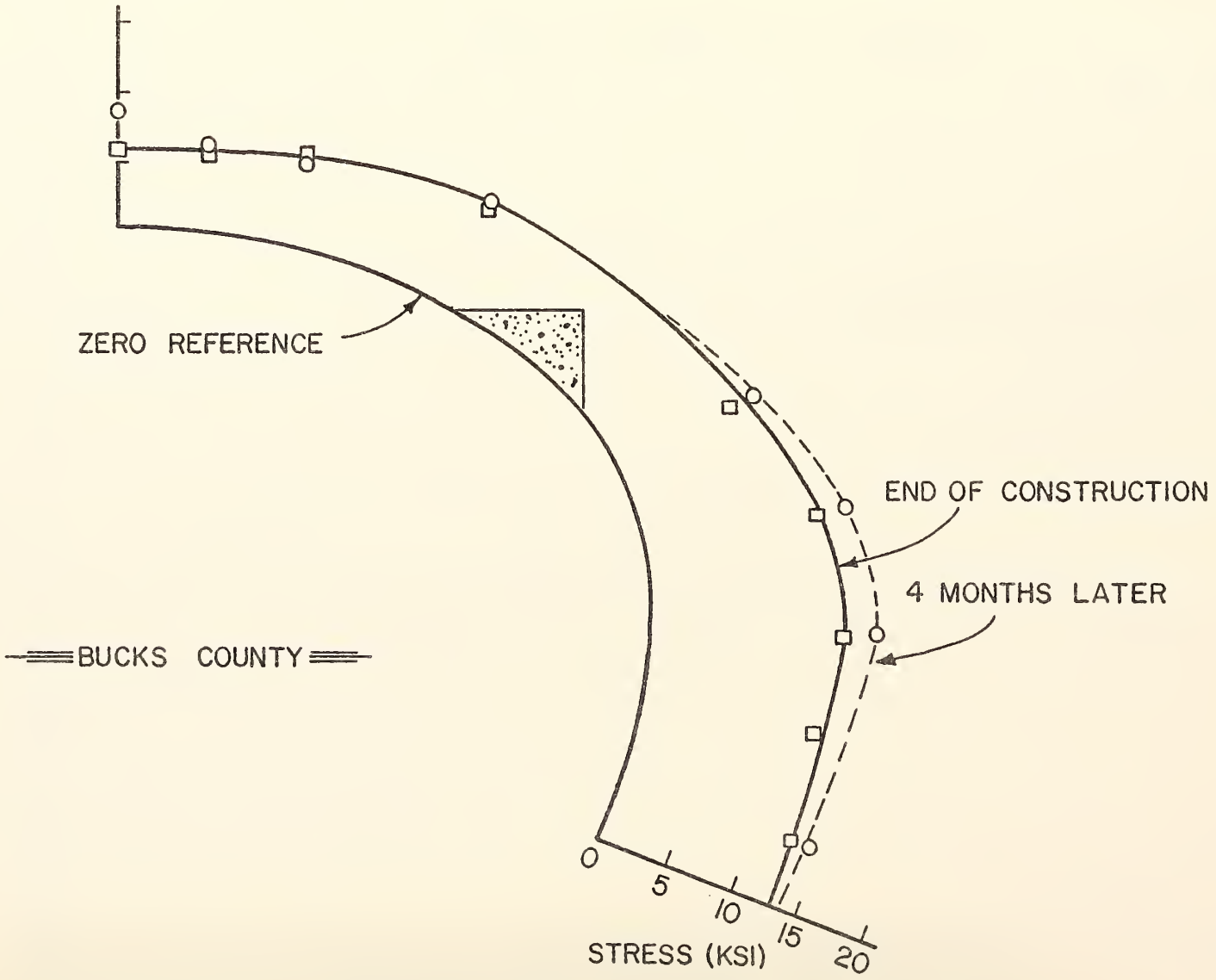

Figure 2.15 Thrust Stress Distribution in Culvert Liner Showing Time Dependent Effects

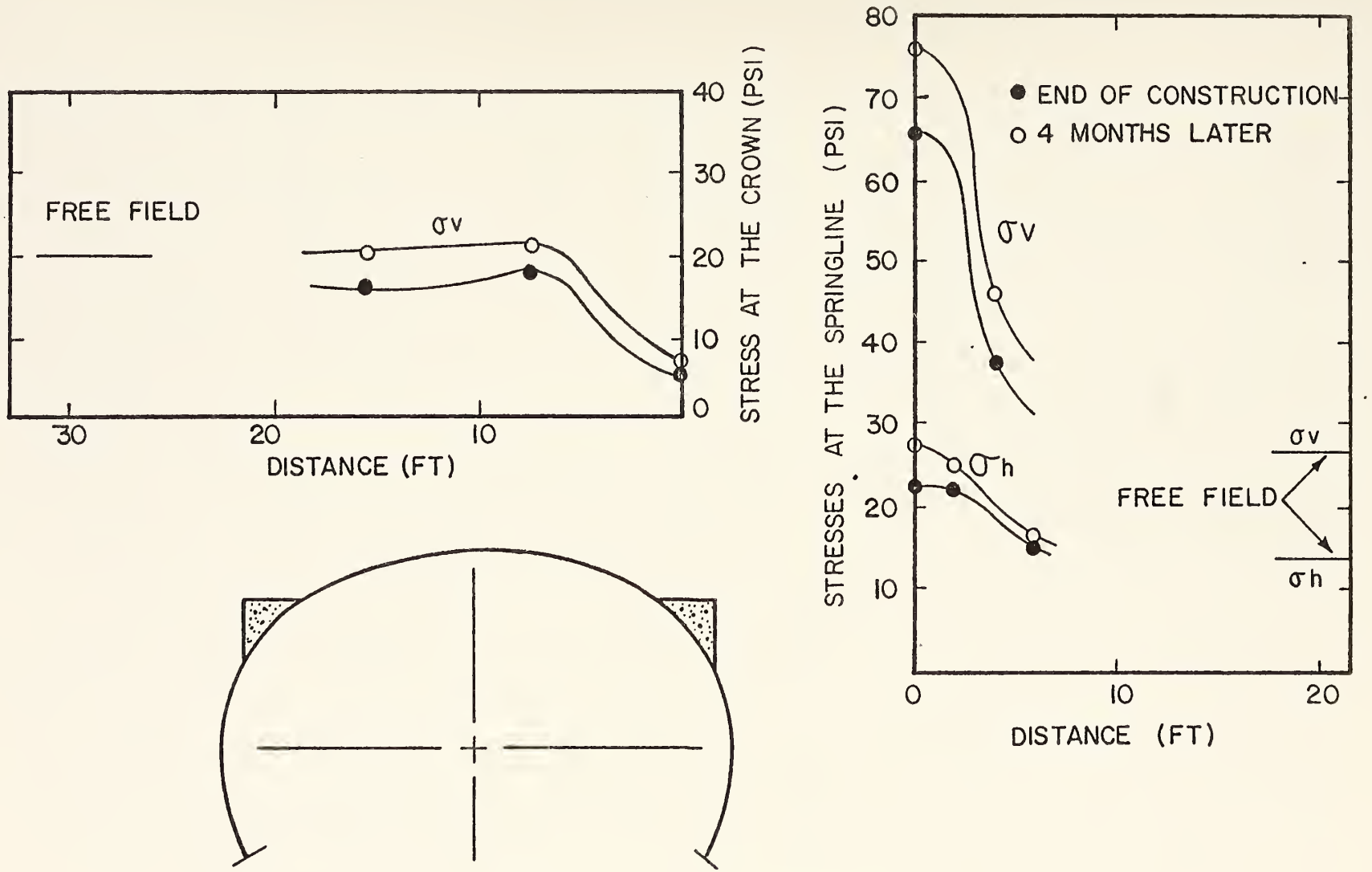

Figure 2.16 Time Dependent Characteristics of Soil Stresses near Crown and Springline (Bucks County)

CHAPTER 3

BASIC MODEL, DEFINITION AND RESULTS

3.1 STATEMENT OF PURPOSE

In this chapter a "basic model" idealization of a long-span culvert is defined along with the corresponding finite element representation. The basic model is used as a fundamental reference throughout this report to ascertain the relative influence of changing various parameters and modeling assumptions. Accordingly, an extensive set of analytical results is presented to provide a data base and an insight for structural behavior of the basic model.

3.2 BASIC MODEL DESCRIPTION

Although the selection of a basic model is somewhat arbitrary, the intent is to choose a model whose parameters are "typical" and/or "average" of long-span systems used in practice.

The long-span configuration chosen is a high profile arch with a 36 ft. (11 m) span, 11 ft. 2 in. (3.4 m) top rise, and 21 ft. 5 in. (6.5 m) total rise. Figure 3-1 illustrates the high profile arch dimensions which is constructed of 5 gage structural steel (6 x 2 inch corrugation), with standard linear elastic properties as shown. The high profile shape was selected because its configuration is somewhere between a low profile and an elliptical shape, all of which are commonly used in practice, and the dimensions are representative of an average size long span.

The high profile arch is anchored into concrete footings 3 ft. (0.92 m) wide and 2 ft. (0.62 m) deep.

At full construction height, the soil is 25 ft. (7.6 m) above the crown of the arch, and the entire soil mass (below, around, and above the arch) is assumed homogenous and linear elastic with a Young's modulus of 2000 psi (13,800 k Pa) and a Poisson's ratio of 0.35, representative of an average elastic soil stiffness. The interfaces between the soil mass, concrete footing, and steel arch

are assumed bonded. Many of the above simplifying idealizations of the basic model will be systematically removed in later studies.

The finite element discretization of the basic model is shown in Figure 3-2 for the case of symmetric loading. Because of symmetry, only half of the system is modeled with a total of 253 elements. Seventeen beam-column elements are connected to form the metal arch with the 17^{th} element buried in the concrete footing. Beam-column elements are defined by two nodes with three degrees of freedom per node, horizontal and vertical displacements, and a rotation. The concrete footing (4 elements) and soil mass (234 elements) are four-node quandrilateral or three-node triangular continuum elements with two degrees of freedom per node, horizontal and vertical displacements. These continuum elements include high order nonconforming displacement functions which have superior characteristics in all basic modes of deformation.

Restraints against all horizontal movement is prescribed for all nodes on the right boundary as well as all nodes on the vertical symmetry line including a rotation constraint for the beam-column element at the crown. All nodes along the bottom boundary are fixed against both horizontal and vertical displacements.

The right boundary is located at a distance of 50 ft. (15.2 m) from the centerline where soil-arch interaction has negligible influence on free field response. Similarly, the bottom boundary is located 25 ft. (7.6 m) below the footing to minimize boundary effects (i.e., it is assumed the arch is constructed on insitu soil whose properties are similar to backfill soil well above the elevation of bedrock).

As yet, the basic model loading conditions have not been defined. This is a difficult subject and requires some elaboration. In general, the loading of a long-span system includes three categories: (1) gravity weight of each soil layer (incremental construction), (2) temporary loads of all compaction equipment, compressing the soil layers, and (3) design live loads of vehiles

traveling over the completed structure. Because of the deep fill height (25 ft.), design live loads are not significant for the basic model configuration. Therefore, they are not included in the basic model. Rather, live loads are considered in a separate study in the next chapter for a shallow cover condition.

The incremental construction configuration adopted for the basic model is shown in Figures 3-2 and 3-3. This selection is the outcome of a preliminary study to determine the minimum number of soil layer increments to produce consistent results. The initial reference configuration, i.e., unloaded system (increment 1), includes the metal arch, concrete footing, and soil up to the springline. The reason that the unloaded system is referenced with soil raised to the springline rather than starting with soil at the footing level is because gravity loaded elements between the springline and the footing tend to "hang" from the arch in tension producing unrealistic results, (special nonlinear soil models and interface elements may be used to correct this problem as discussed later).

Above the reference configuration, seven gravity loaded construction increments (numbered 2 to 8) are used to simulate the sequential placement of soil layers. Soil weight is 120 lb/ft^3 (18.8 k N/m^3). The average soil-layer thickness for the three layers between the springline and the crown is 4 ft. (1.2 m) and 6 ft. (1.8 m) for the four layers above the crown. In usual field practice, soil-layer thickness is between 0.5 to 1.0 ft. (0.15 to 0.3 m), however, results from preliminary analytical studies indicated the coaser layer scheme provides adequate simulation of the construction process.

Loads due to compaction equipment are very difficult to define. Yet, they are extremely important in controlling the deformed shape of the arch because as the soil is compressed vertically, lateral forces are developed pushing the sides of the arch inward. The difficulty in establishing a rigorous

analytical model for compaction is due to the random nature of loading interacting with the highly nonlinear behavior soil as it is compacted from a loose to dense state. Consider, for example, the complexity in defining the location, contact area, and magnitude (including inertia effects) of all compaction equipment traversing each soil layer. Couple this problem with the problem of modeling the soil behavior as each load is applied. A proper soil model must be nonconservative (e.g., plasticity model) so that after the compaction load is removed residual lateral soil stresses will remain, holding the arch in the deformed shape.

In this study, a simplified compaction-load model is proposed which simulates the effect of compaction and is applicable to both linear and nonlinear soil models. Figure 3-4 illustrates the compaction-load technique used with the basic long-span model. To start, a uniform pressure representing all compaction loads is assumed to exist as part of the initial reference configuration and acts on the surface of the initial construction increment (except for the element surface adjacent to the arch). Next, a gravity weighted soil layer is added to the system (increment 2) along with another uniform compaction pressure applied to its surface. However, at the same time, the first compaction pressure is removed by applying an equal but opposite pressure. These pressures squeeze the soil layer and increase lateral pressure on the arch via the Poisson effect. The process is repeated for the next two soil layers. Above the crown the process is terminated by removing the last compaction pressure so that no compaction loads remain in the system.

A compaction pressure of 5 psi (34.4 k Pa) is used with basic model. The motivation for this selection was guided by results presented in the next chapter. For now, analytical results of the basic model are presented.

3.3 BASIC MODEL PERFORMANCE

To set the stage for subsequent studies, a detailed set of structural responses for the arch and surrounding soil mass is presented for the basic model. These results provide insight into the fundamental behavior of the long-span model as well as providing a reference data base.

Three structural responses are of interest in assessing the steel arch performance; displacement, thrust, and moment. As explained in the preceding chapter, displacement and thrust are the most significant responses for design consideration. Figure 3-5 shows the displacement of the crown relative to the footing as a percentage of total arch rise (positive implies peaking) and is plotted as a function of fill-height-ratio. Fill-height-ratio is defined as fill height above the springline divided by top rise of arch. Thus, if the fill-height-ratio is 1, the current soil height is level with the crown. It is observed that maximum peaking occurs when the soil height is at the crown. This behavior conforms with previous experimental observations. Thereafter, the crown reverses direction and rapidly descends back toward its initial position. At a fill-height-ratio of 1.5, the crown has moved down through its initial position and continues to flatten in proportion to increased fill soil. Again, this behavior conforms to the experimental observations, however, the basic model tends to show a higher percentage of flattening.

Also shown is the lateral springline displacement (i.e., length change of total span), normalized by total arch rise (instead of span) permitting direct comparison with crown movement. Naturally, springline movement is opposite in nature to crown movement. The response history for thrust at the springline and crown is shown in Figure 3-6 as function of fill-height-ratio.

Thrust plots normalized by dividing the calculated thrust force in the arch wall by the weight of an imaginary rectangular soil column whose vertical dimensions is final-cover-height above

crown, and whose horizontal dimension is half the span length. Thus, if the normalized thrust value at full cover is greater than 1, then this part of the arch wall is carrying load in excess of soil column weight (negative arching). The figure illustrates that thrust is significantly higher at the springline than at the crown during all stages of fill, and that the springline is experiencing negative arching. Experimental data in the previous chapter confirms this trend. In particular, both experimental and analytical plots show that the springline thrust has a slope of 1.0 when fill is above the crown.

In a similar manner, Figure 3-7 illustrates the moment histories at the crown and springline (actually a little above the springline). Plotted moments are normalized by a reference moment obtained by multiplying the soil column weight by a one-fourth of span length. This reference moment is somewhat arbitrary so that no real significance is inferred if the normalized moment ratio is larger or smaller than 1.0. It is observed that the moments at crown and springline follow trends similar to displacements. However, as will be seen in the next set of figures, moment distribution is highly variable so that the maximum moment occurring slightly above springline is significantly larger than the springline moment. These are the plotted values.

Distribution plots of displacement, thrust, and moment are shown in Figures 3-8, 3-9, and 3-10, respectively, for two fill-height-levels; crown level and final level. Displacement distributions (Figure 3-8) are the deformed shape of the steel arch plotted by adding (and magnifying) displacements to the corresponding points of the undeformed arch after subtracting vertical rigid body movement of the footing. The deformed shapes give a veiw of arch in its maximum peaking position and its maximum flattening position.

Thrust and moment distributions (Figures 3-9 and 3-10) are formed by referencing the undeformed arch as a zero axis and plotting the thrust (or moment) magnitude in the normal direction according

to the sign conventions noted. The striking observation is that for a given fill height thrust varies gradually and is always in compression, whereas moment is highly erratic with five sign changes. These trends also correspond to experimental observations.

To complete the basic model data base, displacements and stresses in the soil mass are shown in the remaining figures of this chapter. First, contour distribution plots of horizontal soil movement is shown in Figures 3-11 and 3-12 for fill soil crown level and at final height, respectively. The next two figures (Figures 3-13 and 3-14) illustrate the vertical soil movement in the same format. Note, vertical displacement contours show the rigid body movement of the footing with respect to the crown.

Figures 3-15 through 3-20 (six figures) depict the complete two-dimensional state of stress in the soil mass for horizontal, vertical, and shear stress. Stress data is displayed by contours for soil fill at the crown and final height. In all cases, it is observed that high stress concentrations occur in the vicinity of the springline and below the footing.

In Figure 3-18, it is interesting to note that the vertical soil stress in the vicinity of the crown is approximately 2/3 of free field pressure (20.8 psi). However, in a localized region 4 ft. (1.2 m) above the springline, the vertical soil stress exceeds free field stress (26.8 psi) by a factor of 5/3. This demonstrates the shortcoming of defining soil arching by only considering the vertical crown pressure. Arching should be defined directly by the thrust carried in the culvert wall as compared to the column weight of soil as previously described.

The last set of data, Figures 3-21 through 3-24, show maximum and minimum principal stress distributions by directed arrows. The length of the arrow shaft is proportional to the stress magnitude. The size of the arrowhead is constant and points in the direction of positive principal stress. Principal stress designations apply to absolute maximum and minimums so that in a free

field situation maximum stress corresponds to vertical stress and minimum corresponds to horizontal stress. Examination of these figures reveals how the presence of the arch culvert disrupts the free field stress paths in the vicinity of the structure.

3.4 Figures 3-1 through 3-24

		Page
Fig. 3-1	Description of basic model idealization.	55
Fig. 3-2	FEM representation of basic model.	56
Fig. 3-3	Construction increment locations.	57
Fig. 3-4	Simplified compaction-load model.	58
Fig. 3-5	Horizontal and vertical deflections.	59
Fig. 3-6	Springline and crown thrust.	59
Fig. 3-7	Springline and crown moment.	59
Fig. 3-8	Deformed shape of arch (magnified 50 times)	60
Fig. 3-9	Thrust distribution in arch.	61
Fig. 3-10	Moment distribution in arch.	62
Fig. 3-11	Horizontal displacements, fill at crown.	63
Fig. 3-12	Horizontal displacements, full fill.	64
Fig. 3-13	Vertical displacement, fill at crown.	65
Fig. 3-14	Vertical displacements, full fill.	66
Fig. 3-15	Horizontal stress, fill at crown.	67
Fig. 3-16	Horizontal stress, full fill.	68
Fig. 3-17	Vertical stress, fill at crown.	69
Fig. 3-18	Vertical stress, full fill.	70
Fig. 3-19	Shear stress, fill at crown.	71
Fig. 3-20	Shear stress, full fill.	72
Fig. 3-21	Minimum stress, fill at crown.	73
Fig. 3-22	Minimum stress, full fill.	74
Fig. 3-23	Maximum stress, fill at crown.	75
Fig. 3-24	Maximum stress, full fill.	76

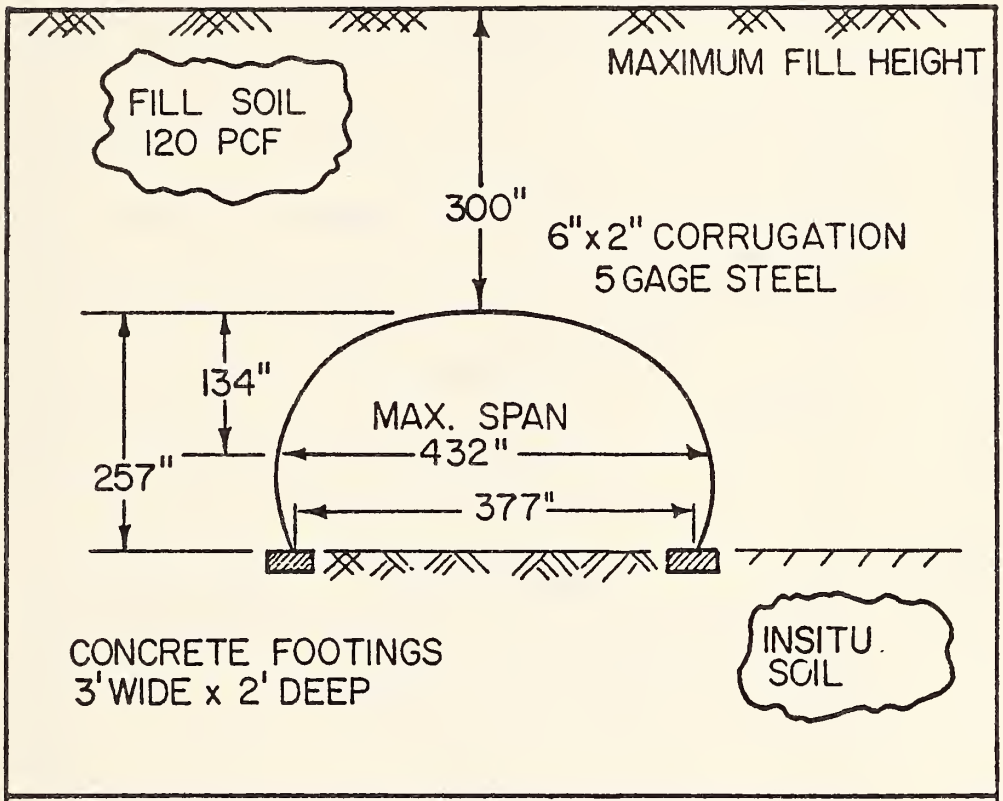

MATERIAL TYPE	YOUNG'S MODULUS psi	POISSON'S RATIO
METAL LINER	3×10^7	0.30
FILL & INSITU SOIL	2×10^3	0.35
CONCRETE FOOTING	3×10^6	0.20

Figure 3.1 Description of basic model idealization

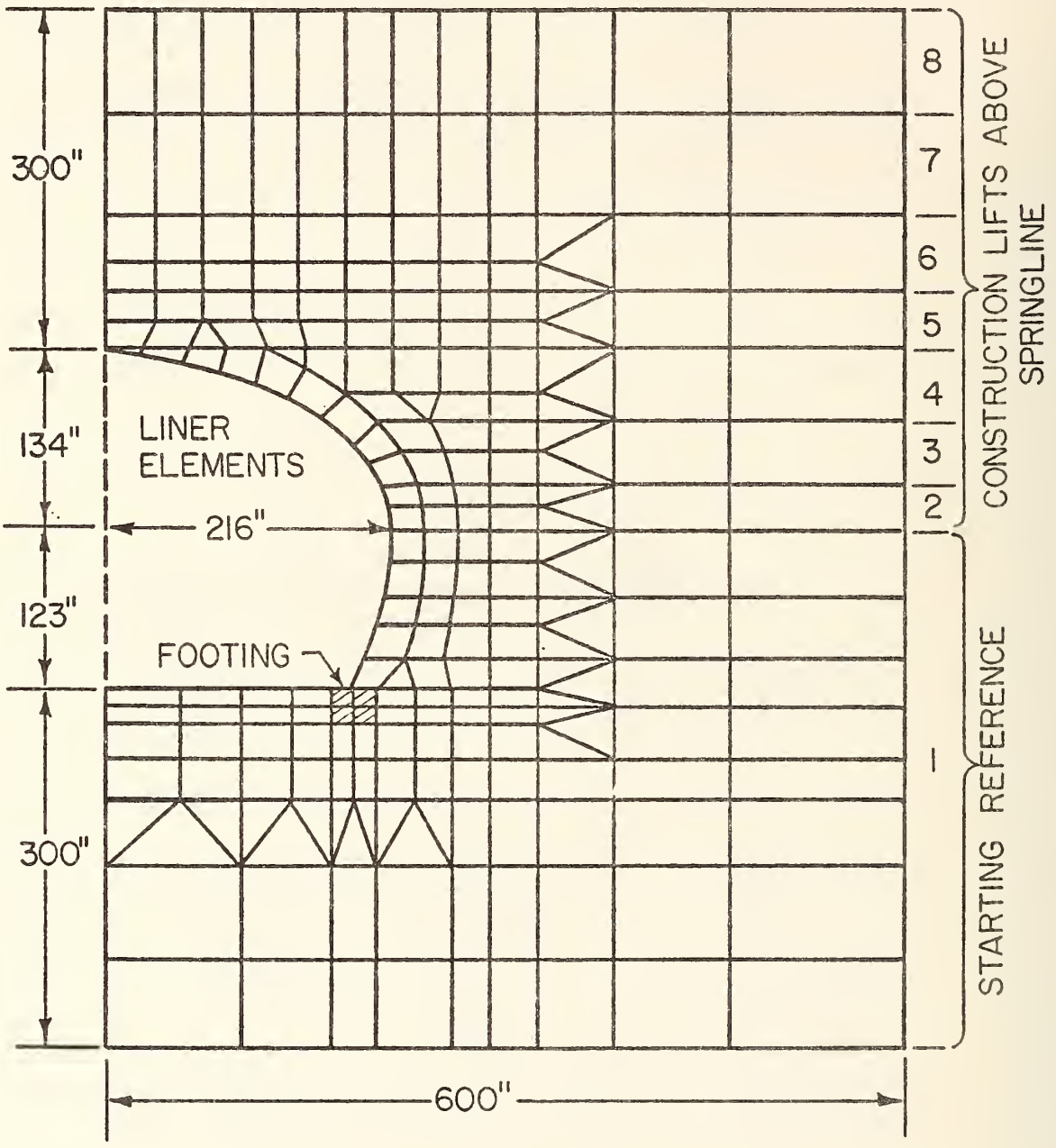

Figure 3.2 FEM Representation of Basic Model

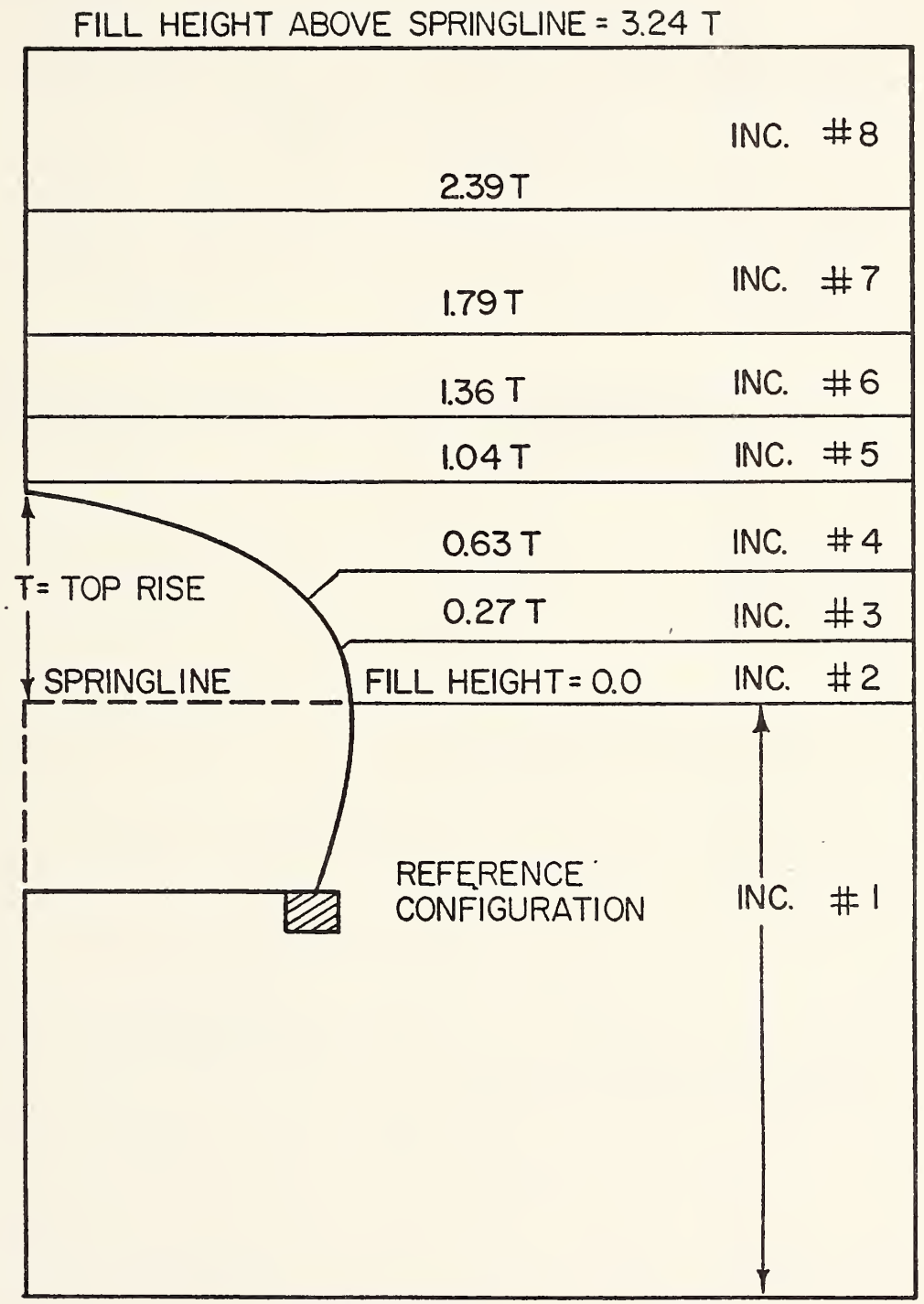

Figure 3.3 Construction Increment Locations

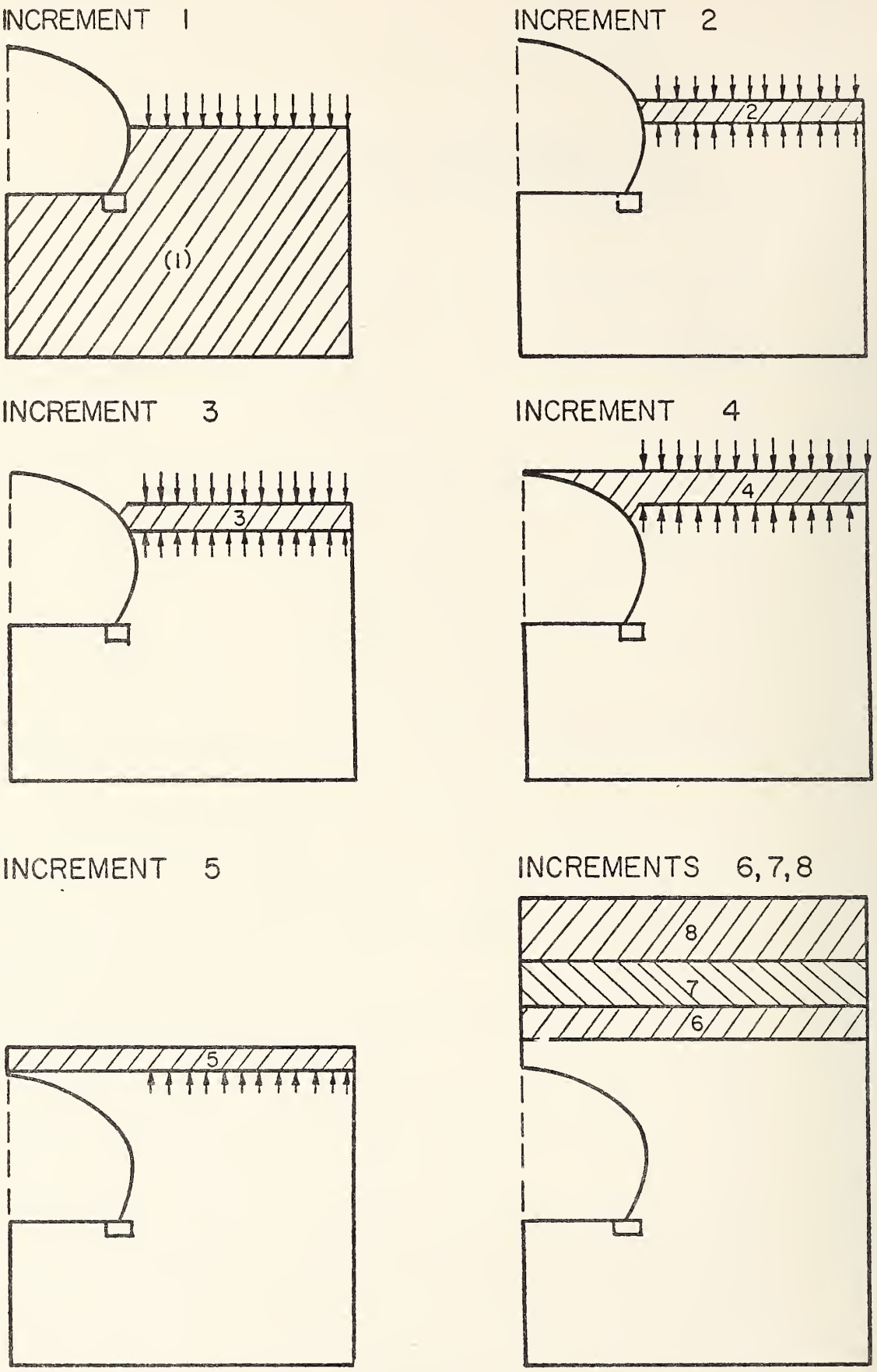

Figure 3.4 Simplified Compaction-Load Model

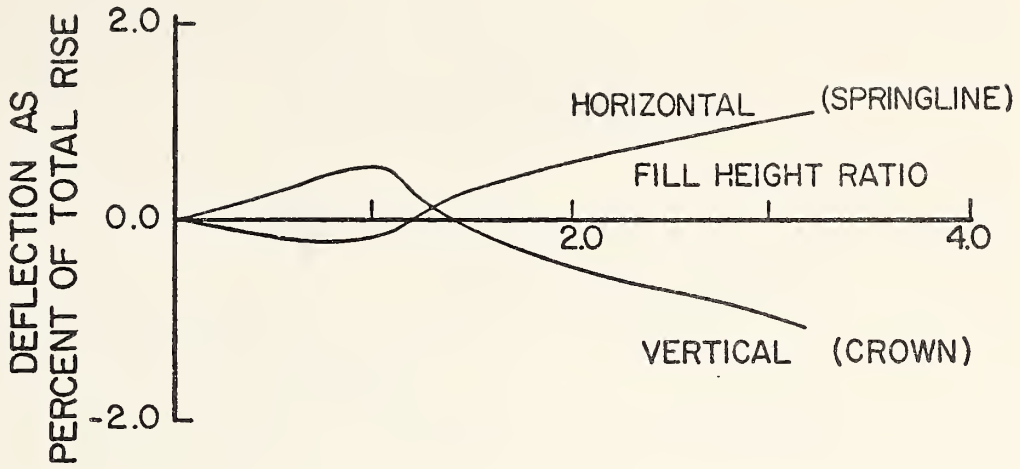

Figure 3.5 Horizontal and Vertical Deflections

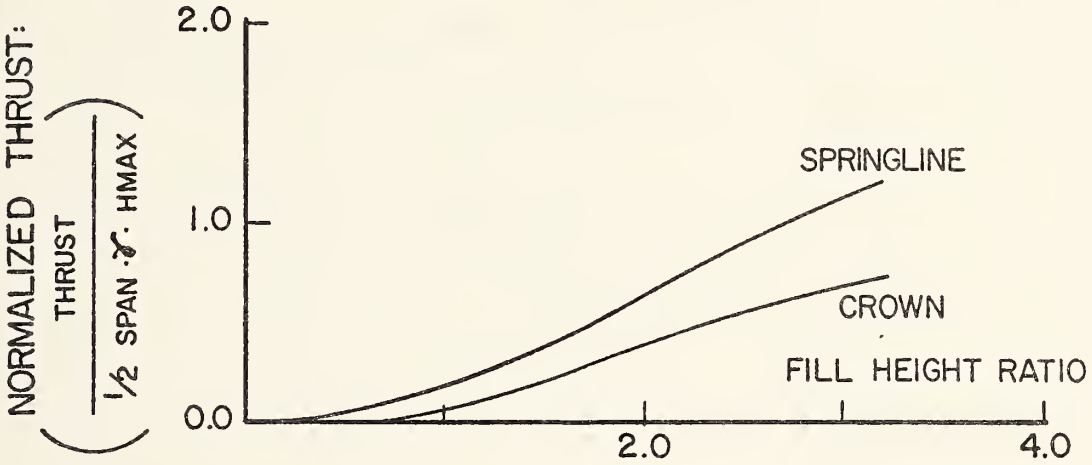

Figure 3.6 Springline and Crown Thrust

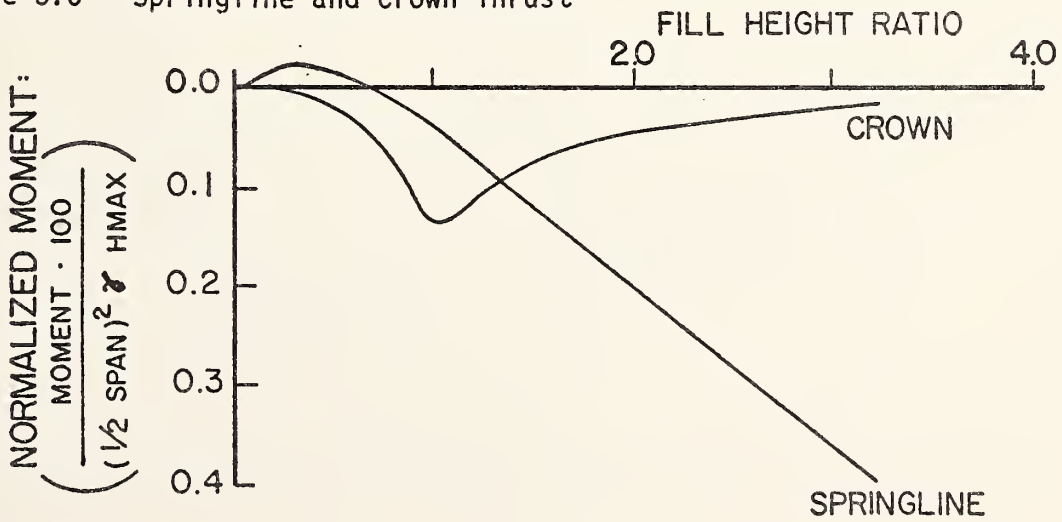

Figure 3.7 Springline and Crown Moment

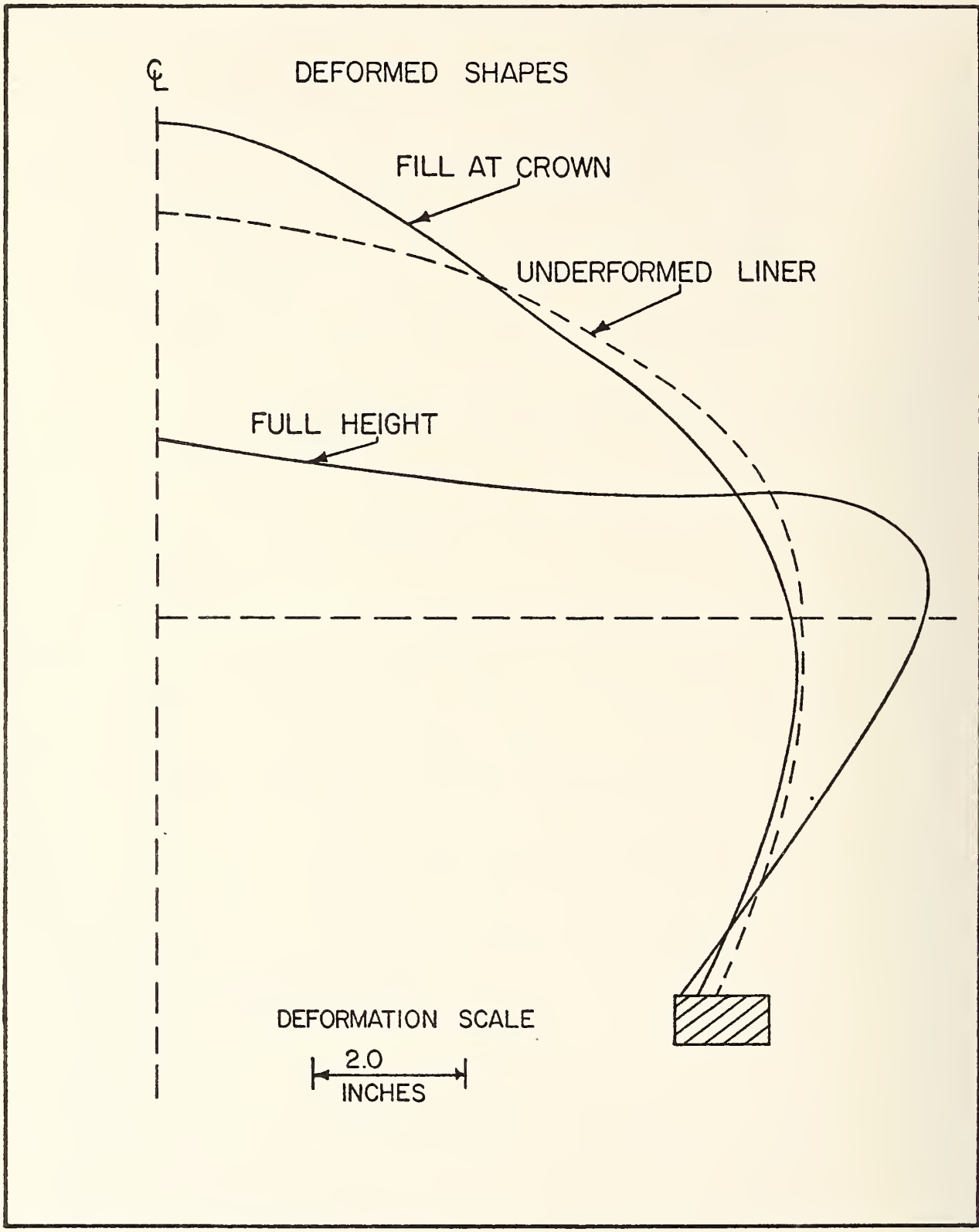

Figure 3.8 Deformed Shape of Arch (magnified 50 times)

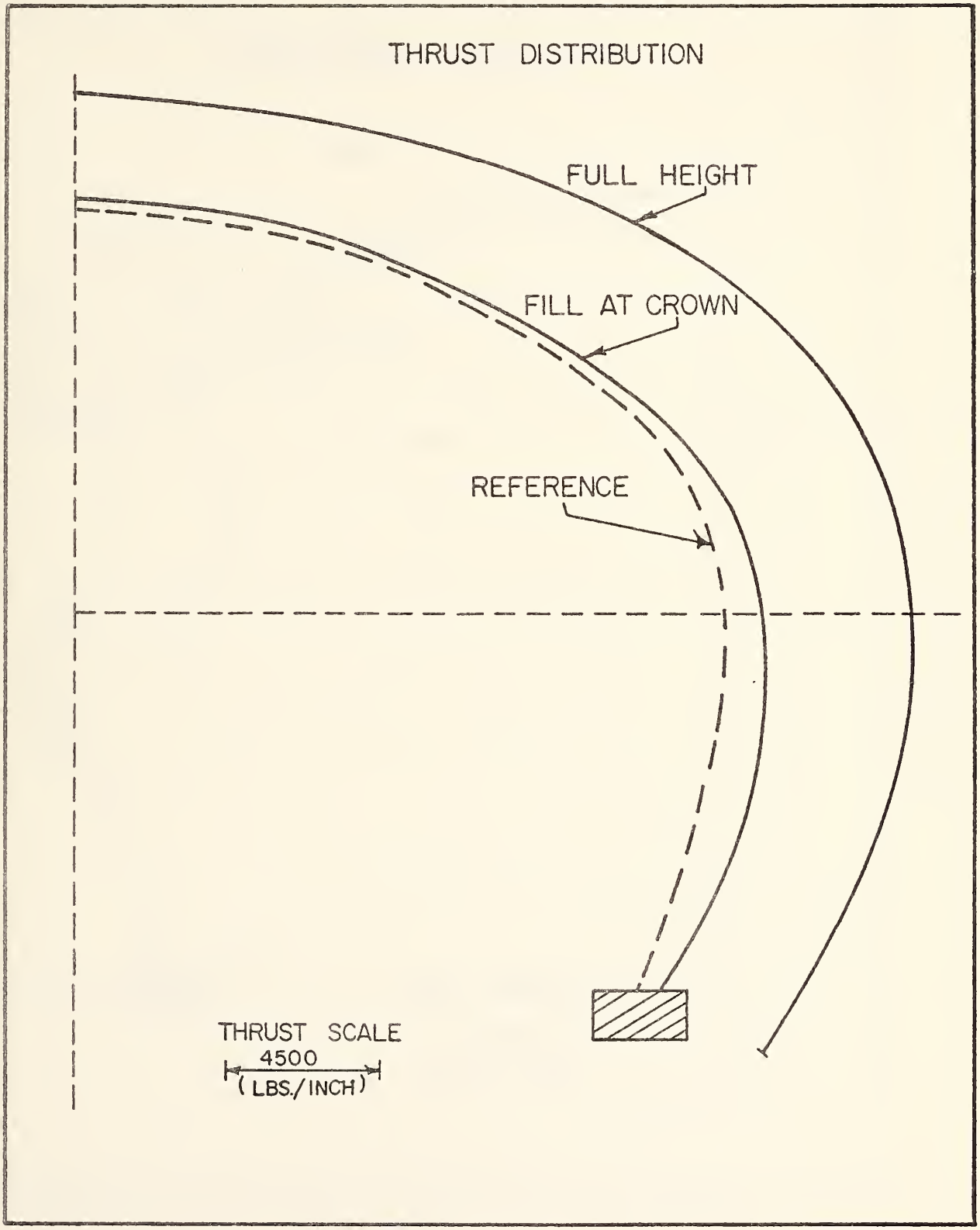

Figure 3.9 Thrust Distribution in Arch

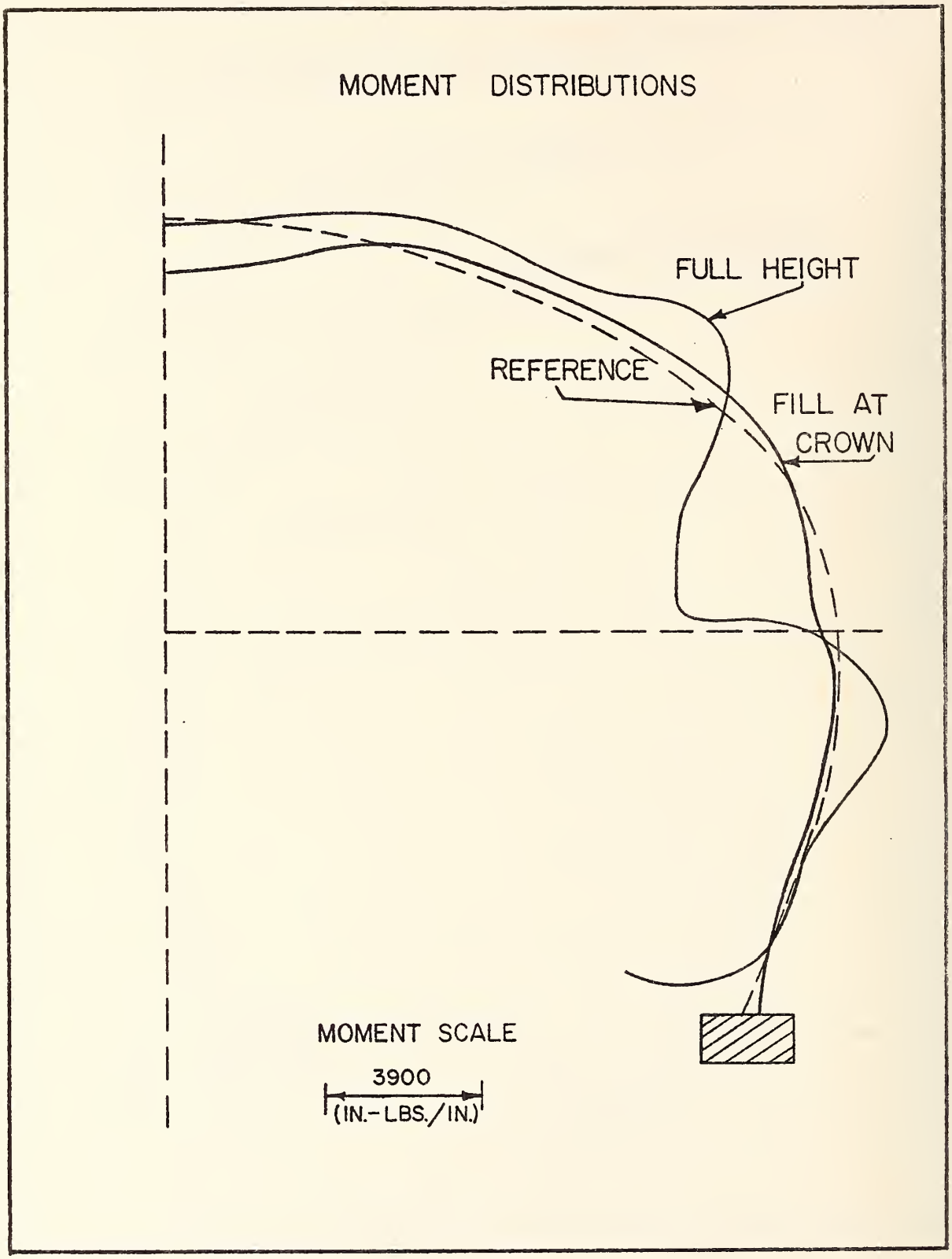

Figure 3.10 Moment Distribution in Arch

HORIZONTAL DISPLACEMENTS

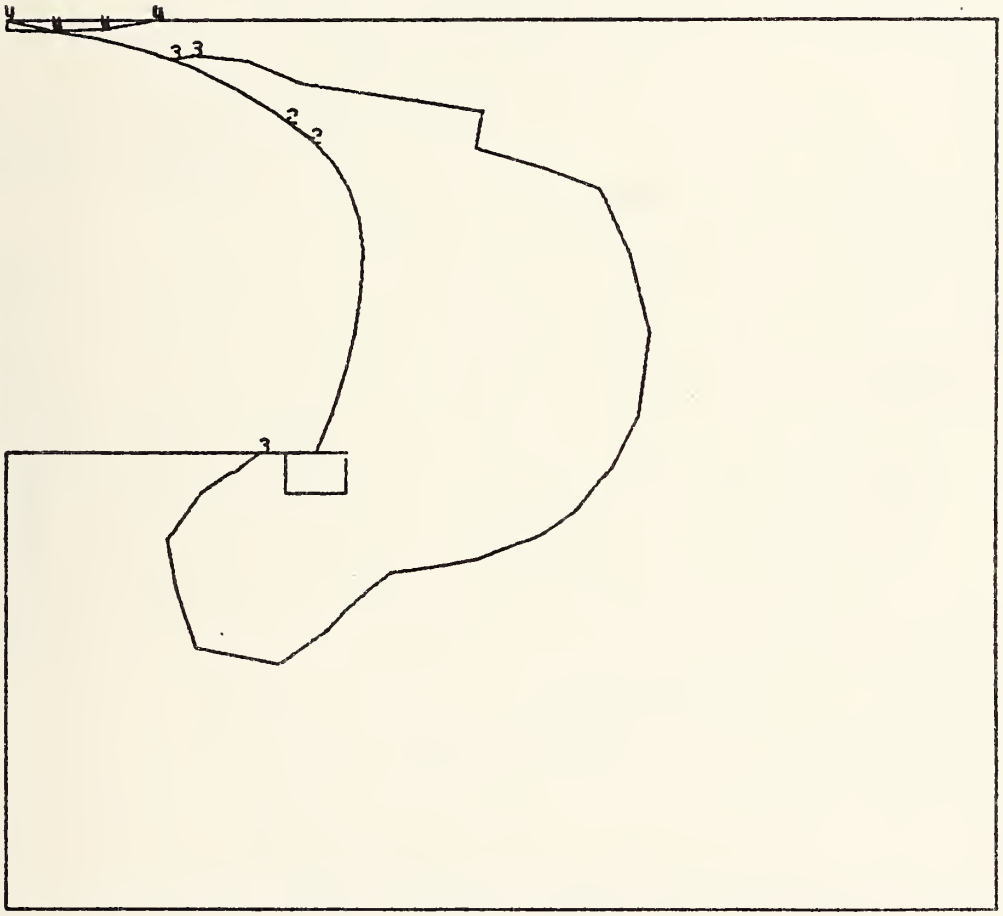

Contour Number	Displacement (inches)
1.	-0.60000
2.	-0.40000
3.	-0.20000
4.	0.00000
5.	0.20000
6.	0.40000
7.	0.60000
8.	0.80000
9.	1.00000
10.	1.20000
11.	1.40000
12	1.60000
13.	1.80000

Figure 3.11 Horizontal Displacements, Fill at Crown

HORIZONTAL DISPLACEMENTS

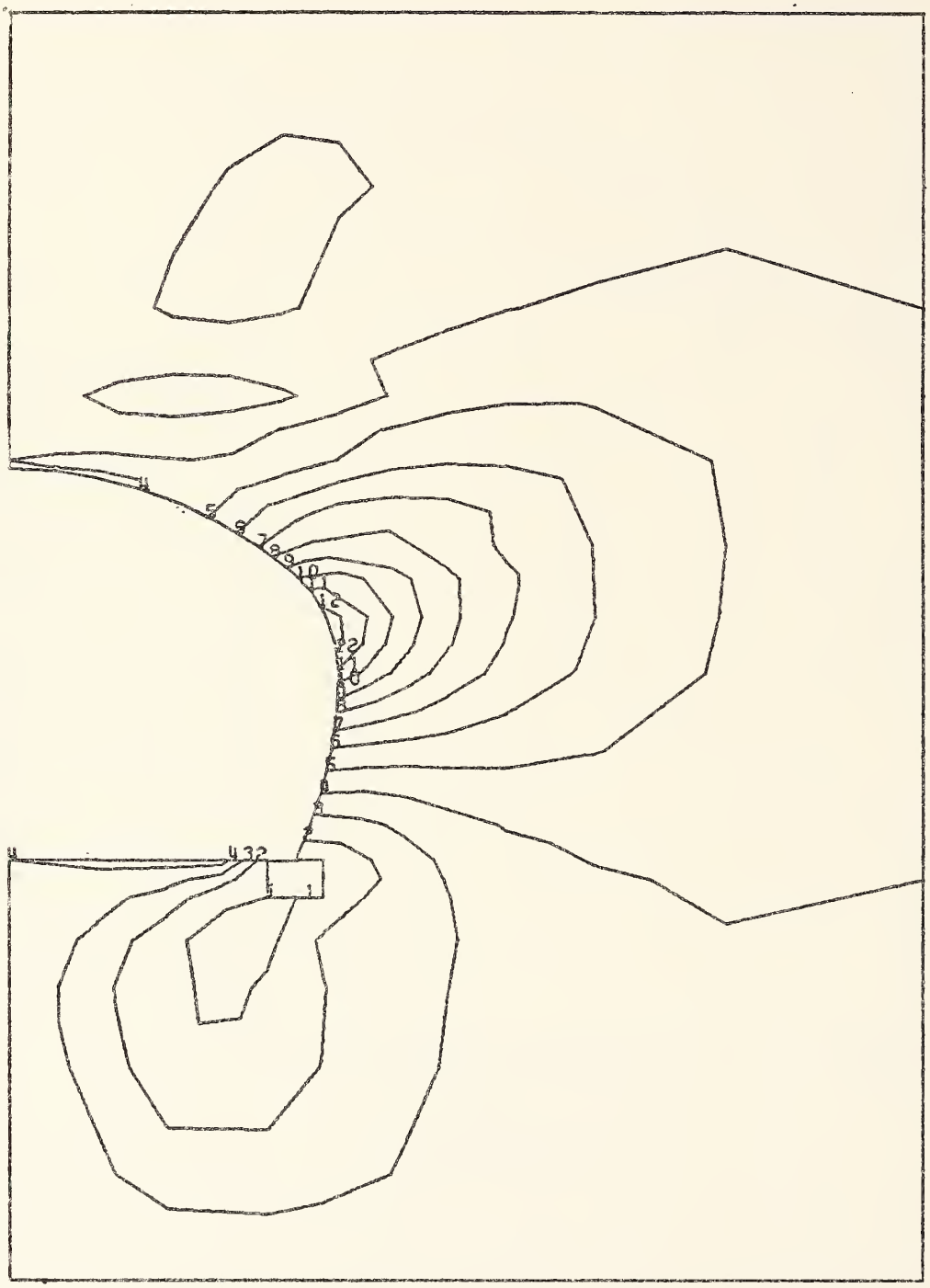

CONTOUR NUMBER	DISPLACEMENT (inches)
1.	-0.60000
2.	-0.40000
3.	-0.20000
4.	0.00000
5.	0.20000
6.	0.40000
7.	0.60000
8.	0.80000
9.	1.00000
10.	1.20000
11.	1.40000
12.	1.60000
13.	1.80000

Figure 3.12 Horizontal Displacements, Full Fill

VERTICAL DISPLACEMENTS

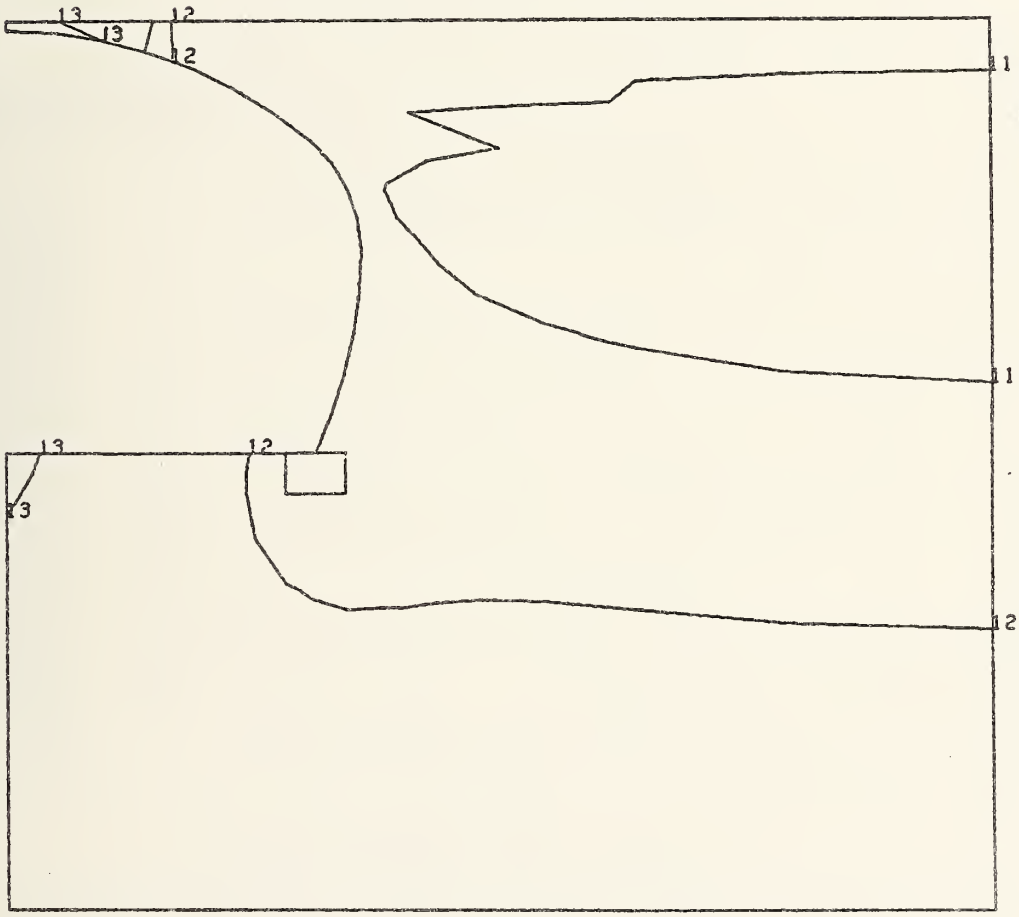

CONTOUR NUMBER	DISPLACEMENT (inches)
1.	-5.99999
2.	-5.49999
3.	-4.99999
4.	-4.49999
5.	-3.99999
6.	-3.49999
7.	-3.00000
8.	-2.50000
9.	-2.00000
10.	-1.50000
11.	-1.00000
12.	-0.50000
13.	0.00000
14.	0.50000
15.	1.00000

Figure 3.13 Vertical Displacement, Fill at Crown

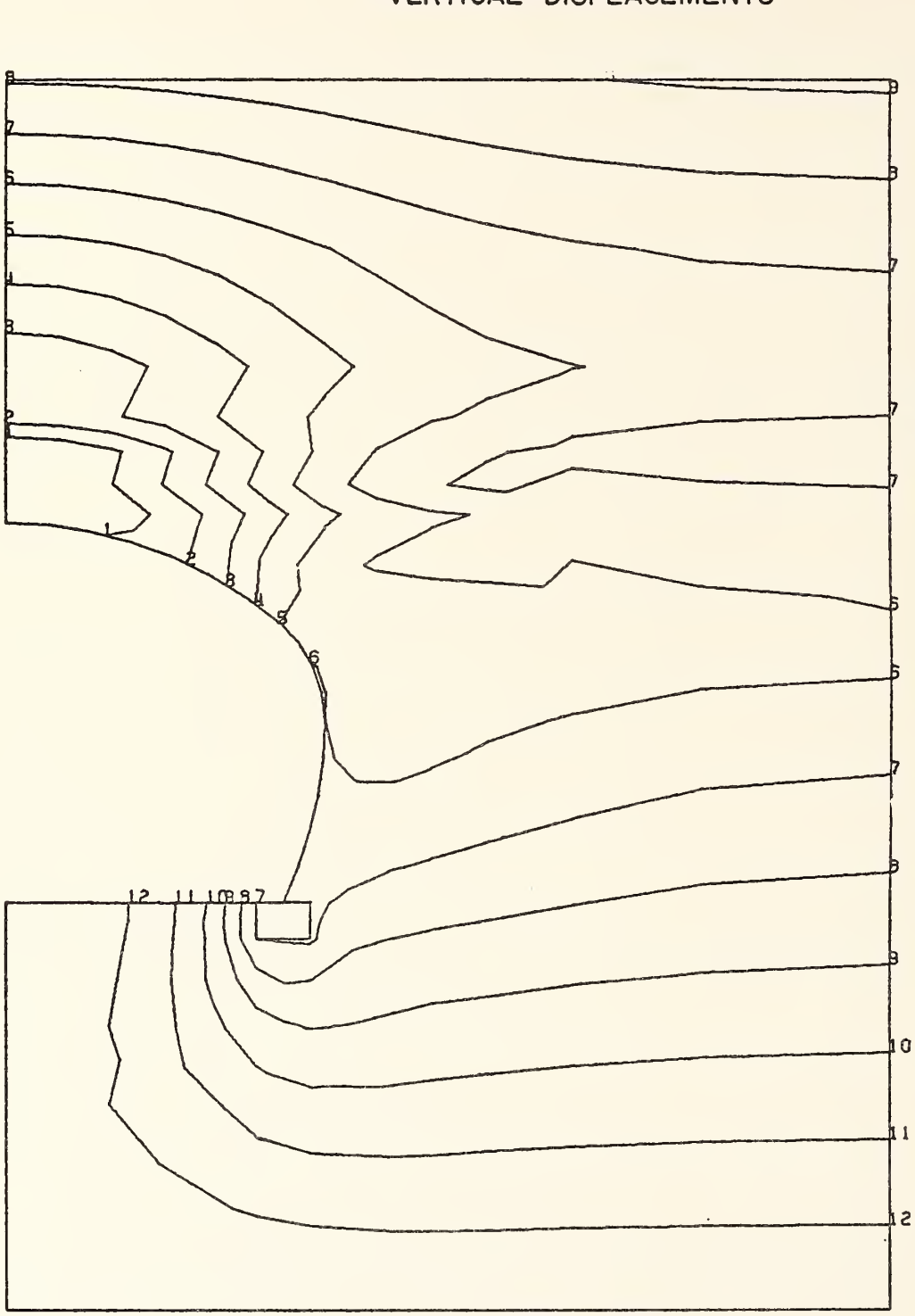

Figure 3.14 Vertical Displacements, Full Fill

HORIZONTAL STRESS

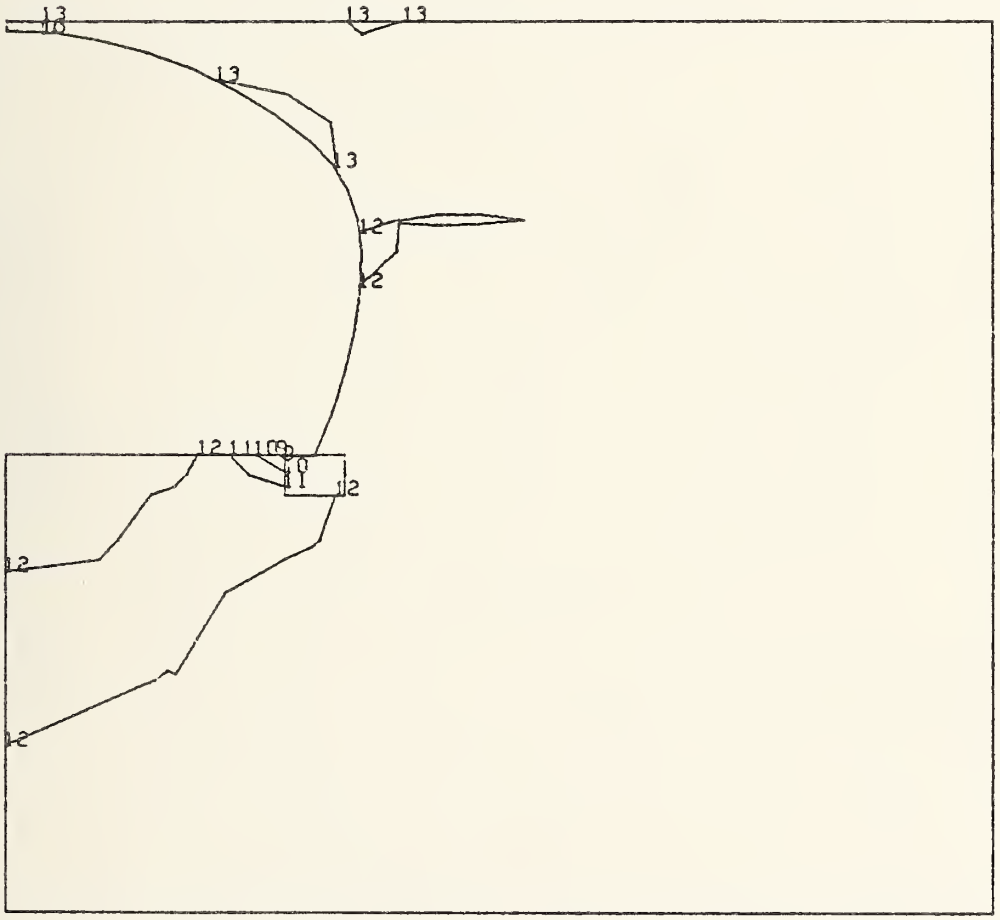

CONTOUR NUMBER	STRESS (psi)
1.	-60.00000
2.	-55.00000
3.	-50.00000
4.	-45.00000
5.	-40.00000
6.	-35.00000
7.	-30.00000
8.	-25.00000
9.	-20.00000
10.	-15.00000
11.	-10.00000
12.	-5.00000
13.	0.00000
14.	5.00000
15.	10.00000
16.	15.00000

Figure 3.15 Horizontal Stress, Fill at Crown

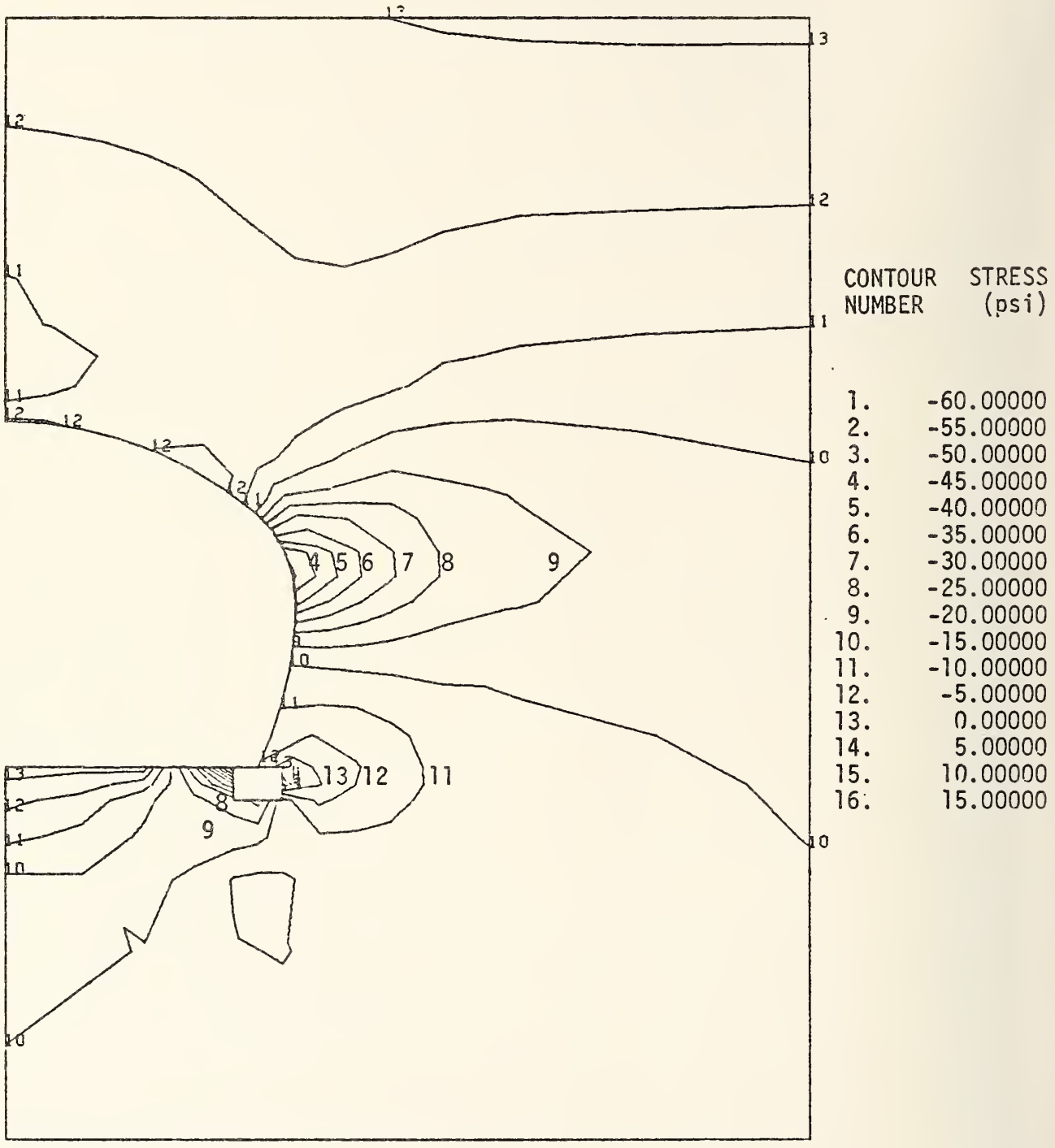

Figure 3.16 Horizontal Stress, Full Fill

VERTICAL STRESS

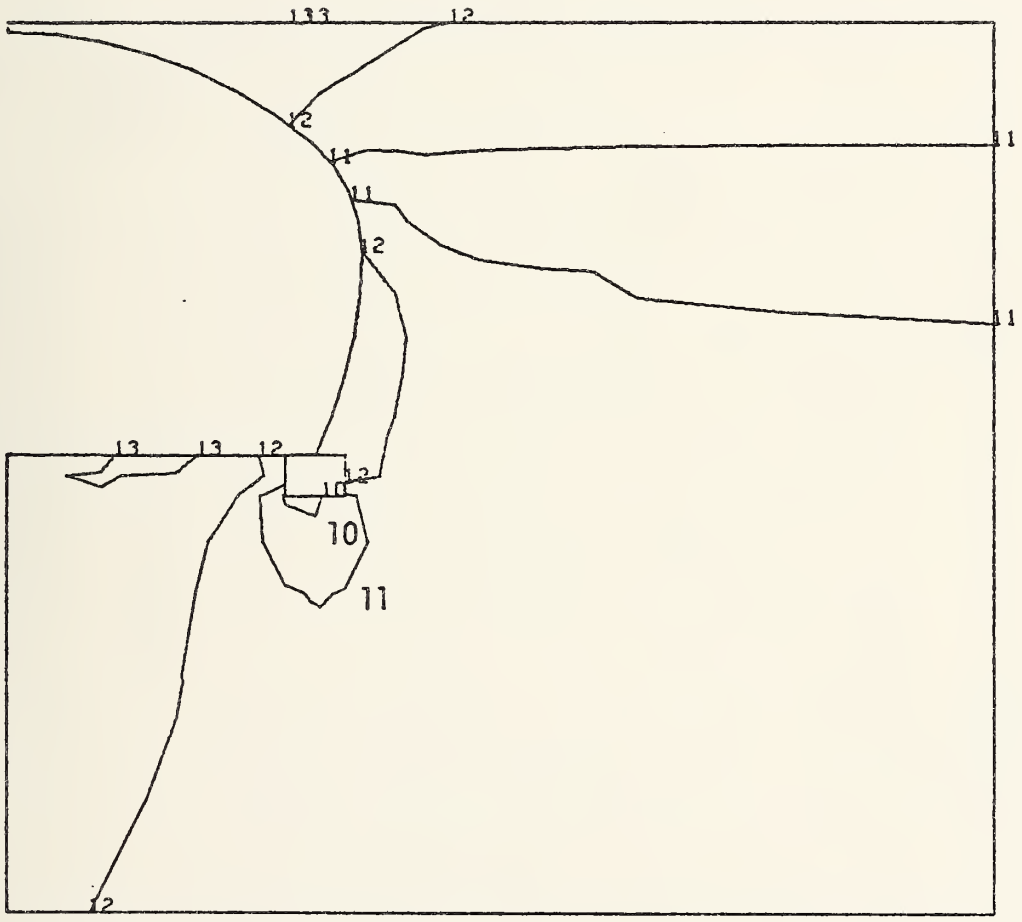

CONTOUR NUMBER	STRESS (psi)
1.	-60.00000
2.	-55.00000
3.	-50.00000
4.	-45.00000
5.	-40.00000
6.	-35.00000
7.	-30.00000
8.	-25.00000
9.	-20.00000
10.	-15.00000
11.	-10.00000
12.	-5.00000
13.	0.00000
14.	5.00000

Figure 3.17 Vertical Stress, Fill at Crown

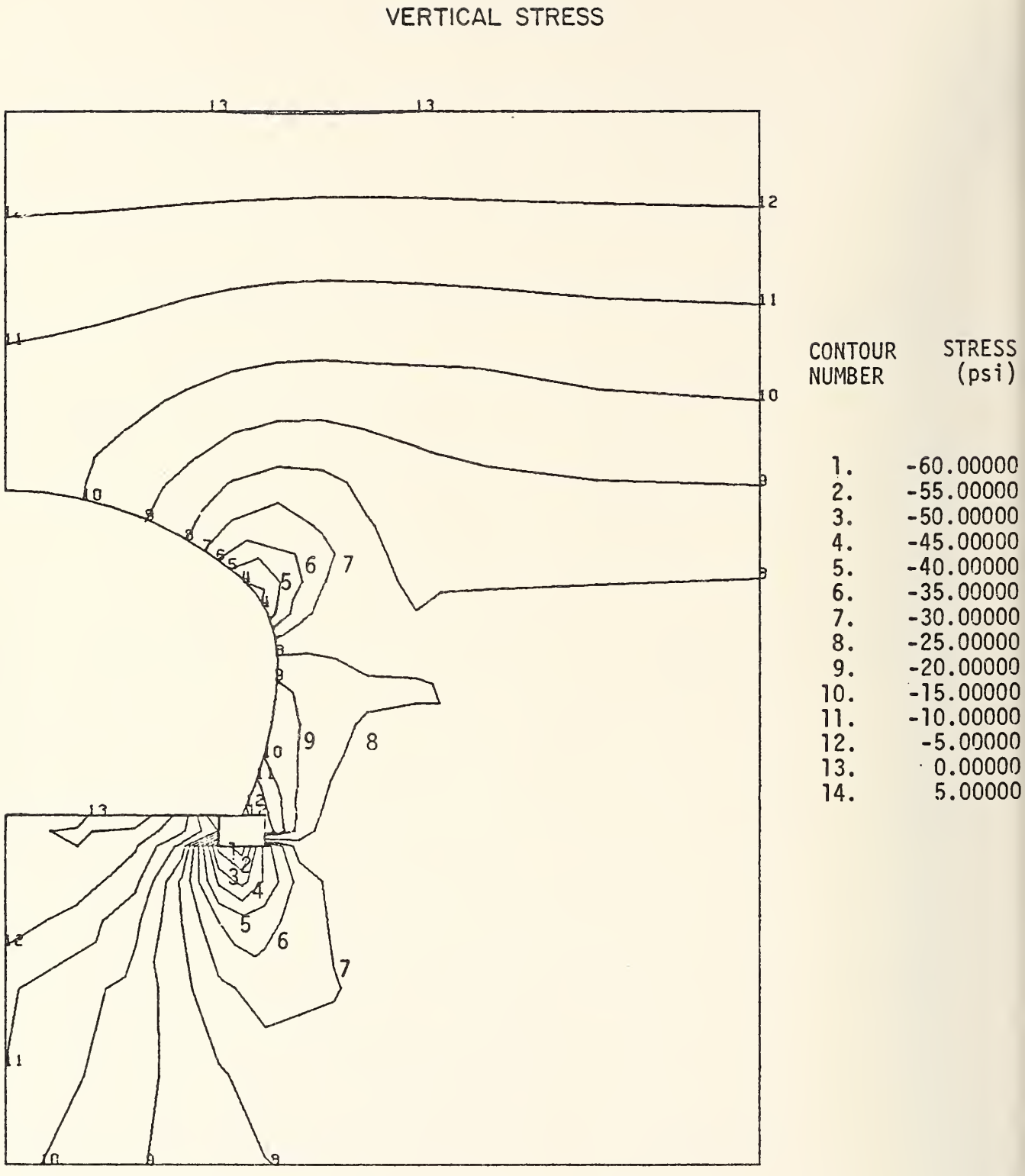

Figure 3.18 Vertical Stress, Full Fill

SHEAR STRESS

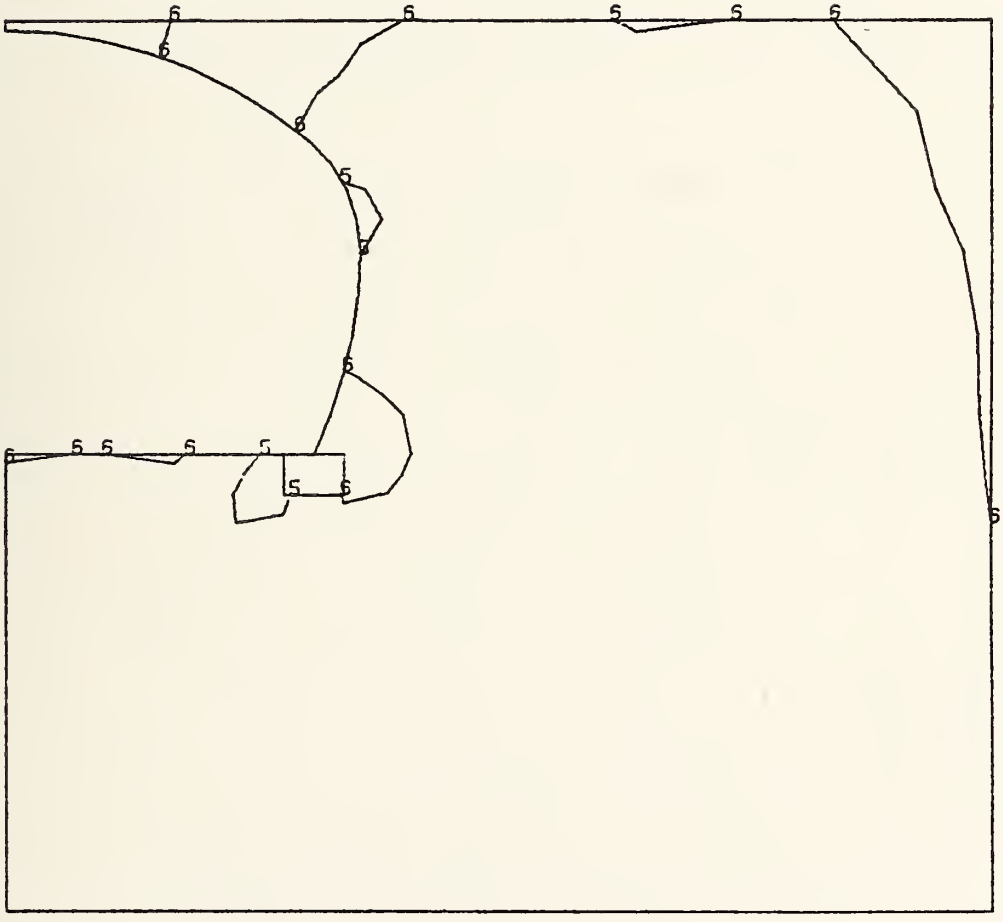

CONTOUR NUMBER	STRESS (psi)
1.	-25.00000
2.	-20.00000
3.	-15.00000
4.	-10.00000
5.	-5.00000
6.	0.00000
7.	5.00000
8.	10.00000
9.	15.00000
10.	20.00000

Figure 3.19 Shear Stress, Fill at Crown

SHEAR STRESS

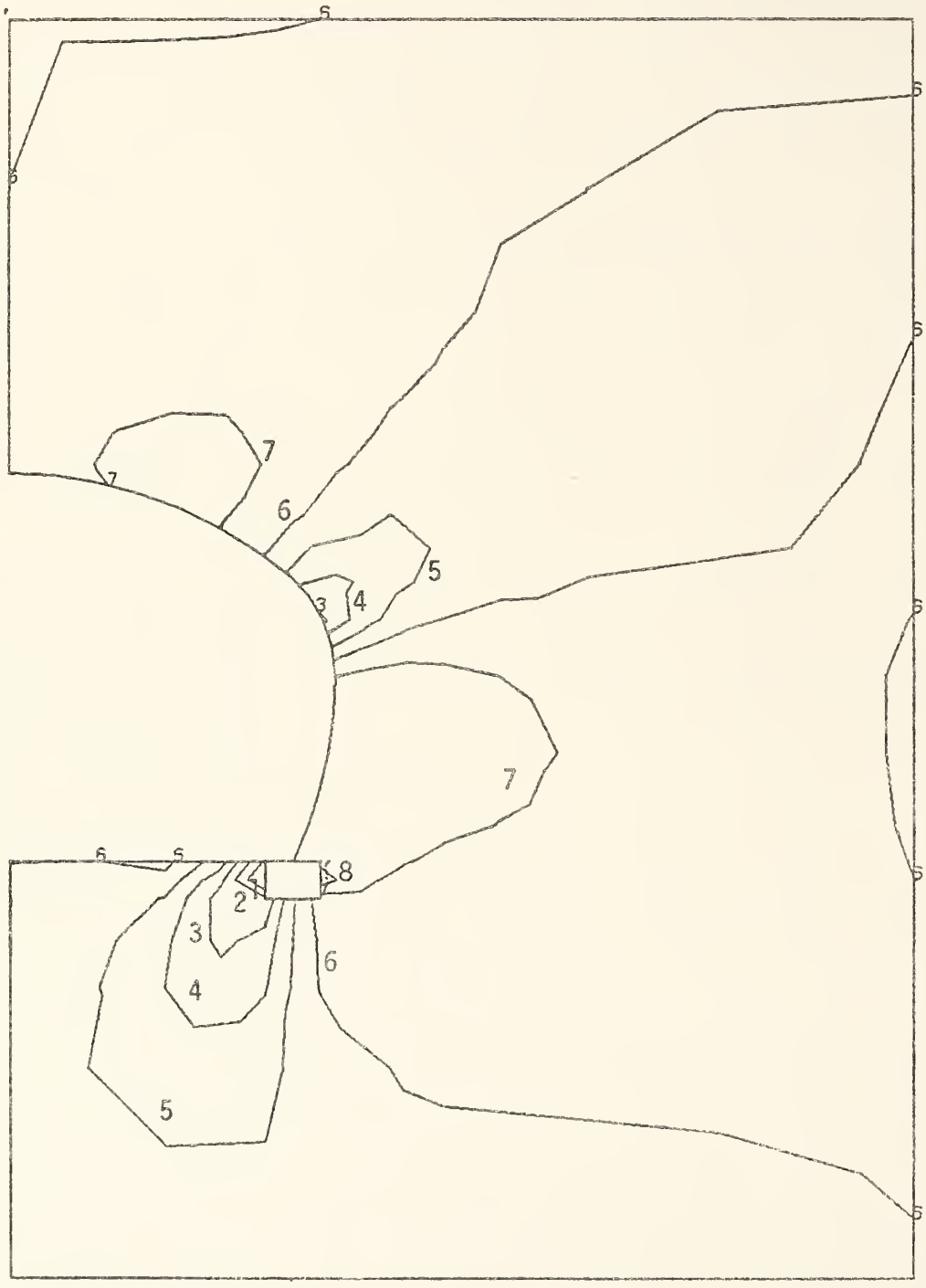

CONTOUR NUMBER	STRESS (psi)
1.	-25.00000
2.	-20.00000
3.	-15.00000
4.	-10.00000
5.	-5.00000
6.	0.00000
7.	5.00000
8.	10.00000
9.	15.00000
10.	20.00000

Figure 3.20 Shear Stress, Full Fill

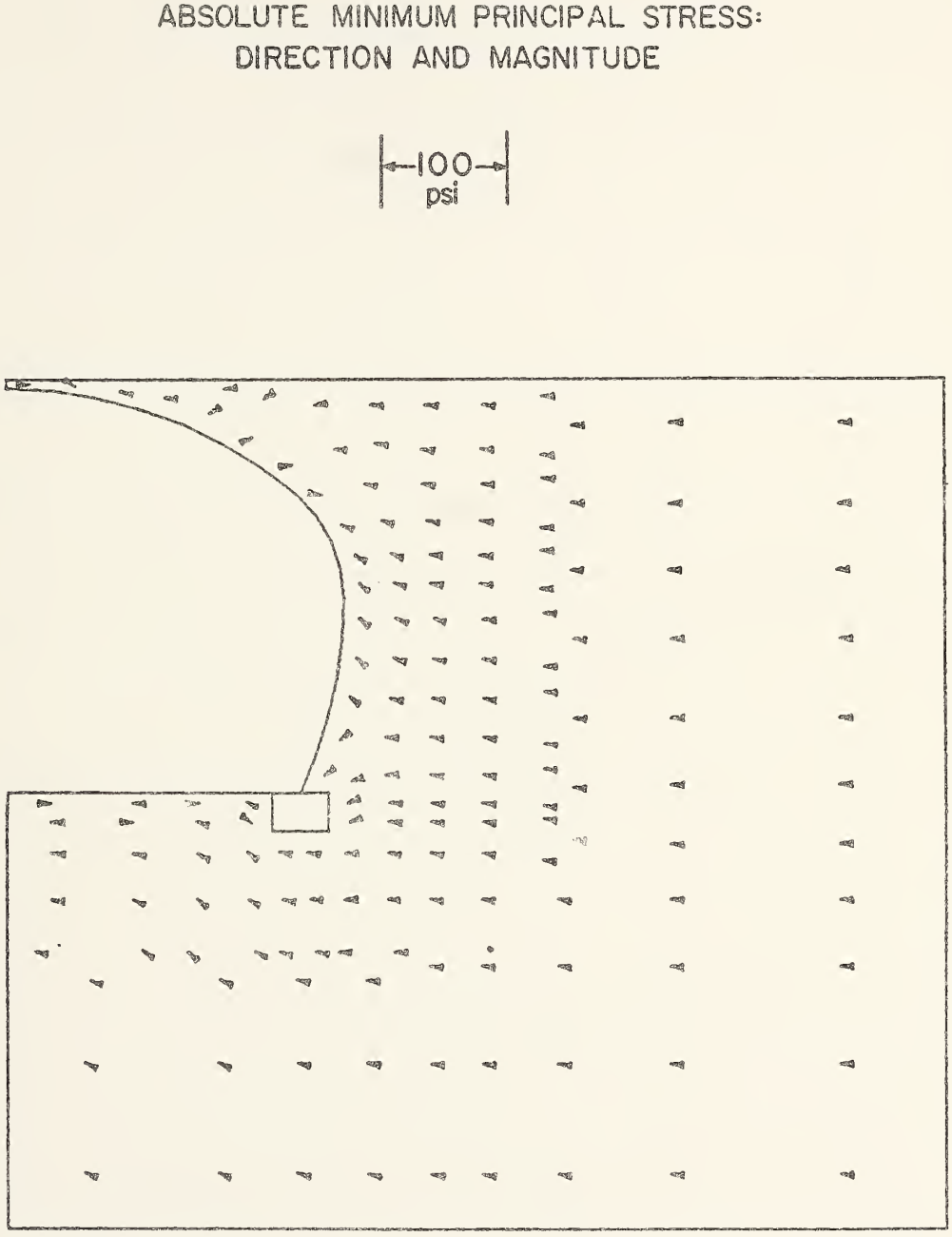

Figure 3.21 Minimum Stress, Fill at Crown

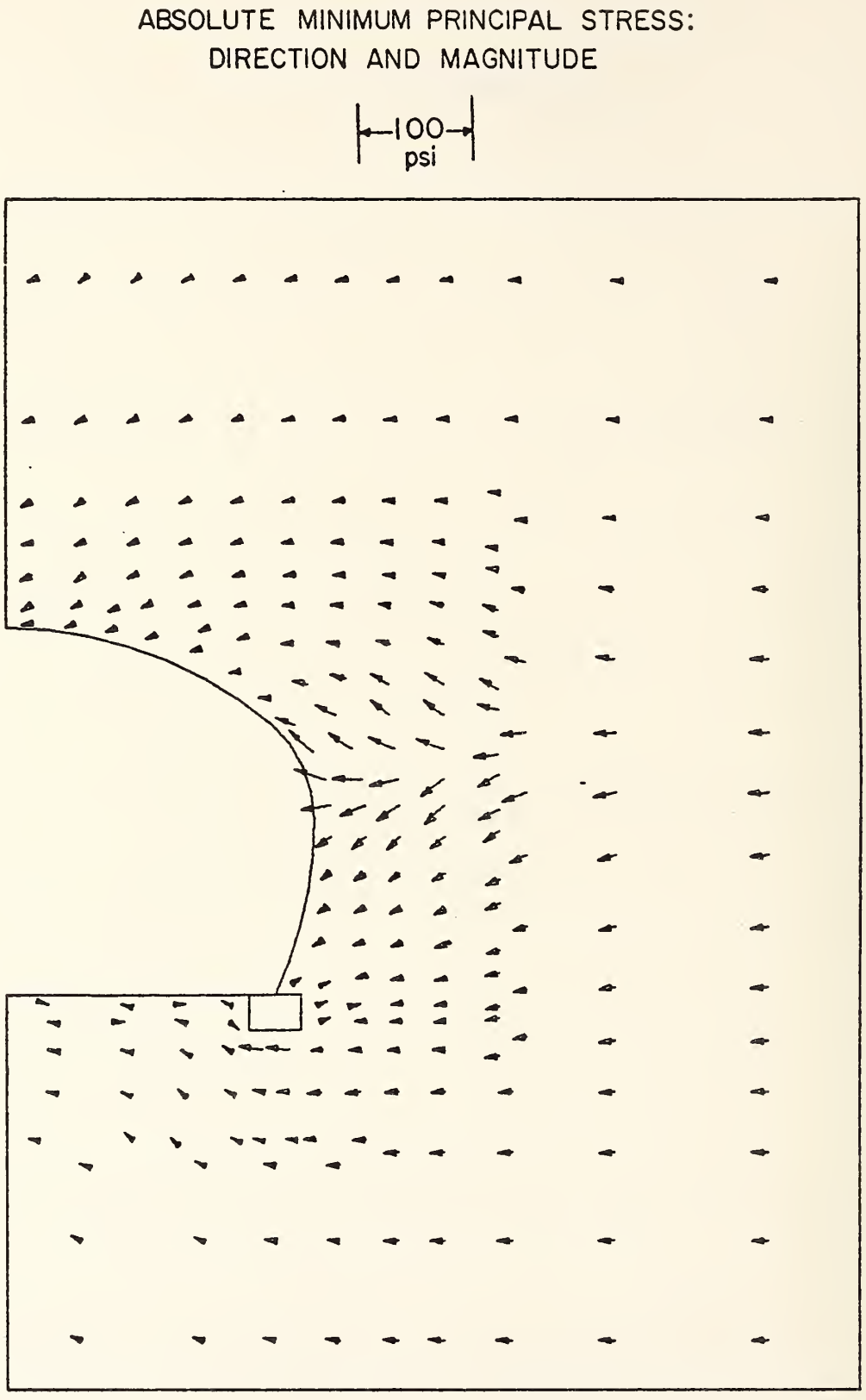

Figure 3.22 Minimum Stress, Full Fill

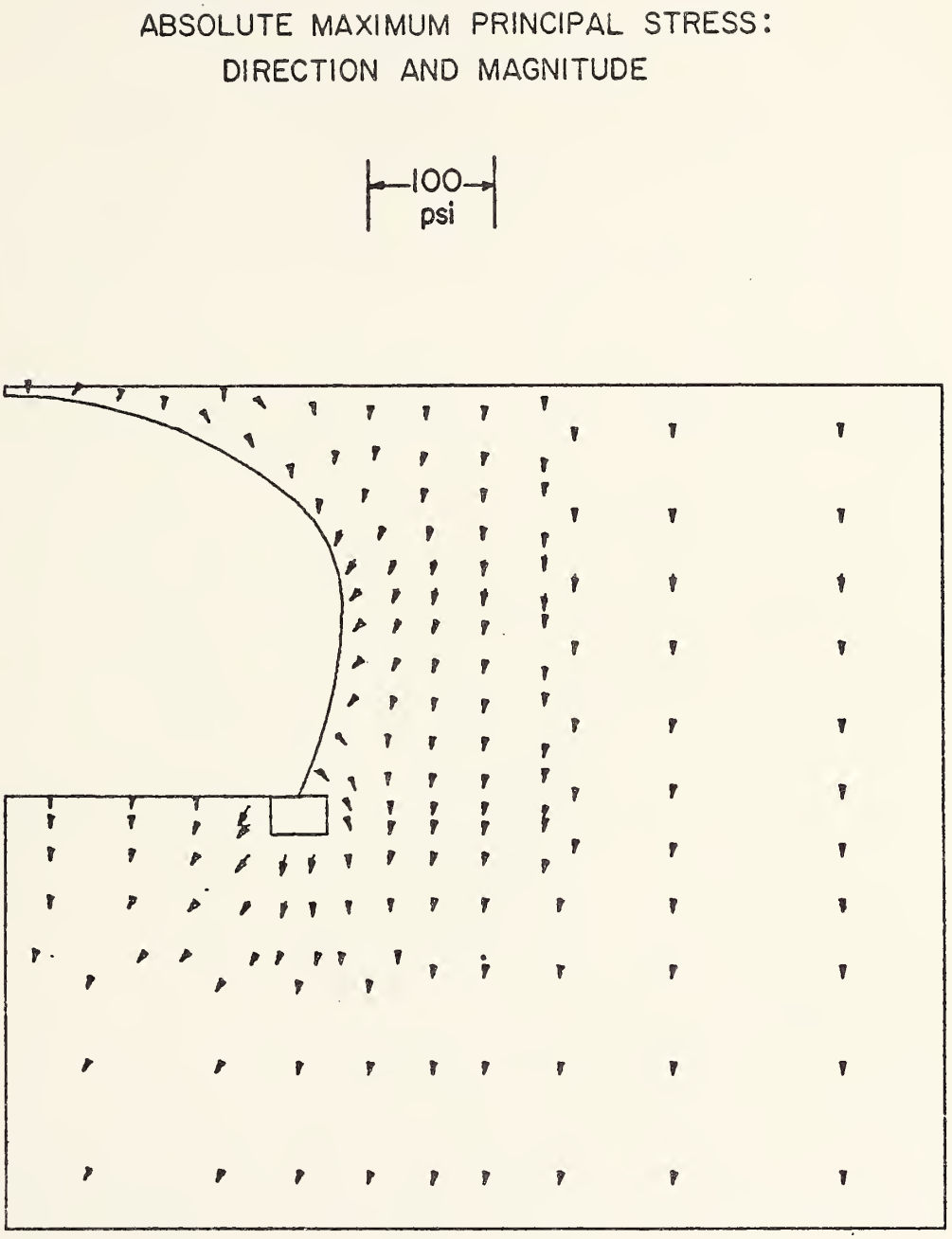

Figure 3.23 Maximum Stress, Fill at Crown

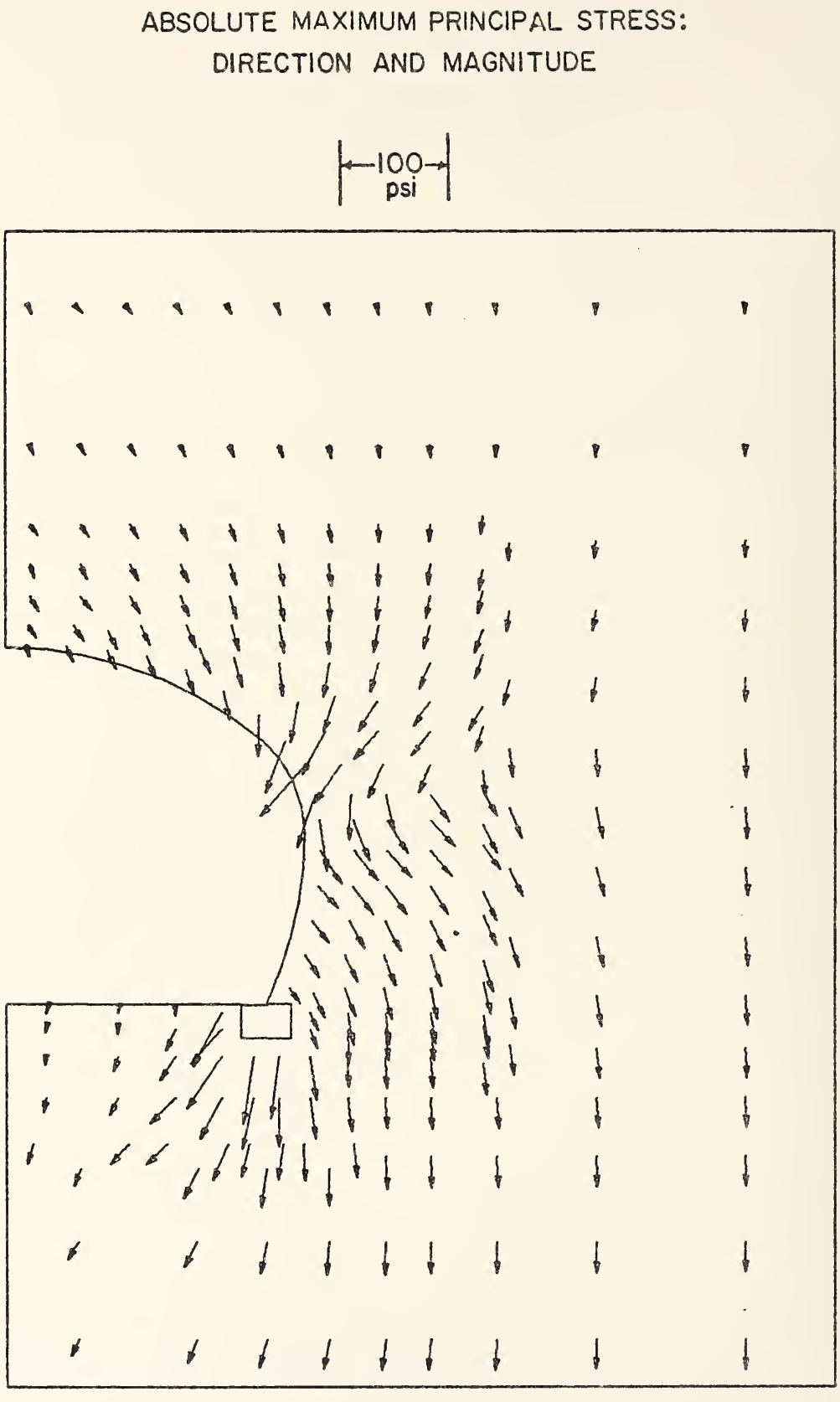

Figure 3.24 Maximum Stress, Full Fill

CHAPTER 4

ANALYSIS OF DEAD AND LIVE LOADING CONDITIONS

4.1 STATEMENT OF PURPOSE

The intent of this chapter is to demonstrate the relative influence of load variations from the basic model. First, the influence of symmetric loading is explored by isolating the effect of gravity loads from compaction loads. Second, the influence of unbalanced (non-symmetric) fill heights is examined. Last, is an investigation of traveling live loads for low cover heights including the consideration of a relieving slab.

4.2 INCREMENTAL GRAVITY vs. COMPACTION LOADS

In the previous chapter, the basic model results were based on the combined loading of incremental gravity layers plus temporary compaction pressures of 5 psi (34.5 kPa). To illustrate the relative influence of each type of loading, two additional solutions are presented, one with just gravity loading, and a second with gravity plus twice the compaction pressure, 10 psi (69.0 kPa). Figures 4-1, 4-2, and 4-3 show these comparisons for crown deflection, springline thrust, and maximum moment (slightly above springline) as a function of fill-height-ratio in the same format of the previous chapter.

Crown Deflection. Examination of the displacement histories in Figure 4-1 shows the significant influence of compaction pressure in controlling the amount of crown peaking during the initial construction stages. Maximum peaking percentages are approximately 0.1, 0.5, and 0.8% for the cases of 0.0, 5.0, and 10.0 psi (0.0, 34.5, and 69.0 kPa) compaction pressures, respectively. Clearly, loading with compaction pressure is more representive of observed performance (Chapter 2) than just gravity loading. At full fill height the percentages of crown flattening for the three cases

are not markedly different. Maximum flattening is slightly reduced as compaction pressure is increased.

Thrust and Moment. In contrast to crown displacement, Figure 4-2 shows that springline thrust is practically unaffected by compaction pressure. In like manner, the maximum moment (slightly above springline) is also insensitive to compaction pressure except for small positive moments developed during the first construction increment.

Monolith. Before leaving this section, it is interesting to compare a monolith gravity loading condition with the incremental loading condition. A monolith system may be imagined by assembling the long-span system with gravity turned off and no compaction loads. Once all the soil is in place, gravity is turned on and the system deforms under its own weight.

A solution of the monolith is superimposed on the previous displacement, thrust, and moment history figures with a dashed line. Although the monolith is not dependent on intermediate fill heights, it is plotted as a straight line assuming that fill height corresponds to a percentage of gravity so that final fill height implies full gravity.

The difference between the monolith solution and the incremented solutions (with and without compaction loads) is apparent during the intermediate stages of construction wherein the monolith is incapable of exhibiting crown peaking and incremental loading responses of thrust and moment. However, at full fill height the monolith responses are reasonably close to the final incremented responses. Thus, the monolith solution may have some practicality for establishing design guidelines such as maximum cover height tables based on allowable thrust and/or deflection.

4.3 NONSYMMETRIC GRAVITY LOADS

Up to now, all loading has been assumed symmetric about the vertical centerline. In this section, the effect of placing soil

layers nonsymmetrically on either side of the arch is examined, an inadvertent but all too common occurrence during field construction. To adjust the basic model for this study, the finite element mesh is doubled by creating a mirror image to form a full mesh model. All parameters of the basic model are unchanged except the construction increment schedule.

Three schedules of soil placement are considered for comparison; alternating sides, alternating layers, and symmetric fill. Figure 4-4 shows the sequential placement of gravity-loaded soil layers for each case. The symmetric fill schedule is defined by three uniformly placed layers identical to the basic model except that the full mesh was used for accuracy checks. For the cases of alternating layers and alternating sides, six sequential layers are considered. In the former case, the soil layers are staggered, first on the left side of arch then on the right side and so on. In the latter case, an extreme unbalance is considered by first placing all three layers on the left side then three layers on the right side.

Deformed Shape. The deformed arch shapes (magnified by 100) for each soil placement scheme are shown side by side in Figures 4-5, 4-6, and 4-7. The figures are ordered in the sequence of soil placement to provide a "stop action" view of the deformations. Rigid body deformation is removed by subtracting off the average vertical displacement of the footings.

In Figure 4-5 the deformed shapes resulting from layers 1 and 2 (or layer 1 on both sides in the symmetric case) are relatively small because only lateral pressures due to Poisson effect of gravity loads are acting on the arch, compaction pressures are ignored in this study. Significant deformations do not occur until a top layer is encountered in the construction sequence wherein the layer weight is acting vertically on the arch (see Figure 4-4). This occurs first for the alternating side load condition after the placement of the layer 3 shown in Figure 4-6.

For the alternating-layer load condition it occurs after layer 5, Figure 4-7. After all loading schemes are completed with fill 0.5 ft. (0.15m) above crown, the resulting deformed shapes are depicted in the bottom row of Figure 4-7. As expected, the deformed shapes of the alternating load schemes are significantly nonsymmetric and exhibit larger deformations than the symmetric case. Permanent lateral offsets of the crown are 0.15 in. (0.38cm) for the alternating-layer condition and 0.34 in. (0.86cm) for the alternating-side condition.

However, the largest deformations occur prior to the final step in which both alternating load conditions exhibit maximum deformations four times greater than the maximum symmetric deformation. Clearly, this demonstrates the importance of balanced construction in field practice.

Thrust Distributions. Figures 4-8, 4-9, and 4-10 show the thrust distributions for the three load cases in the same format as descibed for displacements. Again, significant responses do not occur until a top soil layer is encountered in the construction sequence. This is apparent in Figure 4-9 where the alternating-side load condition exhibits significant thrust on the left side which is fully loaded; however, the other two loading conditions exhibit only a moderate thrust because they have not yet incorporated a top layer on either side. After all loading schedules are completed, the resulting thrust distributions are all remarkably similar and symmetric, differing by less than 6% as shown in Figure 4-10. For both alternating load schemes, maximum thrust occurs during placement of soil layer 5, however, they are only 1% larger than in their final condition.

Moment Distributions. Figures 4-11, 4-12, and 4-13 show the moment distributions for each load case in serial format as before. Positive moments (tension on extrados) are plotted in the arch interior. Significant moments develop when a top layer is placed on the arch as can be observed in Figure 4-12 for the

alternating-side load condition. After all loading schedules are completed, the moment distribution for both alternating load cases are highly non-symmetric (Figure 4-13) and generally larger than in the symmetric case. Maximum moments occur during placement of layer 5 wherein the alternating-side load condition is 60% greater, and the alternating-layer load condition is 30% greater than the symmetric case. In view of the pronounced effect of unbalanced loading it is readily understandable why experimentalists have trouble in recording symmetric strain data during field testing.

4.4 TRAVELING LIVE LOADS

In this section, live loads traveling over the arch culvert model are investigated for three shallow cover heights. The results illustrate how the arch responds as the traveling load approaches the centerline as well as illustrating the reduced influence of live loads as the cover height increases. Results include structural response distributions, influence lines for a traveling point load, and influence lines for an HS 20-44 truck. In addition, the results of placing a concrete relieving slab over the arch are presented to illustrate its effect in reducing live load influence.

The basic model (Chapter 3) is used by creating a mirror image of the finite element mesh to form a full mesh model necessary for the analysis of nonsymmetrical live loads. All other basic model parameters are unchanged except that gravity or compaction loads are eliminated in order to isolate the live load effect.

Three cover heights are considered with ratios of cover height-to-top rise of 0.04, 0.36, and 0.79, hereafter termed cover height one, two, and three, respectively. These configurations are shown in Figures 4-14, 4-15, and 4-16, respectively, along with the locations of four points loads used to simulate a traveling load for each cover height. Actually, the point

loads are uniform strip loads orthogal to the cross-section over a unit slice (plane strain). However, the point load terminology will be used in this writing. Lateral positions of the point loads are identical for each cover height and are located from the centerline in terms of half-span lengths as 1.5, 1.0, 0.5, and 0.0, thereby representing a point load traveling to the centerline beginning 1.5 half-span lengths away. Naturally, the finite element analysis considers each point load as an individual problem so that twelve separate solutions are necessary. In all cases, the point load magnitude is nominally set at 100 lb/in. (175 N/cm).

Response Distributions. Response distributions for deformed shape, thrust, and moments are shown in Figures 4-17, 4-18, and 4-19, respectively. In each figure, responses are shown in three rows corresponding to the three cover heights. For each row, distributions are shown at each load location in progression as the load travels toward the centerline.

Examining the deformed shapes in Figure 4-17, it is observed that maximum deformation is located at the crown and occurs when the load is over the centerline. However, deformations decrease significantly as the cover height is increased. This same trend is observed for moment distributions, Figure 4-19. In particular, the maximum moment is dramatically reduced by a factor of 19 between cover height 1 and cover height 3. The thrust distributions shown in Figure 4-18, are also maximum when the load is over the centerline, however, the point in the arch where maximum thrust occurs is in the 2 o'clock position referenced by an origin at the intersection of the vertical centerline and springline.

Point Load Influence Lines. To gain better insight on the effect of load location and cover height, Figures 4-20, 4-21, and 4-22 show influence lines at key locations in the arch for displacement, thrust, and moment. Crown displacement (as percent of

total arch rise) is displayed in Figure 4-20 as a function of load location from centerline for each cover height. These curves exhibit the same basic trends as the experimental data presented in Chapter 2; however, positive deflection (crown raising) tends to be relatively greater for the experimental data. For cover height 1, the crown is raised when the load is further than 0.6 half-span units from the centerline. However, for cover heights 2 and 3, the crown is not raised when load is anywhere over the arch and only raises slightly when the load is off the arch.

Influence lines for thrust, Figure 4-21, are presented at the 2 o'clock location in the arch where overall maximum thrust occurs. At this location, it is observed that for each cover height thrust decreases steadily as the load moves away from the centerline and becomes negligible when the load is beyond the arch.

Influence lines for crown moment, Figure 4-22, exhibit a bending moment reversal when the load position is in the vicinity of 0.5 half-span units from the centerline. This suggests possible concern for fatigue if heavy live loads and shallow cover heights are used.

Truck (HS 20-44) Influence Lines. The axle loading distribution for a HS 20-44 truck (3 axles) with 20 ft. (6.1m) rear axle spacing is shown in Figure 4-23. Also shown is an equivalent set of strip loads obtained by assuming a uniform spacing between the tires of two or more trucks set side by side as shown. Having defined a set of strip loads it is possible to construct influence lines for this truck (or any other truck) by scaling and superimposing data from the single load influence lines in the previous section.

Figures 4-24, 4-25, and 4-26 show the truck influence lines for crown displacement, 2 o'clock thrust, and crown moment, respectively. The position of the truck is referenced by the distance of the middle axle from the centerline. The relative trends

of the truck influence lines are basically the same as the single load influence lines because the distances from the reference axle to the front and real axle are large, i.e., 0.78 and 1.11 half-span lengths, respectively. Consequently, their superimposed contributions tend to be small compared to the reference axle, and the magnitude of the truck influence lines is primarily controlled by the weight of the middle axle, 2.2 times larger than single-load reference.

To complete this study, Figure 4-27 shows a comparison of dead load vs. live load effects on crown displacement as the cover height increases. Here the truck is positioned with its middle axle over the crown, and the resulting crown deflection decays rapidly as cover height is increased. In contrast, the crown deflection due to dead load of soil above the crown increases steadily with cover height. When the cover height is 0.5 top-rise units above the crown 83% of the total deflection is due to dead load.

Live Loads with Relieving Slabs. The last study in this chapter considers the effect of placing a concrete relieving slab above the crown to spread the live load. Figure 4-28 shows the relieving slab configuration which is 1.0 ft. (0.3m) thick and one span length long, and the top surface is flush with cover height 2, 4.0 ft. (1.2m) above the crown. The concrete is assumed homogenous and uncracked with the same material properties as the arch footing defined in the basic model. A slight alteration of the finite element mesh was required to model the slab thickness with one layer of elements.

The system is loaded with four sequential live loads in the identical manner previously used for the cover height 2 configuration without a relieving slab, thereby providing a direct basis for comparison. Figures 4-29, 4-30, and 4-31 show displacement, thrust, and moment distributions sequentially at each load position for both configurations. It is observed that the relieving

slab substantially reduces structural responses when the load is on the slab. In particular, when the load is at the centerline, maximum displacement, thrust, and moment are reduced by factors; 0.41, 0.57, and 0.13, respectively, in comparison to the corresponding responses without a relieving slab. Apparently, the relieving slab concept is highly beneficial in minimizing live load effects.

Moreover, when the load is centered over the crown, the radius of curvature of the relieving slab surface in contact with the load is 18 times greater than the identical system without a relieving slab. Thus, it may be presumed that the relieving also minimizes bending stress in a flexible pavement covering, such as asphalt, placed over the slab.

4.5 Figures 4-1 through 4-31

		Page
Fig. 4-1	Influence of loading conditions on crown deflection.	88
Fig. 4-2	Influence of loading conditions on springline thrust.	89
Fig. 4-3	Influence of loading conditions on springline moment.	90
Fig. 4-4	Soil-layer placement schemes.	91
Fig. 4-5	Deformed shapes for first two layers.	92
Fig. 4-6	Deformed shapes for second two layers.	93
Fig. 4-7	Deformed shapes for third two layers.	94
Fig. 4-8	Thrust distributions for first two layers.	95
Fig. 4-9	Thrust distributions for second two layers.	96
Fig. 4-10	Thrust distributions for third two layers.	97
Fig. 4-11	Moment distributions of first two layers.	98
Fig. 4-12	Moment distributions of second two layers.	99
Fig. 4-13	Moment distributions of last two layers.	100
Fig. 4-14	Load locations at cover height one.	101
Fig. 4-15	Load locations at cover height two.	102
Fig. 4-16	Load locations at cover height three.	103
Fig. 4-17	Deformed shapes due to live loads.	104
Fig. 4-18	Thrust distribution due to live loads.	105
Fig. 4-19	Moment distributions due to live loads.	106
Fig. 4-20	Influence lines of crown deflection.	107
Fig. 4-21	Influence lines of thrust at 2 o'clock position.	108
Fig. 4-22	Influence lines of crown moment.	109

4.5 Figures 4-1 through 4-31 (continued)

		Page
Fig. 4-23	Loading representation of HS 20-44 truck.	110
Fig. 4-24	Truck influence lines for crown displacements.	111
Fig. 4-25	Truck influence lines for thrust at 2 o'clock position.	112
Fig. 4-26	Truck influence line for crown moment.	113
Fig. 4-27	Crown deflection, live load vs. dead load.	114
Fig. 4-28	Load locations for cover height 2 with relieving slab.	115
Fig. 4-29	Deformed shapes with and without relieving slab.	116
Fig. 4-30	Thrust distributions with and without relieving slab.	117
Fig. 4-31	Moment distribution with and without relieving slab.	118

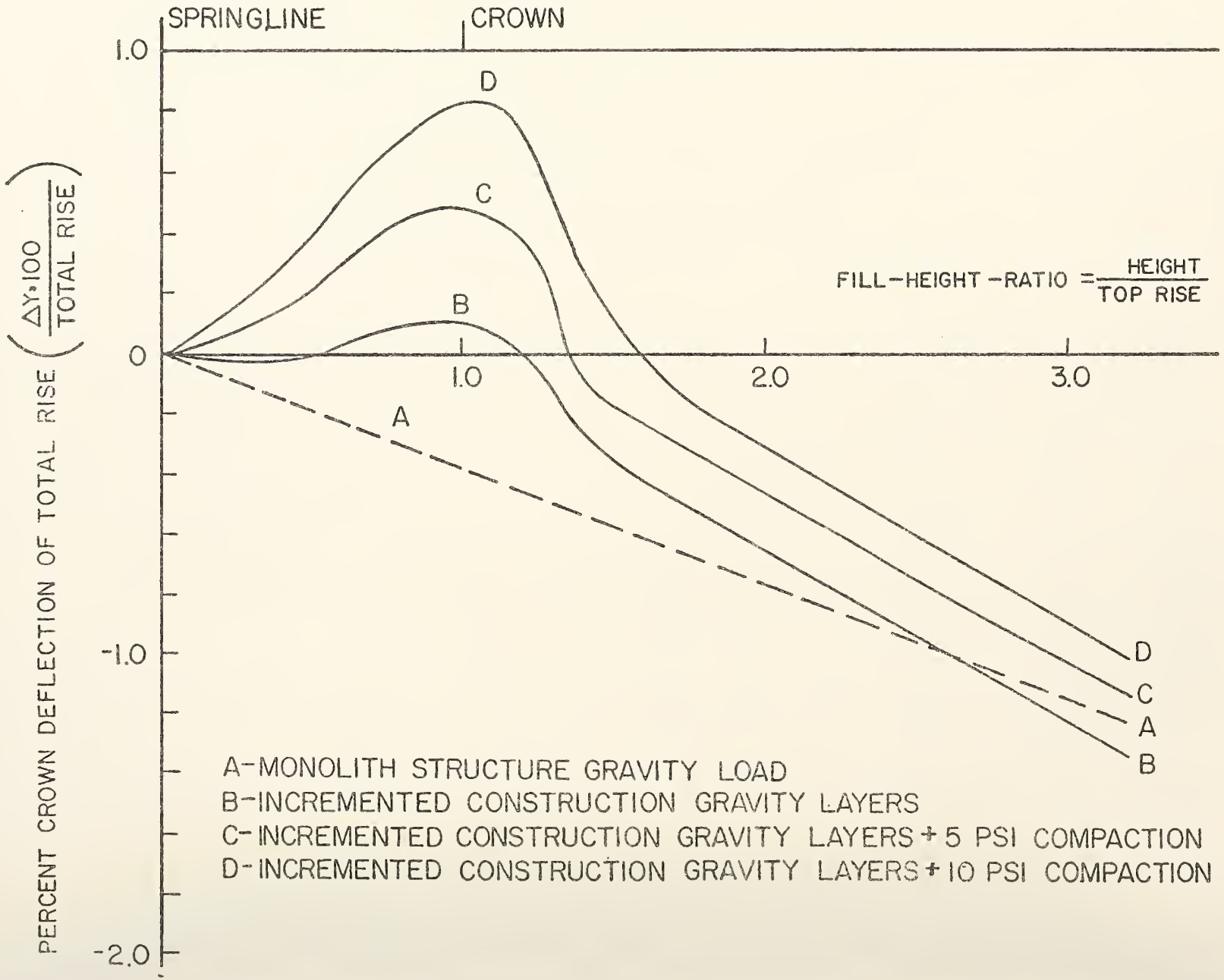

Figure 4.1 Influence of Loading Conditions on Crown Deflection

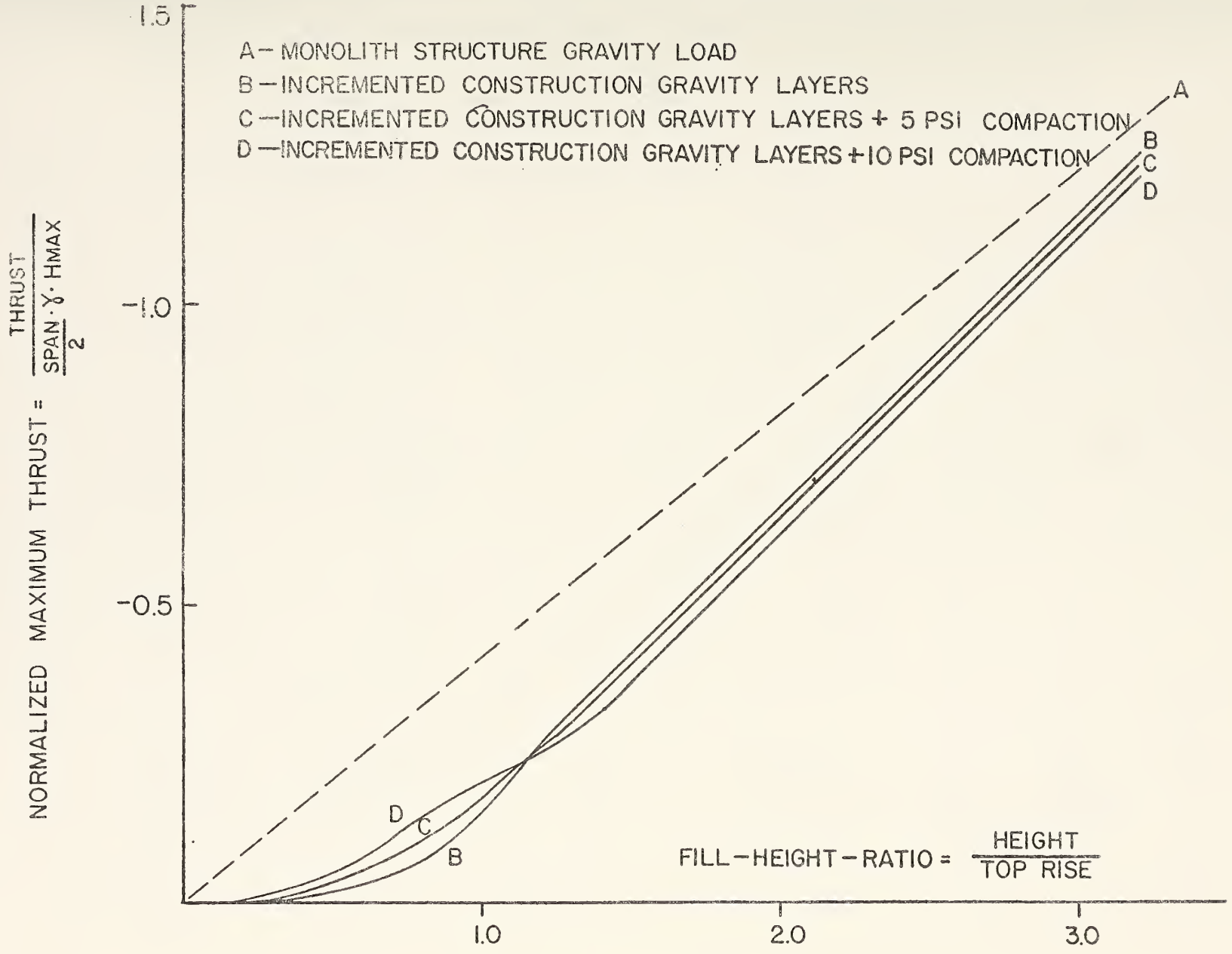

Figure 4.2 Influence of Loading Conditions on Springline Thrust

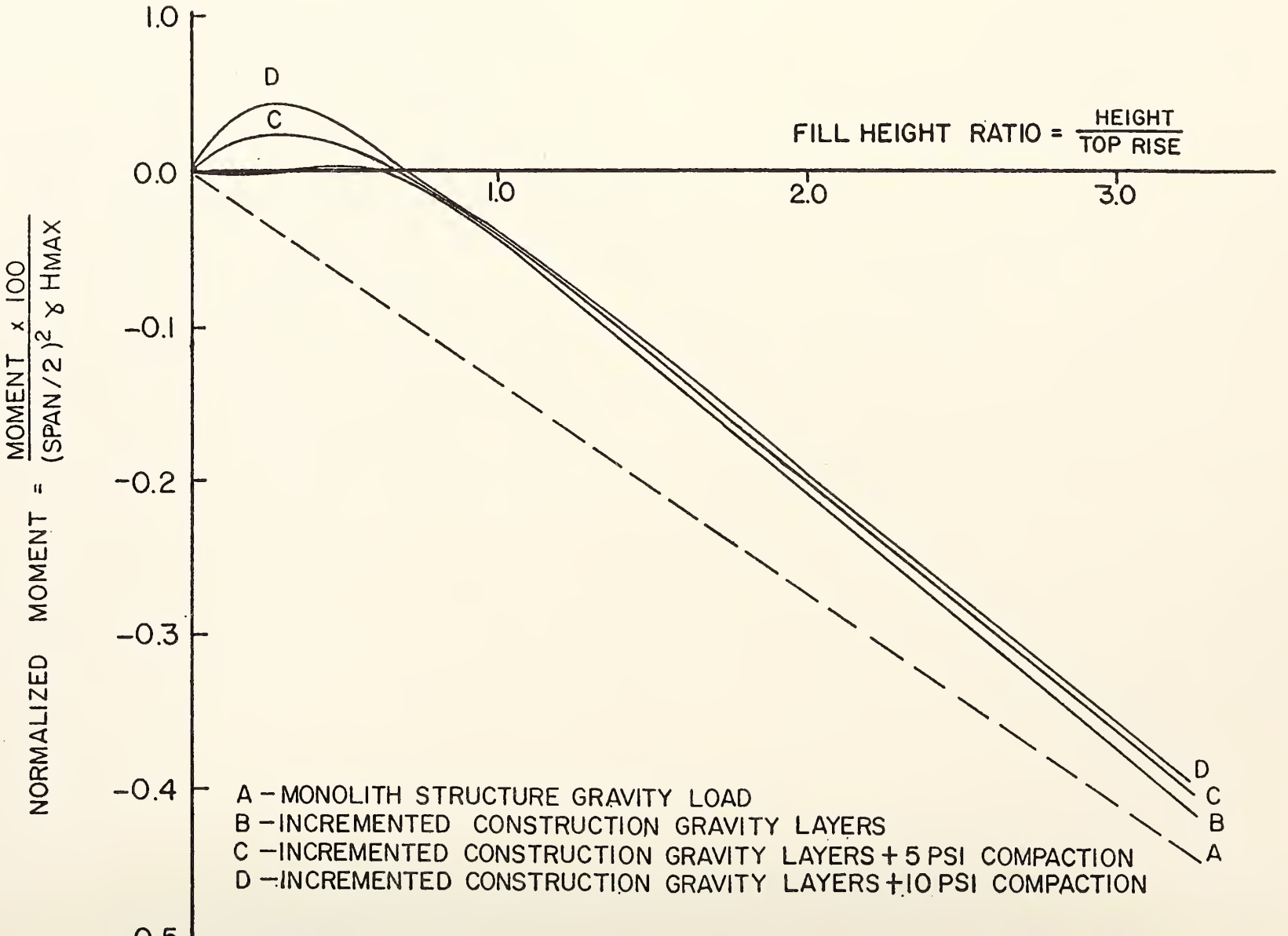
1.0
0.0
-0.1
-0.2
-0.3
-0.4
-0.5
D
C
FILL HEIGHT RATIO = HEIGHT / TOP RISE
1.0
2.0
3.0
NORMALIZED MOMENT = MOMENT x 100 / (SPAN/2)² γ HMAX
A – MONOLITH STRUCTURE GRAVITY LOAD
B – INCREMENTED CONSTRUCTION GRAVITY LAYERS
C – INCREMENTED CONSTRUCTION GRAVITY LAYERS + 5 PSI COMPACTION
D – INCREMENTED CONSTRUCTION GRAVITY LAYERS + 10 PSI COMPACTION
D
C
B
A

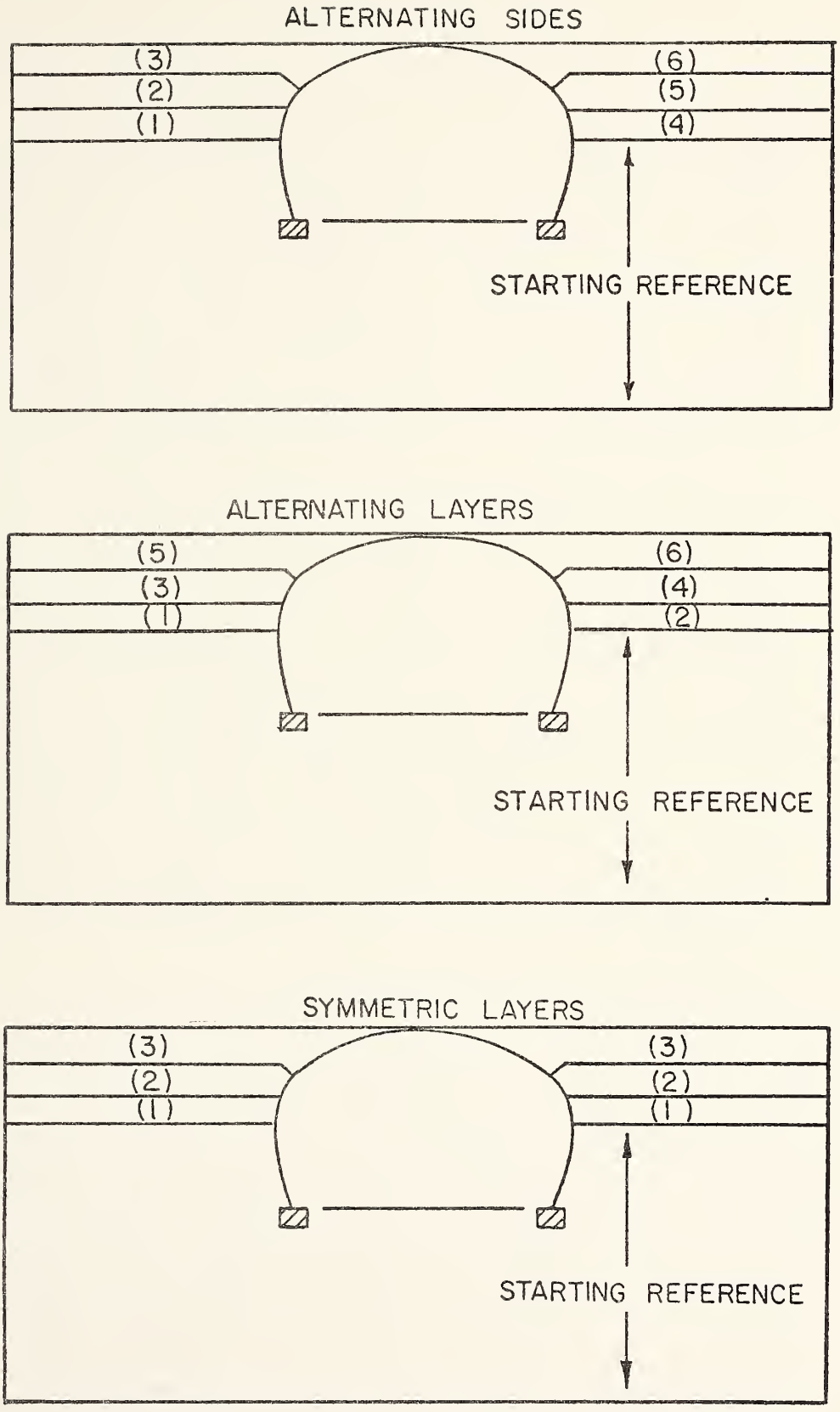

Figure 4.4 Soil-layer Placement Schemes

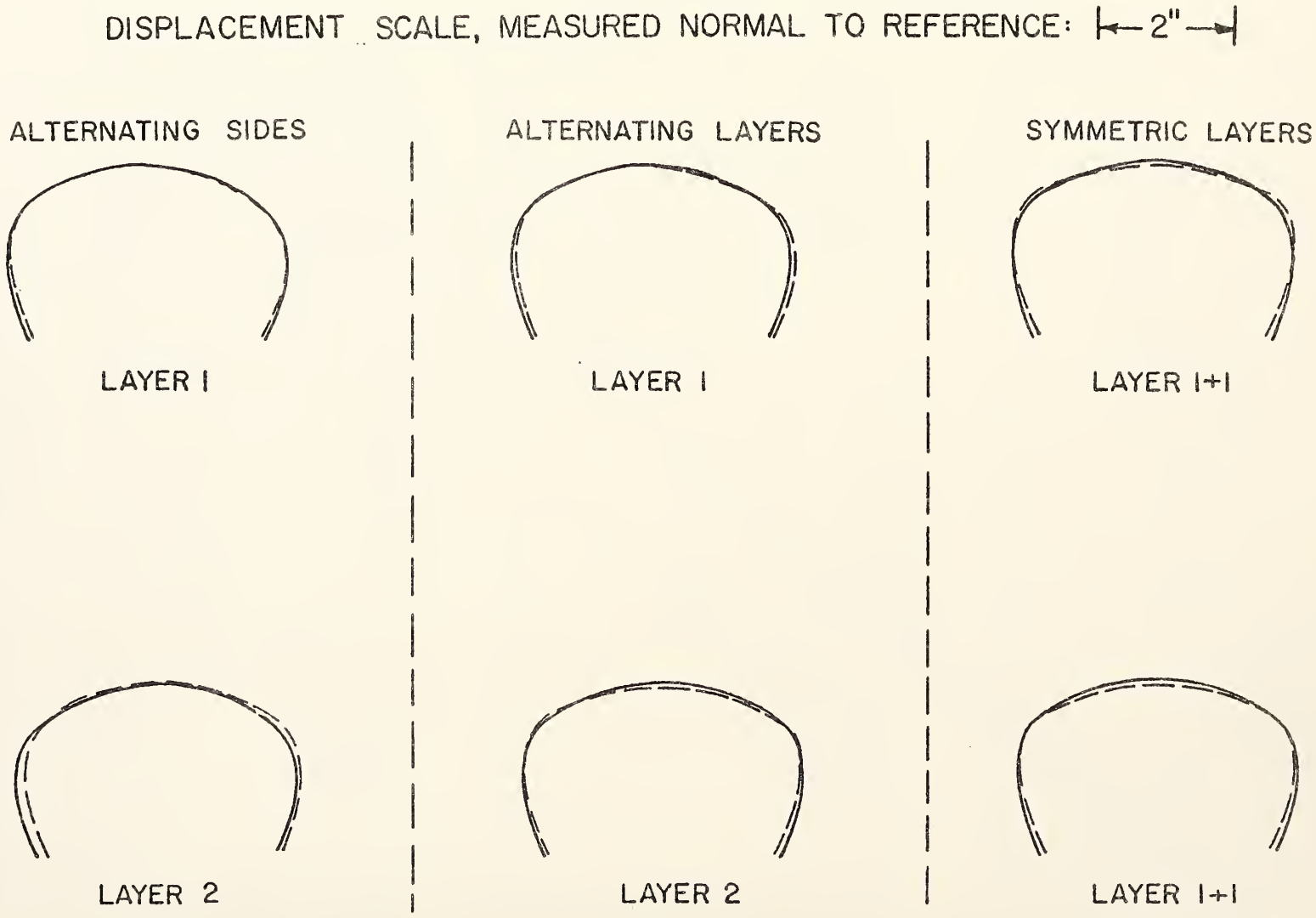

Figure 4.5 Deformed Shapes for First Two Layers

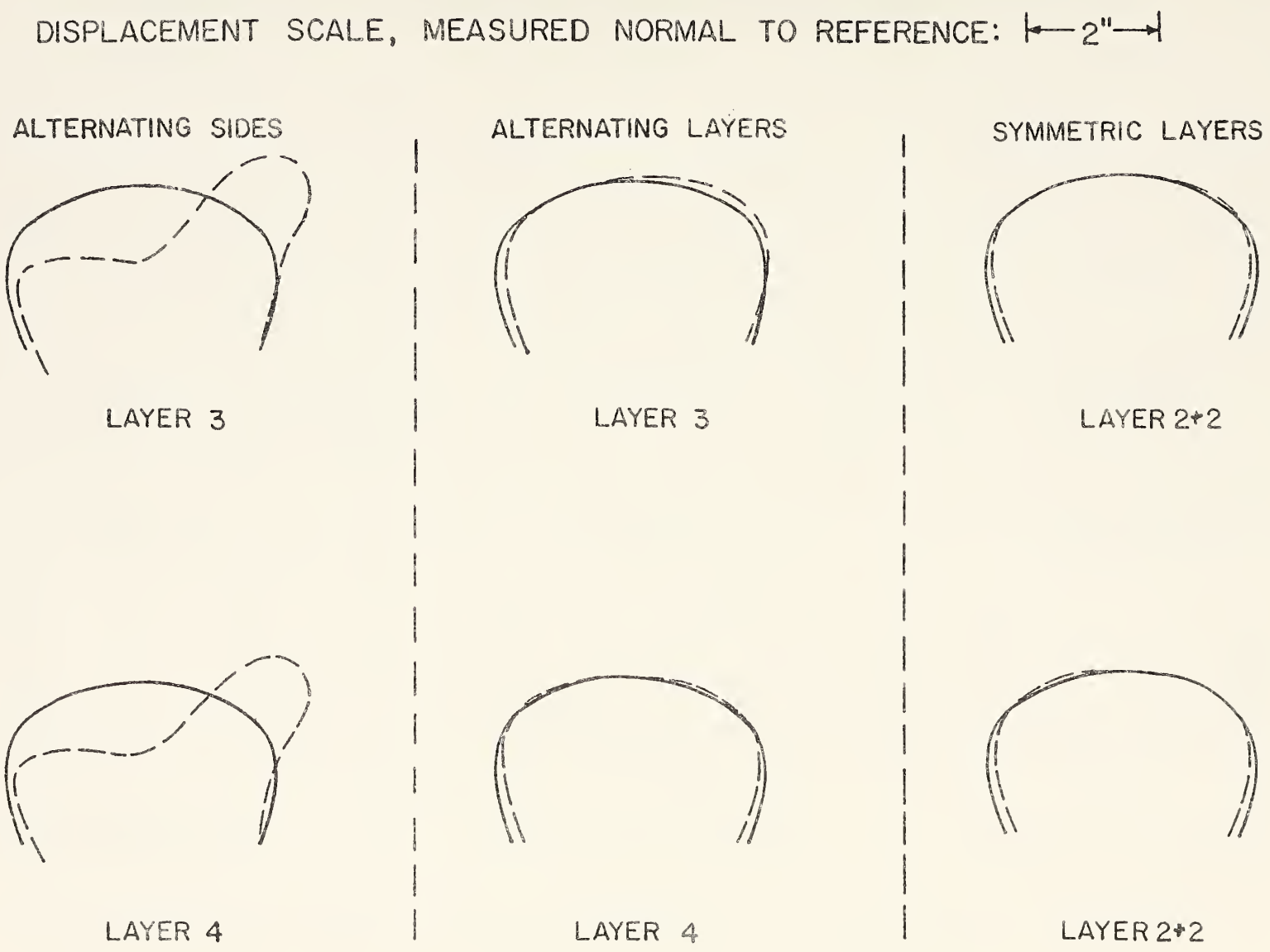

Figure 4.6 Deformed Shapes for Second Two Layers

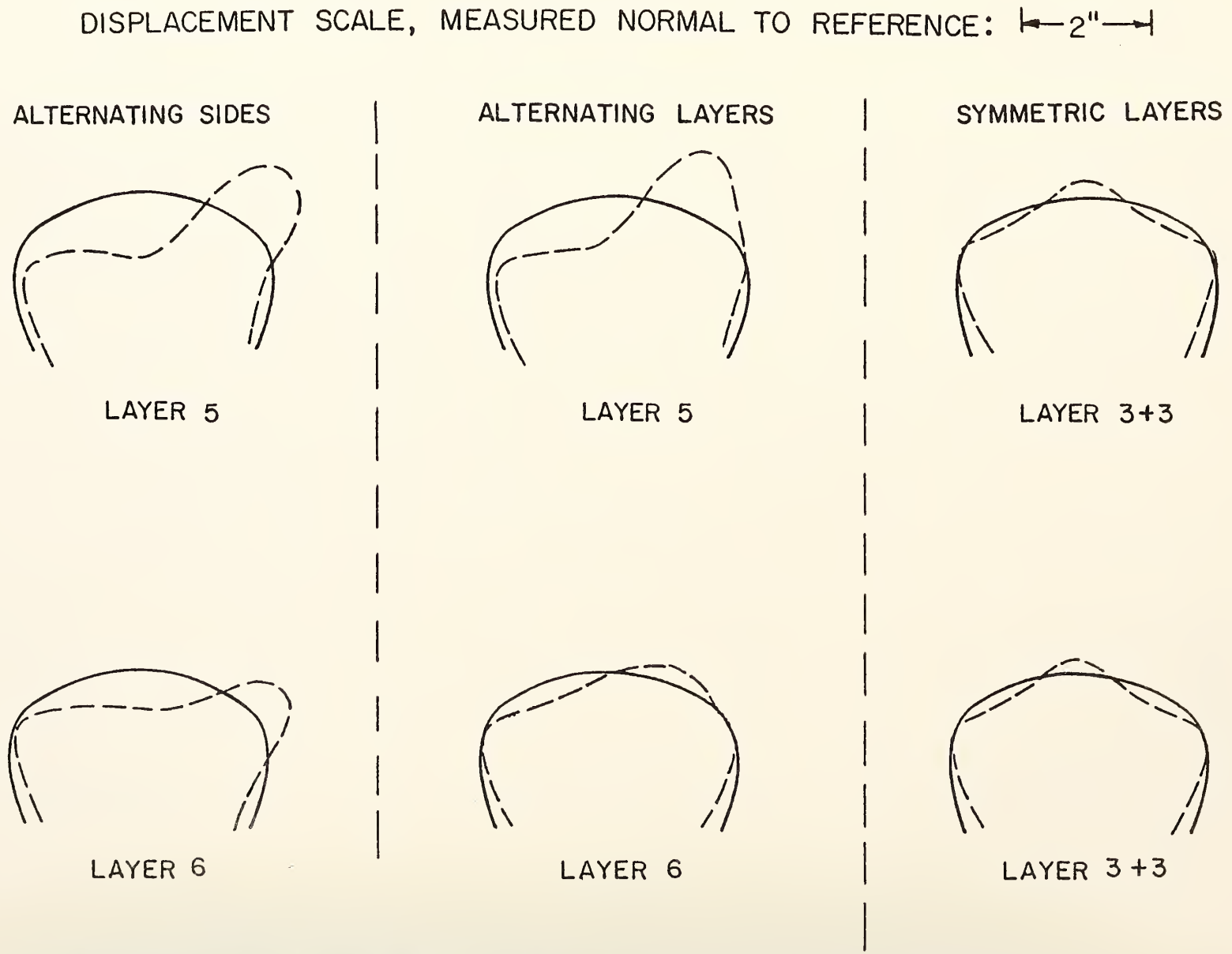

Figure 4.7 Deformed Shapes for Third Two Layers

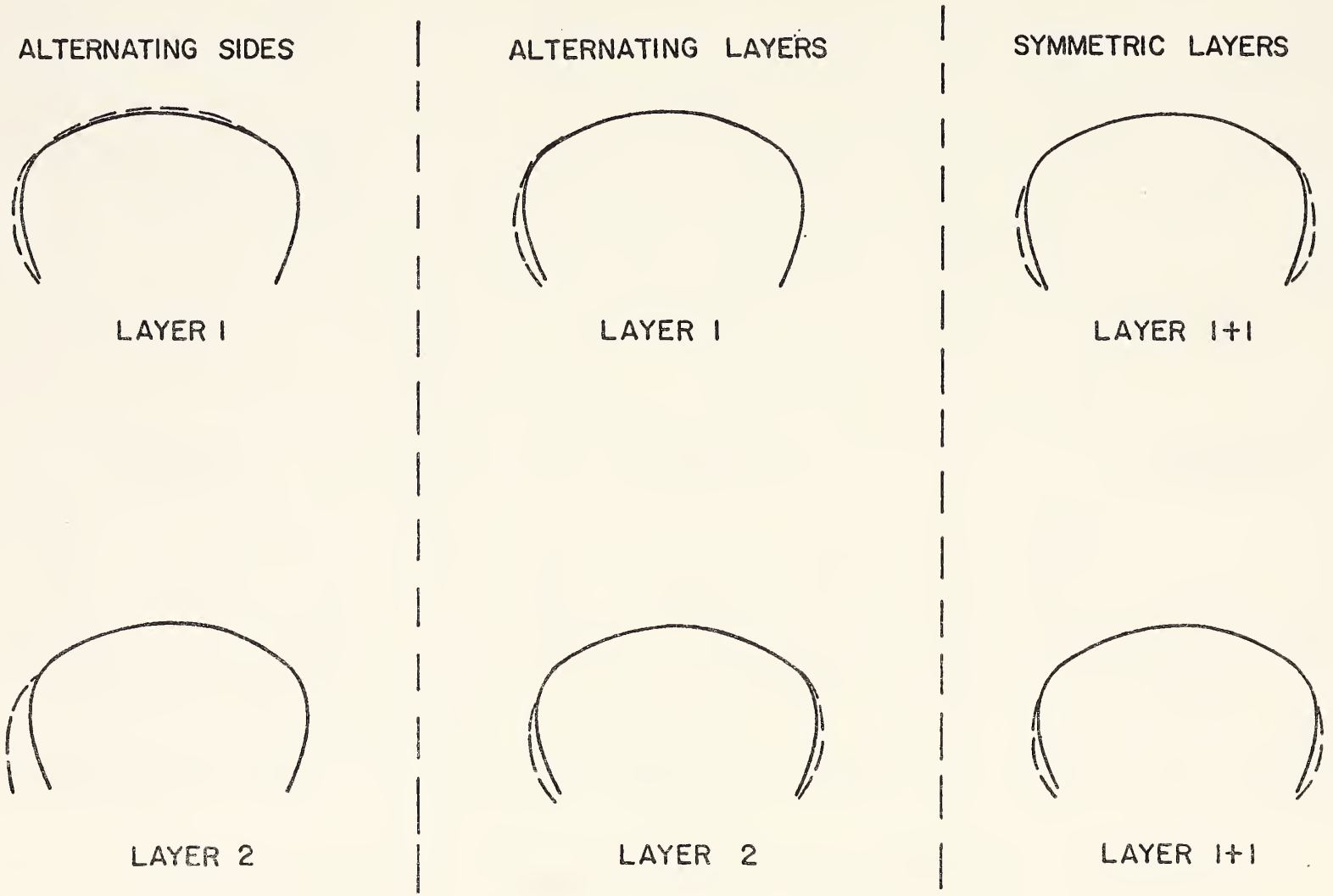

Figure 4.8 Thrust Distributions for First Two Layers

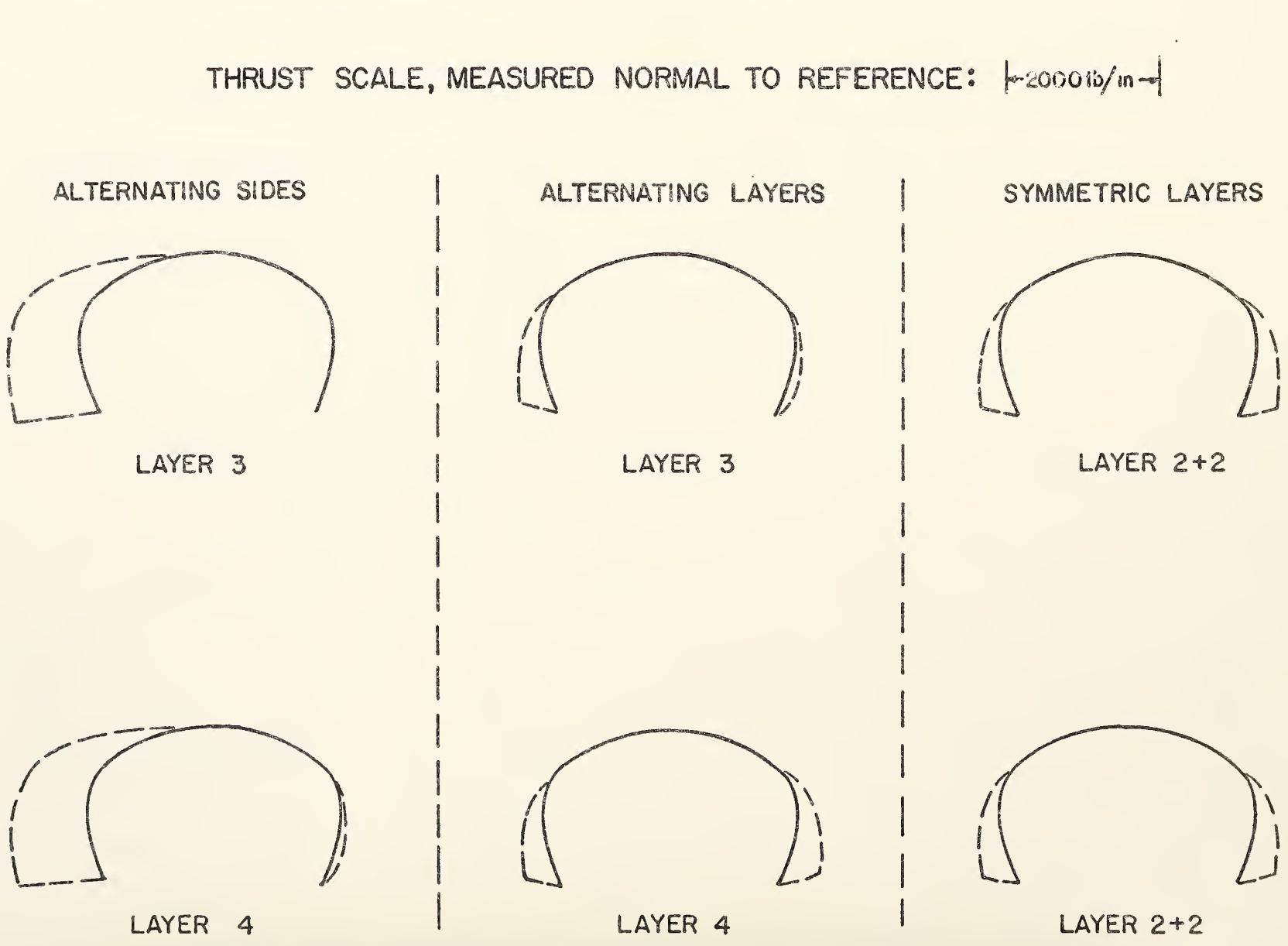

Figure 4.9 Thrust Distributions for Second Two Layers

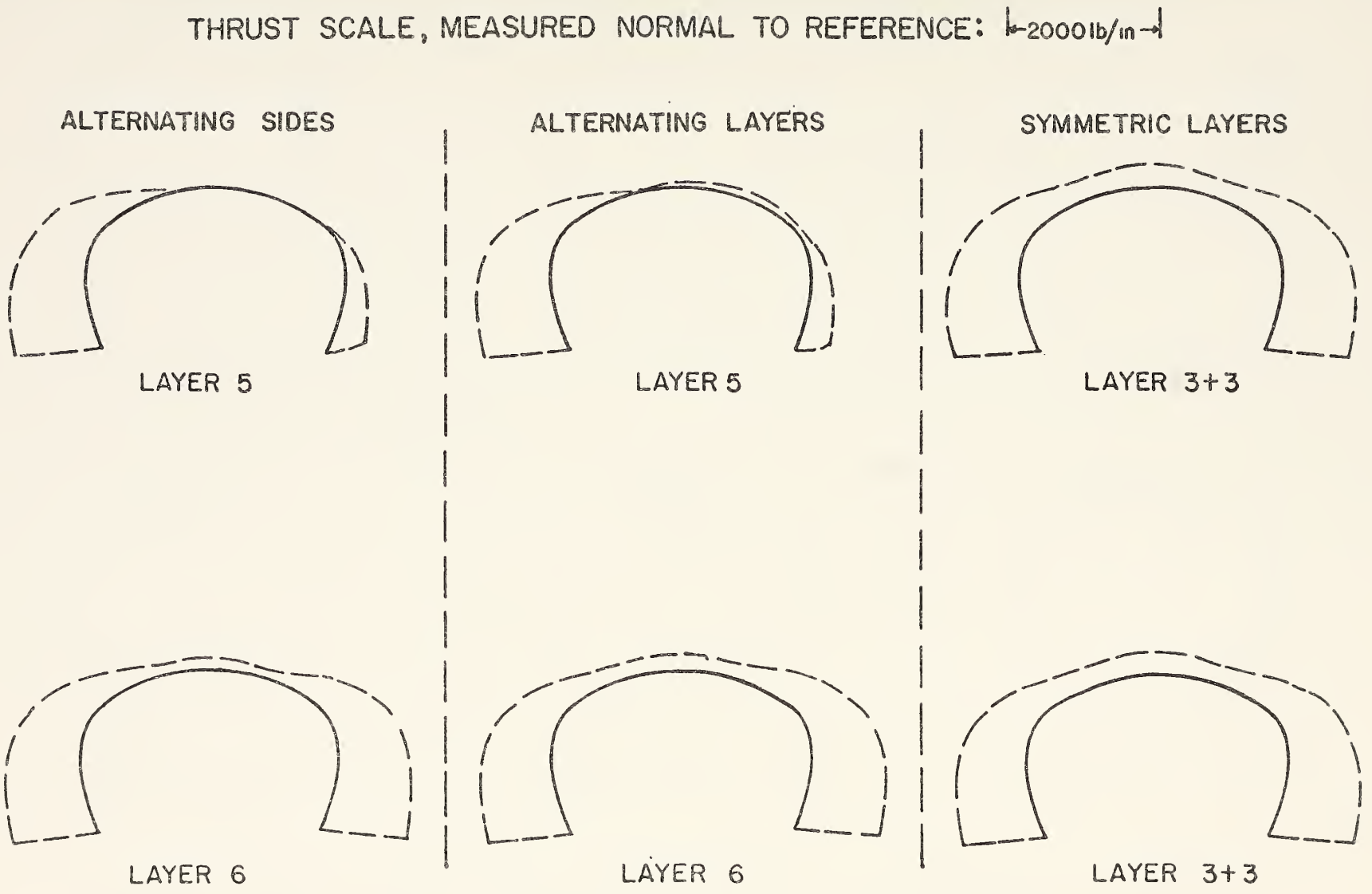

Figure 4.10 Thrust Distributions for Third Two Layers

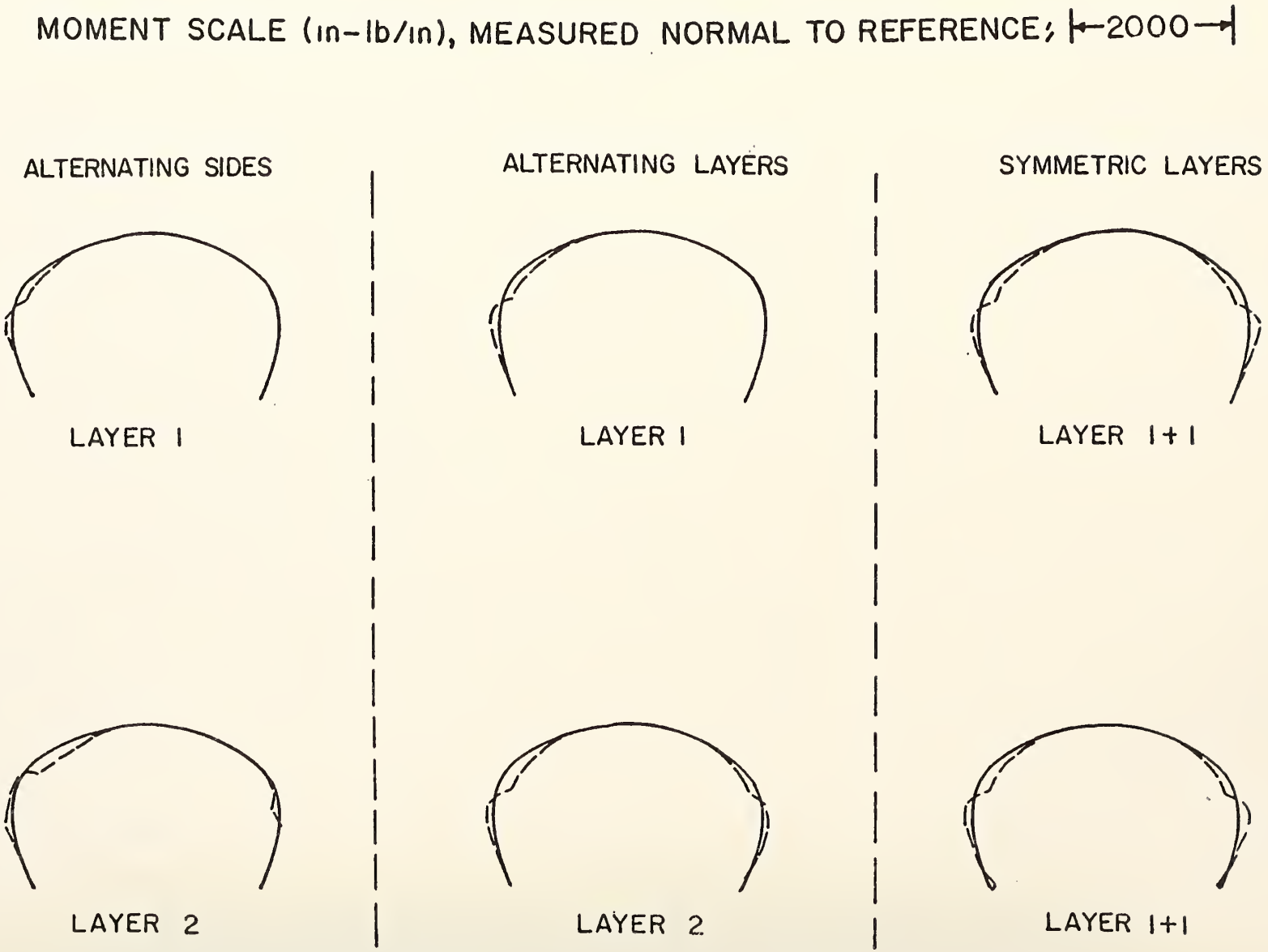

Figure 4.11 Moment Distributions of First Two Layers

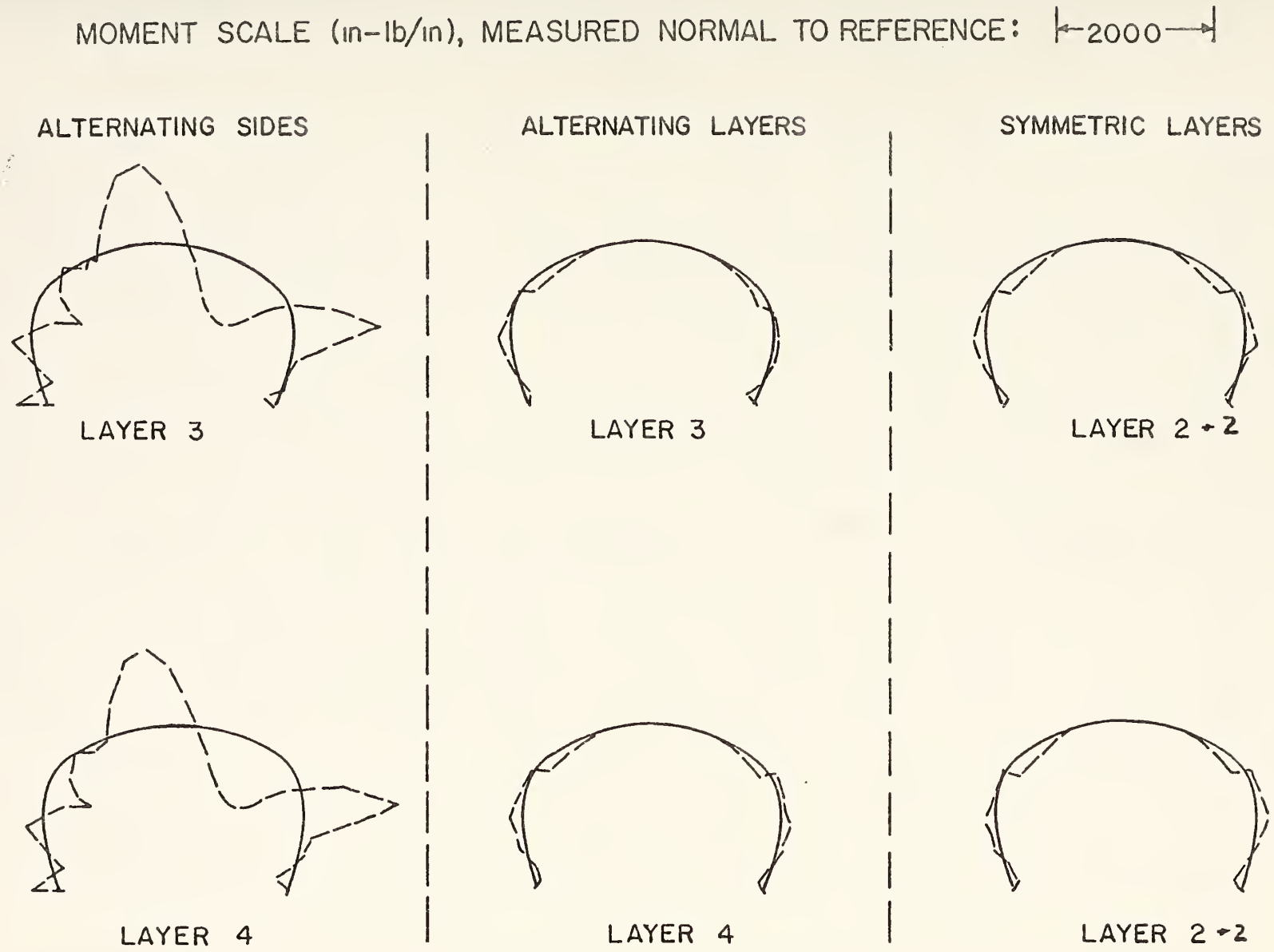

Figure 4.12 Moment Distributions of Second Two Layers

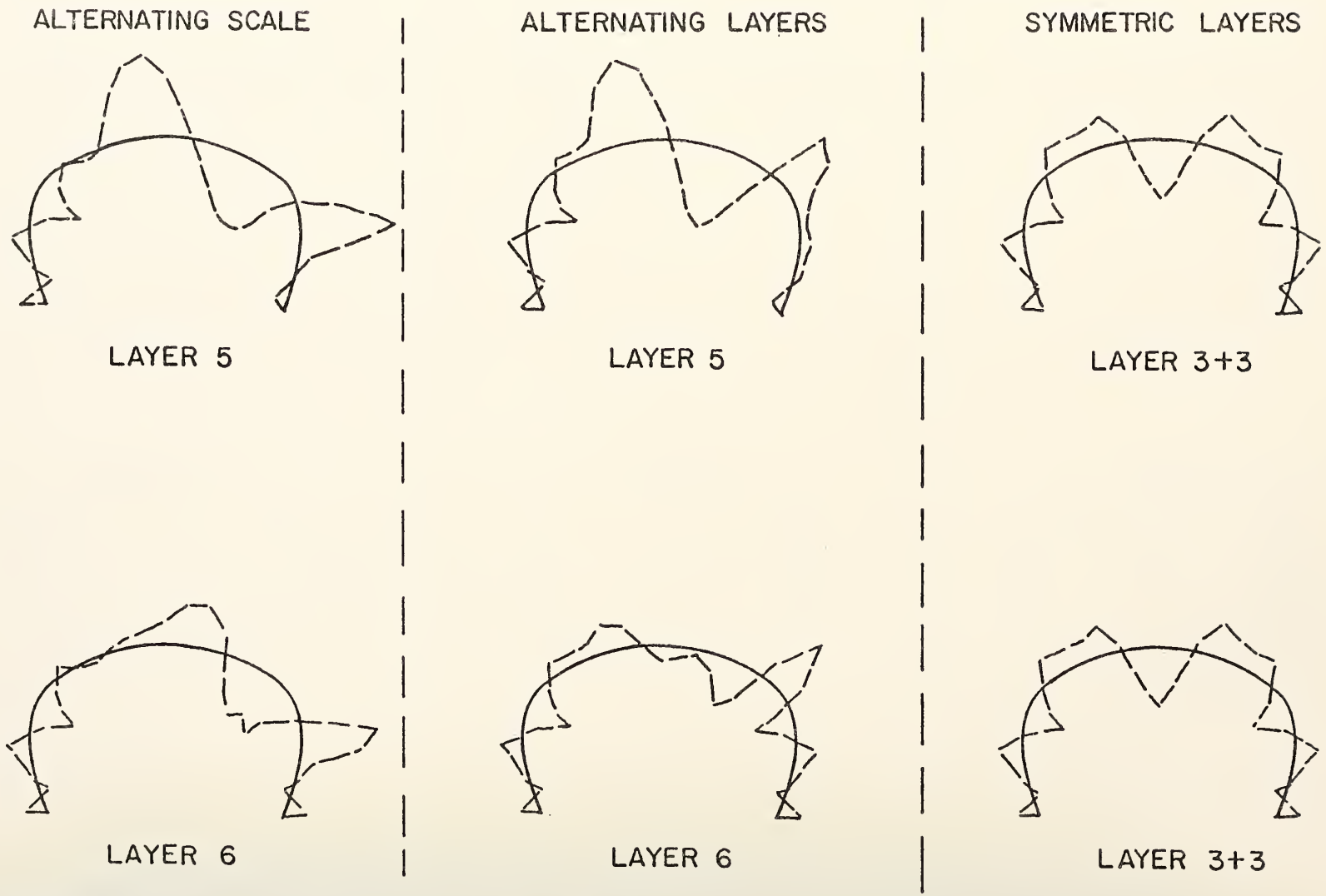

Figure 4.13 Moment Distributions of Last Two Layers

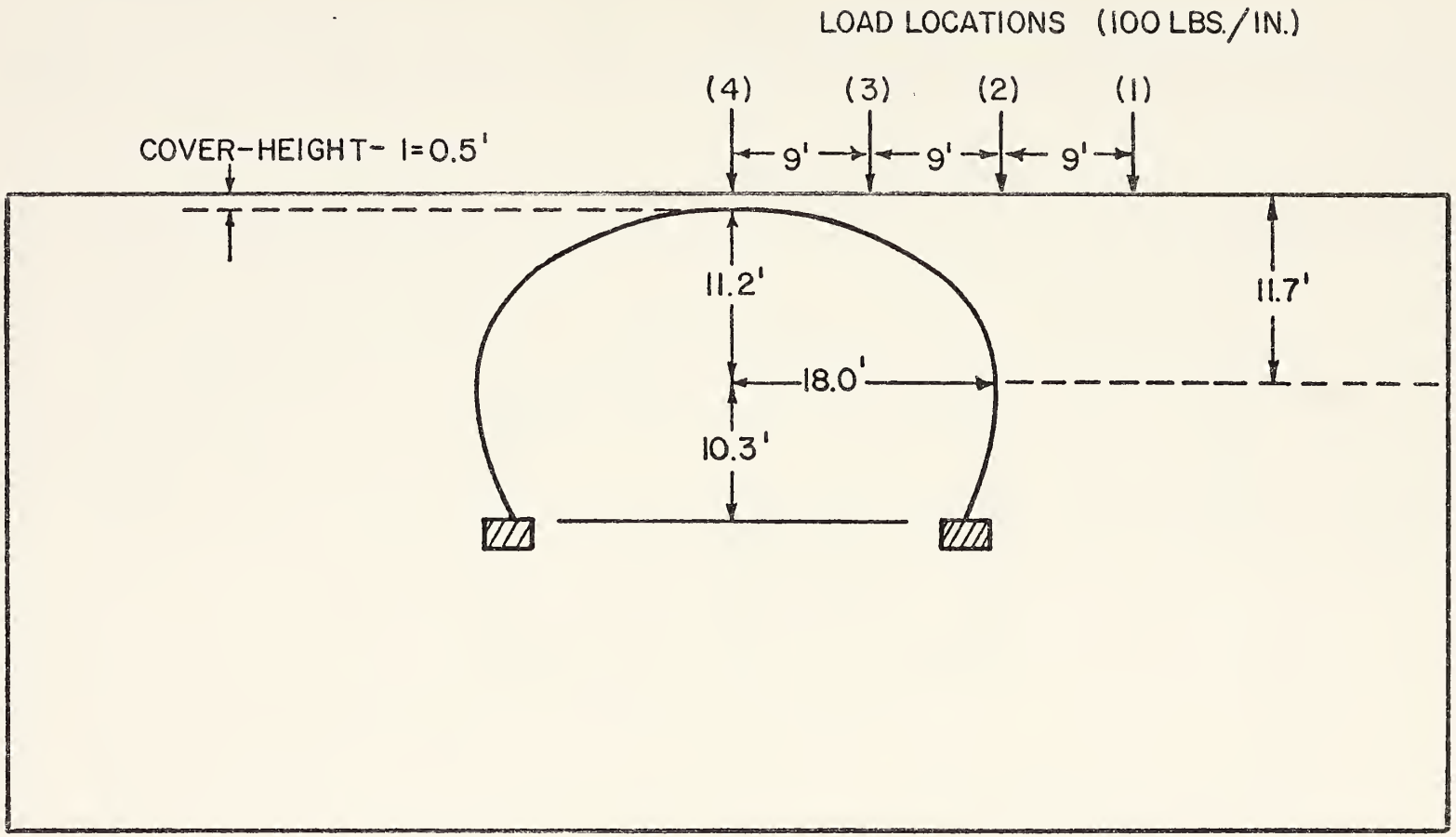

Figure 4.14 Load Locations at Cover Height One

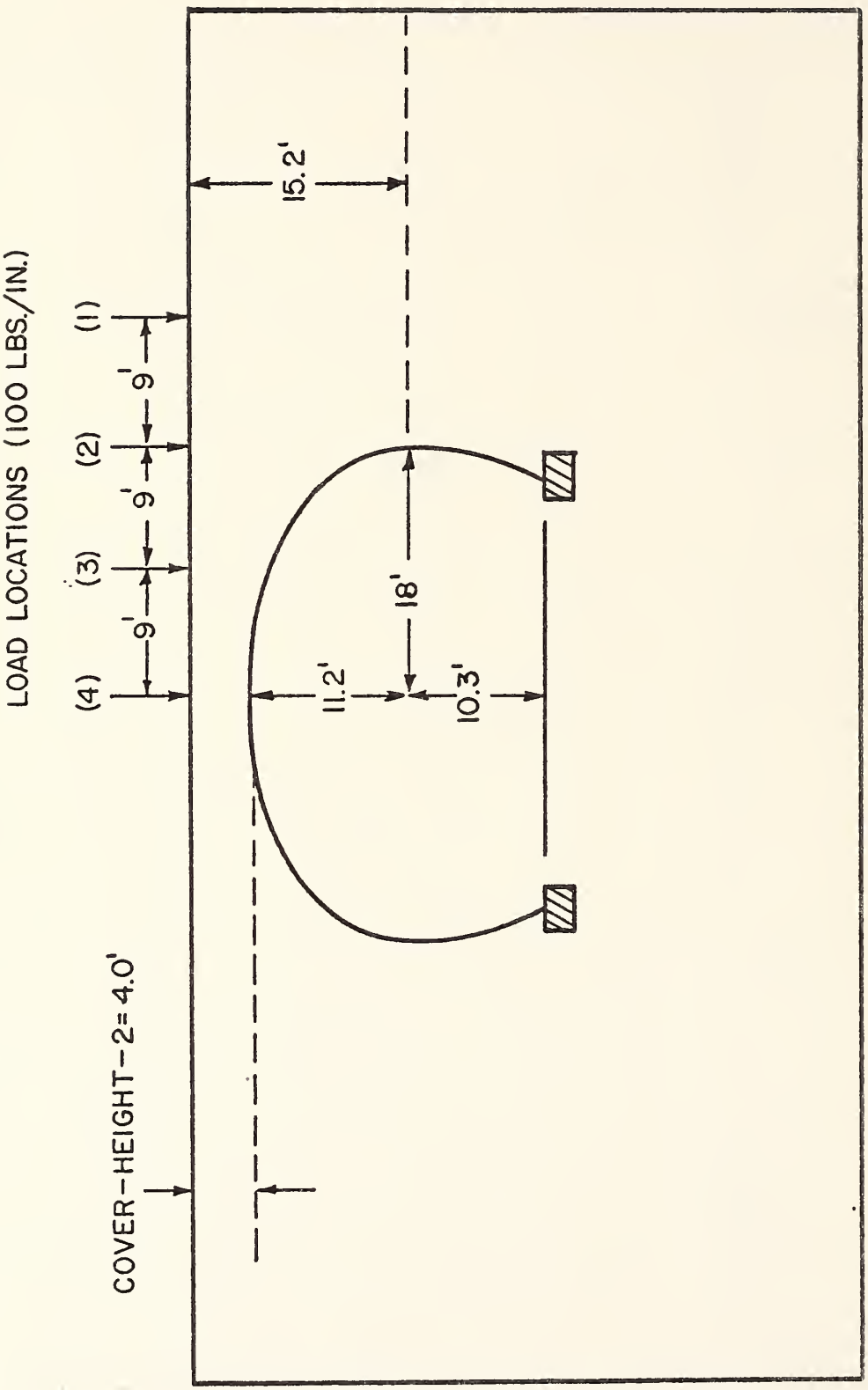

Figure 4.15 Load Locations at Cover Height Two

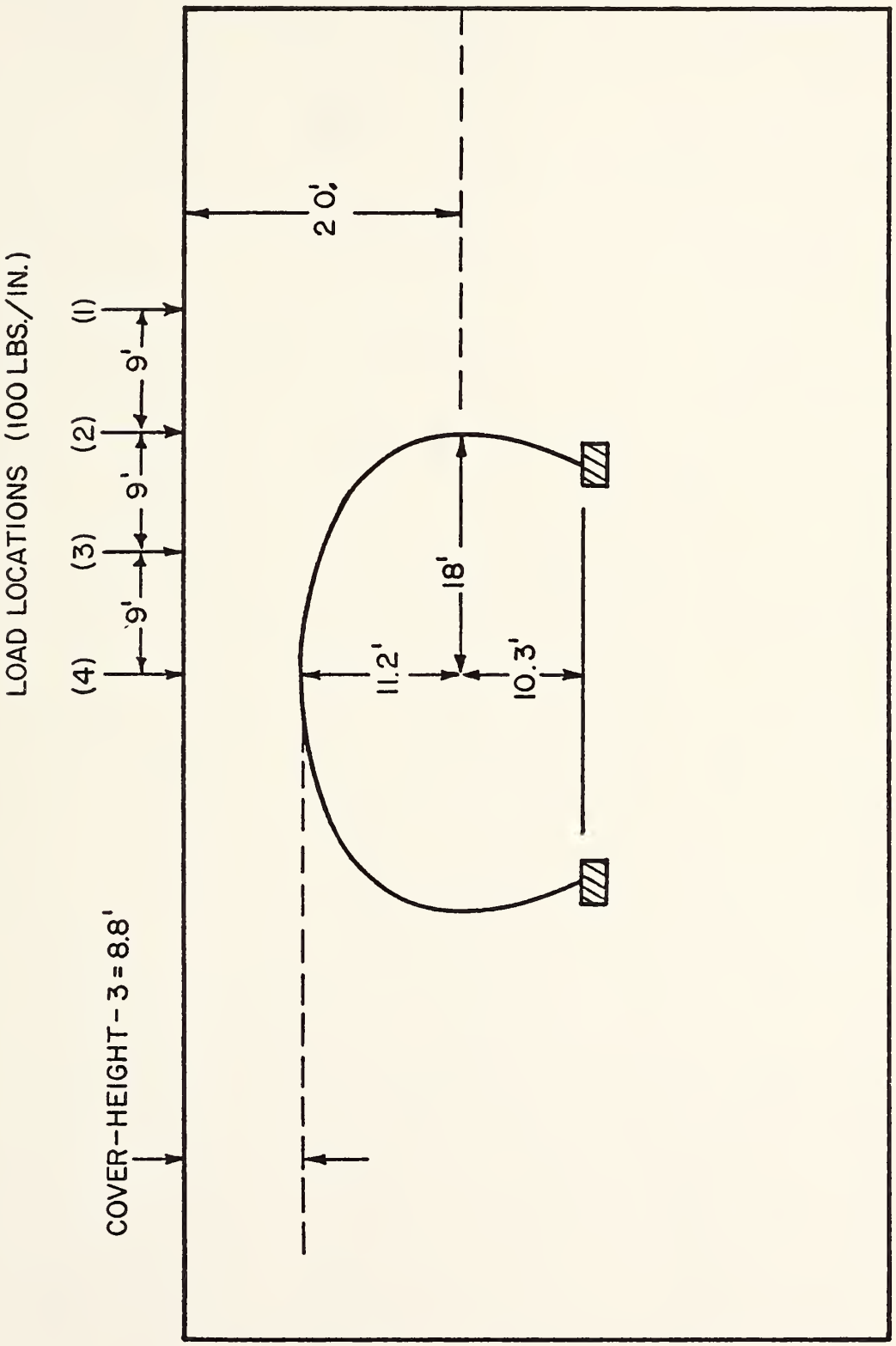

Figure 4.16 Load Locations at Cover Height Three

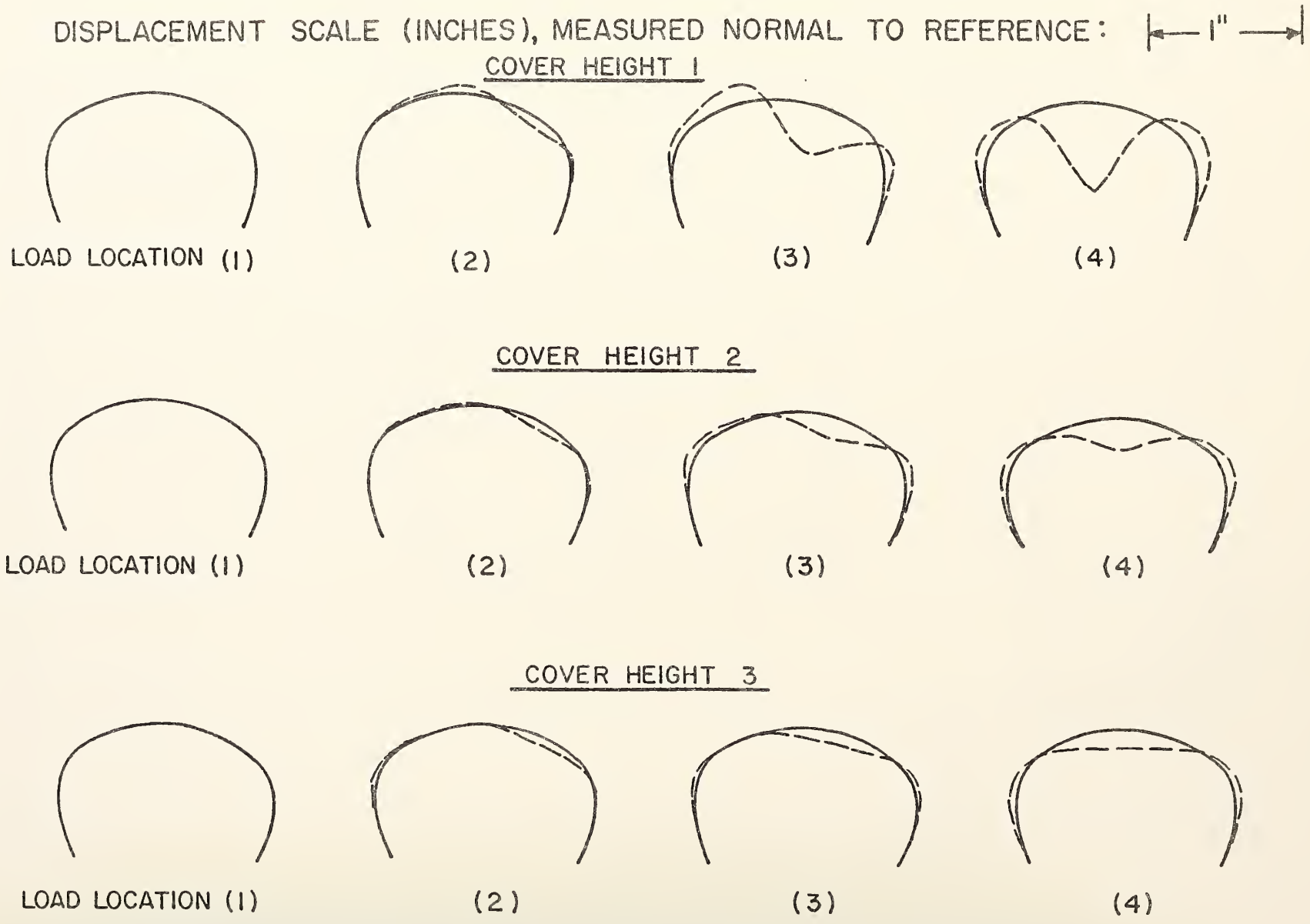

Figure 4.17 Deformed Shapes Due to Live Loads

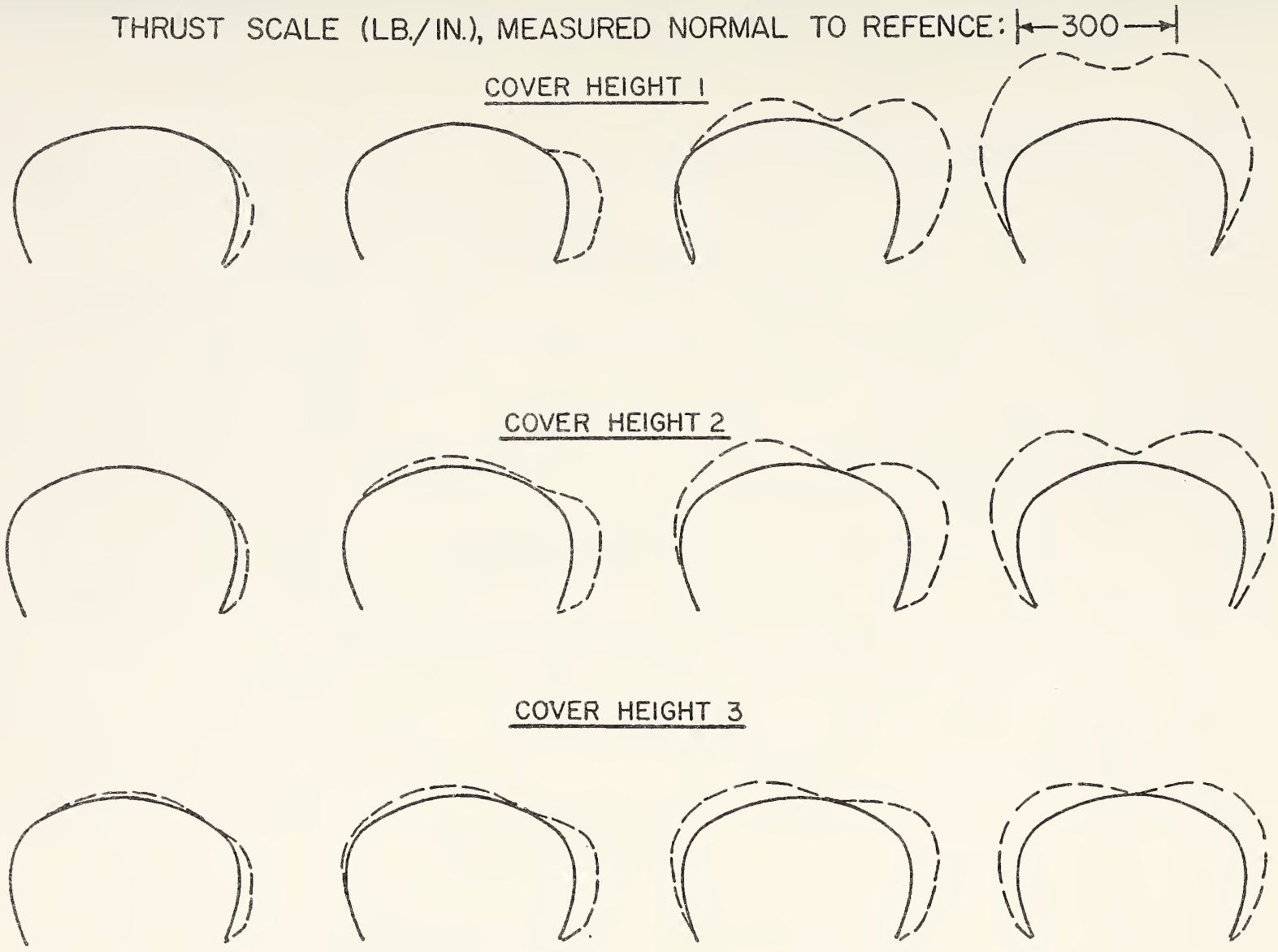

Figure 4.18 Thrust Distributions Due to Live Loads

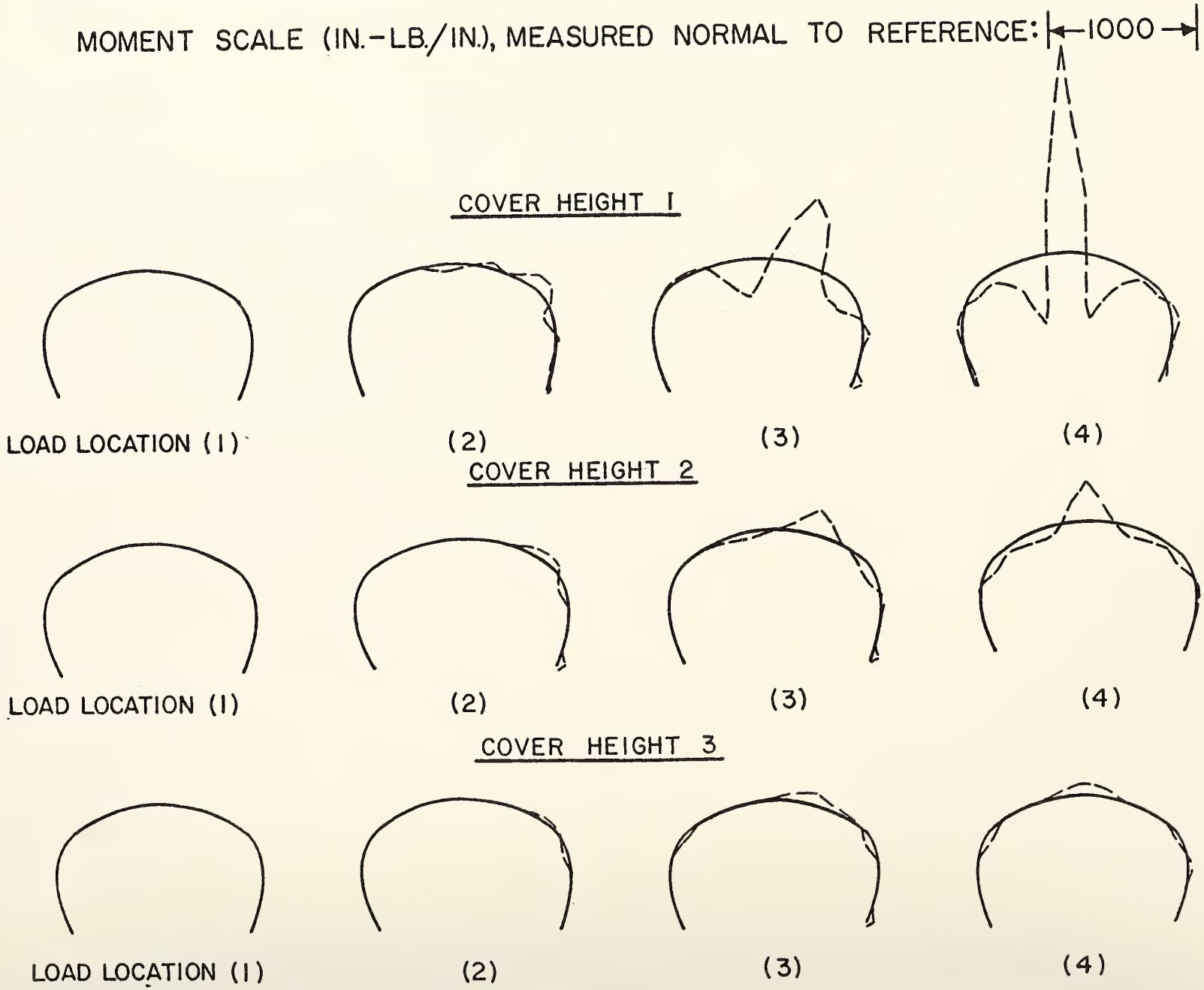

Figure 4.19 Moment Distributions Due to Live Loads

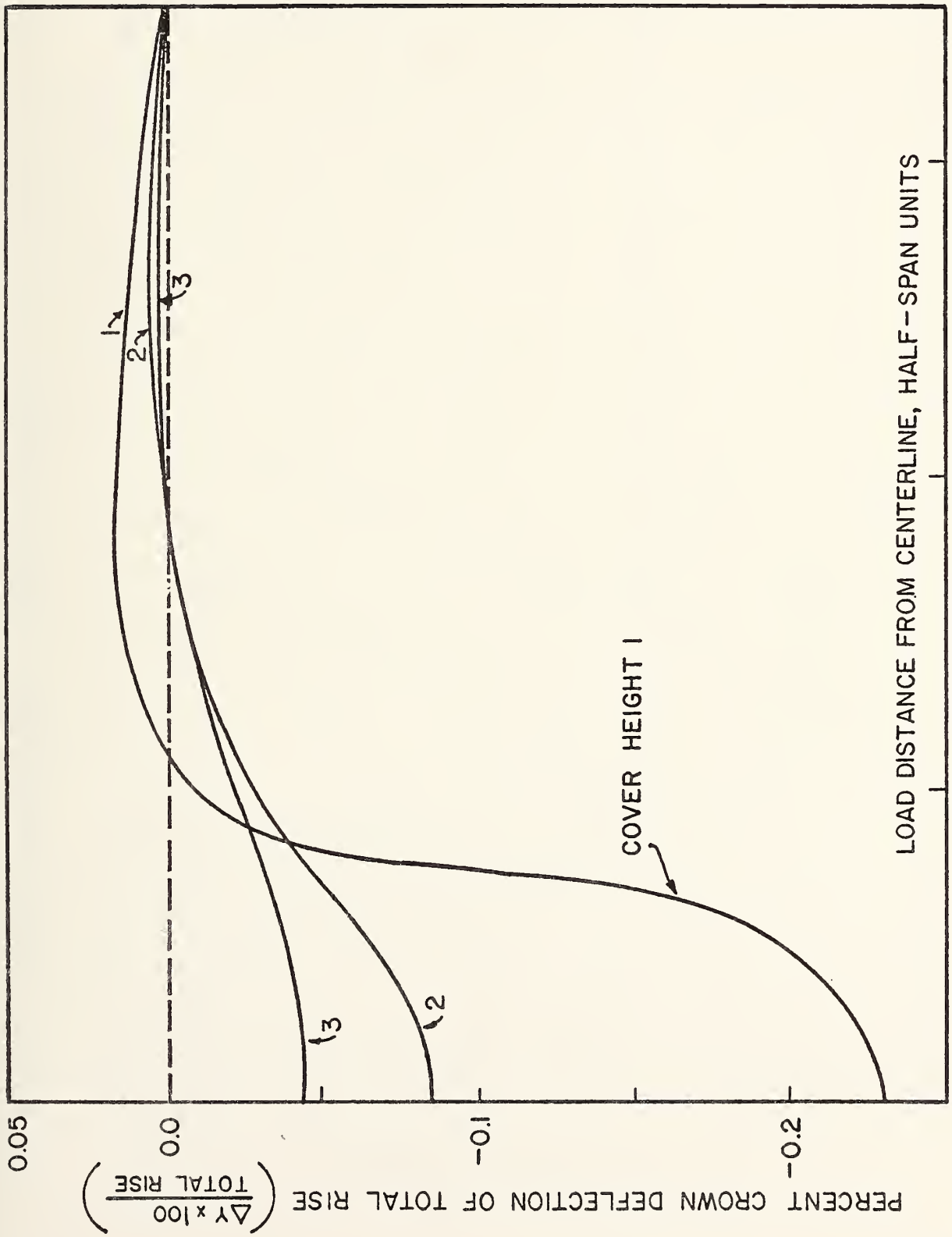

Figure 4.20 Influence Lines of Crown Deflection.

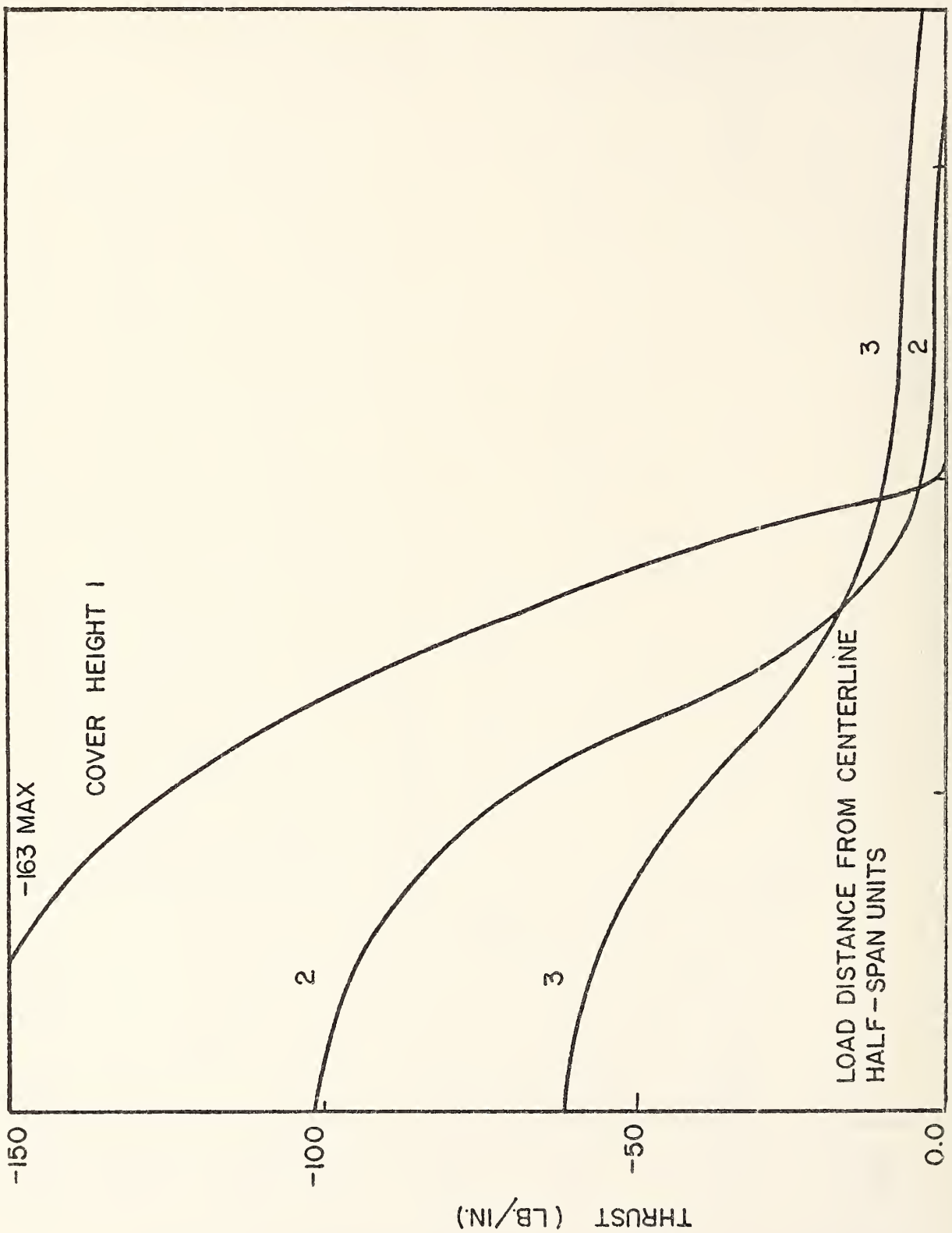

Figure 4.21 Influence Lines of Thrust at 2 O'Clock Position

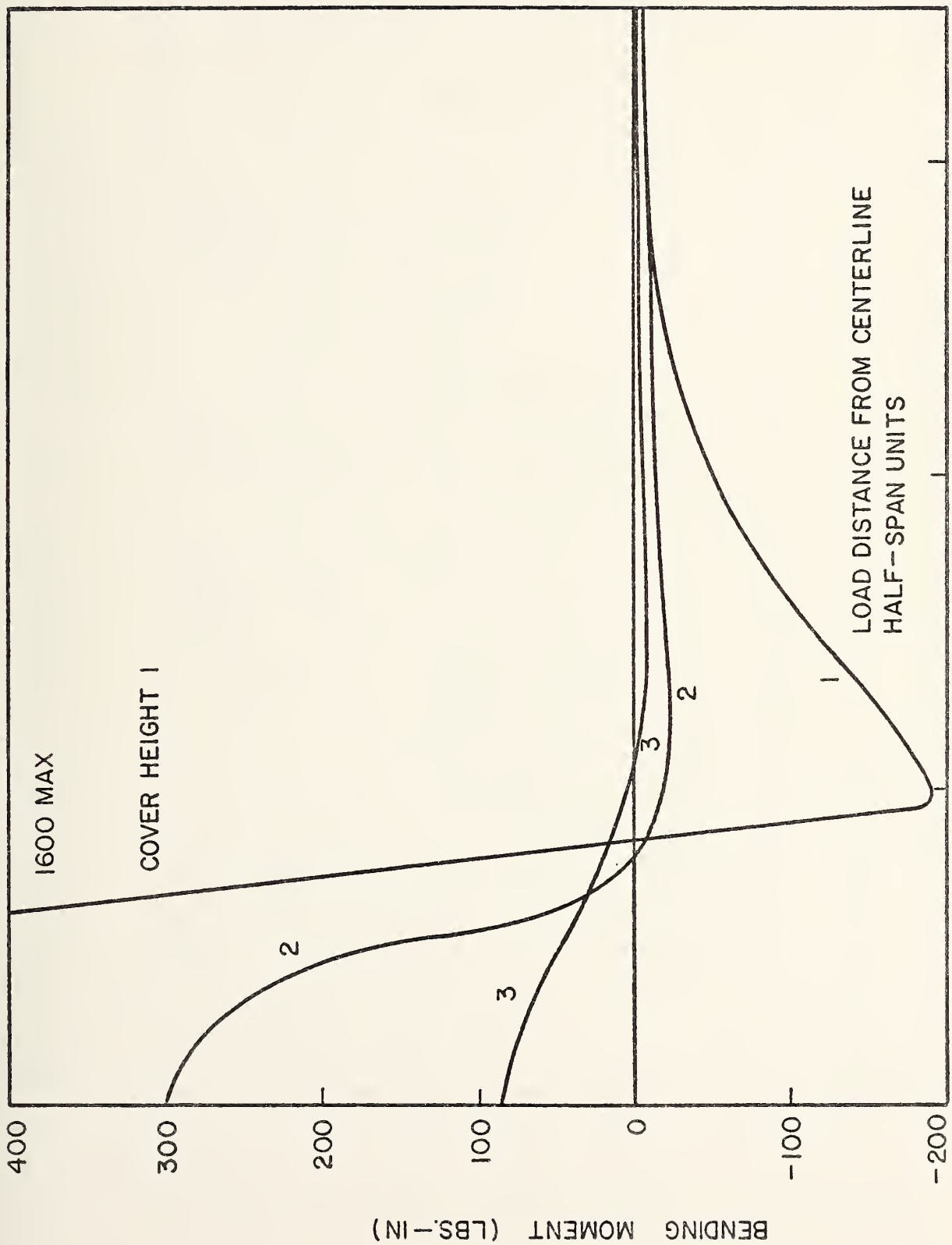

Figure 4.22 Influence Lines of Crown Moment

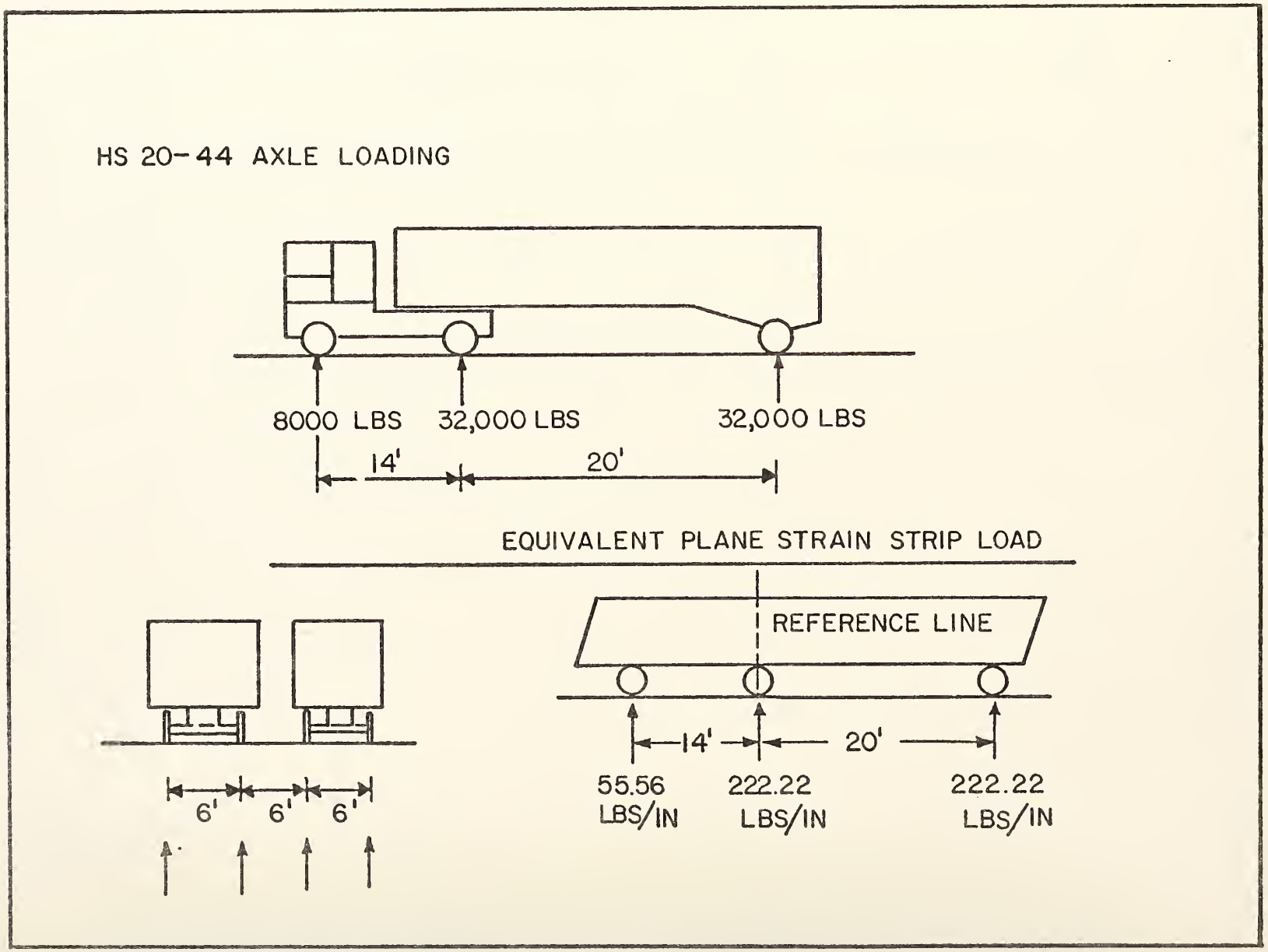

Figure 4.23 Loading Representation of HS 20-44 Truck

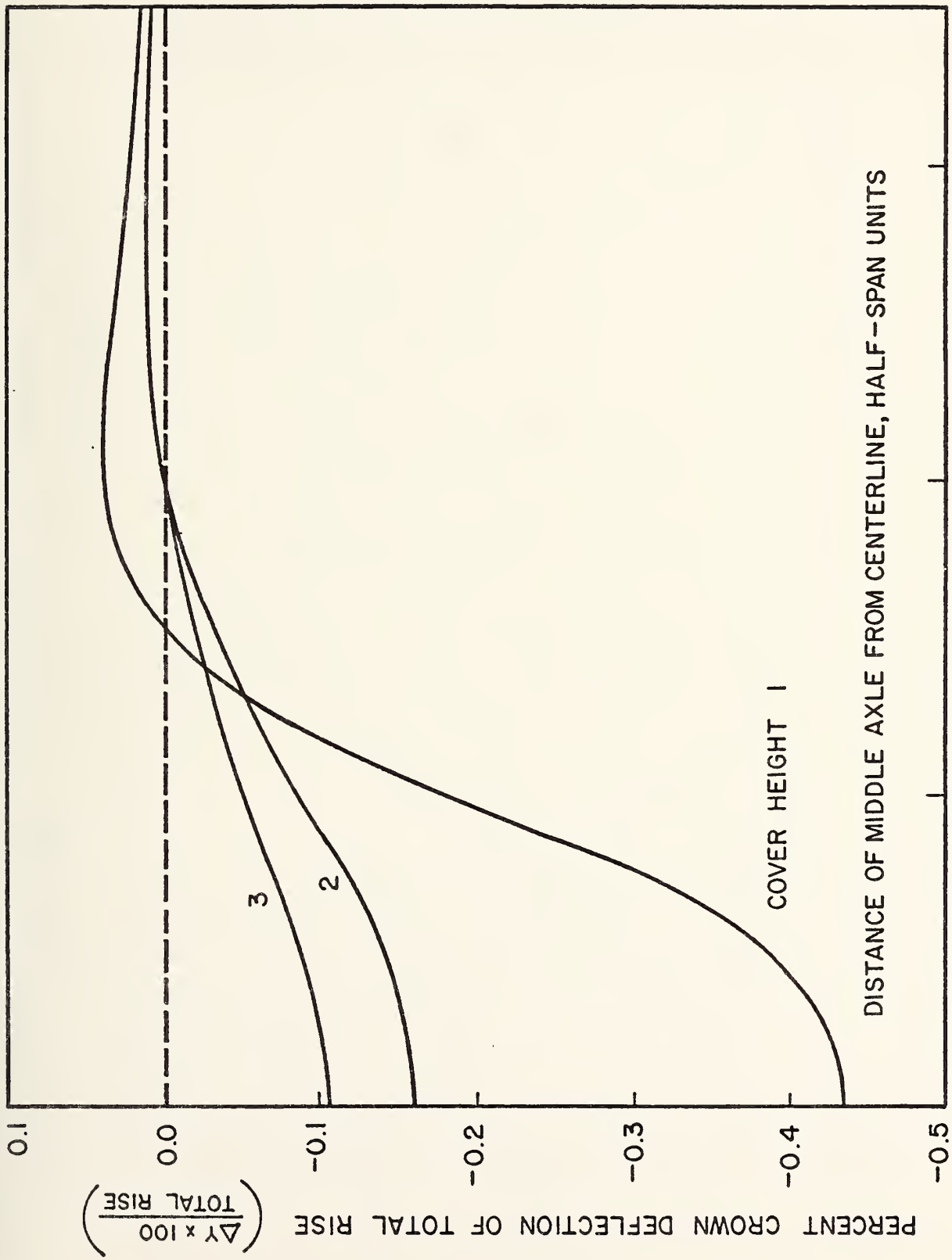

Figure 4.24 Truck Influence Lines for Crown Displacement

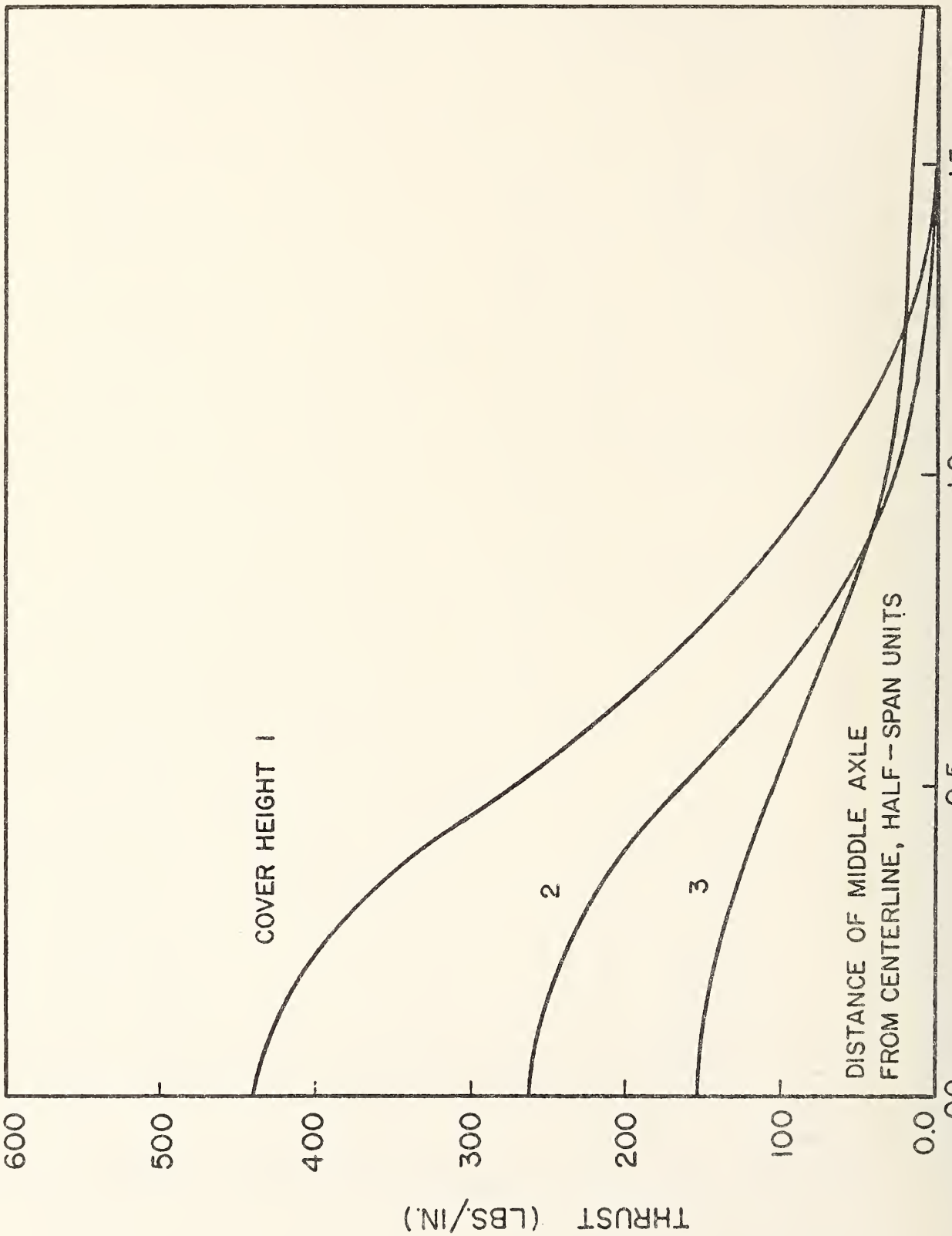

Figure 4.25 Truck Influence Lines for Thrust at 2 O'Clock Position

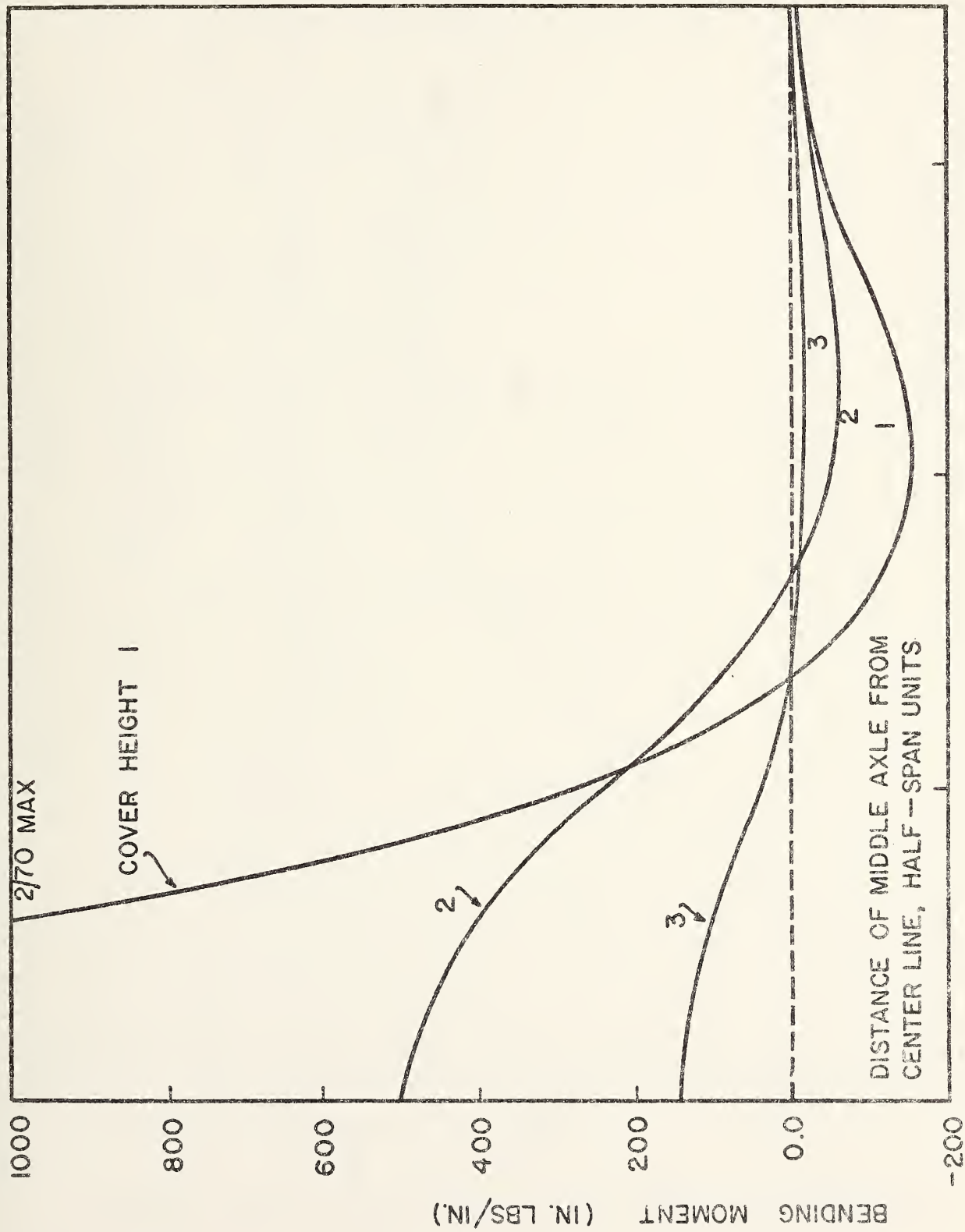

Figure 4.26 Truck Influence Line for Crown Moment

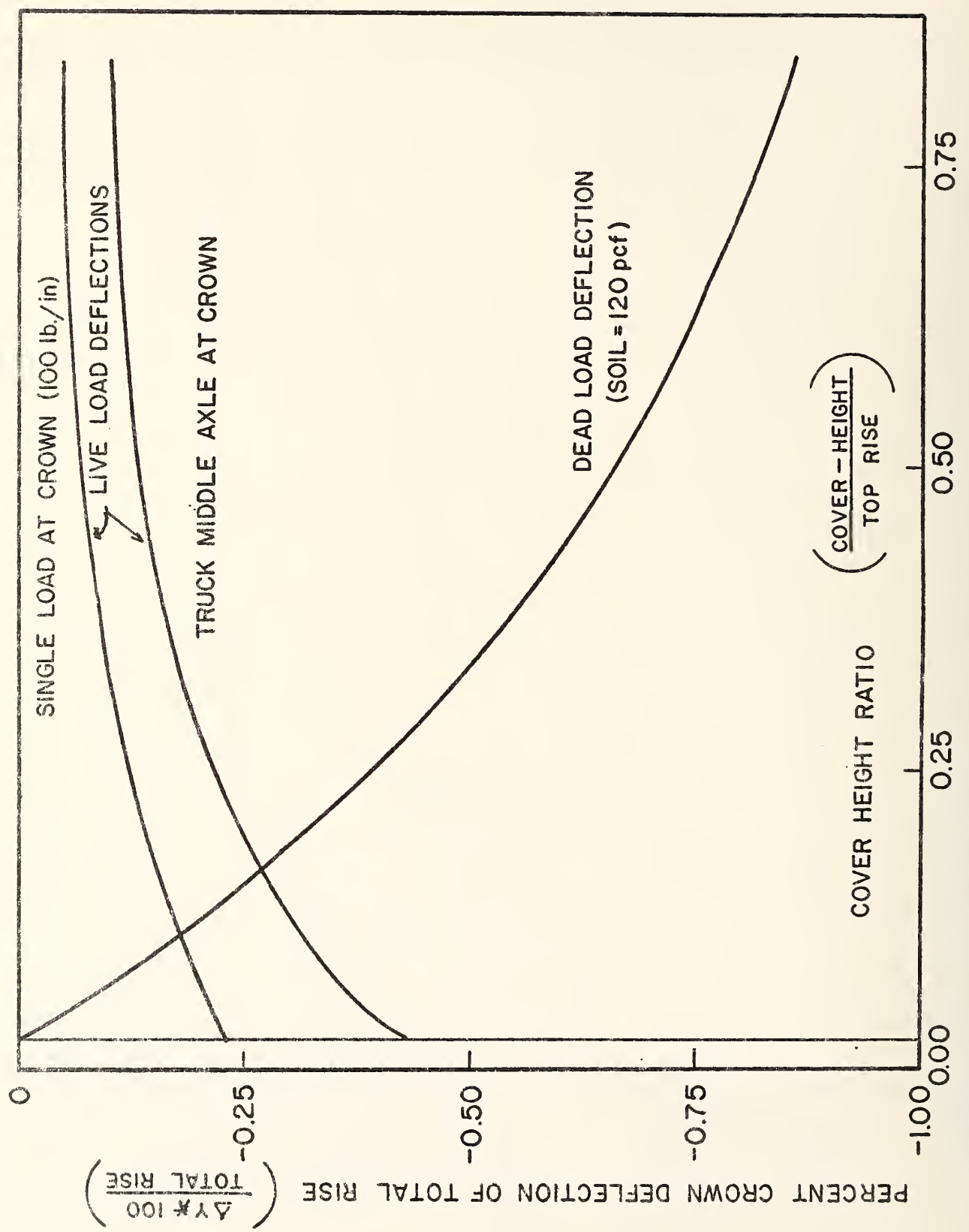

Figure 4.27 Crown Defflecton, Live Load vs. Dead Load

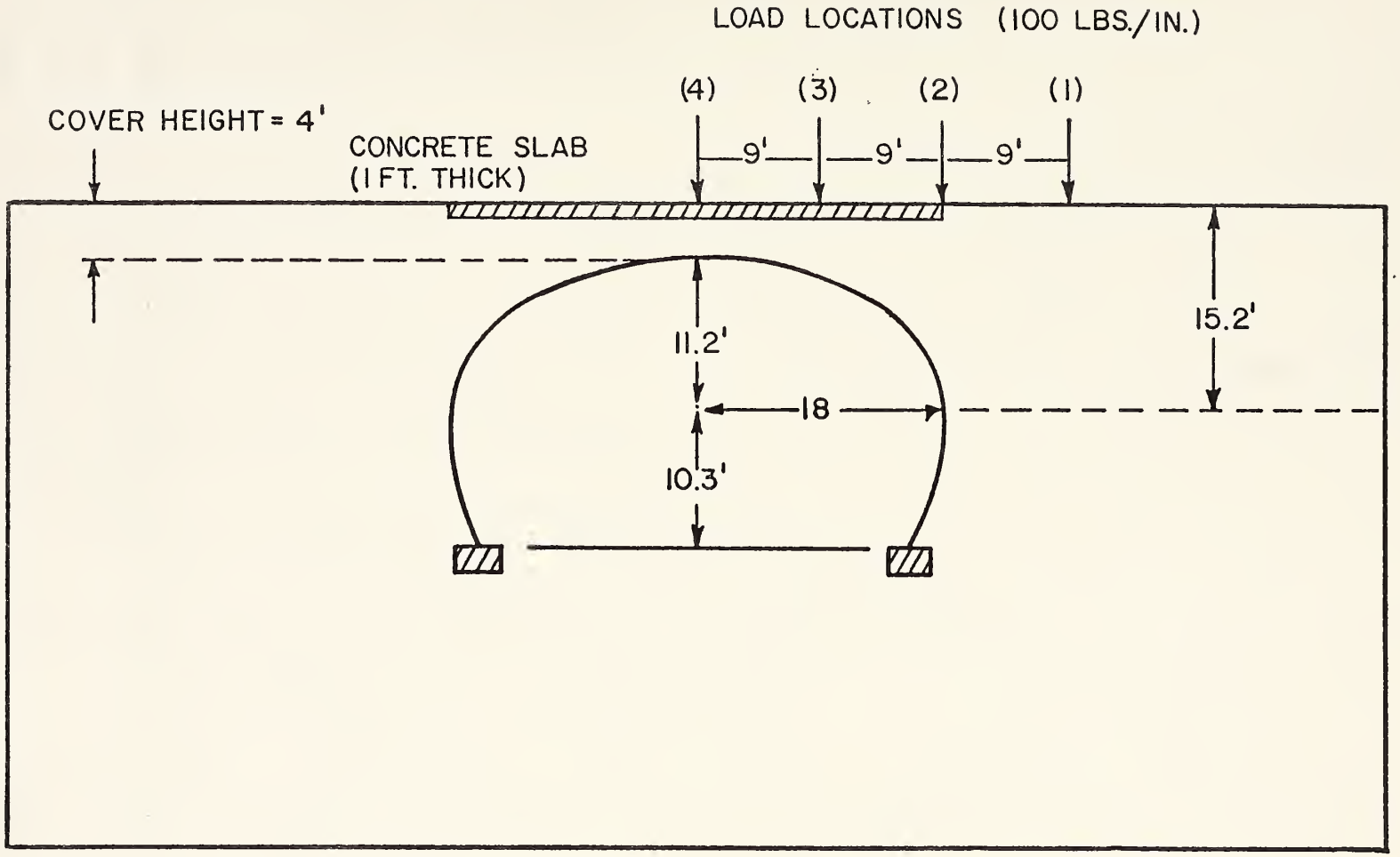

Figure 4.28 Load Locations for Cover Height 2 with Relieving Slab

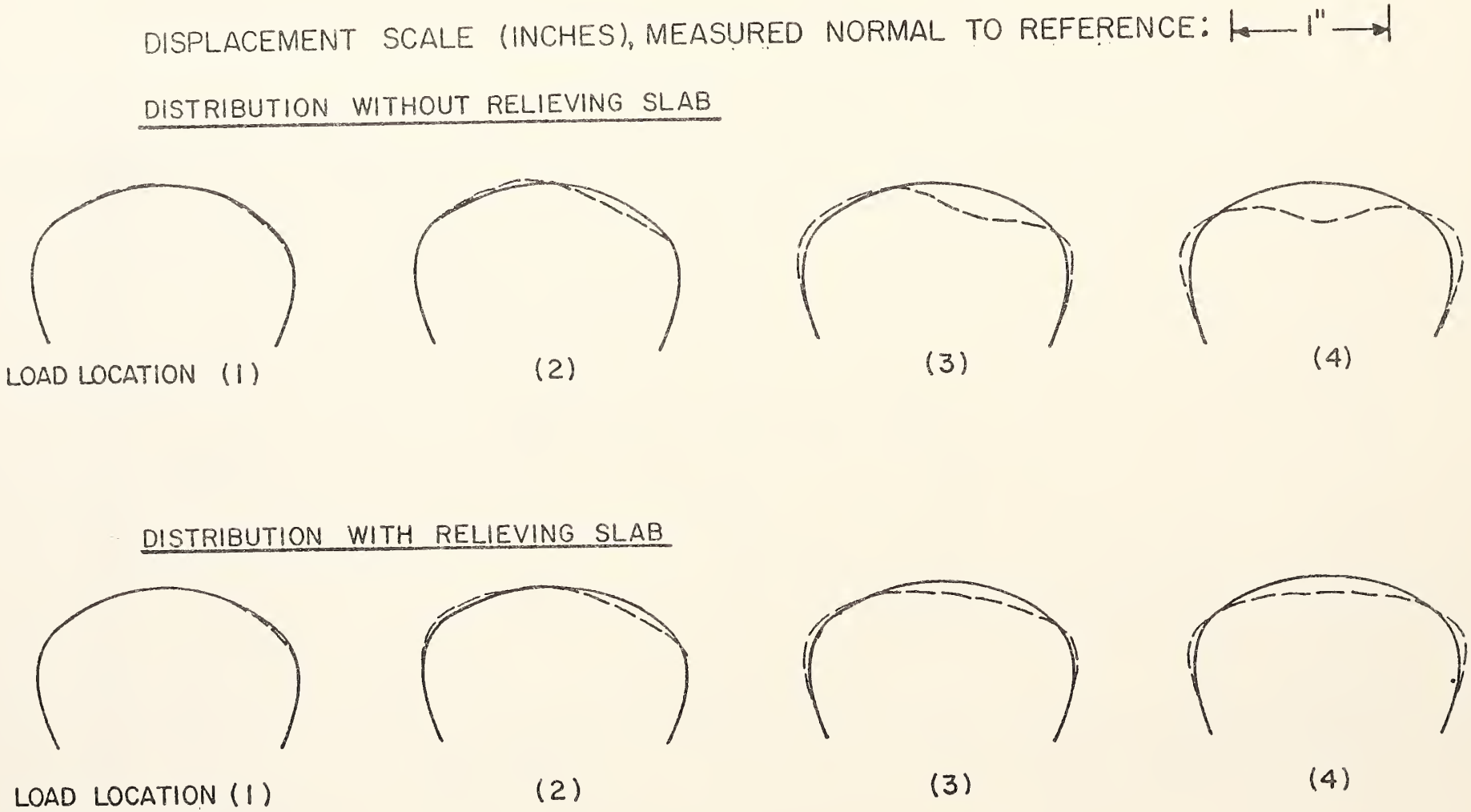

Figure 4.29 Deformed Shapes With and Without Relieving Slab

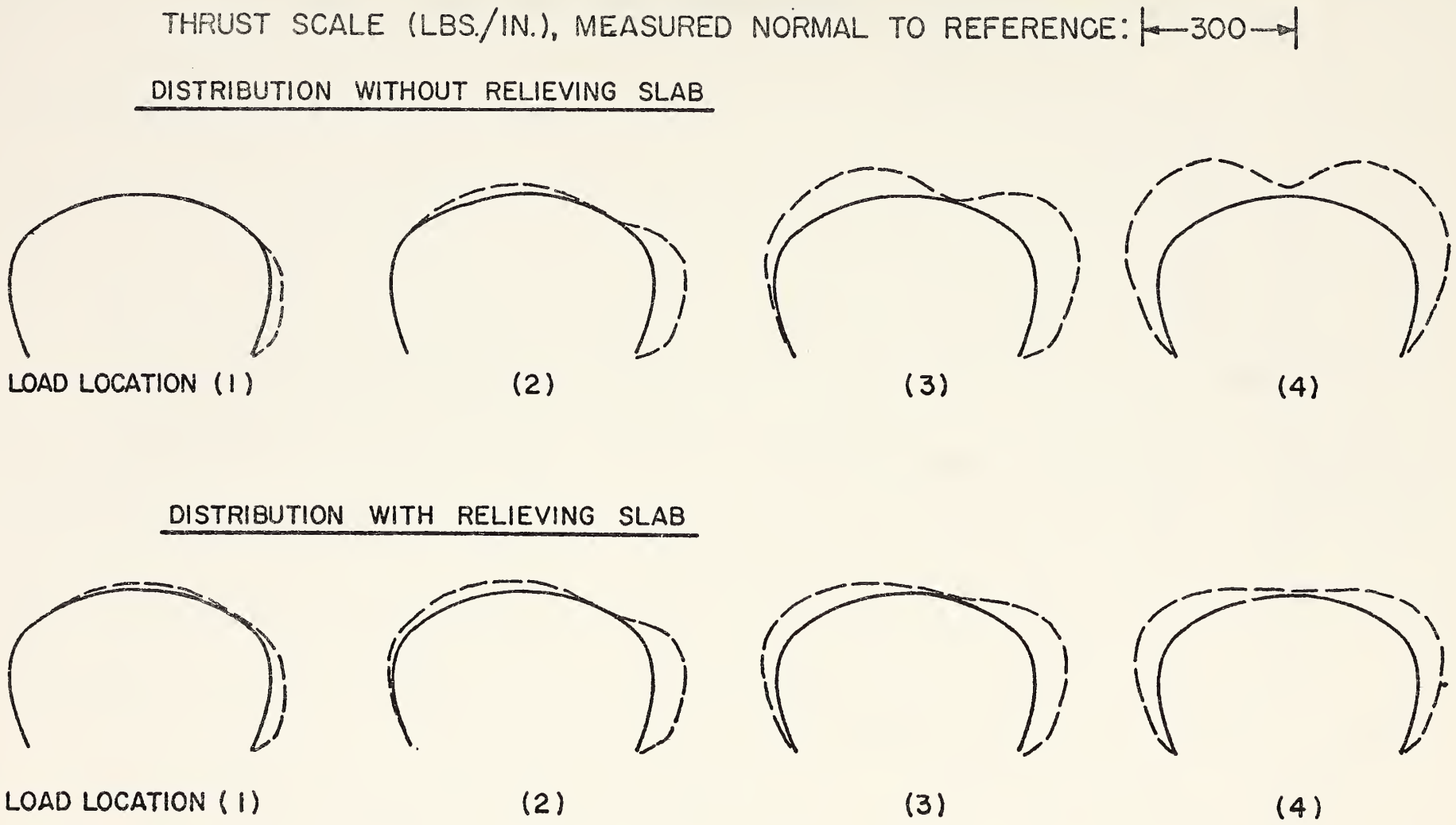

Figure 4.30 Thrust Distributions With and Without Relieving Slab

MOMENT SCALE (IN.-LBS./IN.), MEASURED NORMAL TO REFERENCE: ⊢1000⊣

DISTRIBUTION WITHOUT RELIEVING SLAB

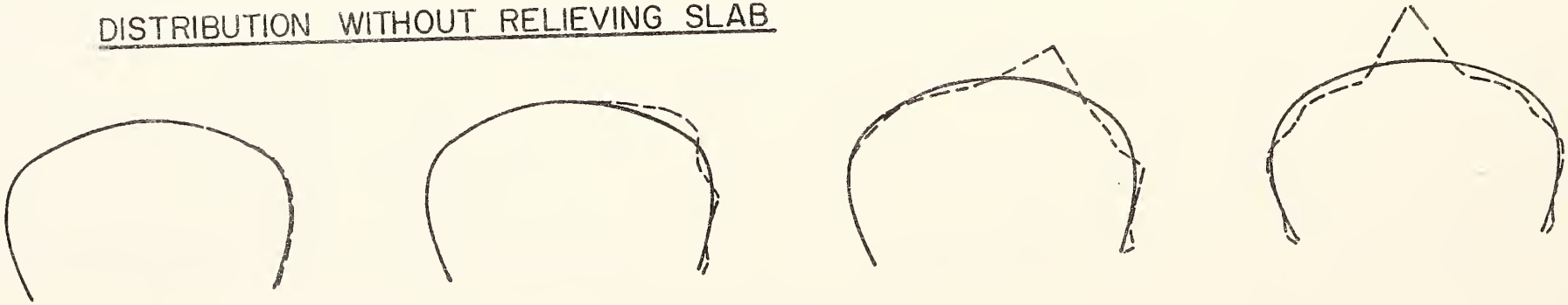

LOAD LOCATION (1) (2) (3) (4)

DISTRIBUTION WITH RELIEVING SLAB

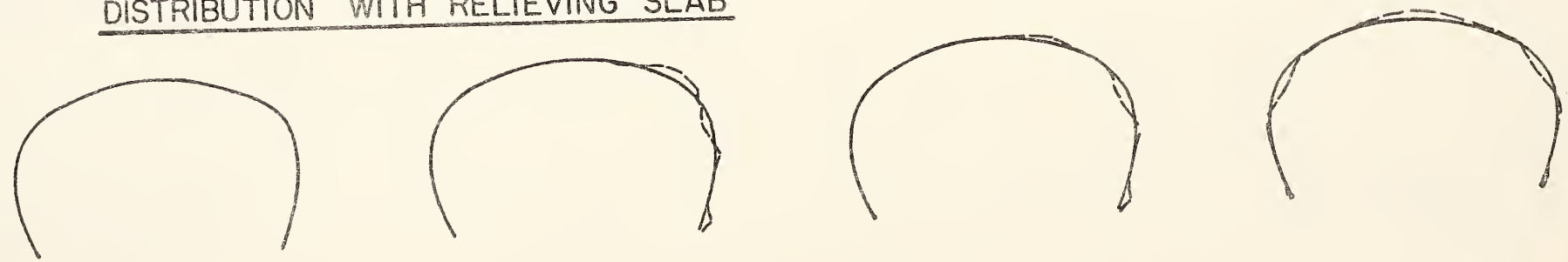

LOAD LOCATION (1) (2) (3) (4)

Figure 4.31 Moment Distributions With and Without Relieving Slab

CHAPTER 5

NONLINEAR STUDIES OF LONG-SPAN BEHAVIOR

5.1 STATEMENT OF PURPOSE

Nonlinear analysis of long-span systems can be generally classified in three catagories. (1) Geometric nonlinearity due to strain-displacement relationship, this includes large deformations (which inherently includes buckling) and large strains. (2) Material nonlinearity due to stress-strain relationship, e.g., nonlinear models of soil and structural liner. (3) Soil-structure interface nonlinearity due to relative slippage and/or separation of soil in contact with the structural liner.

In this chapter, nonlinear effects are investigated by systematically introducing each individual form of nonlinearity into the basic model presented in Chapter 3. Thus, individual nonlinear effects can be isolated and compared with the basic linear solution. The intent of this study is simply to gain insight into relative effects of each nonlinearity and to see if their effect better represents experiment data.

5.2 GEOMETRIC NONLINEARITY

The CANDE computer program used throughout this report is not formulated for large deformations or large strains. Thus, for the purposes of this particular study, the finite element program ADINA (5-1). is used. ADINA is a multi-purpose program oriented to nonlinear solid mechanics with an excellent element library. However, ADINA is not formulated for incremental construction, so that only the monolith form of the basic model is considered. As discussed in the previous chapter, the monolith form differs from the basic model only in that entire fill soil is placed in one increment and without compaction loads.

Figure 5-1 shows the deformed shape of the liner for both large and small deformation theories. Deformed shapes are

determined by adding (and magnifying) displacements to the corresponding points of the undeformed position after subtracting vertical rigid body movement of the footing.

Small deformation solutions are obtained from both the CANDE and ADINA programs and overlay each other in Figure 5-1 with less than 1% discrepancy, thereby providing a degree of confidence in their respective algorithms.

Comparing the large and small deformation solutions, it is observed that the two theories do not differ significantly, differing at most by 8% at the crown. As a general trend, the large deformation responses are slightly higher in magnitude than small deformation responses.

Thrust and moment magnitudes increased in the range of 2 to 6% for the large deformation case.

For the large deformation theory, both Lagrangian and Eulerian coordinate descriptions gave essentially identical results even though the same basic-model elastic properties were used in both descriptions. Therefore, it may be concluded that large strains were not significant and the modest difference between large and small deformation solutions can be attributed to large rotations.

For this example, the influence of large rotations does not significantly alter the solutions of small deformation theory. However, for deeper fill heights, larger spans, and/or less stiff materials, large deformations and hence, buckling could be highly significant.

5.3 SOIL-STRUCTURE INTERFACE FRICTION

In previous studies of the basic model, the soil has been assumed bonded to the structural liner, i.e., infinite friction coefficient between soil and structure. For this study, a spectrum of frictional interface values are considered ranging from fully bonded to completely frictionless.

The analytical model of interface friction is developed in detail in the CANDE Engineering Manual. The development is based on the Coulomb friction hypothesis which in this case implies that relative frictional movement between soil and structure will occur whenever the shear traction stress exceeds the normal interface pressure times the friction coefficient, μ. Thereafter, shear traction is equal to the frictional stress limit unless the relative movement tends to reverse direction in which case rebonding occurs.

To incorporate this frictional behavior into the basic model, special interface elements (available in the CANDE program) are introduced. This entails adding two additional nodes to each node of the structural liner. One node is associated with soil in contact with the structure node, and the other node is a dummy node whose degrees of freedom are Lagrange multipliers representing traction and normal forces across the interface.

Except for the above changes in mesh topology to accomodate the interface elements, the basic model remains the same as defined in Chapter 3.

Crown displacement history as a function of fill height is shown in Figure 5-2 for four cases of friction; μ = 0.0, 0.2, 0.5 and ∞ (basic model). Maximum crown peaking is more than doubled for the intermediate frictional cases as compared to the fully bonded basic model. In the post-peaking range, crown flattening occurs at the same rate for all cases with a near constant offset for the fully bonded case. At full fill height, maximum flattening of the intermediate frictional cases is only one-half that of the fully bonded case.

Crown deflection trends for intermediate frictional cases appear in better agreement with observed experimental data in Chapter 2, e.g., crown deflections pass through the origin at fill-height-ratios greater than 2.0.

Springline thrust histories, shown in Figure 5-3 for the four friction cases, decrease as the frictional coefficient

decreases. A maximum reduction of 16% is observed for the frictionless case as compared to the bonded case.

At full fill height, distribution plots for deformation, thrust, and moment are shown in Figure 5-4 for three friction conditions, $\mu = \infty$, 0.5, and 0.0. As friction decreases, the thrust distribution becomes more uniform, equalizing thrust at crown and springline. No significant change is observed in moment distributions or magnitudes for the three frictional cases except near the crown (see Figure 5-4).

5.4 MATERIAL NONLINEARITY

Stress-strain relationships for fill soil and structural liner are the fundamental areas of material nonlinearity of long-span systems. These are discussed in turn.

Soil Nonlinearity. The analytical treatment of soil is one of the most significant parameters for predicting deformed shape and bending moments of long-span structural liners. This is demonstrated in the next chapter for a range of linear soil stiffness wherein it is shown deformed shaped is inversely proportional to soil modulus. Naturally, this same trend applies to nonlinear soil models, however, the soil stiffness distribution is dependent on stress/strain state and loading history. Thus, the response is highly dependent upon the particular nonlinear soil model being considered.

Among investigators in the field of soil-structure interaction, there is no unaniminty of opinion on the correct nonlinear soil model. Generally, nonlinear soil models are classified in two groups; plasticity models and variable modulus models. The former group is based on the theory plasticity, which in general requires specification of a yield condition, hardening rule, and flow rule. Examples of plasticity models applied to soils are the Drucker-Prager, Mohr-Coulomb, and capped models (5-2).

Variable modulus models are based on the hypothesis that stress increments are related to strain increments by an elastic constitutive matrix whose components are dependent stress/strain state and loading history. Many variable modulus models have been proposed in the literature and differ among themselves in form and technique. Examples are; Duncan (5-3), Hardin (5-4), Kondor (5-5), and Corotis (5-6). One commonality among these models is that soil stiffness is increased (in varying degrees) as confining pressure increases.

For this study, no attempt is made to compare and contrast the various nonlinear soil models. Rather, the fundamental effect of increased stiffness due to confining pressure (overburden loading) is examined by using the overburden-dependent soil model described in the CANDE Engineering Manual. The overburden-dependent model is a rudimentary variable modulus model that increases soil stiffness (Young's modulus) for each individual soil element dependent on current verticle pressure on the element plus one-half the overburden pressure (soil lift) placed above the element during the current construction increment. Table 5-1 gives Young's modulus (secant) as a function of vertical overburden pressure used in this study. These values are taken from the CANDE Engineering Manual and represent a granular soil with good compaction. Poisson's ratio is constant at 0.35.

Figure 5-5 shows a comparison of crown displacement history for the basic model with overburdent dependent soil modulus and the standard elastic case (Young's modulus = 2000 psi (13,800 kPa)). A greater amount of peaking is observed for the overburden dependent model because during early stages of construction overburden pressure is small, producing soil moduli less than the standard elastic case. As the fill height increases, the overburden dependent model increases stiffness so that crown flattening is somewhat less than the elastic case.

Table 5-1: Overburden-dependent Model

Overburden Pressure (psi)	Secant Young's Modulus (psi)
5.0	1100.0
10.0	1300.0
15.00	1500.0
20.0	1650.0
25.0	1800.0
30.0	1900.0
40.0	2100.0
50.0	2250.0

1 psi = 6.895 kPa

At full fill height, the maximum thrust is reduced 1% and maximum moment is reduced 11% for the overburden-dependent model as compared to the standard basic model.

Although only modest changes in structural responses were observed by introduction of the overburden-dependent soil model, one should not conclude nonlinear soil models are not significant. On the contrary, some variable modulus models can have a pronounced effect on structural responses. The simple overburden-dependent model used in this study does not include stiffness reduction due to increased deviatoric stresses which is characteristic of soils. Nor did it include variations in Poisson's ratio.

Structure Nonlinearity. Unlike soil nonlinearity, material nonlinearity for steel structures is well defined and can be represented by an elastic-perfectly plastic relationship within the working range for long spans. For this study, yield stress of the steel liner is 33,000 psi (228,000 kPa) with no special consideration for seam strength, i.e., seam and wall properties are assumed identical (Chapter 7 provides a discussion on seam slippage). Except for the introduction of the elastic-plastic model for steel, all parameters remain as defined for the basic model.

For this long-span system, initial outer fiber yielding begins when the fill height is 1.10 top-rise units above the crown. The yielding occurs slightly above the springline on the liner extrados as a consequence of combined bending and thrust. Bending stress contributes 61% and thrust stress contributes 39% of initial yielding.

At full fill height (1.6 top-rise units above crown), metal yielding extends upward from the springline covering 22% of the liner perimeter from springline to crown. Maximum plastic penetration is 44% of the corrugated cross-section occuring at the point of initial yielding.

Crown displacements and thrust force are not effected by metal yielding, i.e., less than 0.2% difference between linear and nonlinear results. However, maximum moment is reduced by 14% due to plastic hinging.

5.5 SUMMARY OF NONLINEAR EFFECTS

Large deformation theory produces a slight increase (8%) for maximum crown displacement as compared to small deformation theory. Other structural responses are in closer agreement. Differences between large and small deformation solutions are attributed to rotations not strains.

Low values of interface friction between structure and soil increase crown peaking on the order of 100% compared to the fully bonded assumption. Contrarily, maximum flattening is reduced by 50%. Thrust is reduced and becomes more uniform as friction decreases. Models with intermediate values of friction appear to give the best representation of observed behavior.

Nonlinear material models for soil (overburden-dependent) and structure (elastic-plastic) do not significantly alter responses for displacements and thrusts for the basic model. However, for other soil-structure systems these effects may be more significant.

5.6 Figures 5-1 through 5-5

		Page
Fig. 5-1	Deformed shapes (magnified) for small and large deformation theories.	128
Fig. 5-2	Effect of interface friction on crown displacements.	129
Fig. 5-3	Effect of interface friction on springline thrust.	130
Fig. 5-4	Distribution plots for three interface friction conditions.	131
Fig. 5-5	Comparison of overburden-dependent and elastic soil models on crown deflection.	132

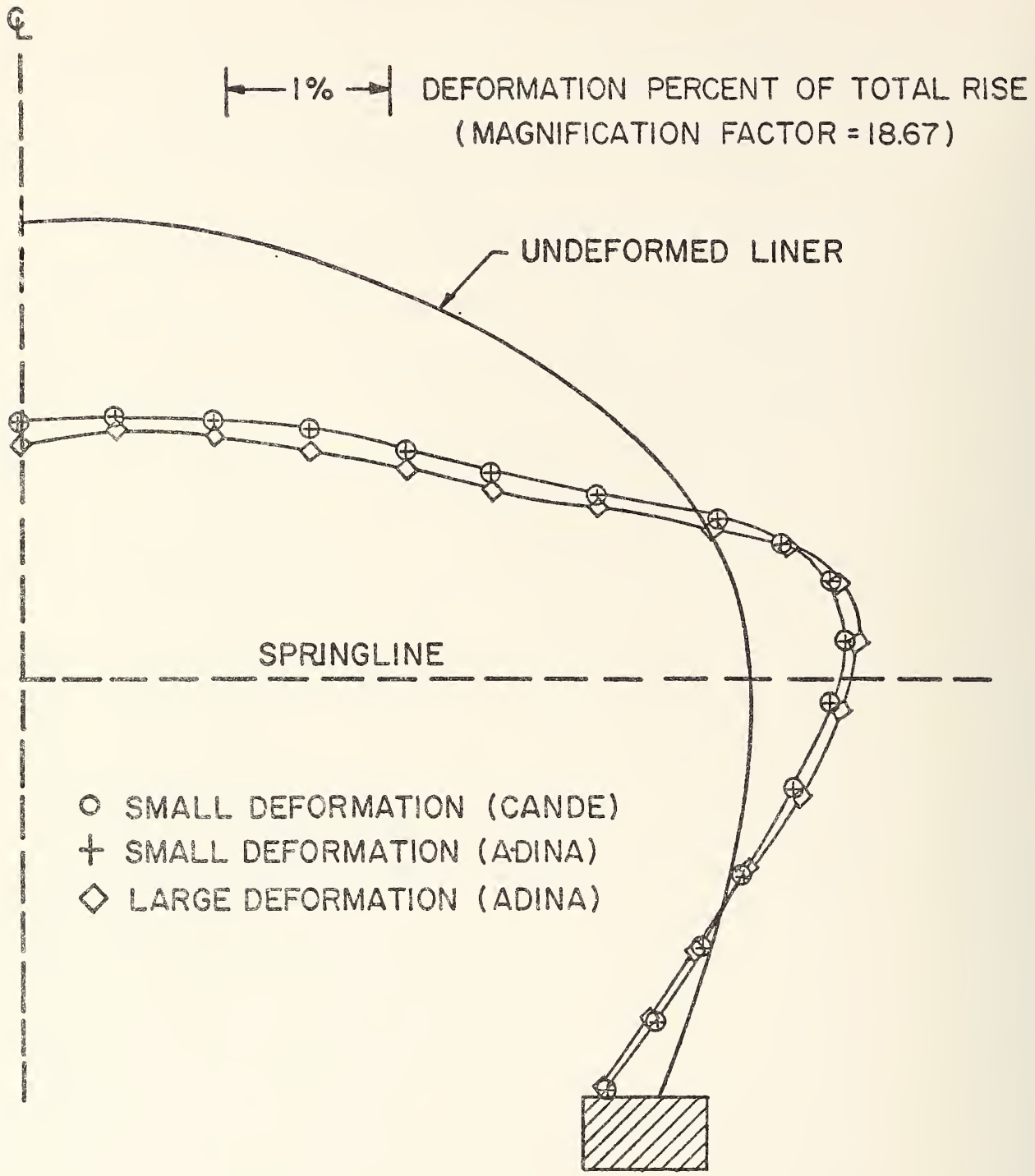

Figure 5.1 Deformed Shapes (Magnified) for Small and Large Deformation Theories

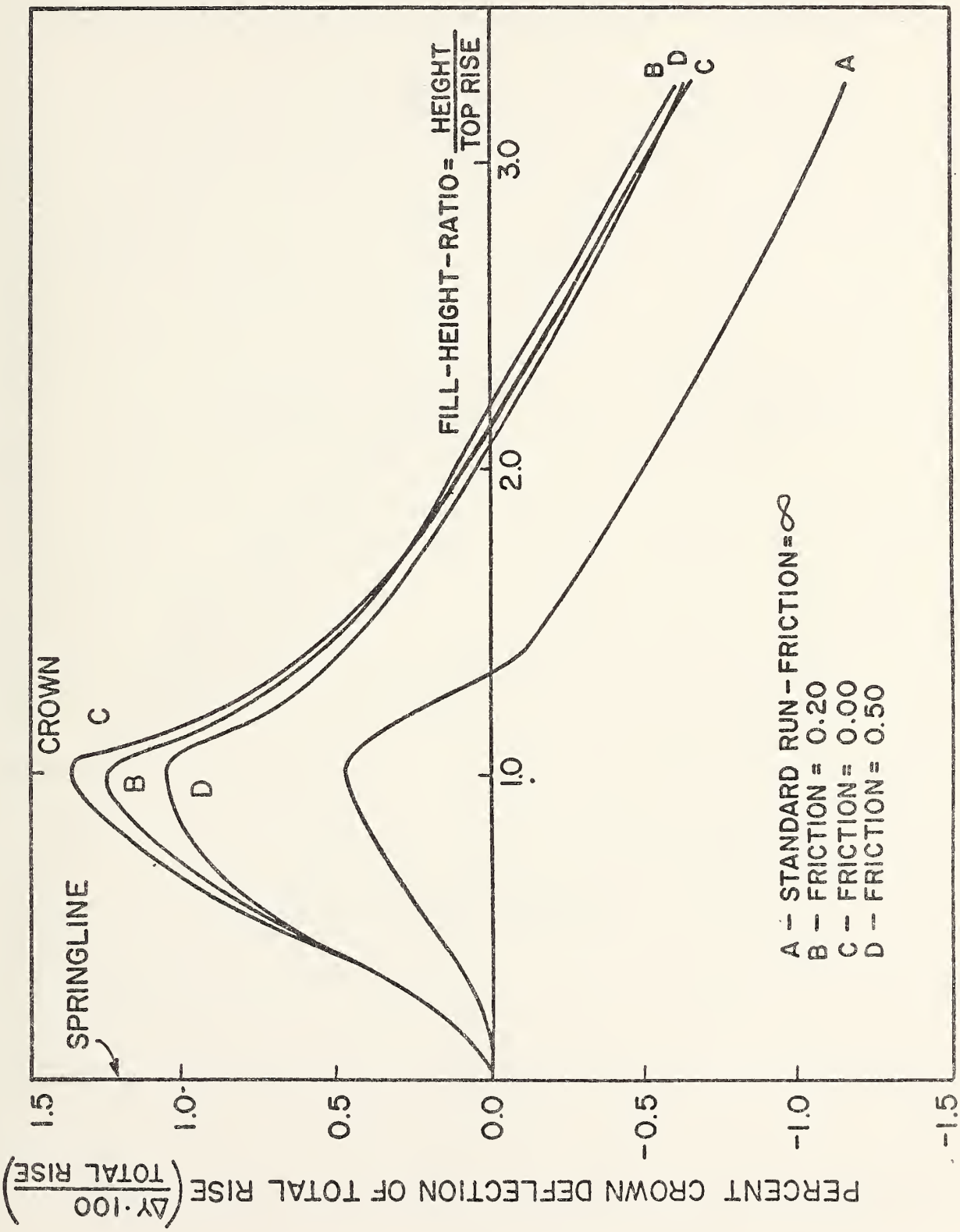

Figure 5.2 Effect of Interface Friction on Crown Displacements.

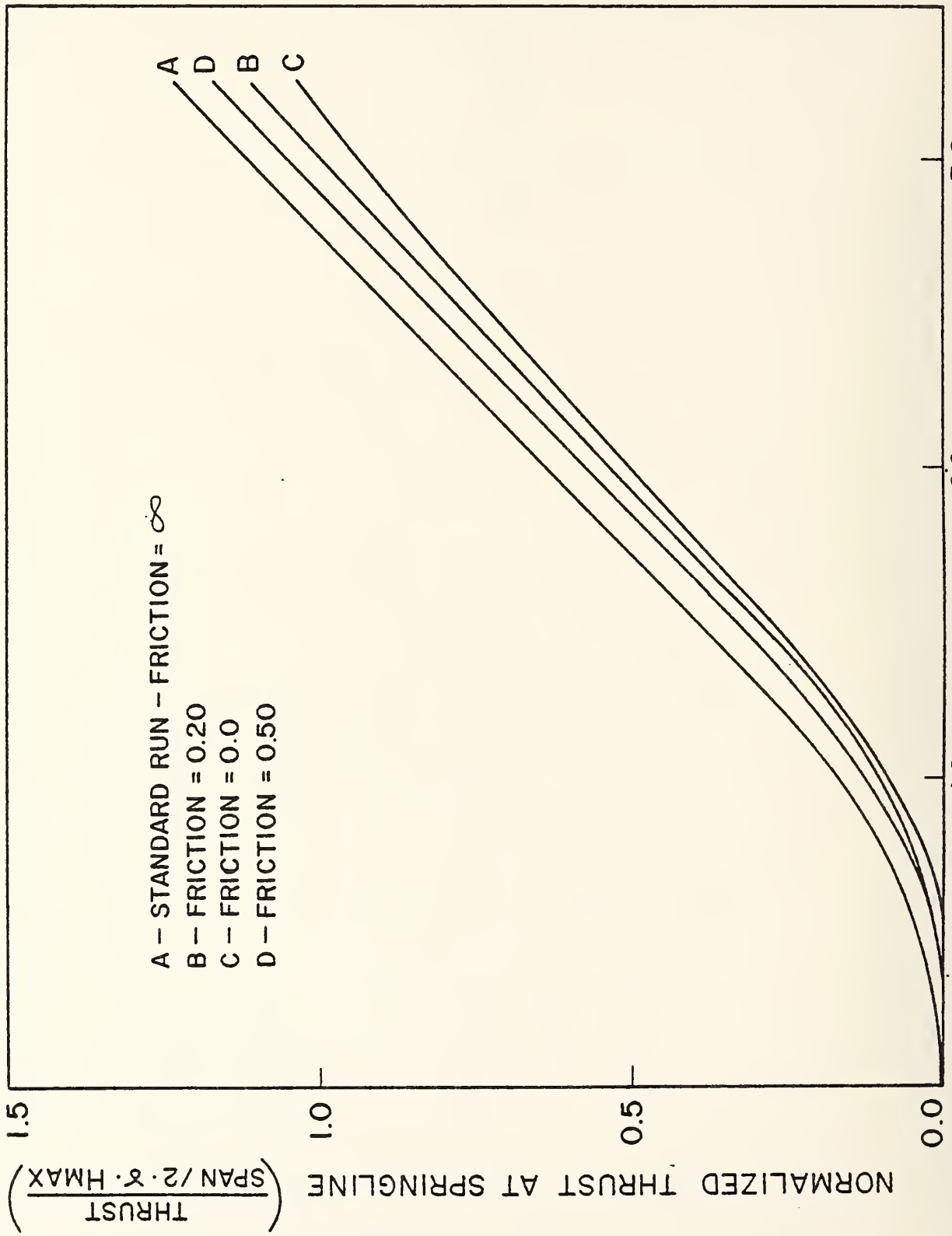

Figure 5.3 Effect of Interface Friction on Springline Thrust.

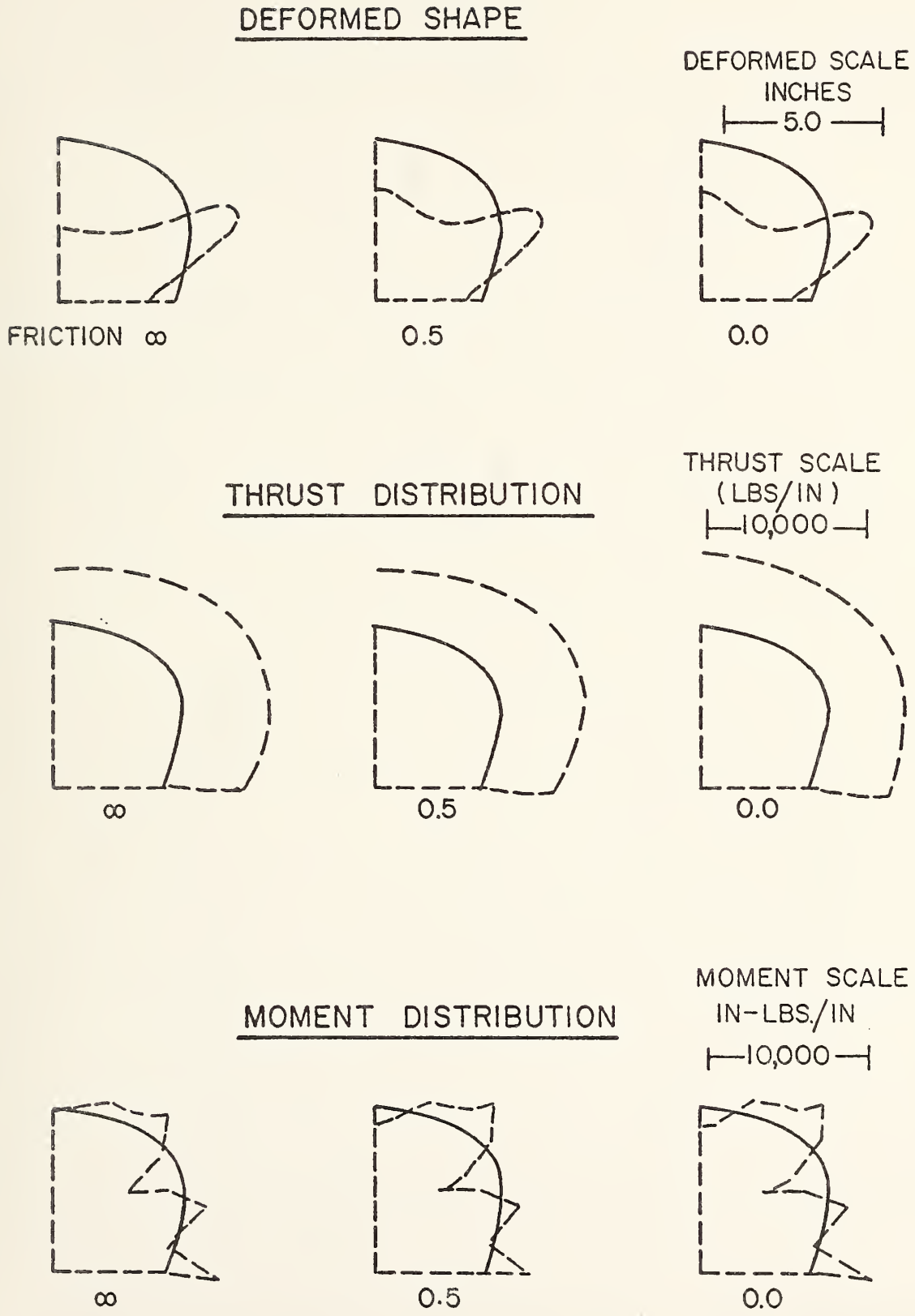

Figure 5.4 Distribution Plots for Three Interface Friction Conditions

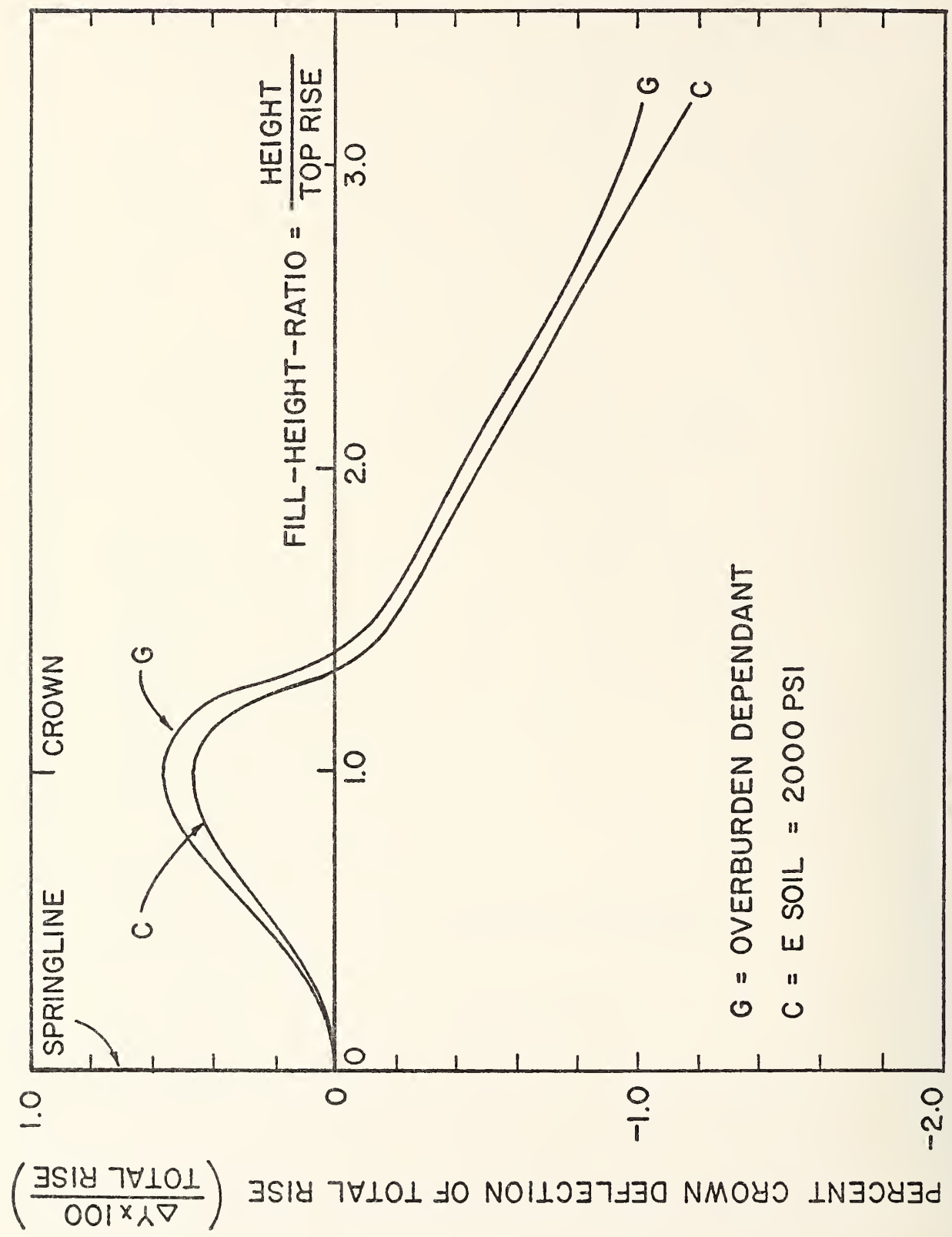

Figure 5.5 Comparison of Overburden-Dependent and Elastic Soil Models on Crown Deflection

CHAPTER 6

PARAMETER STUDIES OF CONVENTIONAL LONG SPANS

6.1 STATEMENT OF PURPOSE

For conventional long-span systems, the major structural design specifications include the following fundamental parameters; soil stiffness (quality and compaction), footing width for arches, liner thickness, liner shape, liner scale, and special manufacturing features. In this chapter, the relative influence of these fundamental parameters are analytically examined to provide insight into their effectiveness for enhancing long-span structural performance. In addition, this study provides a background for new design concepts presented in Chapter 7.

To ascertain the relative merits of the above fundamental parameters, the basic high profile arch system defined in Chapter 3 is used as reference. Selective alterations of the basic model are introduced to isolate the effect of each parameter variation. In all cases, linear material properties are assumed. Structural performance is evaluated by crown deflection (peaking and flattening), maximum thrust, and maximum moment. Table 6-1 contains a summary of key structural response ratios for all parameter variations and will be discussed in turn.

6.2 SOIL STIFFNESS

In conventional long-span installations, soil stiffness is controlled by the compaction method and structural quality of the backfill soil. For this study a narrow but practical range of soil stiffness is considered by halving and then doubling Young's modulus of the basic model backfill soil (13800 kP_A or 2000 psi). All other parameters are left unchanged.

Figure 6-1 shows crown deflection history during the

Table 6-1: Structural Response Ratios at Full Fill Height*

Structural Response Ratio	Soil Stiffness		Footing Width		Liner Thickness		Liner Shape		Liner Scale		Special Features		
	One-half (1000 psi)	Double (4000 psi)	Narrow (2 ft)	Wide (4 ft)	Light Cage (10)	Heavy Cage (1)	Low Profile	Horizontal Ellipse	Small Scale (2/3)	Large Scale (3/2)	Thrust Beam	Soil Bin	Stiff Ribs
Crown Displacement	1.99	0.52	0.97	1.03	1.02	0.99	0.83	2.17	0.61	1.61	0.99	1.09	0.85
Maximum** Thrust (near springline)	1.01	0.98	0.99	1.01	0.99	1.00	0.95	0.90	0.63	1.62	1.02	1.01	1.01
Maximum Moment (near springline)	1.69	0.58	0.99	1.01	0.69	1.23	1.09	0.71	1.03	0.93	1.06	1.00	12.10
Springline Horizontal Displacement	1.98	0.49	0.97	1.02	0.99	1.00	0.98	1.35	0.57	1.65	0.99	1.01	0.65

*Each ratio is formed by dividing the response of the varied system by the corresponding response of the basic model (unvaried system).
For reference, response values of the basic model are:
Relative crown displacement = -3.002 inches
Maximum thrust = -5522 lbs/in
Maximum moment = -3878 in-lbs/in
Springline displacement = 1.69 inches (for half-span)

**Both maximum moment and maximum thrust generally occur in liner slightly above springline.

placement of fill soil from the springline to maximum fill height for the three cases of fill soil modulus. It is observed that maximum crown peaking and maximum flattening occurs in almost inverse proportion to the soil stiffness. Thus, soil stiffness is highly significant in controlling deformations.

In contrast, Figure 6-2 shows that springline thrust, which is maximum thrust, is not significantly changed by increased soil stiffness.

Maximum moments, like displacements, are reduced with increased soil stiffness but to a lesser degree. Table 6-1 shows ratios of maximum moment using the basic model result as a divisor. A moment increase factor of 1.69 is reported for the one-half modulus and a decrease factor of 0.58 for the double modulus.

6.3 FOOTING WIDTH

In general, footing widths to support arch-shaped long spans are designed according to the bearing capacity of supporting soil. However, assuming identical soil conditions with sufficient bearing capacity, it is reasonable to assume that a narrow footing will deflect further into the supporting soil than a wide footing. Consequently, it is conjectured that a narrow footing may induce a greater degree of positive arching and improve structural performance. This notion is examined below.

The footing width of the standard basic model is 3.0 ft (0.91 m). To determine the influence of footing width a narrower and wider footing width of 2.0 ft (0.61 m) and 4.0 ft (1.22 m) are incorporated into the finite element mesh geometry. In all cases, the footing material is concrete with a depth of 2.0 ft (0.61 m). All other system parameters remain unchanged.

Figures 6-3 and 6-4 show crown deflection and springline thrust histories are virtually the same for the three footing widths, i.e., only a slight reduction in structural responses

are observed as footing width decreases.

At full fill height, the narrow footing settled 0.36cm more than the "standard" footing, and the wide footing settled 0.35cm less than the standard. Apparently, these small differences in settlement are not enough to induce any significant amount of positive soil arching.

Key Structural response ratios are summarized in Table 6-1.

6.4 LINER THICKNESS

The common range of liner gage (thickness) for long-span systems with 6x2 inch corrugated steel structural plate is gages 1 through gage 10. The basic model is gage 5. Increases of liner thickness (i.e., decrease of gage number) provides an increase of cross-sectional area and moment of inertia in the liner wall.

For this study, gages 10, 5, and 1, representing the spectrum of common useage, are analyzed to determine their relative effect on long-span performance. As always, the basic model is used as reference with the only change being the cross-sectional properties of the liner. Sectional properties are shown in the insert of Figure 6-5. Gage 10 has 37% less area and 38% less moment-of-inertia than gage 5, whereas gage 1 has 29% more area and 31% more moment of inertia than gage 5.

Figures 6-5 shows that crown displacement is practically unaffected by changes in gage (less than 5%) even though the bending stiffness (moment of inertia) is more than doubled from gage 10 to gage 1. This is because the soil stiffness dominates liner stiffness and controls the deformed shape as previously discussed. Of course, in early stages of construction when fill soil is below the springline, the soil mass is too small to dominate the system. Here, stiff liners are useful to maintain shape and provide lateral resistance for compaction.

Springline thrust history, Figure 6-6, is also practically

insensitive to liner gage. Therefore, thrust stress, which is of design importance, is reduced in direct proportion to the liner thickness.

As indicated in Table 6-1, maximum moment is increased as liner thickness increases. Maximum moment for gage 10 steel is 23% greater than for gage 5 steel. However, the sectional modulus increases by 22% so that maximum bending stress is practically independent of gage.

6.5 LINER SHAPE

Three fundamental long-span shapes are analyzed and compared: high profile arch (basic model), low profile arch, and horizongal ellipse. Each of these shapes have the same top rise, span, and curvature above the springline. Thus, the finite element representation of geometry and loading above the springline is the same for each structure.

To model the ellipse, the bottom half of the basic mesh is replaced with a mirror image of the top half forming a horizontal ellipse with a total rise of 268 in. (6.87 m). For the low profile arch, additional soil elements are added to the basic high profile arch model raising the floor and footing to an elevation 14 in. (0.36m) below the springline and reducing the total rise to 148 in (3.76m). One beam-column element is used between the springline and footing and another is anchored in the footing to provide continuity of the liner into the footing.

Except for the above modifications, all other characteristics of the ellipse and low profile arch models are identical to the basic high profile arch model.

Figure 6-7 illustrates the history of crown deflection for each shape as a percentage the high profile rise 257 in. (6.56m) used as a common-reference. Thus, the deflection histories may be compared directly. Deflections of the high and low profile arches follow similar trends with the high profile arch being

slightly more flexible. However, the ellipse exhibits very little peaking but excessive flattening, more than twice that of the arch shapes. This same trend was observed in the experimental data presented in Chapter 2. Apparently, the ellipse is strong in resisting lateral pressures (small peaking) but weak in carrying overburden pressure (flattening).

Springline thrust histories, shown in Figure 6-8, reveals that maximum thrust is 10% less in the ellipse than the high profile arch. Also, as shown in Table 6-1, maximum moment is 29% less than the high profile arch.

Differences in structural responses between the high and low profile arch are not too significant.

6.6 LINER SCALE

In order to get an indication of size effects, the geometry of the basic model is scaled up by a factor of 3/2 and also scaled down by a factor 2/3. All horizontal and vertical model coordinates are scaled (up and down) except the vertical height of cover above crown is maintained constant at 25 ft (7.6 m) so that the same overburden load is applied to each scaled model. All other system parameters including sectional properties of the liner remain as defined for the basic model.

Since the top-rise distance changes according to scale, crown deflection and springline thrust histories as a function of fill-height-ratio cannot be meaningfully plotted on a common scale as in previous studies. Rather, Table 6-2 gives crown deflection and springline thrust values for fill heights at crown level and full fill height.

At full fill height, Table 6-1 shows key response ratios of the scaled models to the basic model. Displacements and thrusts change in almost direct proportion to the scale factor. However, maximum moments remain relatively constant, independent of the scale factor.

Table 6-2: Scale Effects on Crown Displacement and Springline Thrust

Scale of Basic Model	Fill Height at Crown		Full Fill Height	
	Crown Displacement (inches)	Springline Thrust (lbs/in)	Crown Displacement (inches)	Springline Thrust (lbs/in)
0.67	0.582	- 404.0	-1.84	-3464
1.00	1.20	- 862.0	-3.00	-5522
1.50	2.40	-1860.0	-4.83	-8945.0

6.7 SPECIAL FEATURES

In order to improve the structural performance of long-span systems, several special features have been added to the long span systems by various manufacturers. Some commonly used features are; thrust beam, soil bin, and rib stiffeners shown in Figure 6-9 along with comments on their intended purpose.

For this study, the above special features are incorporated into the basic model to compare their relative merits. Note, however, the finite element idealizations do not mimic all the intended functions of each special feature (e.g., improved soil compaction). This must be kept in mind when interpreting results.

To model the thrust beam, triangular continuum elements are added to the basic mesh to form a triangular concrete cross-section measuring 41 in. (1.05 m) on the horizontal leg and 28 in. (0.72 m) on the vertical leg. The acute angle is located 145 in. (3.69 m) off the center line. Material properties are identical to the concrete footing given in Chapter 3, and the thrust beam is assumed part of the initial configuration.

Modeling of the soil bin is approximated by superimposing a steel superstructure on the liner as shown in the insert of Figure 6-10. Section properties of the ribs and connection members represent smeared averages over the rib spacing intervals to accomodate the plane strain analysis. The fin is continuous and has the same properties as the liner.

The last special feature, shaped rib stiffeners, are incorporated into the basic model by uniformally increasing the sectional properties of the liner. Again, section properties are approximated by a smeared average over the rib spacing interval. For this example, the composite liner moment of inertia is 5.0 in^4/in (82.0 cm^4/cm) and the composite liner cross-sectional area is 0.44 in^2/in (1.12 cm^2/cm). Properties approximate a curved I-beam (12WF36) spaced at 5 ft (1.5 m) intervals and bonded to

the liner. Note the stiffened liner is nearly 40 times stiffer in bending than the unstiffened liner.

Figure 6-10 shows the crown displacement history for each special feature system as well as the basic model. As might be expected, the rib-stiffeners and soil bin substantially limit peaking because of the vast increase in crown bending stiffness. However, as the fill height is increased, the soil bin structure exhibits slightly more flattening than the other structures. The thrust beam structure provides a modest reduction in peaking, but for the most part behaves like the basic model without special features. At least one attribute of the thrust beam not modeled by this analysis is that higher soil compaction (soil stiffness) can be achieved in the soil adjacent to the thrust beam.

Springline thrust history, shown in Figure 6-11, reveals that none of the special features alter the maximum thrust.

At full fill height, Table 6-1 shows that maximum moments are not significantly altered due to the special features except for the case of the rib-stiffeners. Here, the moments are dramatically increased by an order of magnitude due to the large increase in bending stiffness.

6.8 SUMMARY OF CONVENTIONAL PARAMETERS

The most influential parameter in controlling long span deformations is soil stiffness, i.e., deformation is inversely proportional to soil stiffness. Since liner deformation is primarily due to bending (as opposed to membrane contraction) bending moments are also inversely proportional to soil stiffness. However, thrust is insensitive to soil stiffness. Evidently, the selection of a soil model is crucial for predicting the deformed shape of the liner.

Reducing footing widths (within practical ranges) does not promote positive soil arching to any significant extent. All

structural responses are practically insensitive to variations in footing width.

Liner thickness within the range of standard gage sizes (6x2 in. corrugation) has negligible effect on controlling liner deformation when fill soil is above the springline. In other words, soil stiffness dominates the system so that the deformed shape is not reduced when using a heavier gage. As a consequence, the maximum moment increases in proportion to the bending stiffness because the deformed curvature is near constant. Thrust force remains insensitive to liner gage, therefore, thrust stress is reduced in proportion to the sectional area.

With regard to liner shape, high and low profile arches exhibit similar structural responses except the high profile is slightly more flexible. In contrast, the horizontal ellipse exhibits much less peaking but excessive flattening compared to arches.

Increasing the liner scale increases deformation and thrust proportionally. However, maximum moments are not significantly changed.

Special features; thrust beam, soil bin, and rib stiffeners, exhibit no marked difference in crown flattening at full fill height. However, during early stages of construction, the crown stiffened structures (soil bin and rib stiffeners) exhibit significantly less peaking than the unstiffened structures. Maximum thrust is nearly the same for all special feature structures. Indeed, for all the conventional parameters considered in this chapter thrust force is not significantly changed.

6.9 Figures 6-1 through 6-11

		Page
Fig. 6-1	Effect of soil stiffness on crown deflection.	144
Fig. 6-2	Effect of soil stiffness on springline thrust.	145
Fig. 6-3	Effect of footing width on crown deflection.	146
Fig. 6-4	Effect of footing width on springline thrust.	147
Fig. 6-5	Effect of liner gage on crown deflection.	148
Fig. 6-6	Effect of liner gage on springline thrust.	149
Fig. 6-7	Effect of liner shape on percent crown deflection.	150
Fig. 6-8	Effect of liner shape on springline thrust.	151
Fig. 6-9	Special features with long spans.	152
Fig. 6-10	Effect of special features on crown deformation.	153
Fig. 6-11	Effect of special features on springline thrust.	154

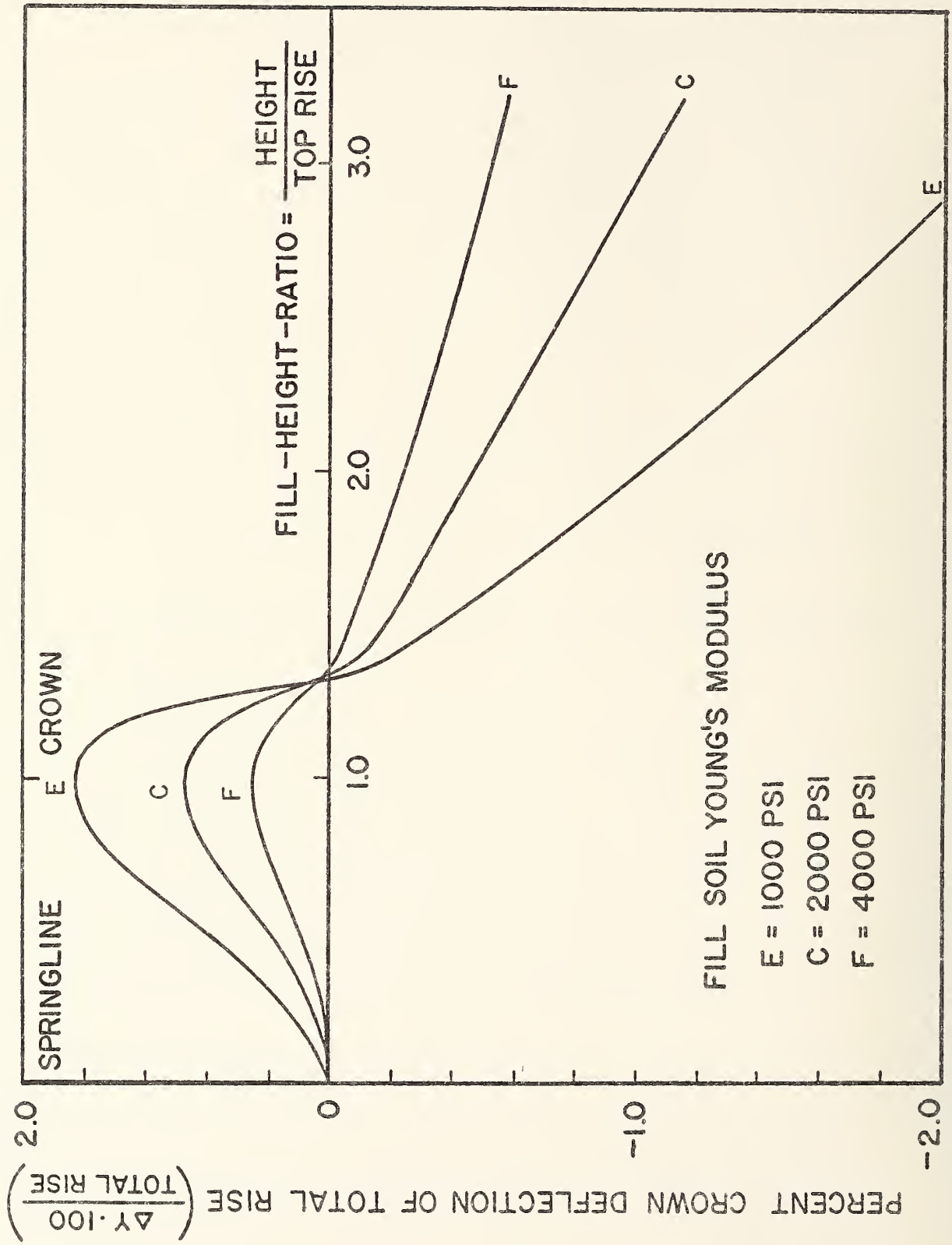

Figure 6.1 Effect of Soil Stiffness on Crown Deflection.

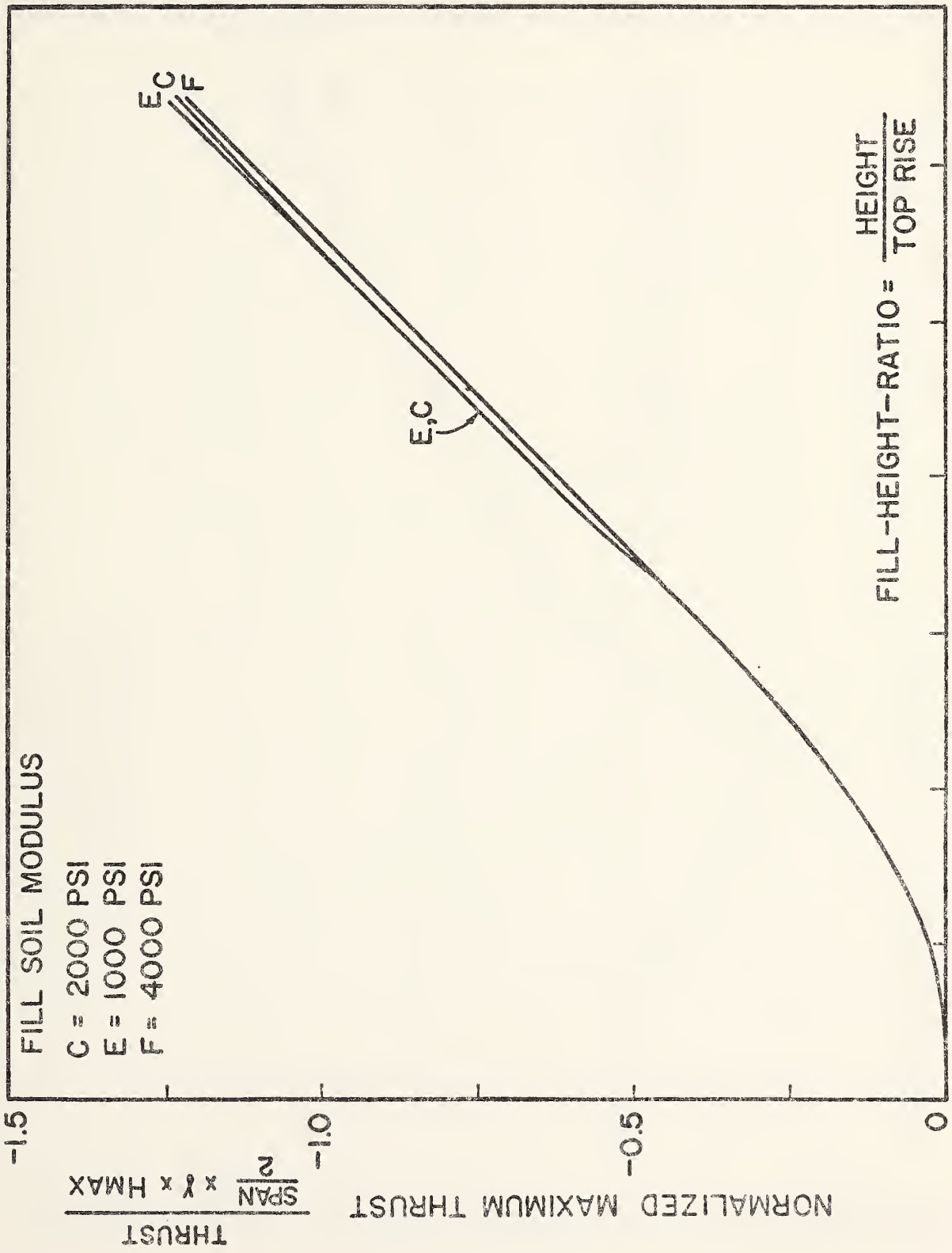

Figure 6.2 Effect of Soil Stiffness on Springline Thrust.

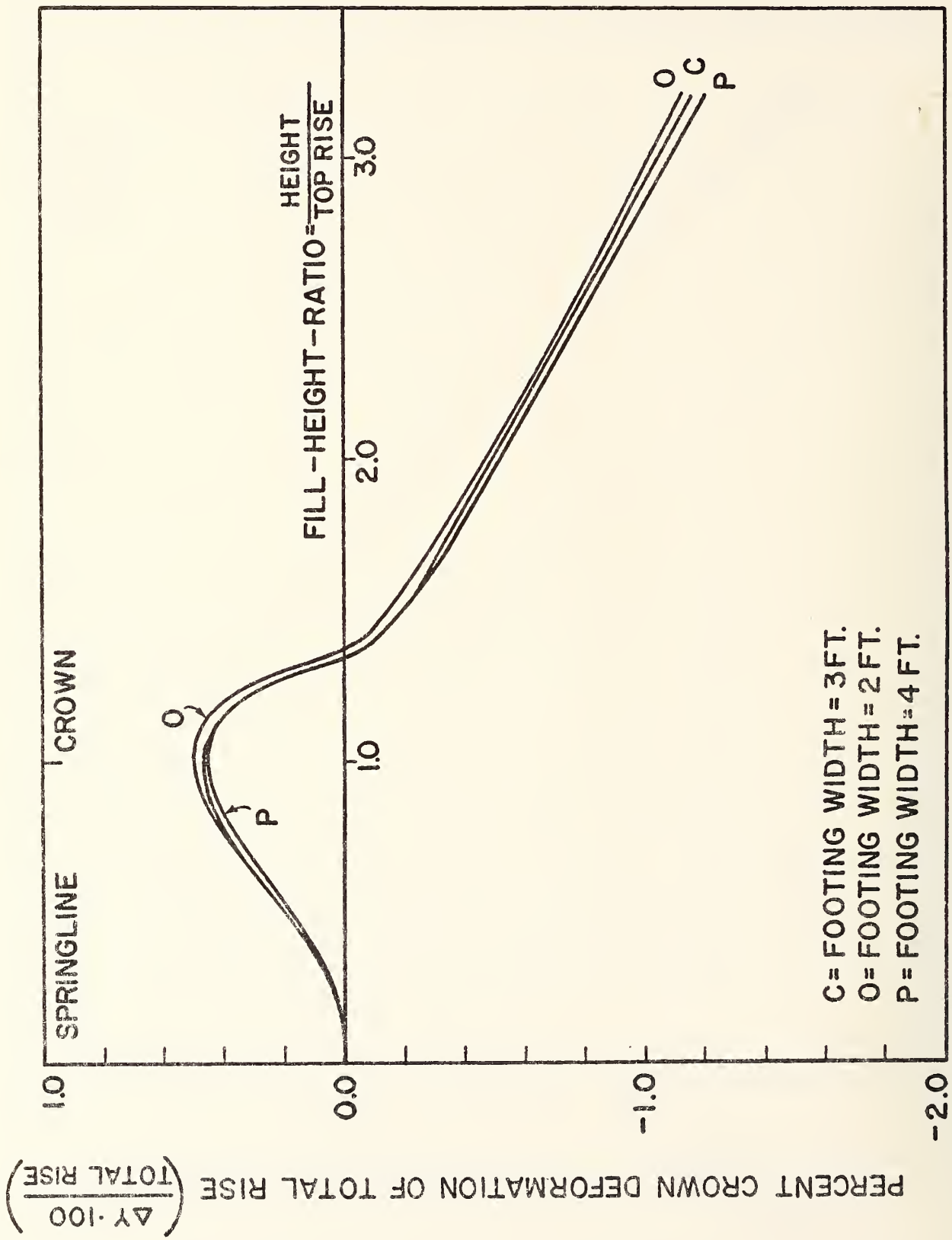

Figure 6.3 Effect of Footing Width on Crown Deflection.

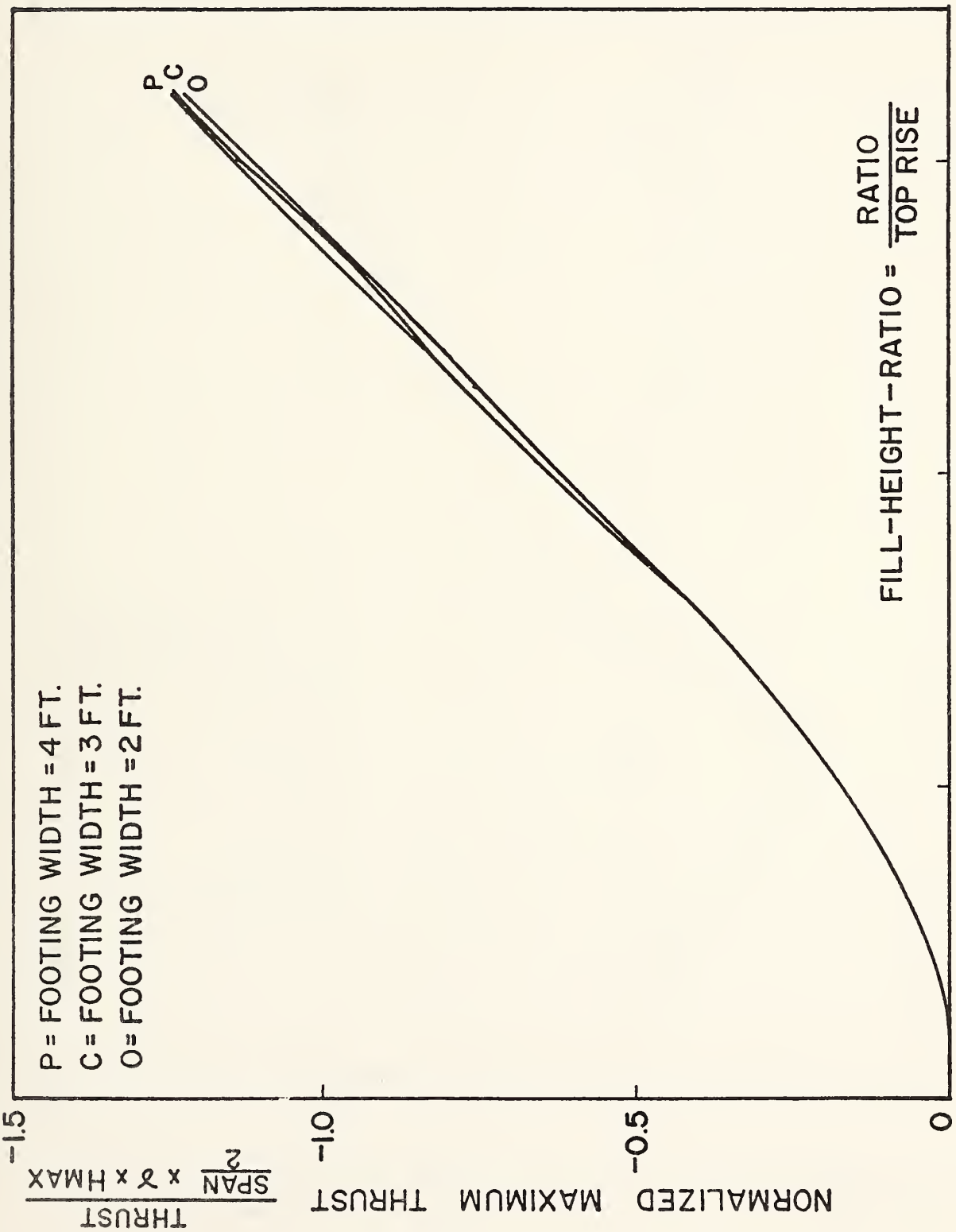

Figure 6.4 Effect of Footing Width on Springline Thrust.

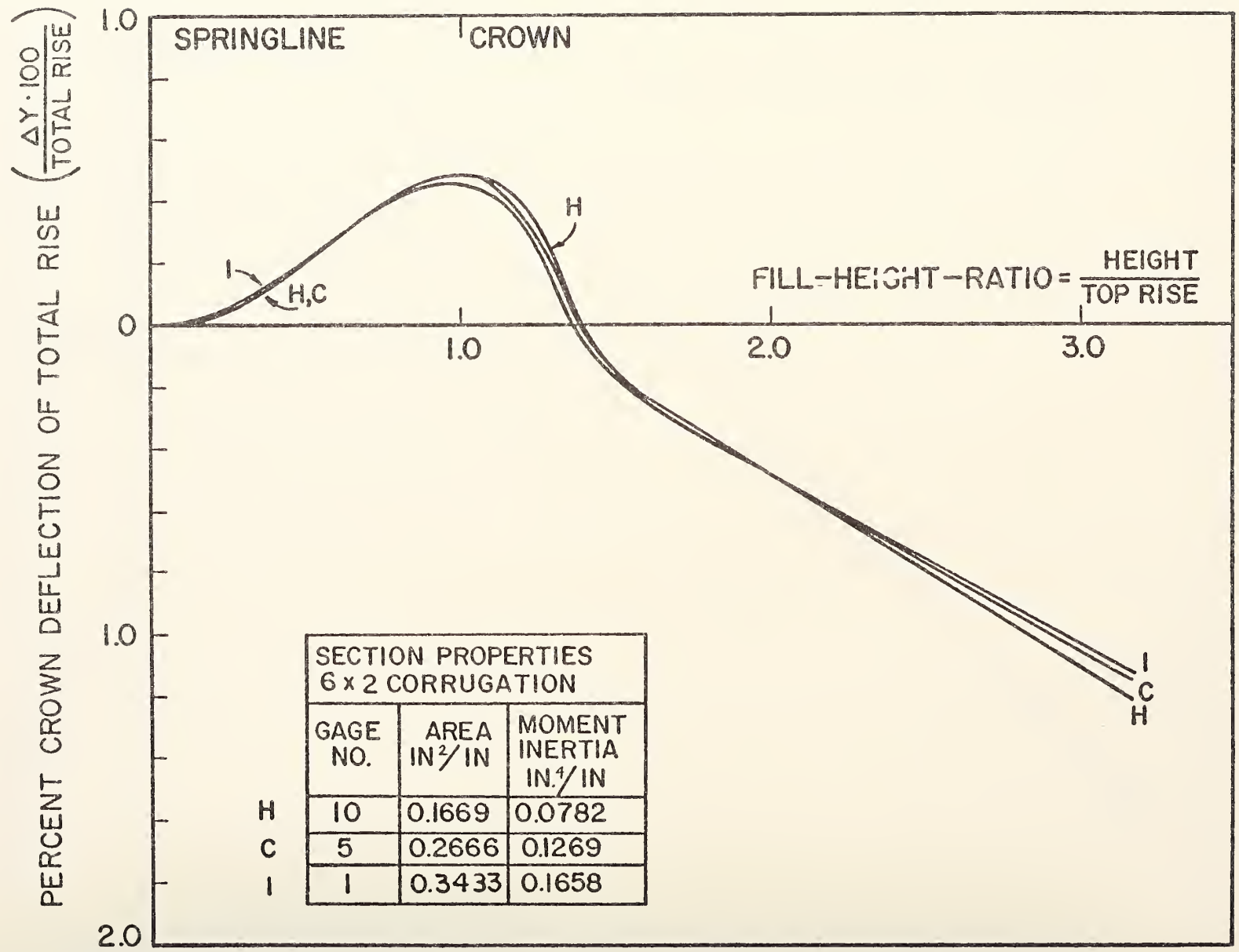

Figure 6.5 Effect of Liner Gage on Crown Deflection.

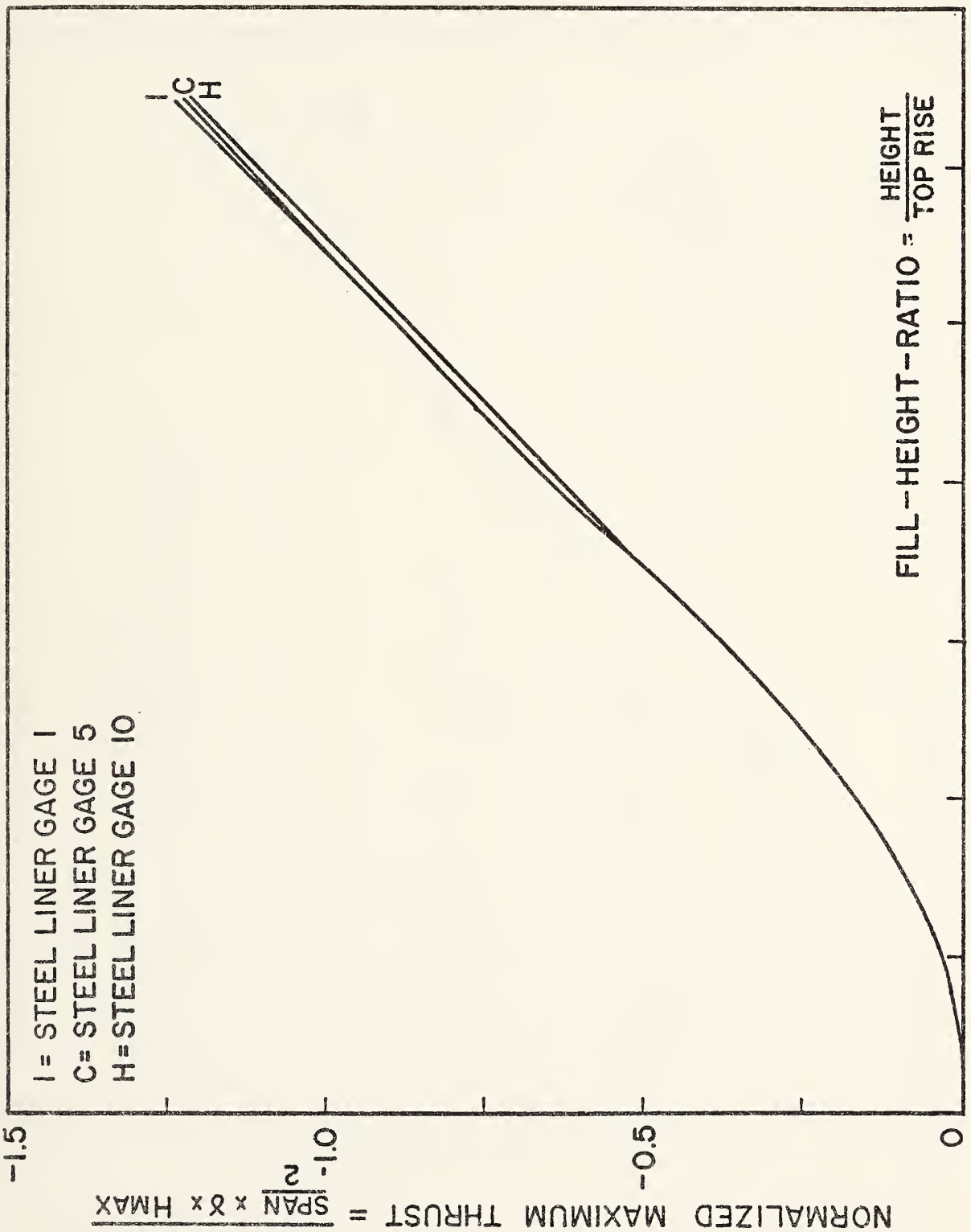

Figure 6.6 Effect of Liner Gage on Springline Thrust.

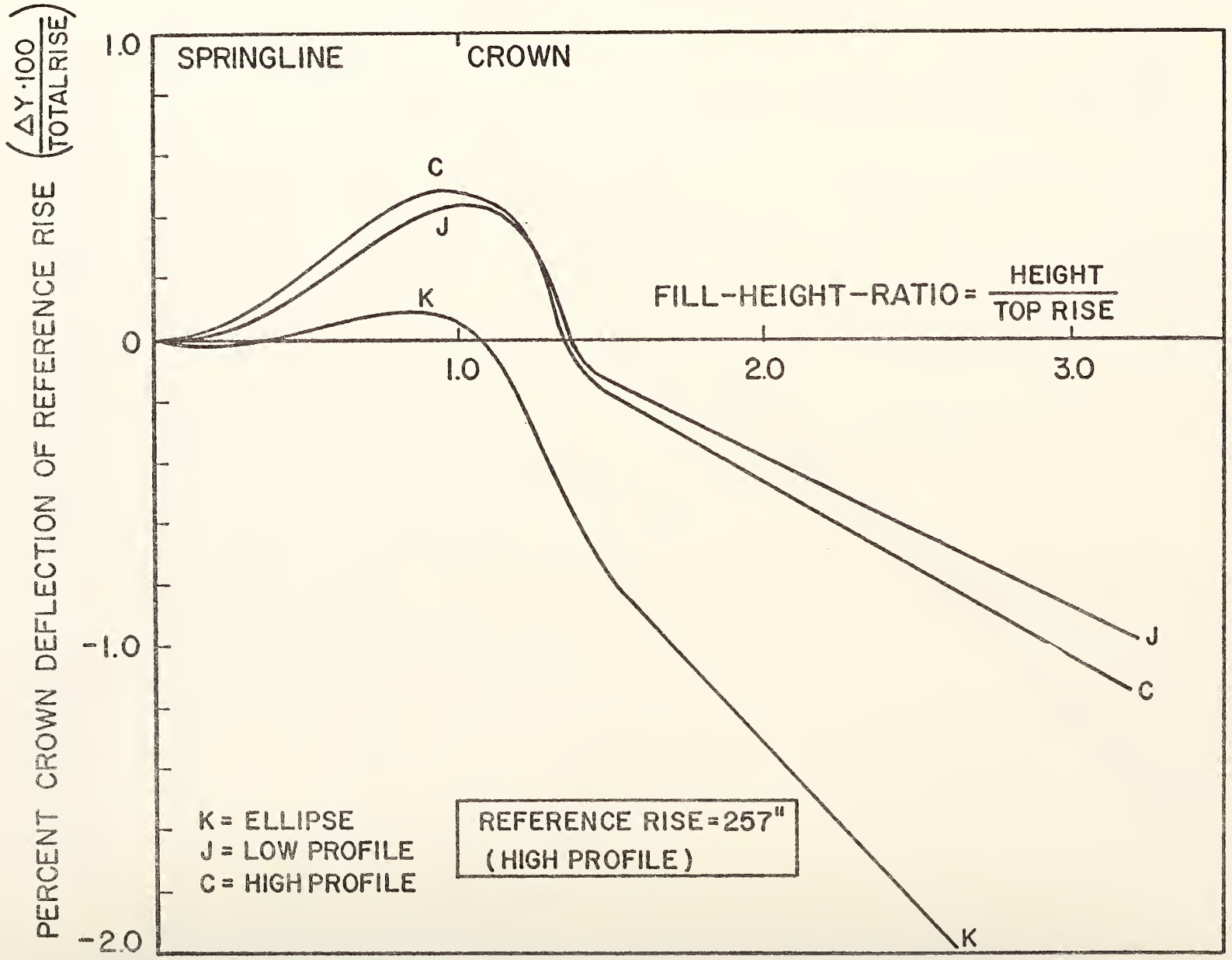

Figure 6.7 Effect of Liner Shape on Percent Crown Deflection.

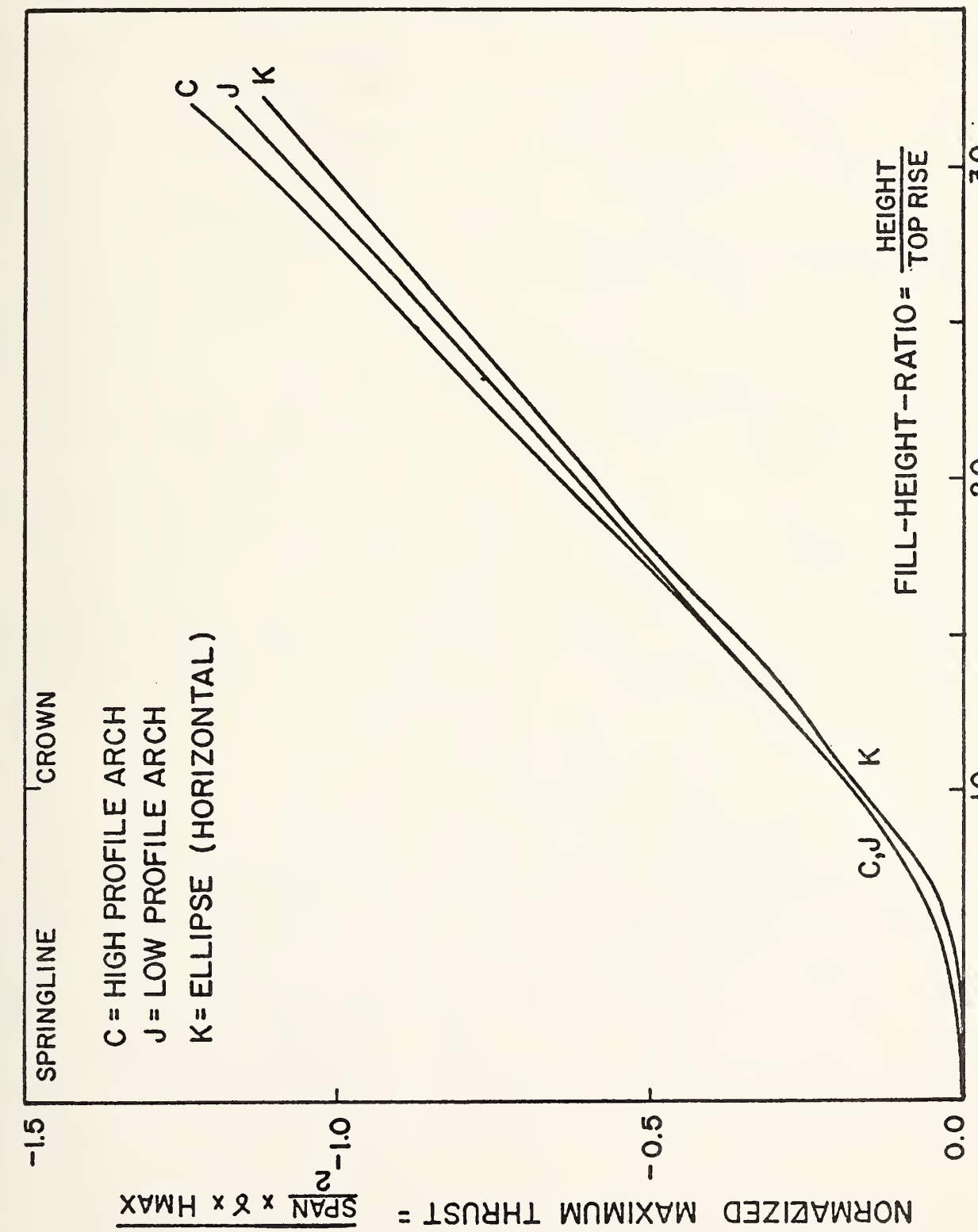

Figure 6.8 Effect of Liner Shape on Springline Thrust.

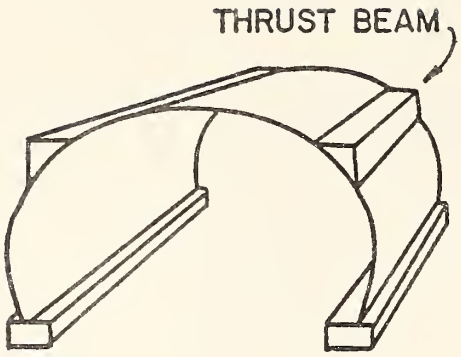

2A. LONGITUDINAL THRUST BEAM

INTENDED PURPOSES

- ANCHORS BASE OF TOP ARCH.
- PROVIDES STIFF SUPPORT WHERE SOIL IS DIFFICULT TO COMPACT.
- PROVIDES VERTICAL FACE FOR SOIL COMPACTION AND LATERAL SUPPORT.
- PROVIDES LONGITUDINAL SUPPORT.

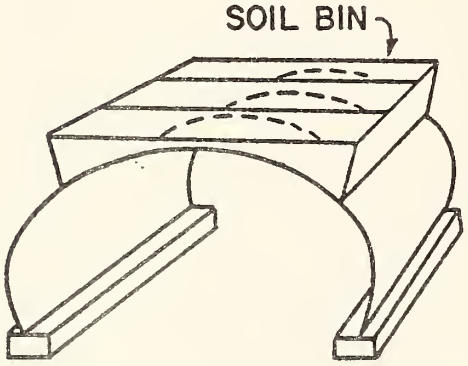

2B. SOIL-BRIDGE BINS

- FORMS THE KEYSTONE OF THE COMPRESSION SOIL ARCH.
- PROVIDES TOP ARCH STIFFNESS TO REDUCE INITIAL PEAKING AND SUBSEQUENT FLATTENING.
- PROVIDES BIN TO TOP LOAD THE STRUCTURE DURING EARLY BACK-FILLING STAGES.

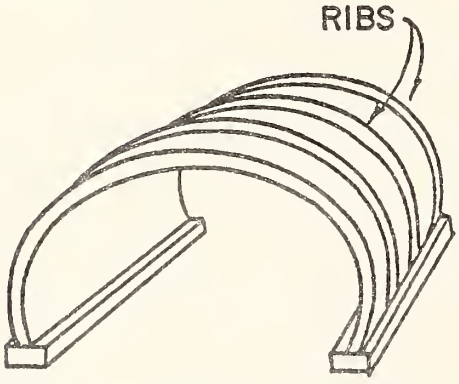

2C. CIRCUMFERENTIAL RIB STIFFENERS.

- PROVIDES INCREASED STIFFNESS TO PERMIT SOIL COMPACTION WITHOUT EXCESSIVE PEAKING.
- PROVIDES STIFFNES TO PRECLUDE LOCAL BUCKLING AND EXCESSIVE FLATTENING DURING OVER-BURDEN LOADING.

Figure 6-9 Special Features with Long Spans

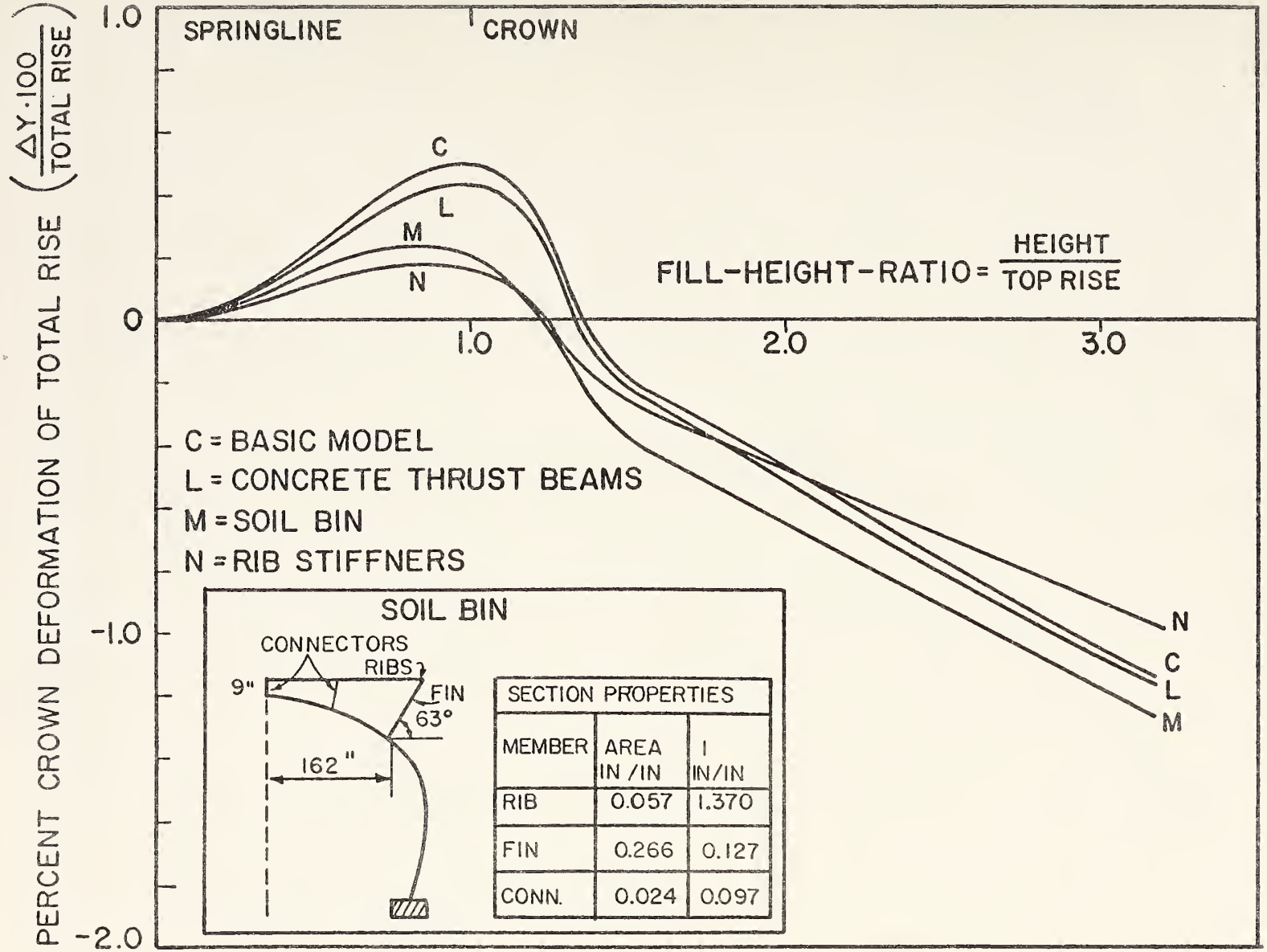

Figure 6.10 Effect of Special Features on Crown Deformation.

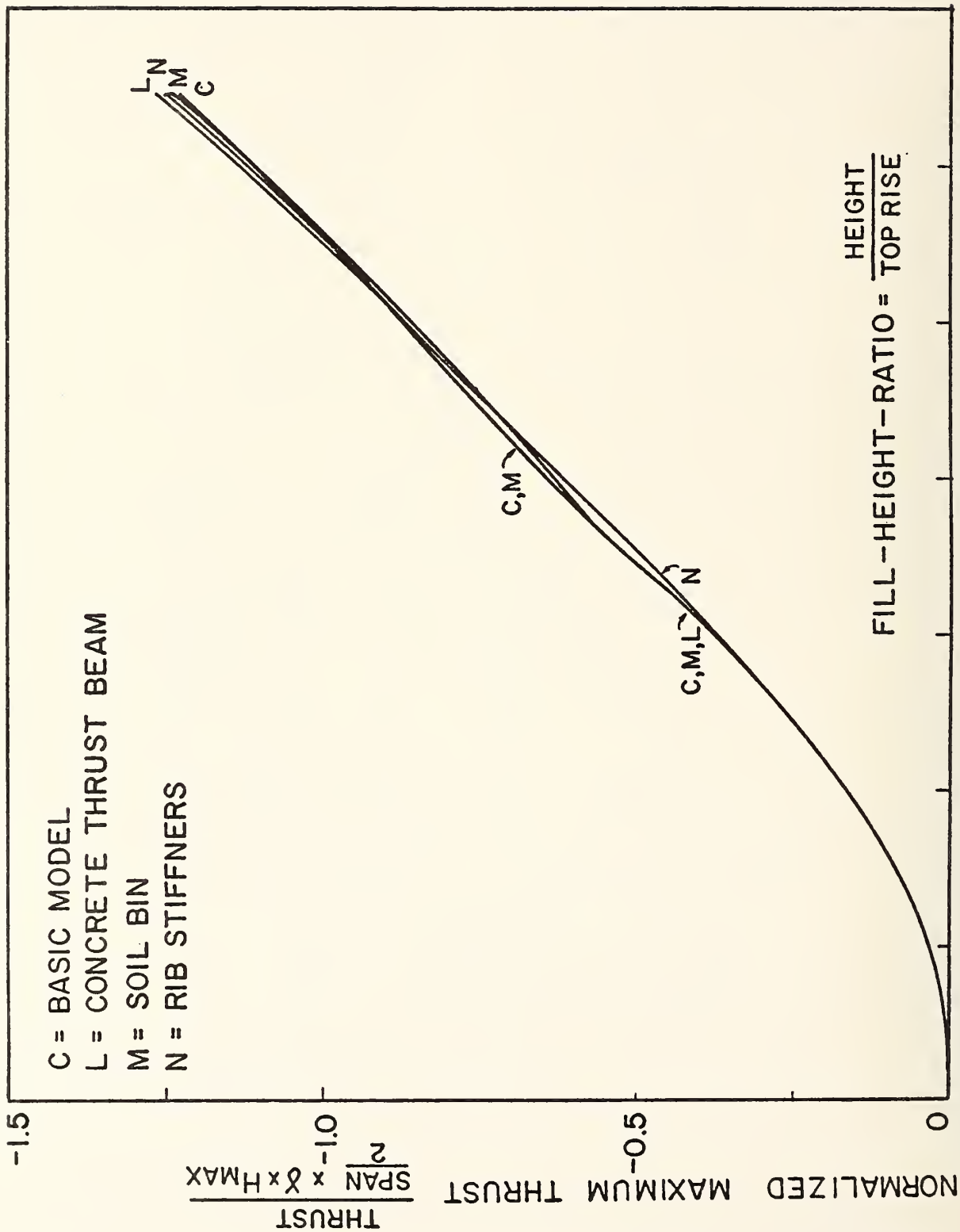

Figure 6.11 Effect of Special Features on Springline Thrust.

CHAPTER 7

PARAMETER STUDIES OF NEW CONCEPTS FOR LONG SPANS

7.1 STATEMENT OF PURPOSE

In this chapter new concepts to improve the structural performance of long-span systems are discussed and analytically evaluated. Methods of enhancing long span structural performance can be catagorized in two groups; improvements to the soil system, and improvements to the metal liner. In both catagories, the objective is to limit structural distress of metal liner (e.g., displacements and stresses) and to maintain integrity of the entire long-span system.

With regard to improving the soil system, the following techniques are examined; incorporation of reinforced earth, selective soil stabilization, and special placement of soft inclusions. The merits of utilizing a concrete relieving slab above the crown of shallow buried culverts to minimize the effects of live loads has already been discussed in Chapter 4.

For the metal liner, potential improvements to be discussed are; slotted bolt connections, squeeze block footings, and increased bending stiffness.

Some of the techniques above have no precedent in current long span installations. Thus, they can only be evaluated by using finite element models. To this end, the basic model (Chapter 3) is modified to accomodate each special technique and the results are compared with the unmodified basic model to ascertain relative merits.

In the following, each of the new concepts is presented and discussed in order.

7.2 REINFORCED EARTH

The purpose of reinforced earth is to stiffen and strengthen

the soil in one direction (usually horizontally) by introducing small amounts of reinforcing materials like metal strips, bars, or fabric within soil layers, such that, tensile stresses in the reinforcing strips are developed by frictional shear force between soil particles and strips. The resulting composite material behaves approximately like an orthotropic continuum whose stiff direction is dependent on the tensile stiffness of the reinforcement.

Current applications of reinforced earth are primarily directed toward highway applications such as, retaining walls, quay walls, foundation slabs, etc. Appendix B provides a summary review of reinforced earth applications, characteristics, costs, design and construction, experimental findings, and analytical models.

Objective and Scope. There is no precedent of reinforced earth applications to long-span systems. Thus, the objective of this study is directed toward fundamental considerations of applying reinforced earth to improve long-span structural behavior. Specifically, the following areas are investigated:

(1) Influence of percentage of reinforcement to soil (by area),

(2) Effect of connected vs. unconnected reinforcement to metal liner,

(3) Effect of selective placement of reinforcements.

To investigate the above objectives, portions of the basic model soil zones which are to be considered reinforced earth are modeled as an orthotropic material whose stiffness in the horizontal direction is increased dependent on the percentage and stiffness of reinforcement. The orthotropic representation is based on the "unit cell" concept and is derived in Appendix B. For all cases in this study, the horizontal reinforcing strips are characterized by steel with Young's modulus = 30×10^6 psi (207×10^6 kPa). Only the percentage of steel per "unit cell" area is varied and is given by:

$$\text{Percent Reinforcement} = (A_{steel}/A_{spacing}) \times 100$$

where A_{steel} is the cross-sectional area of the steel strip, and $A_{spacing}$ is the cross-sectional area of the unit cell defined by the product of lateral and vertical reinforcement spacing distances.

Influence of Percent Reinforcement. For the first study, reinforced earth is introduced into the entire fill soil zone above the footing as indicated in Figure 7-1. Three percentages of reinforcement are considered, namely; lightly reinforced 0.05%, moderately reinforced 0.10%, and heavily reinforced 0.20%. All other parameters and loading conditions remain the same as the basic model (Chapter 3).

Figure 7-2 depicts the crown deflection as a function of fill height for the three percentages of reinforcement as well as dramatically reduced for all percentages of reinforcement to the extent it is practically nil for moderate and heavy reinforcement. As fill height is increased, the rate of crown flattening is approximately reduced by one-half for all cases of soil reinforcement vs. the unreinforced reference case. However, the reduction of crown flattening must be viewed with some skepticism because the analytical model of reinforced earth does not consider the nonlinear effect of stiffness reduction due to horizontal compressive strain in the strips. At fill-height-ratios greater than 1.5 some reinforced elements were observed to change into compressive strain so that horizontal stiffness would in reality be reduced.

Springline thrust as function of fill height is shown in Figure 7-3 for the three reinforcement percentages and reference condition. Here, it is observed that soil reinforcement has no effect in reducing thrust.

Distribution plots around the liner at full fill height are shown in Figure 7-4 for displacements, thrust, and moment.

Inspecting these distributions reveals that displacements and moments are generally reduced as percent reinforcement is increased except for moments near the footing. Thrusts, on the otherhand, remain nearly the same for all cases except near the crown wherein the reference case (0% reinforcement) experiences approximately 30% less thrust than the reinforced cases. However, thrust is maximum at the springline so that for design purposes thrust considerations are the same.

Effect of Connected vs. Unconnected Reinforcement. In some highway applications (Appendix B) it has been suggested not to connect the metal reinforcing strips to the structure (e.g., wall, abutment, etc.). Motivations for this are; potential better performance, reduced labor and material costs, and ease of construction. Also, unconnected strips may occur inadvertently from construction negligence and/or premature connection failure.

Sharing these motivations and concerns for long span applications, this study compares the results of connected vs. unconnected reinforcement strips. To simulate unconnected reinforcement strips in the finite element model, a narrow zone of soil in contact with the liner is left unreinforced as shown in Figure 7-1b. The remaining soil is moderately reinforced (0.10%) and may be compared with the connected, moderately reinforced case in the previous study.

Figure 7-5 shows peaking of the crown is increased for the unconnected reinforcement vs. the connected reinforcement, however, as compared to the reference case (0% reinforcement), the unconnected case substantially reduces crown peaking by nearly 80%. In the flattening range the connected and unconnected cases behave approximately the same.

Springline thrust is shown in Figure 7-6. As in the previous study, maximum thrusts are not significantly altered by the introduction of reinforced earth, however, the unconnected

reinforcement case results in slightly less thrust than either the connected or unreinforced case.

Comparison of displacement, thrust, and moment distribution plots at full fill height are shown in Figure 7-7 for connected reinforcement, unconnected reinforcement, and no reinforcement. In general, the structural responses for the connected and unconnected reinforcement are similar and significantly reduce displacements and moments from the reference condition. Thus, it may be economically advantageous to use unconnected reinforcement strips for long span applications.

Effect of Selective Placement of Reinforcement. Thus far in the investigation, reinforcement has been distributed throughout the entire fill soil zone above the footing. In this section, reinforcement is selectively placed in two regions; along "liner-sides" (Figure 7-1c) and "above-crown" (Figure 7-1b). The objective is to ascertain what regions of reinforcement are most effective in minimizing structural responses. To provide a comprehensive basis of comparison, the subsequent plots also show the reference case (no reinforcement) and "full-region" reinforcement. In all soil zones containing reinforcement the percent of reinforcement is moderate (0.10%) and connected conditions are assumed.

Figure 7-8 shows crown peaking is identical for the unreinforced condition and the above-crown reinforced condition because the peaking condition occurs with fill soil level with the crown. Thus, the above-crown reinforcement is not yet introduced into the system. Maximum peaking for liner-side reinforcement is somewhat greater than that occuring from full-region reinforcement, however, both of these cases are significantly lower than the unreinforced reference condition. In the flattening range, full-region and liner-side reinforcement conditions are similar, reducing maximum flattening by approximately 50% as compared to the reference condition. The above-crown reinforcement condition only reduces maximum flattening by 20%.

Springline thrust as a function of fill height is shown in Figure 7-9 for the four conditions. As before, the introduction of soil reinforcement does not significantly alter the maximum thrust. A very slight reduction in thrust is observed for the above-crown reinforcement condition.

Finally, distribution plots at full fill height are shown in Figure 7-10. Of significant interest, it is observed that all structural response distributions are approximately the same for the full-region and liner-side reinforcement conditions. Since these distributions are more favorable with regard to minimizing displacements and moments, it may be concluded that liner-side reinforcement is optimum for cost-effectiveness. This conclusion is further demonstrated by the similarlity of structural response distributions for the unreinforced and above-crown reinforcement conditions , indicating little or no improvement is gained by placing reinforcement above the crown.

Summary Reinforced Earth. Moderate amounts of reinforced earth laid in horizontal rows can reduce crown peaking by 90% or more. Further, the rate of crown flattening with respect to increasing fill height can be reduced by 50%. Maximum thrust (at the springline) is not appreciably altered by the introduction of soil reinforcement, however, thrust at crown is increased by 30% but is still less than at the springline. Nonetheless, this increases the concern of buckling in the vicinity of the crown.

The placement of reinforcement along the sides of the liner is nearly as effective in reducing the structural responses as reinforcing the entire fill soil region. Reinforcement above the crown has little effect. Thus, liner-side reinforcement appears to be optimum with regard to cost-effectiveness.

Unconnected reinforcement is almost as effective in reducing structural responses as connecting the reinforcement

to the liner. Thus, economic considerations may favor unconnected reinforcement. However, for ultimate capacity, this conclusion is probably invalid.

7.3 SOIL STABILIZATION

In Chapter 6, it was demonstrated that increasing the soil modulus (stiffness) of the entire fill soil resulted in proportional decreases of deformations and moments in the metal liner. If similar reductions in structural responses can be achieved by selectively stiffening the soil in small local regions, then economic advantages are apparent. Therein lies the motivation of this study.

Local regions of soil can be stiffened by compaction and/or utilizing high quality structural soil such as well graded granular material, however, the maximum stiffness achievable has a limited range. A more effective method of increasing soil stiffness (and strength) is by soil stabilization, i.e., mixing the soil with additives such as lime, lime-fly ash, or portland cement. Stiffnesses of natural soils can be increased up to one hundred times or more by stabilization techniques.

Appendix A provides a summary review of soil stabilization techniques including; construction practices, engineering properties, and relative costs.

Objective and Scope. In this study, the effectivenss of soil stabilization (stiffness) for reducing structural distress in long-span systems is investigated for cases where stabilized soil is placed along the sides of the metal liner. Specifically, the objectives are to determine;

(1) Effect of stabilized soil stiffness,

(2) Effect of stabilized soil zone width.

The basic long-span model (Chapter 3) is used as a reference basis. Select regions of stabilized soil adjacent to the liner sides are treated as an isotropic elastic continuum

with Young's modulus values of 4, 20, and 100 times the fill soil modulus. These modulus values respresent the practical range of stiffness increases from soil stabilization (see Appendix A). In all cases, Poisson's ratio is constant at 0.35. Except for increased soil stiffness in stabilization zones, the analytical model for soil stabilization is identical to the basic model.

Effect of Stabilized Soil Stiffness. Figure 7-11a shows the stabilized soil zone adjacent to the metal liner and extending laterally one-fourth span length beyond the springline. Vertically, the zone extends from the footing to a height 88% of the total rise.

For this configuration, Figure 7-12 shows crown displacement as a function of fill height for three stiffness values of soil stabilization (4, 20, and 100 times soil modulus). Also, shown is the reference condition (basic model) without soil stabilization. It is evident that even modest soil stabilization ($E_{stiff}/E_{soil} = 4$) reduces crown peaking and subsequent flattening by 35% as compared to the reference condition. Stiffer, and hence more expensive, stabilized soils further limit crown movement, however, a point of diminishing returns is reached. For example, crown peaking is reduced by 51% for intermediate stiffness ($E_{stiff}/E_{soil} = 20$), and by 54% for high stiffness ($E_{stiff}/E_{soil} = 100$). Thus, little is gained from the more expensive stabilized soil.

Springline thrust history is shown in Figure 7-13 for the three stabilized soil stiffnesses and reference condition. Throughout this report maximum thrust has generally occurred in the vicinity of the springline. Thus, Figure 7-13 gives the mistaken impression that maximum thrust is reduced as stabilized soil stiffness is increased. However, this is not the case. Indeed, springline thrust is reduced as stiffness increases but the location of maximum thrust is shifted above

the springline toward the 2 o'clock position. As a result, the actual maximum thrusts increase slightly (3%) rather than decrease.

Distribution plots of displacements, thrusts, and moments at full fill height are shown in Figure 7-14. Here the location shift of maximum thrust is clearly apparent. Also, peak moments are concentrated in the locations of maximum thrust.

Effect of Stabilized Soil Zone Width. Figure 7-11b shows three width variations of the stabilized soil zone defined as W_1 = 1/3 span, W_2 = 1/4 span, W_3 = 3/8 span. The effect of stabilized soil width is considered for these three cases for a constant stabilized soil stiffness $E_{stiff}/E_{soil} = 20$.

Crown displacement histories are shown in Figure 7-15. Peaking and flattening are reduced by 36, 51, and 58% for successive increases in stabilized zone width as compared to the unstabilized condition.

Springline thrust histories are plotted in Figure 7-16. Here it is observed that the smallest width, W_1, produces 13% increase in springline thrust, whereas the larger widths, W_2 and W_3, produces a slight reduction. However, the location of maximum thrust for widths W_2 and W_3 are shifted from springline (3 o'clock position) toward the 2 o'clock position. As a result, the maximum thrust increases by 3% for widths W_2 and W_3 compared to the unstabilized condition.

Distribution plots at full fill height are shown in Figure 7-17. In general, deformations and moments decrease as the stabilized soil width increases, however, with diminishing returns.

Summary of Stabilized Soil. Introduction of stabilized soil adjacent to the sides of the metal can reduce maximum deformation by 50% or more, however, maximum thrusts increase slightly by 3 to 5%. Stabilized soil stiffnesses on the order of 10 to 20 times the fill soil stiffness with a width of 1/4 span length appear to be optimum with regard to cost-effectiveness.

7.4 SOFT INCLUSIONS

The concept of placing soft inclusions above culverts dates back to the early part of this century wherein soft organic matter or loosely compacted soil was placed in the trench directly above the culvert crown in an attempt to promote positive soil arching. This technique termed "imperfect trench" (see Chapter 8) is recognized in current design practices for traditional culverts.

For long-span systems this technique occurs naturally to some degree because of the inability to compact heavily above the crown. However, no special soft materials have been used in practice.

As mentioned above, soft inclusions can be formed with soft organic materials (e.g., hay, cornstalks, etc.) or loosley compacted soil. However, organic materials tend to decompose and are generally no longer recommended. Loosely compacted soils are better in this regard but the relative stiffness is difficult to control and predict.

As an alternative, soft inclusions can be formed from manufactured materials such as plastic foams and polystyrene scraps. Also, processed natural material such as expanded shale and clay could be used. Such materials offer better quality control and lower ranges of stiffness then traditional techniques, however, the costs are greater.

Appendix A offers a summary review of soft materials with potential applications to culverts and long spans including engineering properties and relative costs.

Objective and Scope. Soft inclusions placed above the crown of the basic long-span model are investigated to ascertain the effectiveness of promoting positive soil arching and reduction of distress in the metal liner. Specifically, the objectives are to investigate:

(1) Effect of soft inclusion stiffness

(2) Effect of soft inclusion vertical dimension

In addition, a combined study with stabilized soil is examined to determine:

(3) Effect of soft inclusion + stabilized soil.

As before, the basic long-span model (Chapter 3) is used as a reference basis. To simulate soft inclusions, the only change in the basic model is the assignment of lower Young's modulus values to the soft inclusion zone. Reduced modulus ratios of 0.5, 0.2, and 0.1 are used to characterize the practical range of soft inclusions (Appendix A). Poisson's ratio is 0.35 for all soil and soft inclusion zones. Also, the body weight of the soft inclusion zone is assumed the same as the fill soil in order to isolate the effect of soft inclusion stiffness without changing the loading.

Effect of Soft Inclusion Stiffness. Figure 7-18a shows the location and dimensions of the soft inclusion in contact with crown for which the three modulus ratios are considered.

Crown displacement histories are shown in Figure 7-19 wherein it is observed that peaking and flattening are adversely affected (increased) by the soft inclusion. Maximum flattening increases by 34% for the softest case.

Springline thrust history, shown in Figure 7-20, is reduced but only slightly by the soft inclusions. Maximum thrust reduction is only 6% for the softest case. This is a disappointing result because it was anticipated that the soft inclusion would promote significant positive arching, and hence, substantially reduce thrust.

Distribution plots at full fill height, Figure 7-21, reveal increases in deformations and moments as the modulus of soft material is decreased. Thrust magnitudes and distributions are not significantly changed.

Effect of Soft Inclusion Height. Figure 7-18b shows three height variations of the soft inclusion defined in terms of total rise as $H_1 = 0.36D$, $H_2 = 0.79D$, and $H_3 = 1.39D$. The width is unchanged and the soft material modulus is constant, 0.2 times the fill soil modulus.

Crown deflection histories, shown in Figure 7-22, demonstrate an increase in crown flattening as the height of the soft inclusion increases. Crown peaking increases the same amount for the three heights because when the fill soil is at crown level the increased heights are not yet included in the system.

Again, the results for springline thrust are disappointing, Figure 7-23. No significant reduction is observed, i.e., less than 6%.

Distribution plots shown in Figure 7-24 exhibit the same trends as the previous study. A general increase in deformations and moments with no significant reduction in thrust.

Effect of Soft Material + Stabilized Soil. A combination of soft material and stabilized soil is shown in Figure 7-18c along with zone dimensions and material parameters. The intent here is to determine if the interaction of the stiff and soft inclusions results in more favorable responses than either method applied individually.

Figures 7-25, 7-26, and 7-27 show these comparisons for crown deflection, springline thrust, and response distributions as before. Inspection of these figures indicates that soil stabilization by itself is more effective for reducing liner deformations than the combination of soft and stiff inclusions. However, maximum moments are most effectively reduced by the combined system. Reductions in maximum thrust are not significant for any of the cases.

Summary of Soft Inclusions. Soft inclusions placed above the crown do not appear beneficial in reducing structural responses. In fact, moments and displacements tend to increase as the soft inclusion zone is heightened and/or made softer. The desired result of reducing maximum thrust did not occur to any significant extent for all the cases considered. Thus, the concept does not appear fruitful for long span applications similar to this study.

7.5 IMPROVEMENTS TO METAL LINER

Thus far, the studies in this chapter have been restricted to evaluating techniques to improve long spans by altering the soil characteristics, i.e., reinforced earth, soil stabilization, and soft inclusions. In this section the discussion is focused on considering alterations of the metal liner (structure).

There are two basic strategies (seemingly opposed) of altering the structure in an attempt to improve performance of the soil-structure system; (1) general increase of structure bending stiffness, and (2) selective reduction of structure ring compression stiffness. These notions are elaborated below.

Structure Stiffness Increase. Methods and results of increasing structure stiffness were discussed in the previous chapter. Here, highlights of that study are reviewed in the context of this discussion.

The simplist but most limited method of increasing structure stiffness is by increasing the metal gage. Assuming standard structural corrugation size (6 x 2 inch), the effect of increasing gage, (1) does not change deformations, (2) increases moments in proportion to increased bending stiffness (bending stress near constant), and (3) does not change thrust force (thrust stress reduced in proportion to cross-sectional area increase).

Special features such as soil bins, rib stiffeners, and/or specialized large corrugations used to increase bending stiffness exhibit the following trends: (1) crown peaking is reduced in early stages of construction but at full fill height the deformation of the special features are controlled by the soil, (2) thrust is not changed, and (3) moments increase.

In general, the added structural stiffness provided by special features do little to improve the structural responses on their own merit. Perhaps the real worth of special features is to provide a higher degree of lateral resistance to inward

moving during early stages of construction. This, in turn, allows a greater amount of soil compaction and increased soil stiffness. Analytically, this must be modeled with a non-linear soil model.

Reductions in Ring Compression. One commonality in all the analytical results presented is the insensitivity of maximum thrust to variations in system parameters. Maximum thrust is a key design consideration and none of the techniques investigated thus far, appear to have any significant influence on thrust.

Thrust is regulated by the ring compression stiffness of the liner. As noted above, varying liner gage over the available range of gages does not alter maximum thrust response because even the smallest practical gage size results in relatively high ring compression stiffness.

Ring compression stiffness can be reduced by squeeze-block-footings (7-1). In practice, this has been achieved by letting the liner bear on wood blocks within the footing. In principle, this is akin to making the footing appear softer in bearing so that the structure will move down and promote positive soil arching. In the previous chapter, the influence of footing width was found to have negligible influence on thrust. This suggests squeeze block footings may also be of limited value. However, more realistic analytical models of squeeze block footings should be examined before discarding this technique.

Perhaps the most direct and effective method of controlling ring compression stiffness is the slotted bolt-hole concept. Here, slots, instead of holes, are cut in the corrugated structural plate for longitudinal seam connections. The slot-joints are bolted together in their extended position. As fill soil is raised, ring compression thrust increases until the slotted-joint frictional resistance is exceeded producing controlled joint slippage. Overall, the structure circumferentially shortens and forces positive soil arching. Frictional

resistance is controlled by bolt torque and slot width. ARMCO Steel Company has introduced a "keyhole" slot with the slot width slightly smaller than the bolt hole (7-2).

An analytical model of this concept has not been attempted for this study. Conceivably, the interface element in CANDE could be modified to simulate the slotted bolt hole behavior. This would require patient development and experimental data, Thus, it is left to a future study.

Simplified approaches of modeling joint slippage have been attempted (7-3) by artificially reducing the cross-sectional area of liner wall to produce reduced ring-compression stiffness. However, this approach appears oversimplified and does not replicate the elastic-plastic nature of joint slippage. For example, a reduction in wall area by a factor of 6 resulted in only 10% decrease of thrust. A realistic model of joints must show a plateau of nearly 100% reduction of thrust as frictional slip occurs.

7.6 Figures 7-1 through 7-27

		Page
Fig. 7.1	Reinforcement Zones in Basic Model.	172
Fig. 7-2	Influence of percentage of reinforcement.	173
Fig. 7-3	Influence of percentage of reinforcement.	174
Fig. 7-4	Distribution plots at full fill height, complete and connected reinforcement.	175
Fig. 7-5	Connected vs. unconnected reinforcement to liner.	176
Fig. 7-6	Connected vs. unconnected reinforcement to liner.	177
Fig. 7-7	Distribution plots af full fill height for reinforcement connection.	178
Fig. 7-8	Effect of selective placement of reinforcements.	179
Fig. 7-9	Effect of selective placement of reinforcements.	180
Fig. 7-10	Distribution plots at full fill for selective reinforcements.	181
Fig. 7-11	Stabilized soil zones.	182
Fig. 7-12	Crown displacements for increased stabilized soil stiffness.	183
Fig. 7-13	Springline thrust for increased stabilized soil stiffness.	184
Fig. 7-14	Effect of stiff soil modulus on structural distributions.	185
Fig. 7-15	Crown displacement history for stabilized soil widths.	186
Fig. 7-16	Springline thrust history for stabilized soil widths.	187
Fig. 7-17	Effect of stiff soil zone width on structural distributions.	188

7.6 Figures 7-1 through 7-27 (cont'd)

		Page
Fig. 7-18	Soft inclusion zones.	189
Fig. 7-19	Crown displacement histories for various moduli of soft inclusion.	190
Fig. 7-20	Springline thrust history for various moduli of soft inclusions.	191
Fig. 7-21	Effect of soft inclusion modulus on structural distributions.	192
Fig. 7-22	Crown displacement histories for various soft material heights.	193
Fig. 7-23	Springline thrust histories for various soft materials.	194
Fig. 7-24	Distribution plots for variations of soft material height.	195
Fig. 7-25	Crown displacement histories for soft and stiff inclusions.	196
Fig. 7-26	Springline thrust histories for soft and stiff inclusions.	197
Fig. 7-27	Distribution plots for soft and stiff inclusions.	198

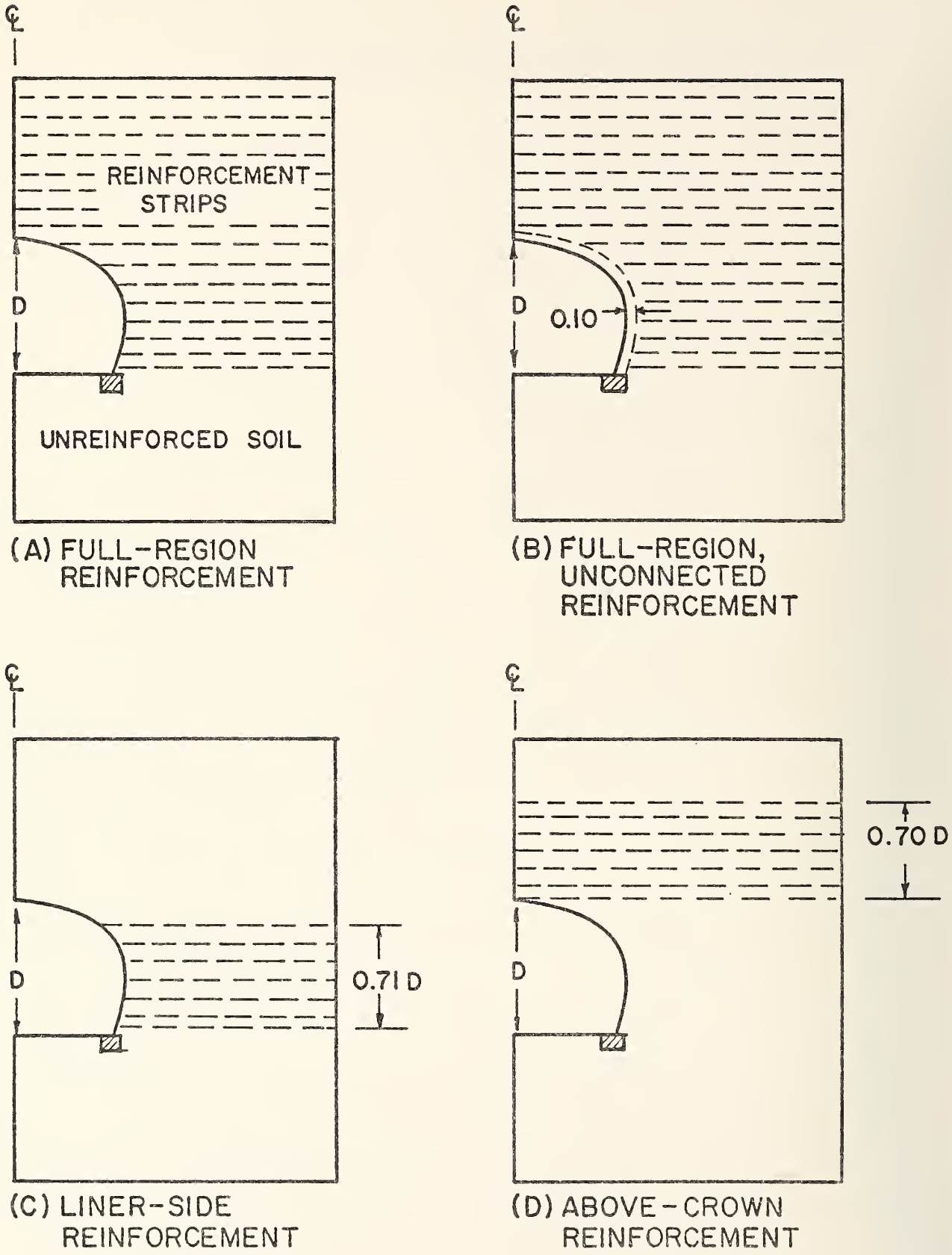

Figure 7.1 Reinforcement Zones in Basic Model.

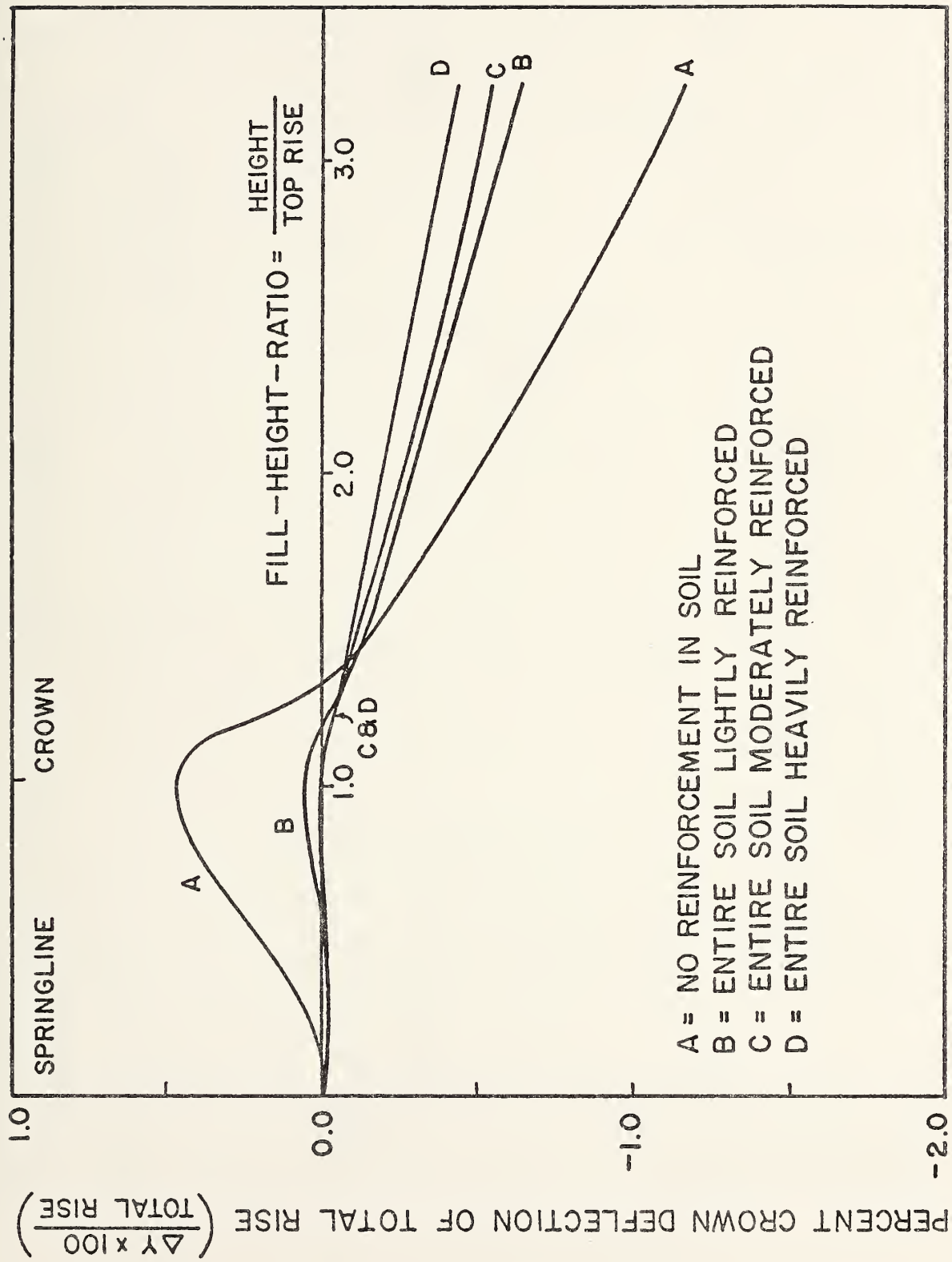

Figure 7.2 Influence of Percentage of Reinforcement.

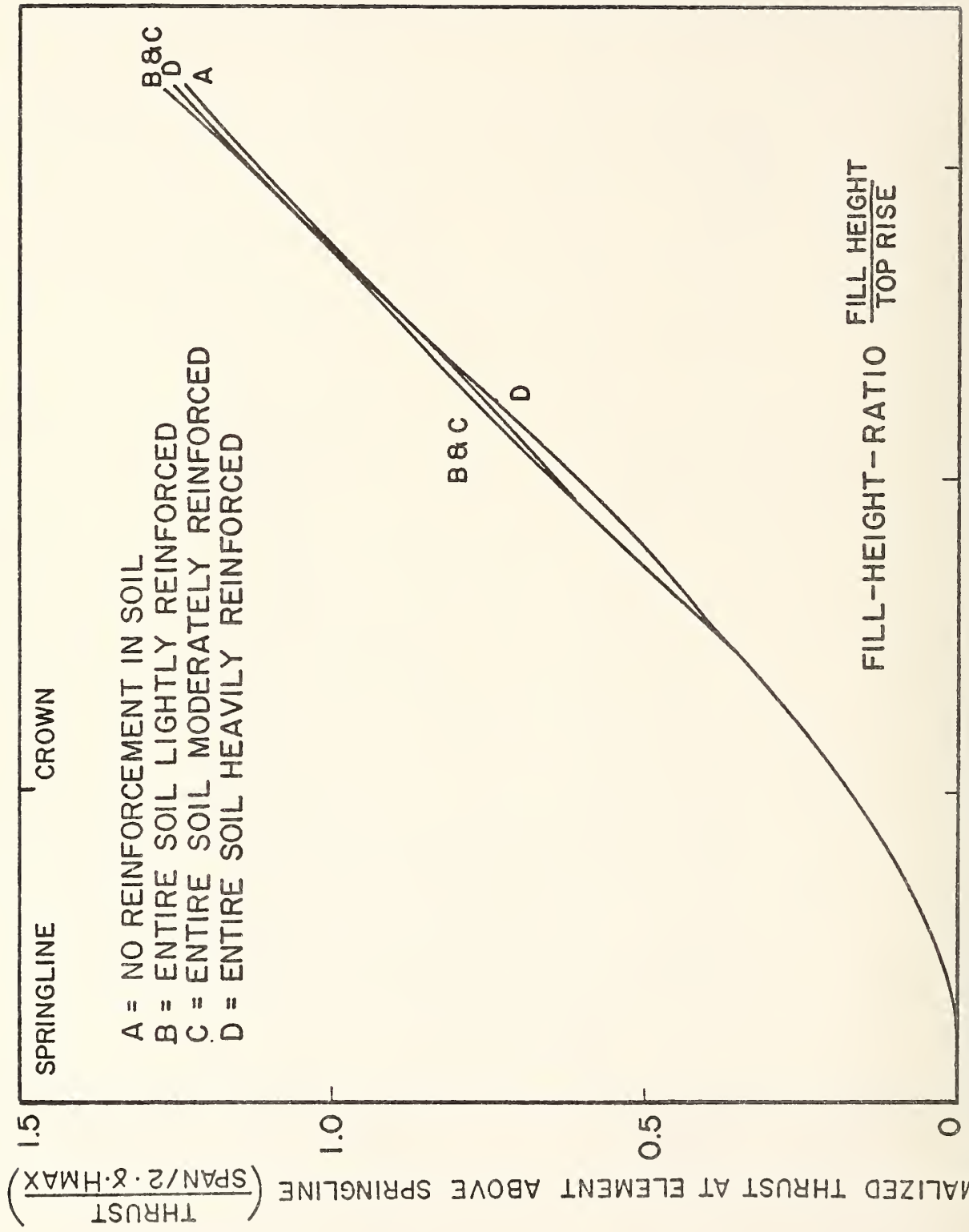

Figure 7.3 Influence of Percentage of Reinforcement.

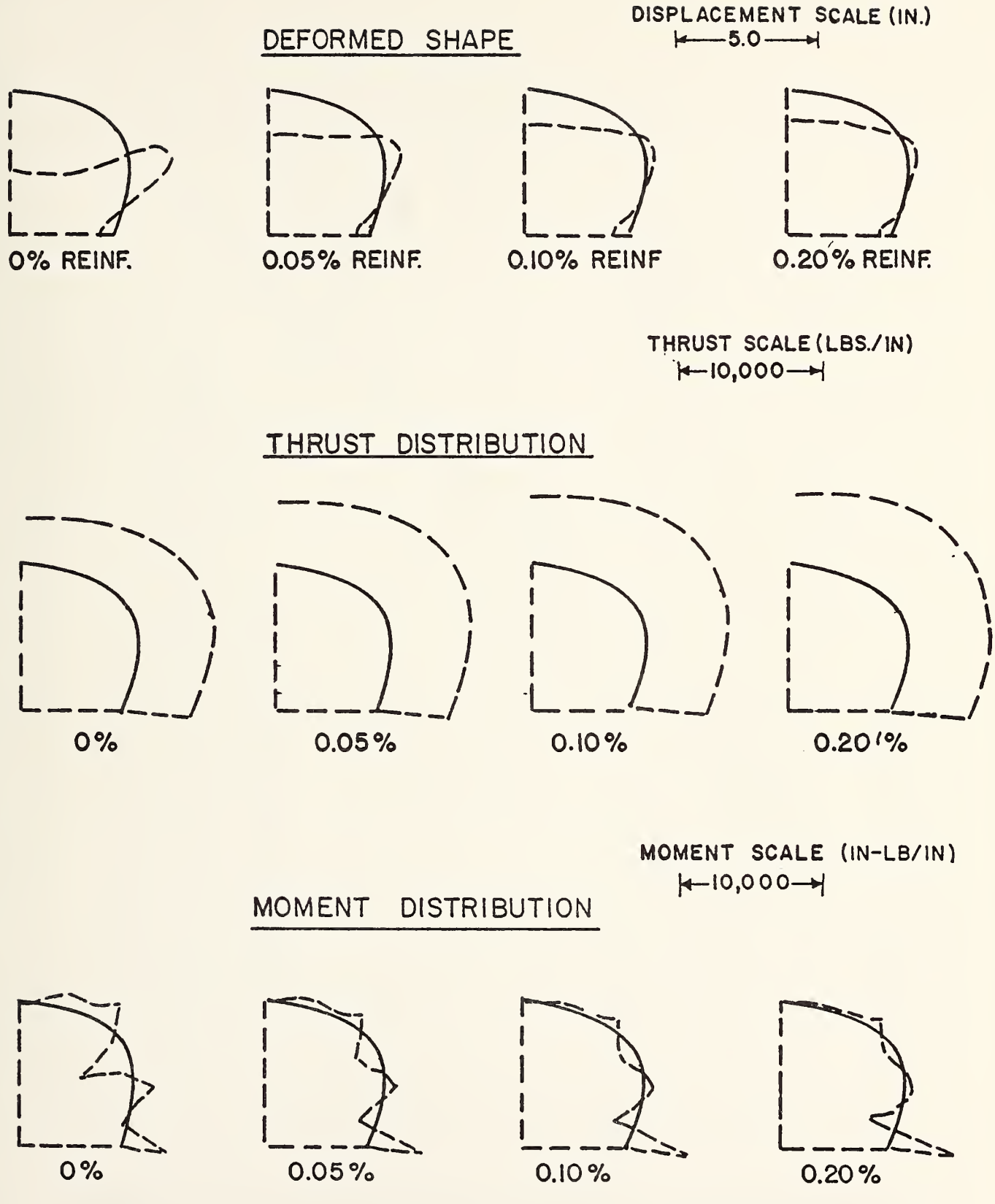

Figure 7.4 Distribution plots at Full Fill Height, Complete and Connected Reinforcement.

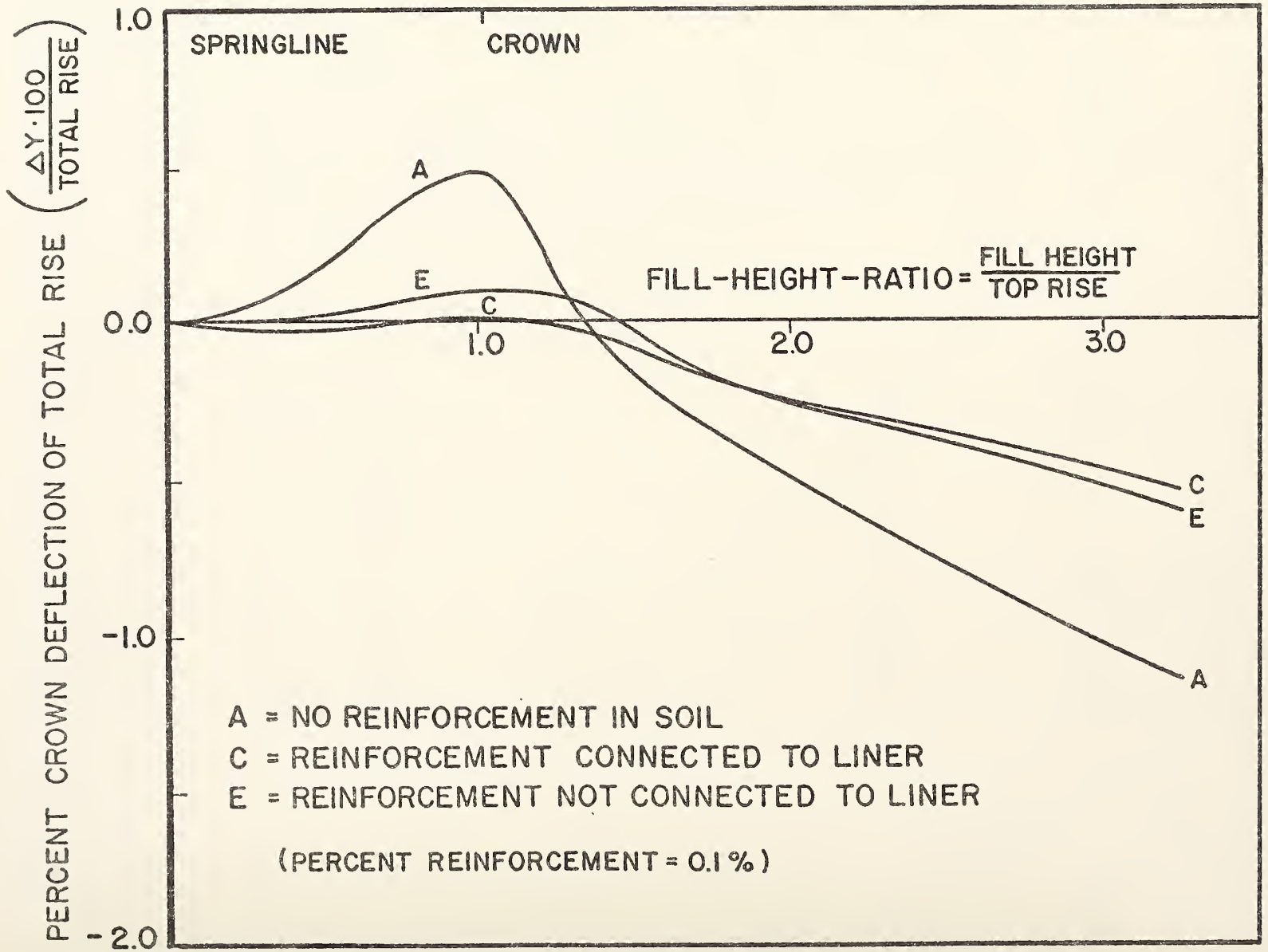

Figure 7.5 Connected vs. Unconnected Reinforcement to Liner.

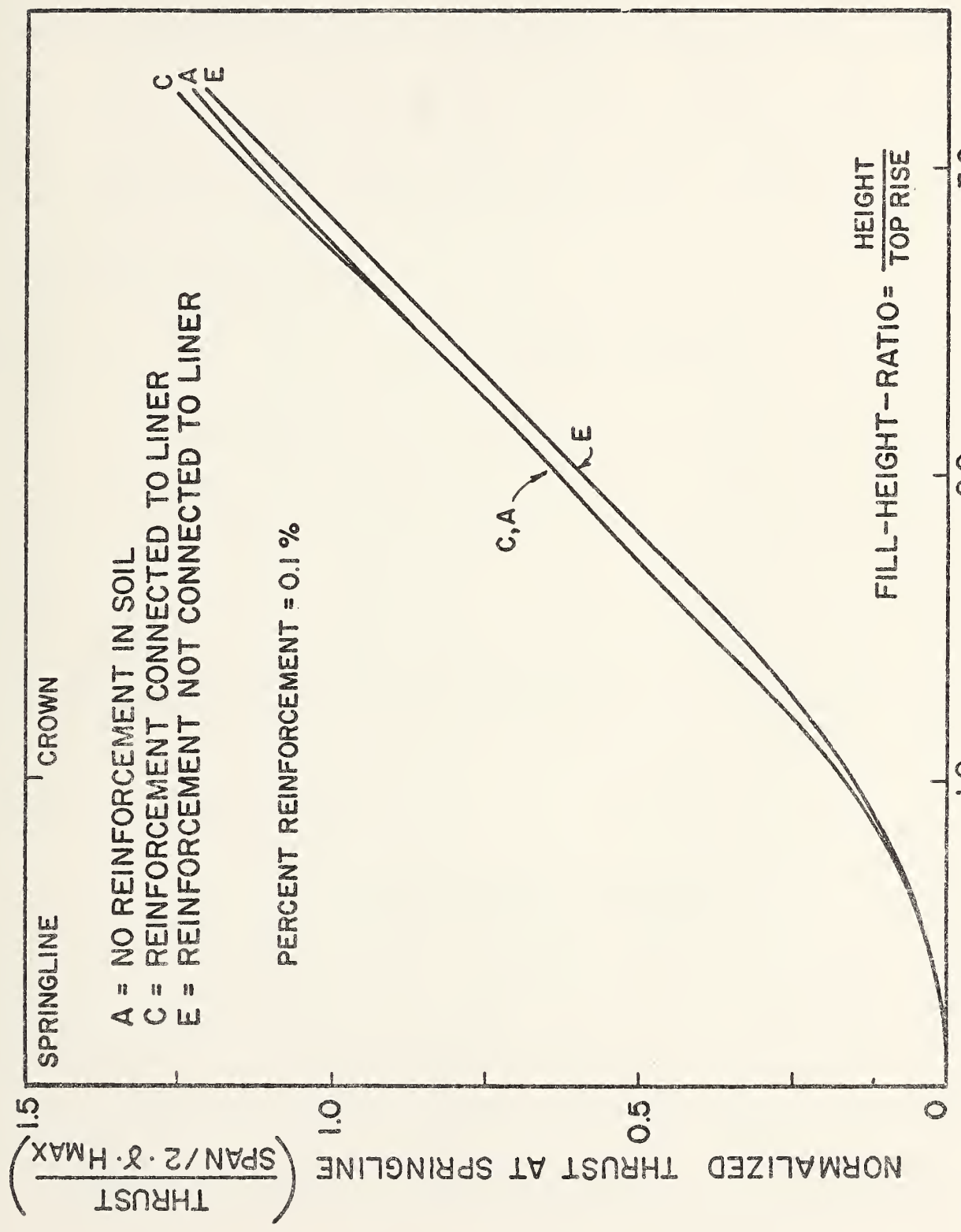

Figure 7.6 Connected vs. Unconnected Reinforcement to Liner.

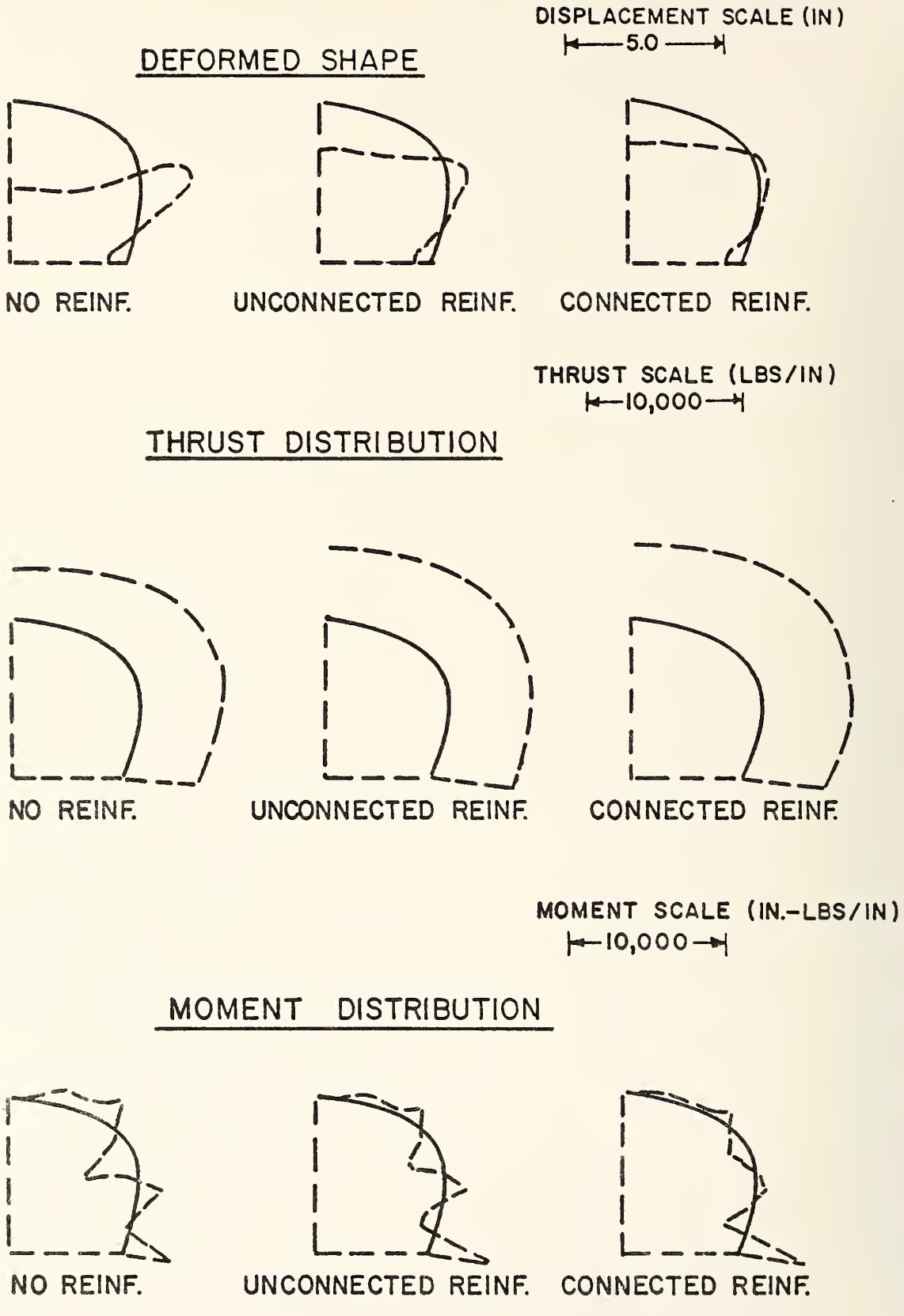

Figure 7.7 Distribution Plots at Full Fill Height for Reinforcement Connection.

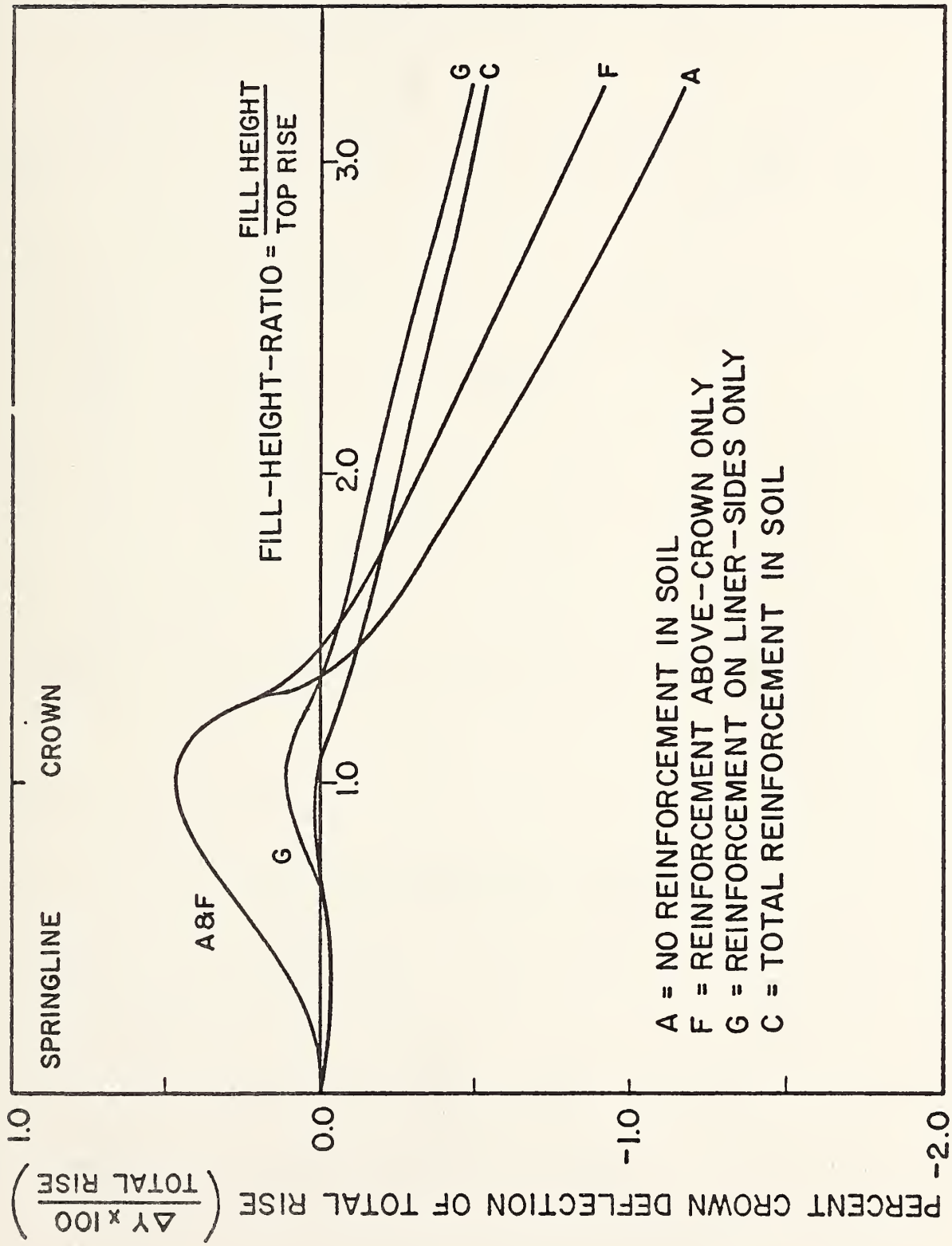

Figure 7.8 Effect of Selective Placement of Reinforcements.

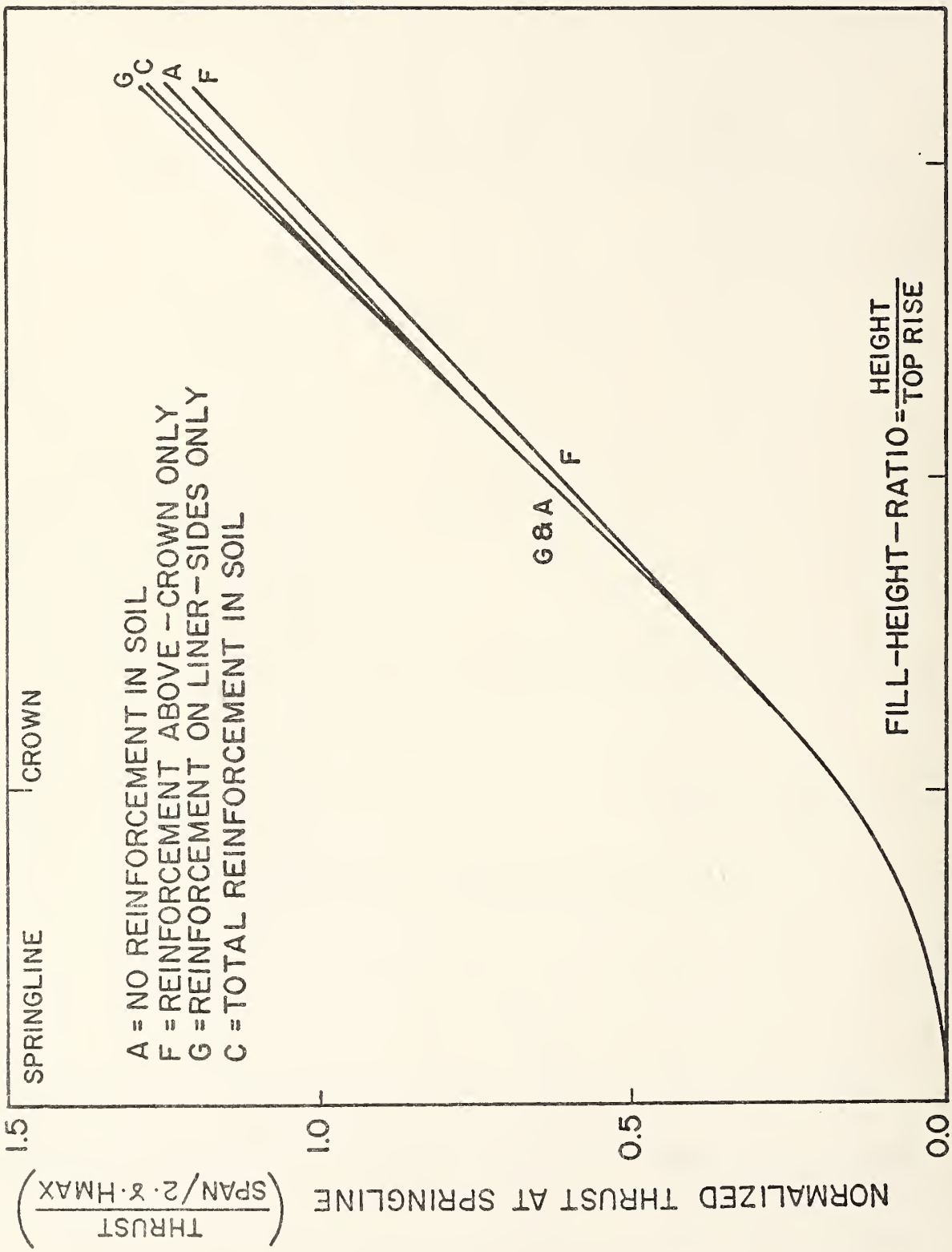

Figure 7.9 Effect of Selective Placement of Reinforcements.

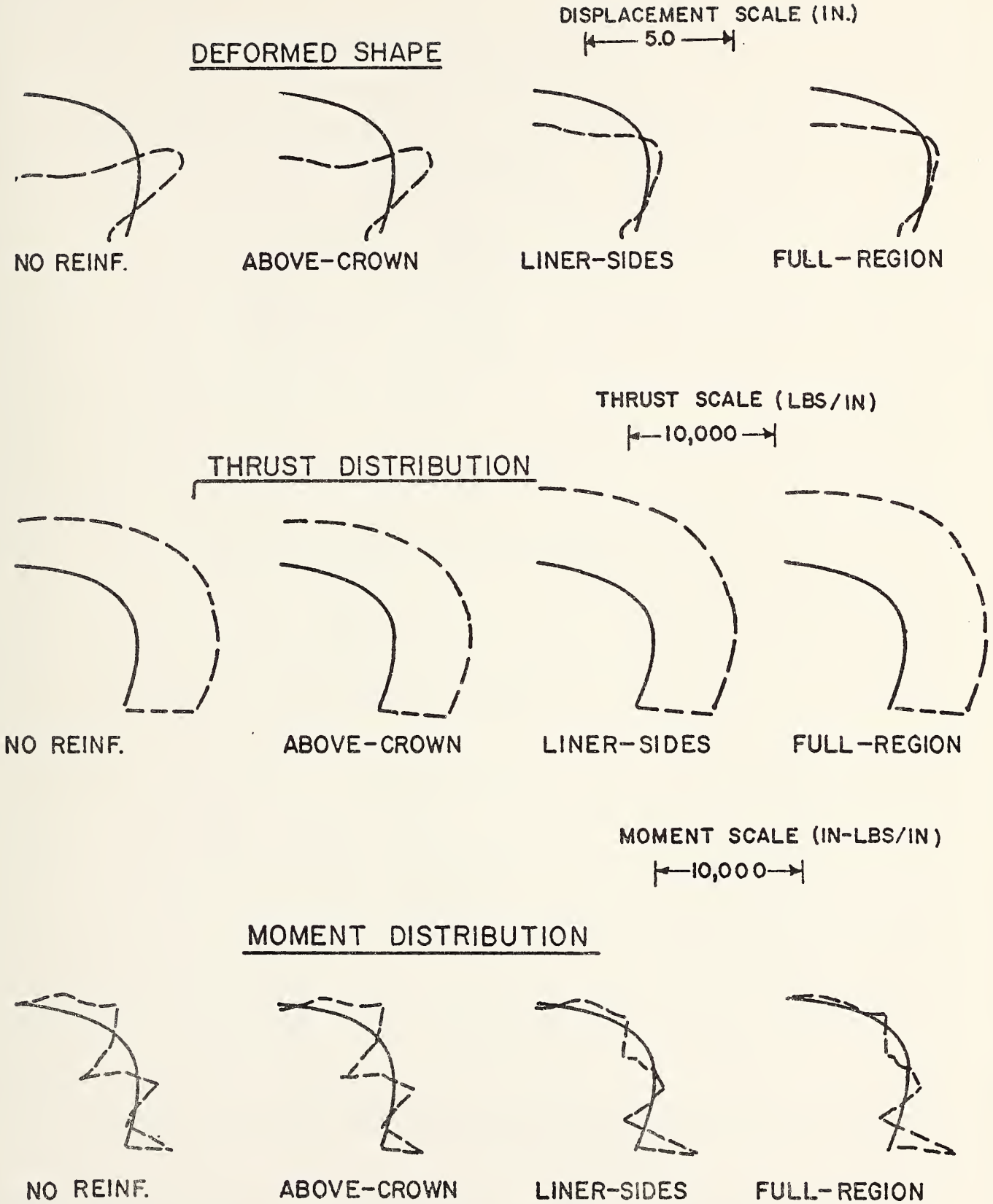

Figure 7.10 Distribution Plots at Full Fill for Selective Reinforcements.

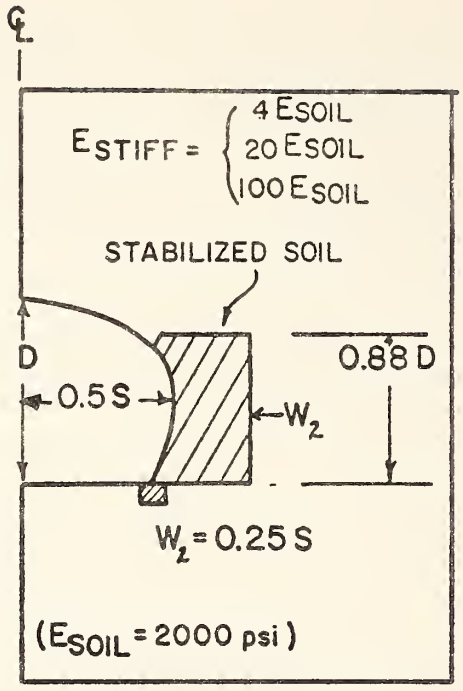

(A) CONSTANT ZONE WIDTH, VARIABLE MODULUS

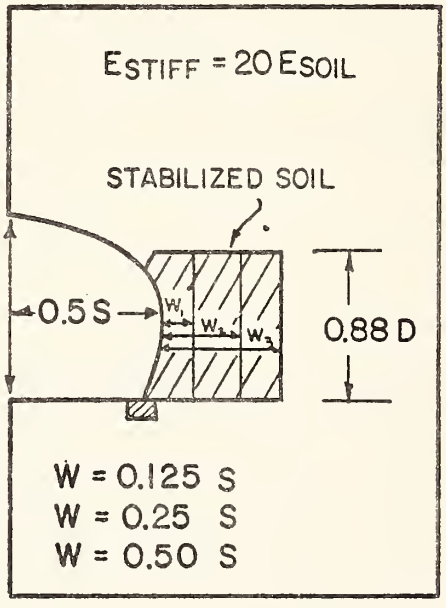

(B) CONSTANT MODULUS, VARIABLE ZONE WIDTH

Figure 7.11 Stabilized Soil Zones.

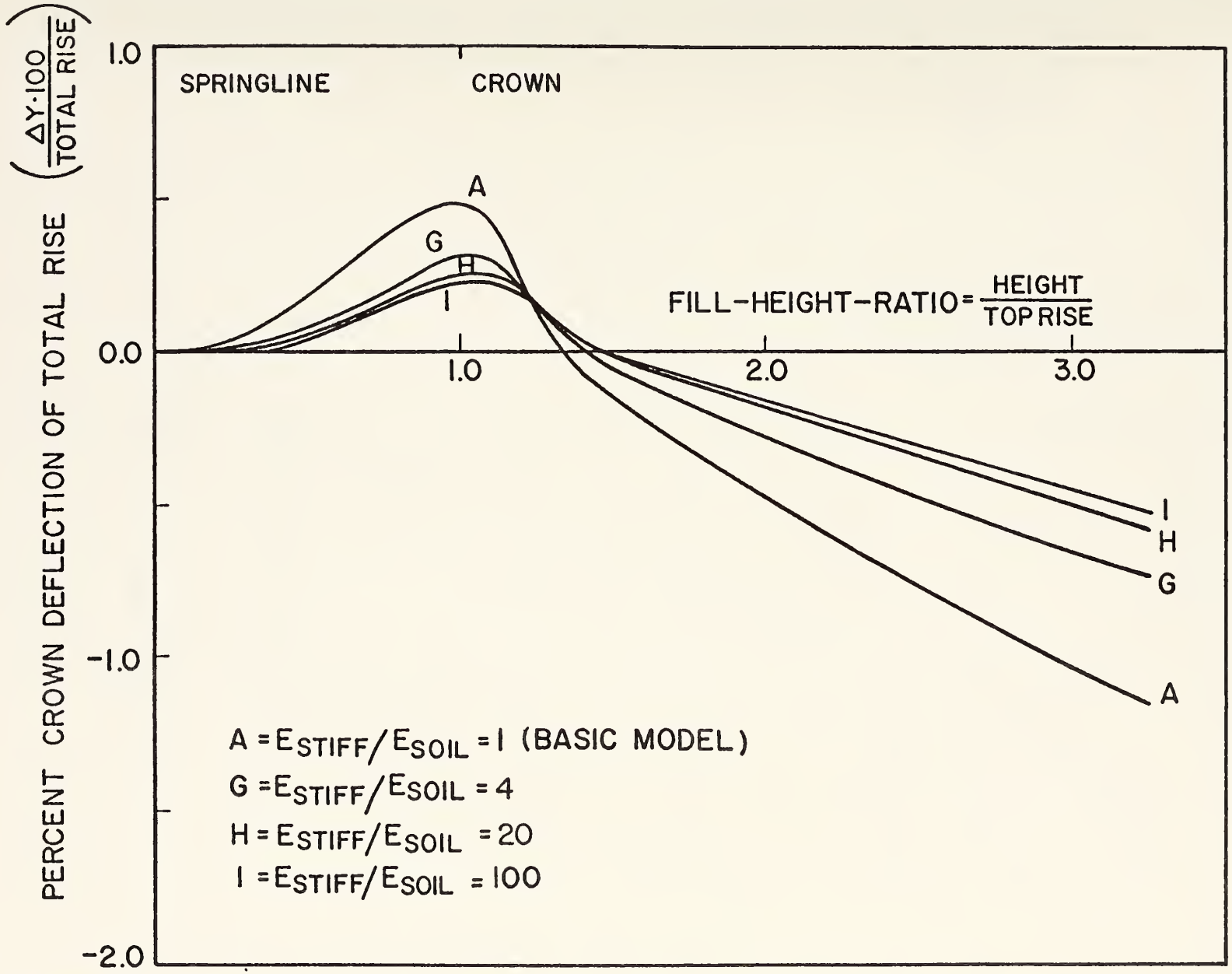

Figure 7.12 Crown Displacements for Increased Stabilized Soil Stiffness.

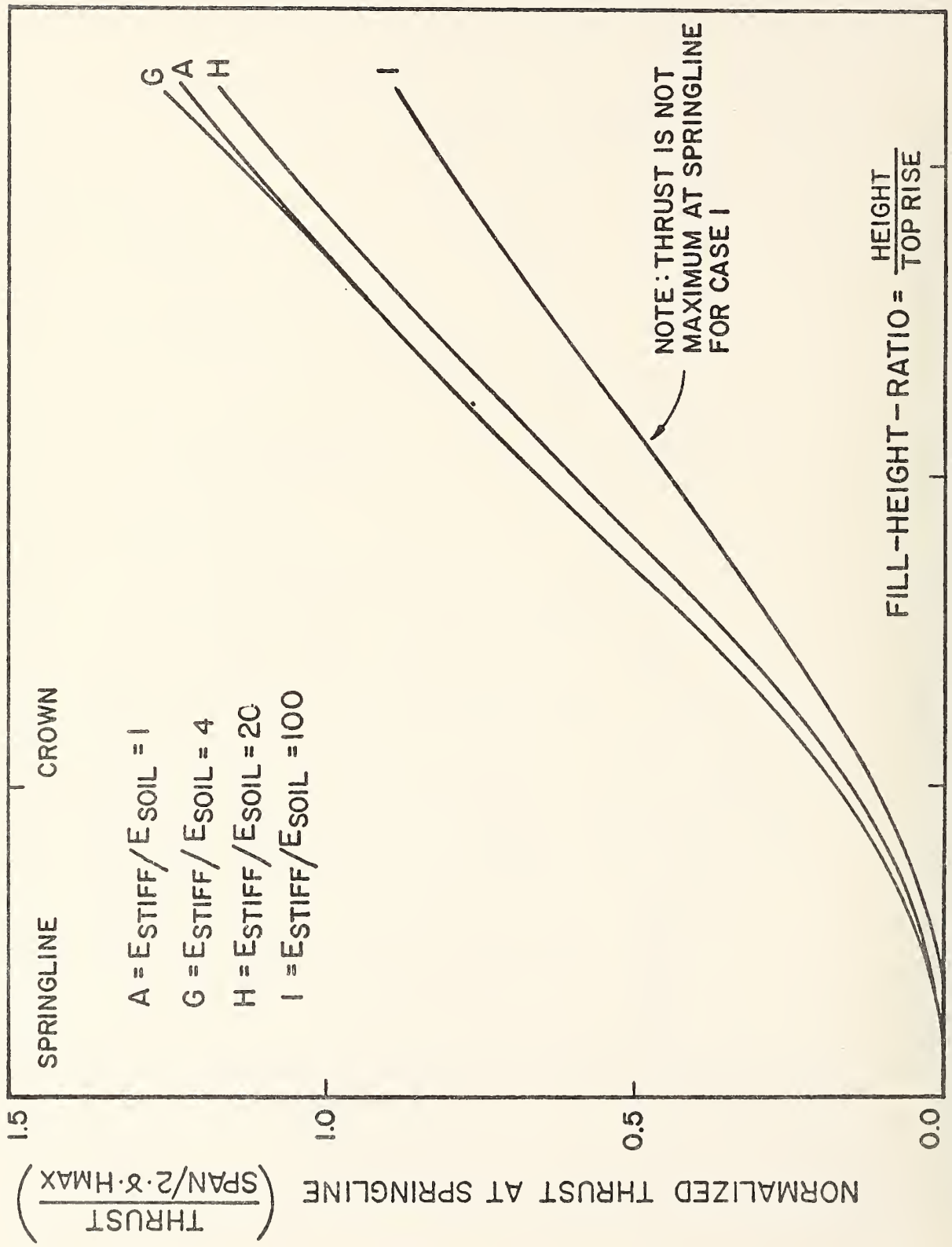

Figure 7.13 Springline Thrust for Increased Stabilized Soil Stiffness.

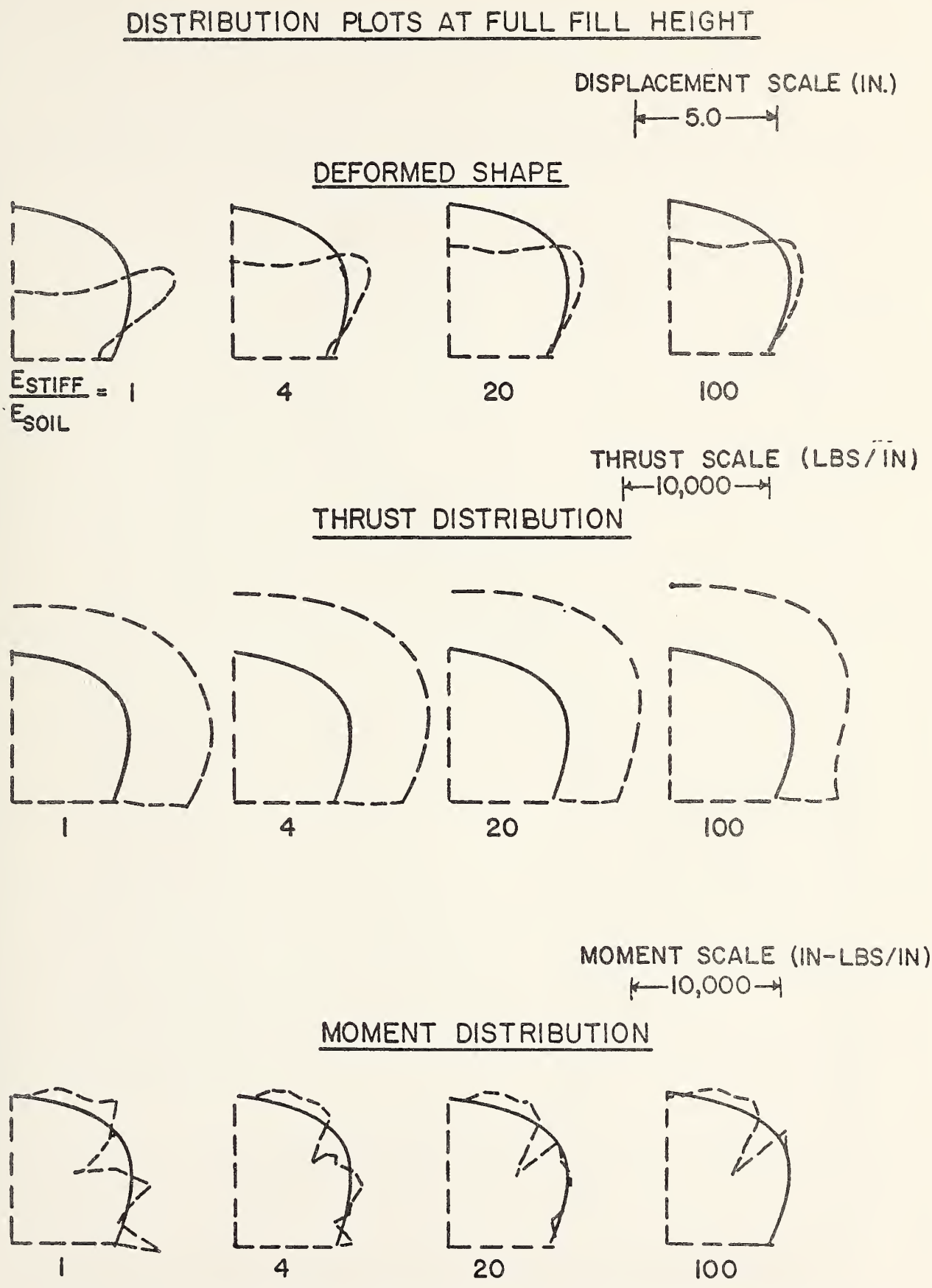

Figure 7.14 Effect of Stiff Soil Modulus on Structural Distributions

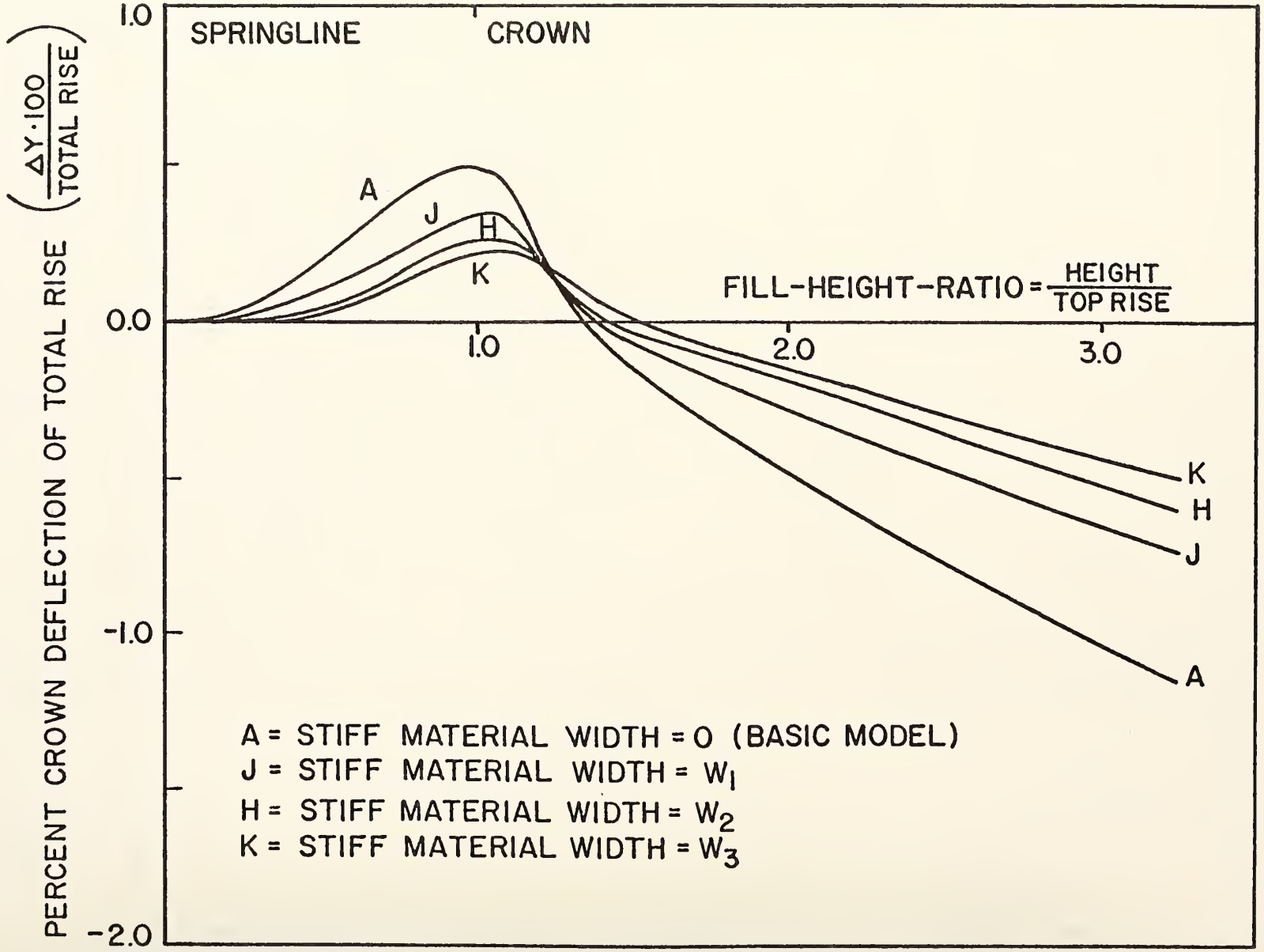

Figure 7.15 Crown Displacement History for Stabilized Soil Widths.

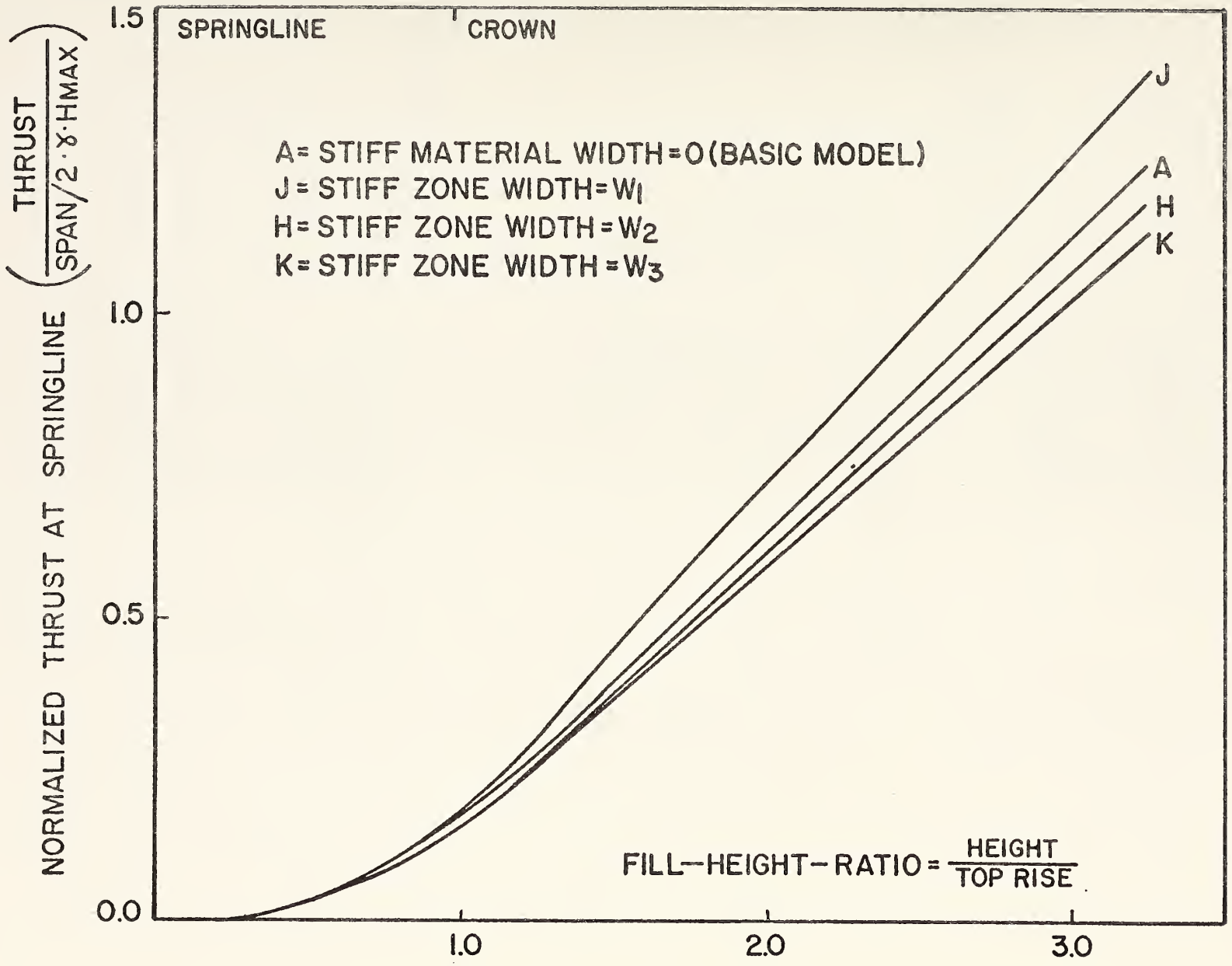

Figure 7.16 Springline Thrust History for Stabilized Soil Widths.

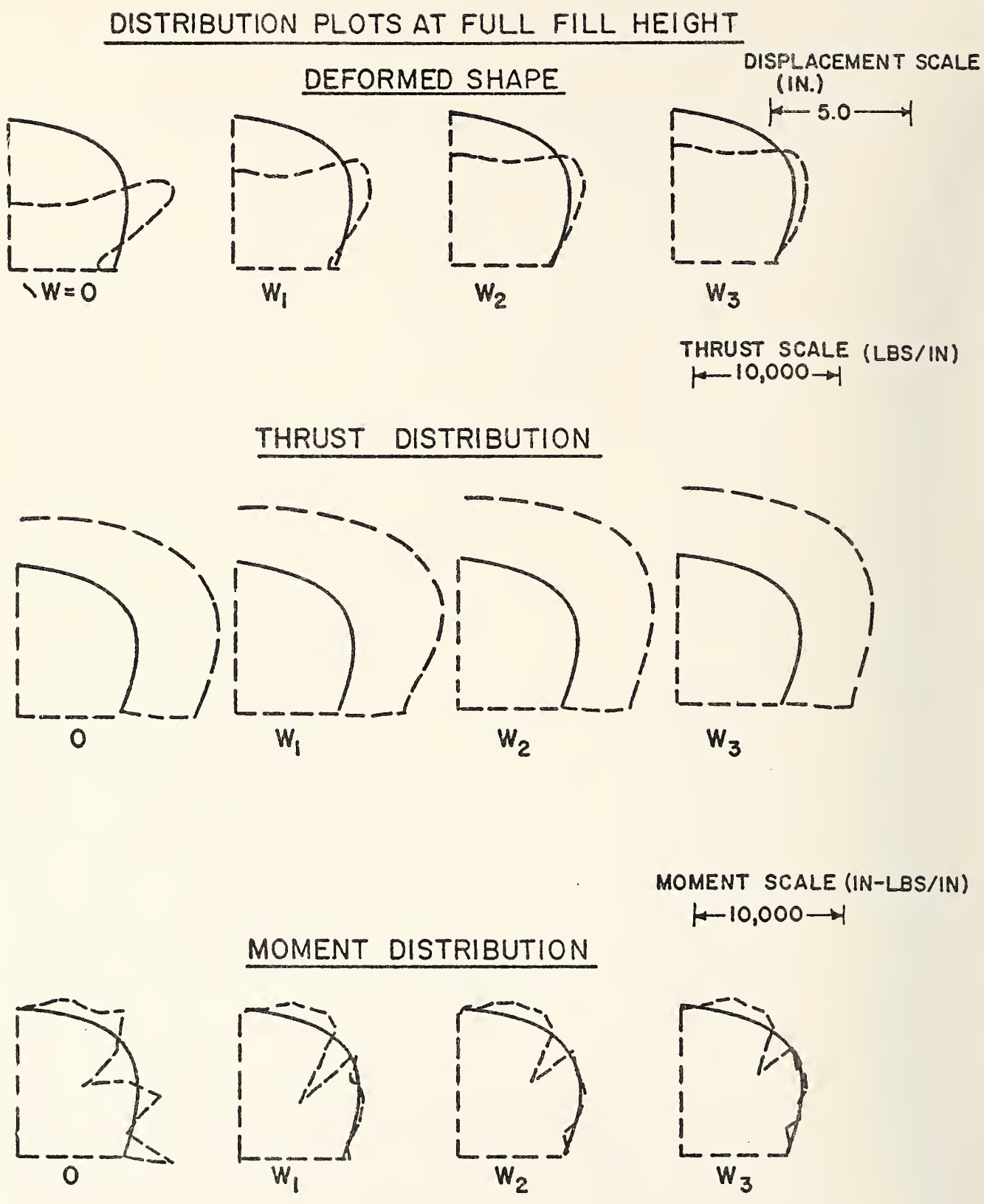

Figure 7.17 Effect of Stiff Soil Zone Width on Structural Distributions.

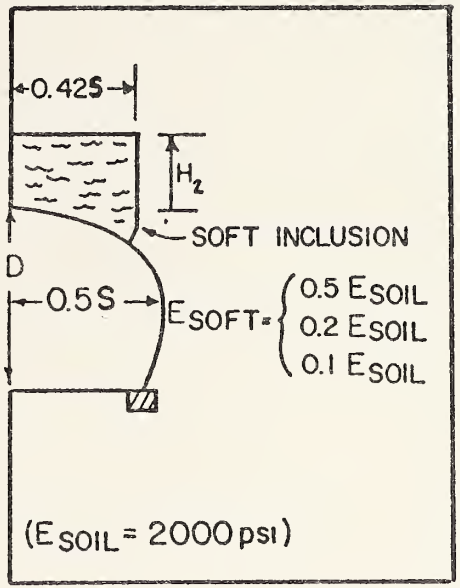

(A) CONSTANT DIMENSIONS, VARIABLE MODULUS

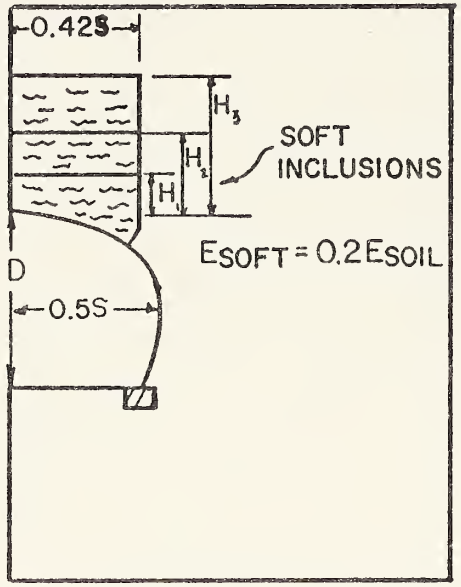

(B) CONSTANT MODULUS, VARIABLE HEIGHTS

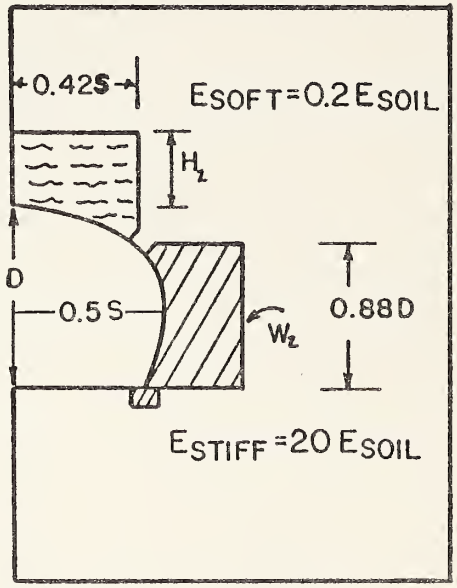

(C) COMBINED SOFT MATERIAL PLUS STABILIZED SOIL

Figure 7.18 Soft Inclusion Zones.

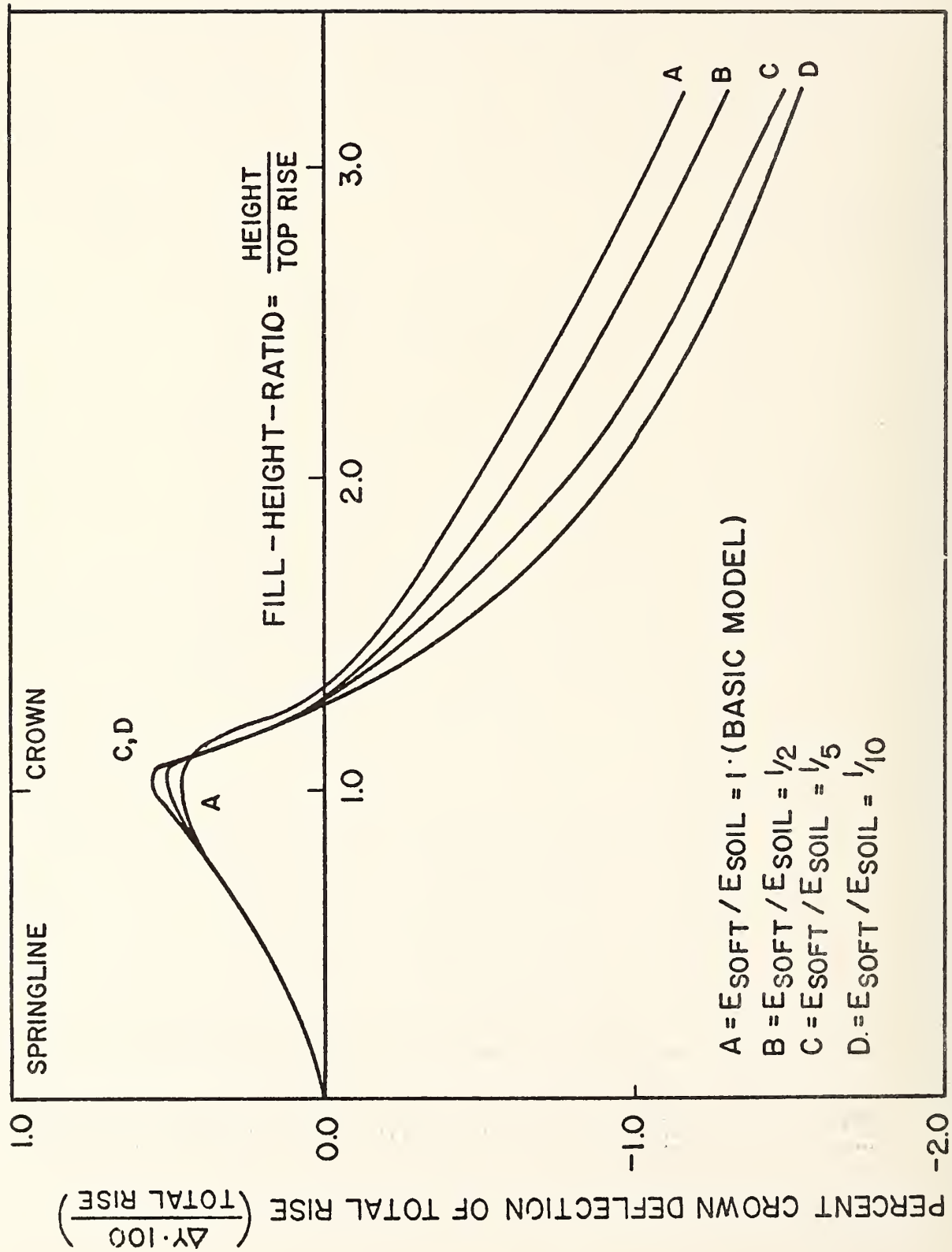

Figure 7.19 Crown displacement histories for various moduli of soft inclusion.

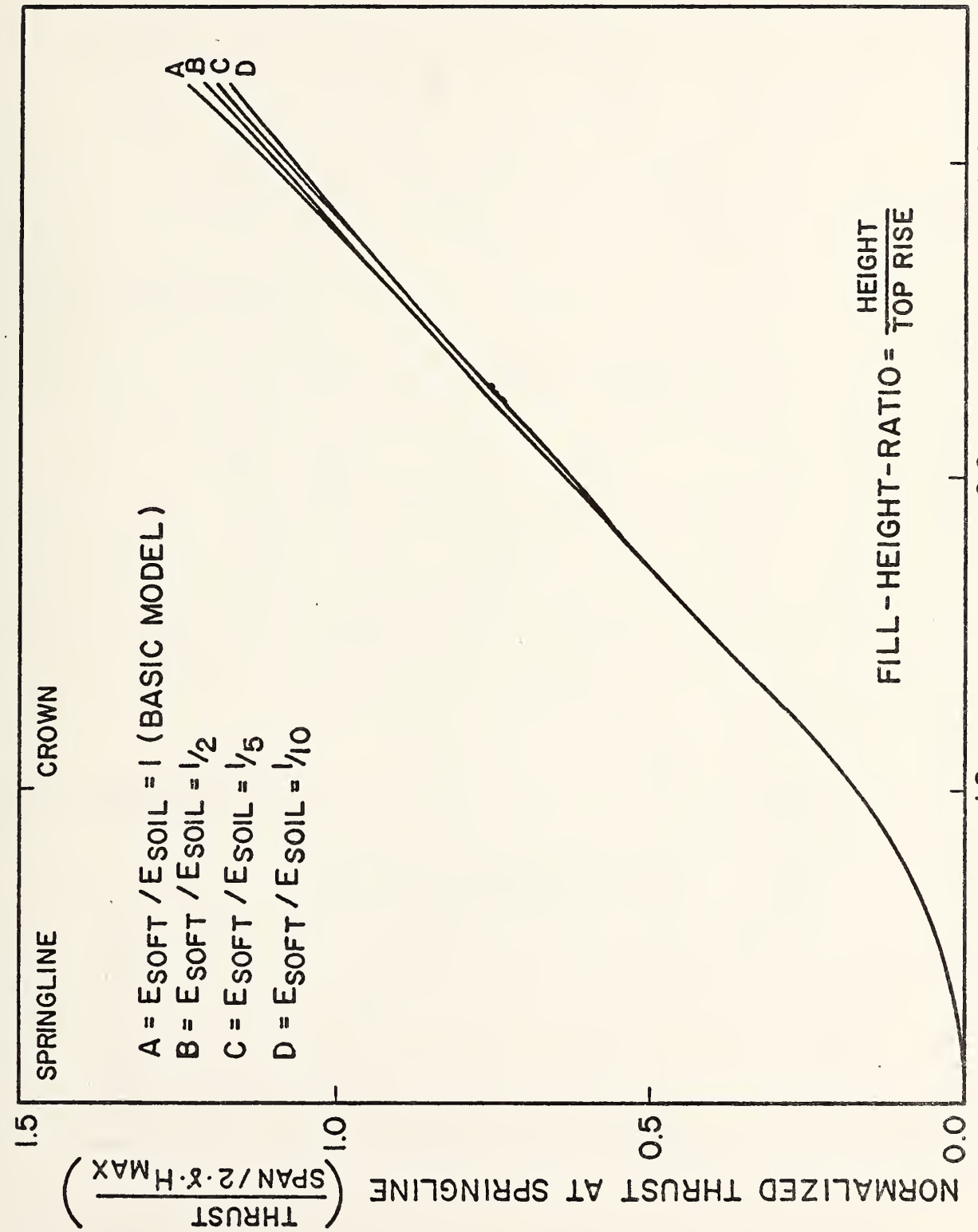

Figure 7.20 Springline Thrust History for Various Moduli of Soft Inclusions.

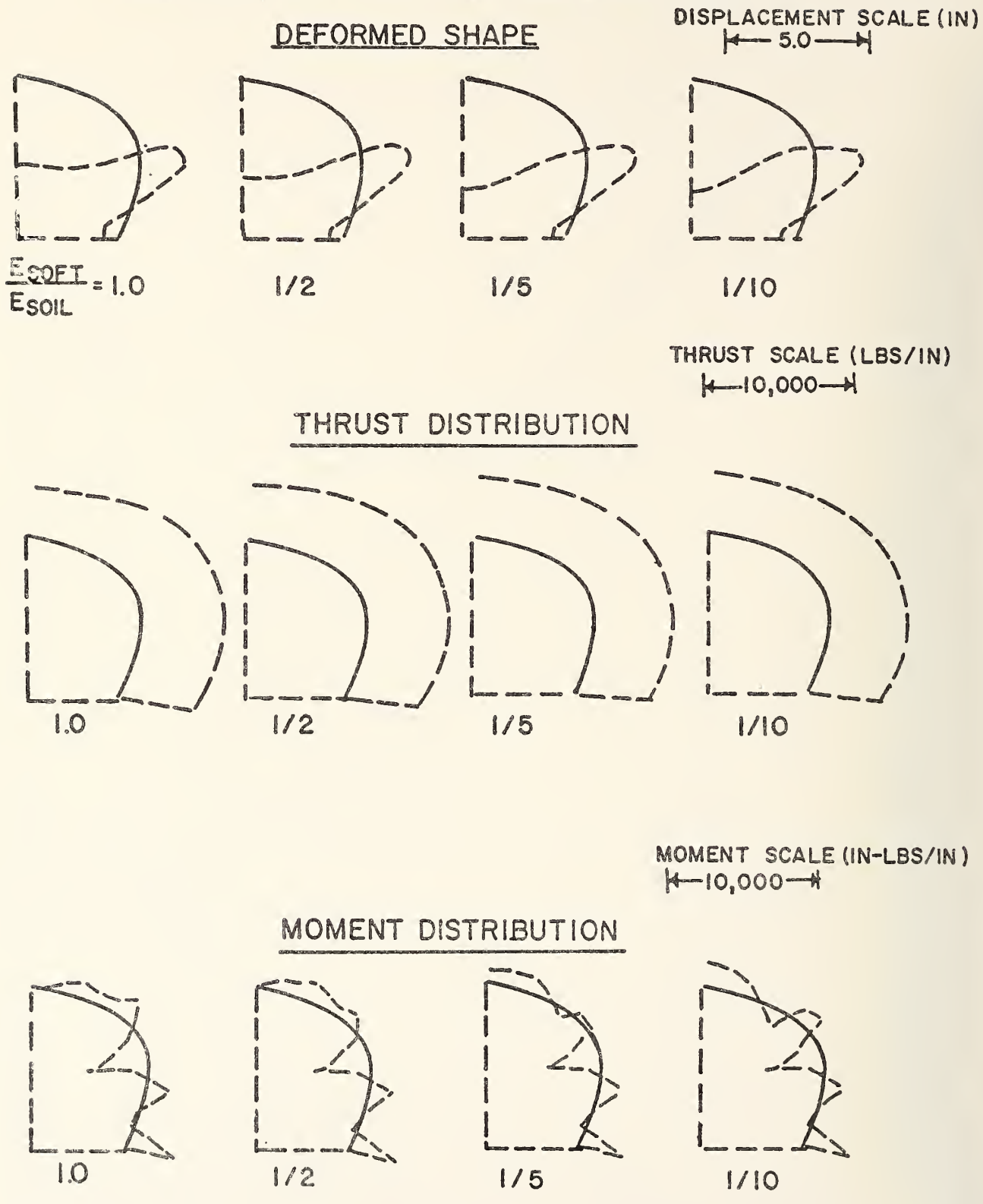

Figure 7.21 Effect of Soft Inclusion Modulus on Structural Distributions.

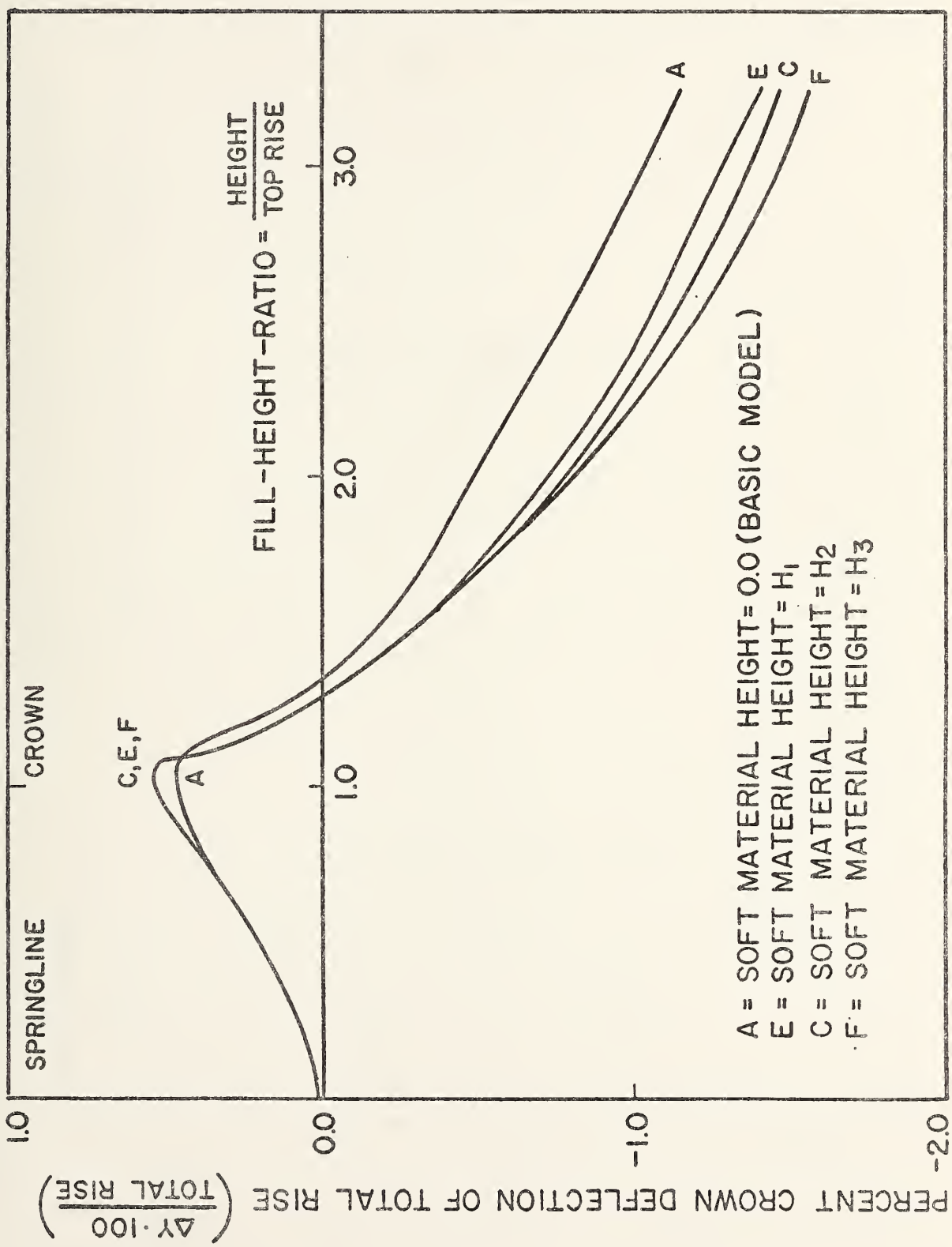

Figure 7.22 Crown Displacement Histories for Various Soft Material Heights.

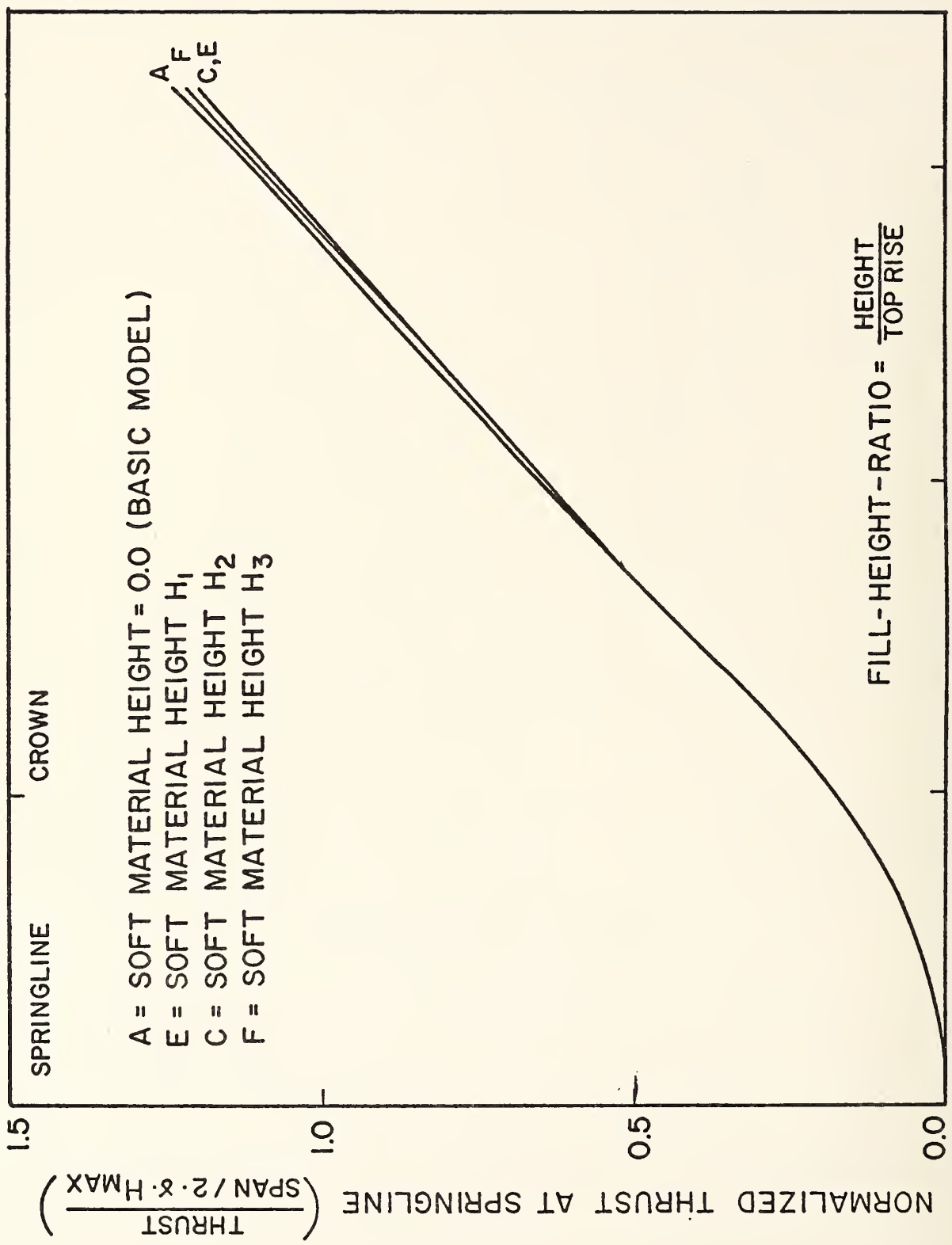

Figure 7.23 Springline Thrust Histories for Various Soft Materials.

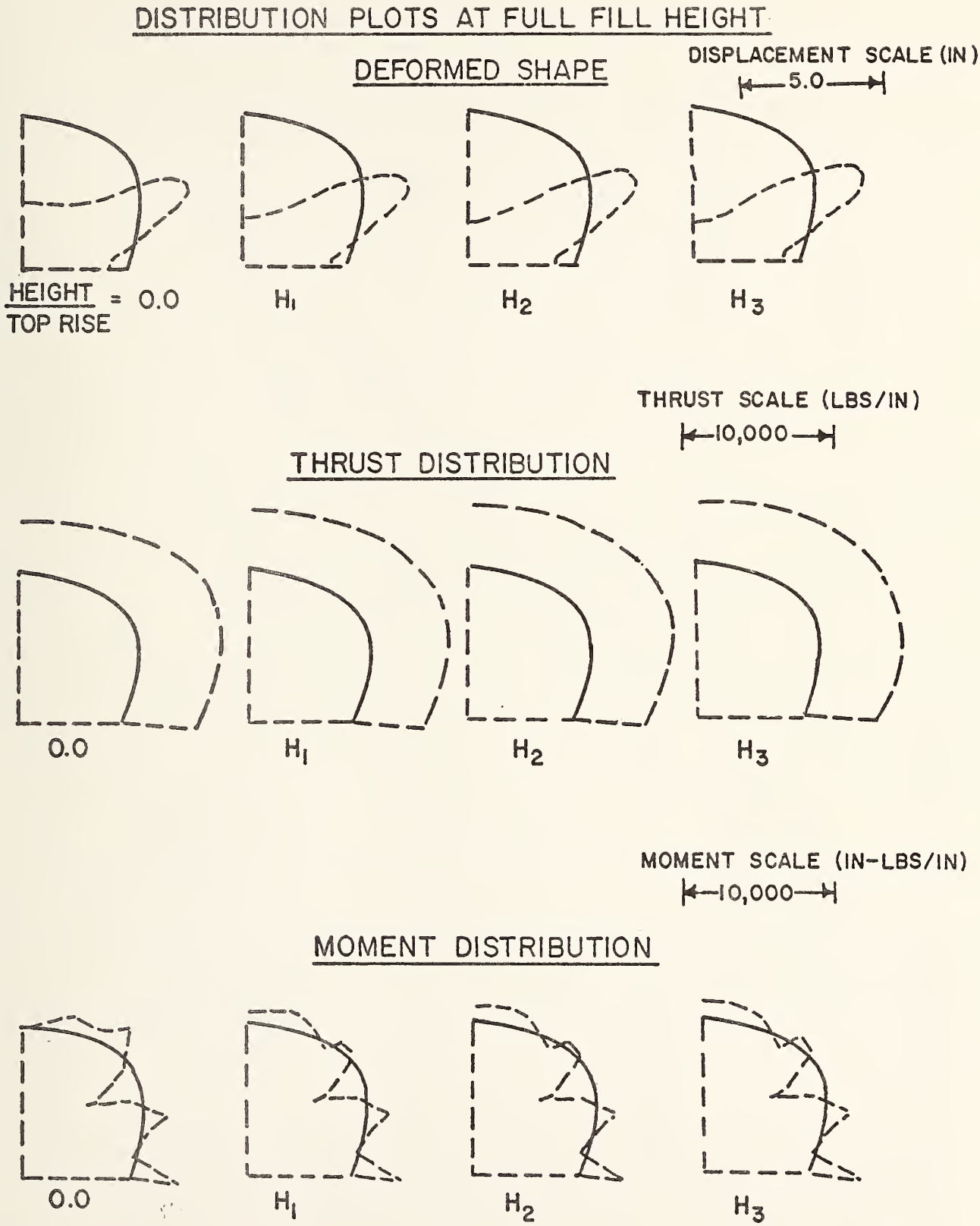

Figure 7.24 Distribution Plots for Variations of Soft Material Height.

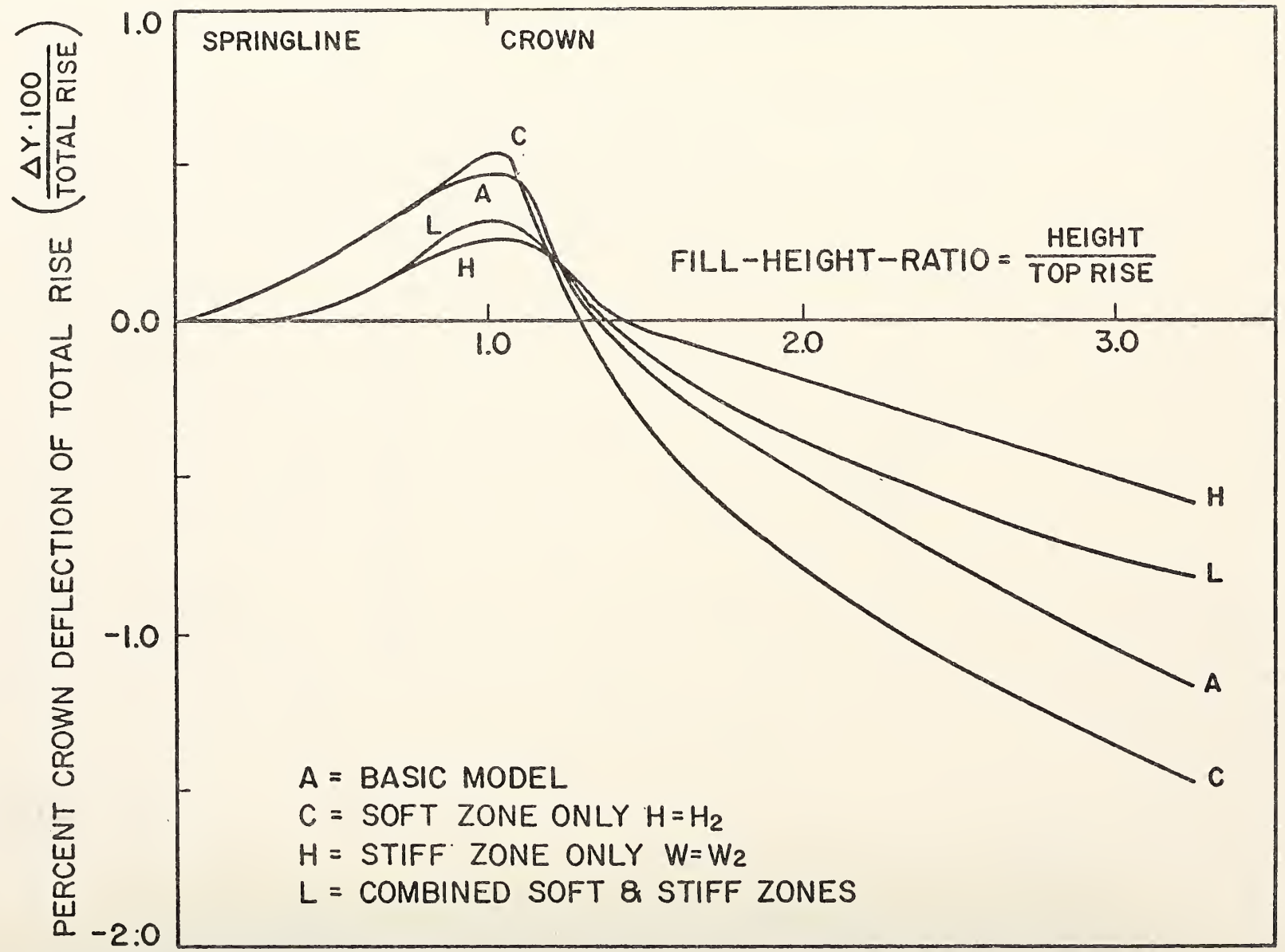

Figure 7.25 Crown Displacement Histories for Soft and Stiff Inclusions.

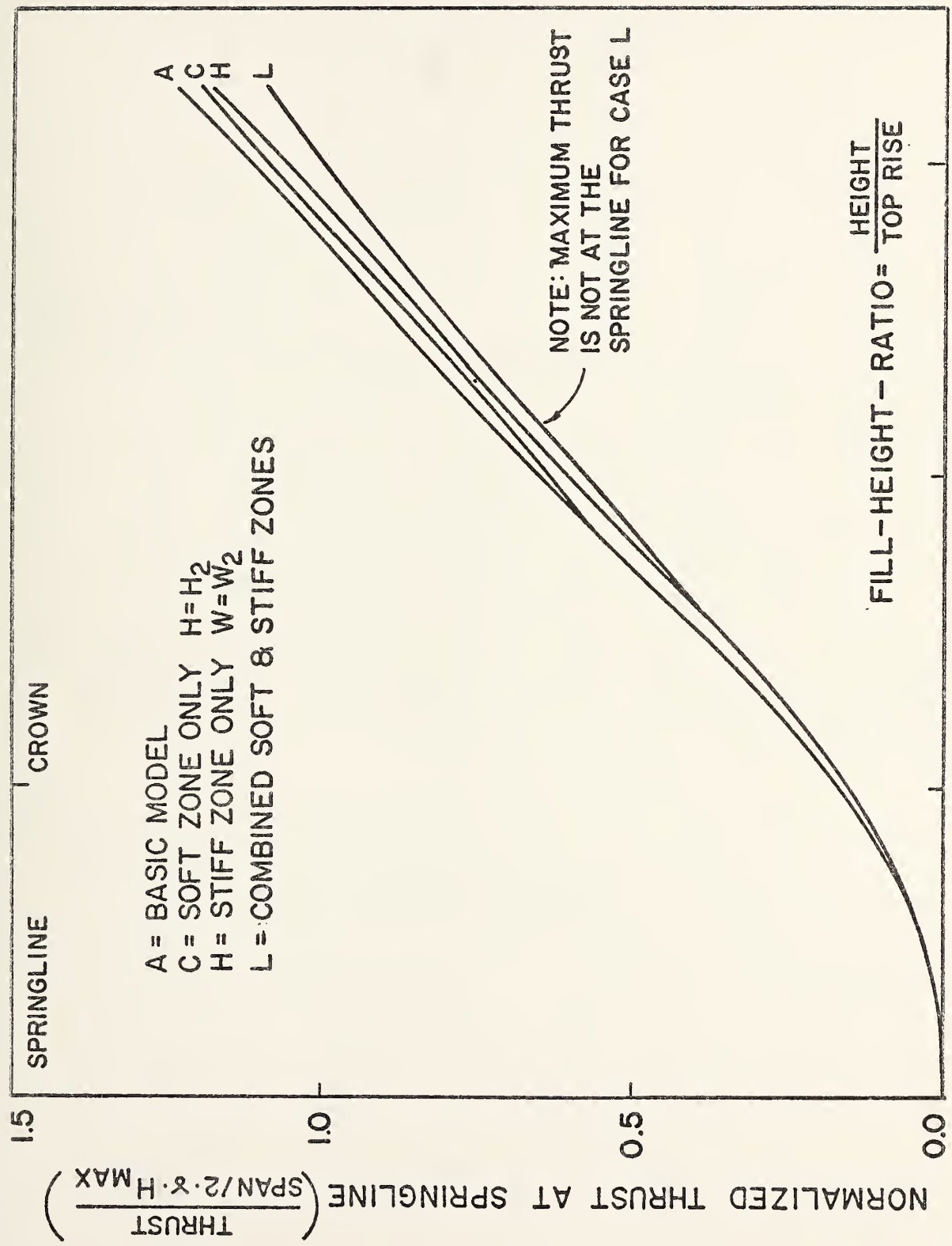

Figure 7.26 Springline Thrust Histories for Soft and Stiff Inclusions.

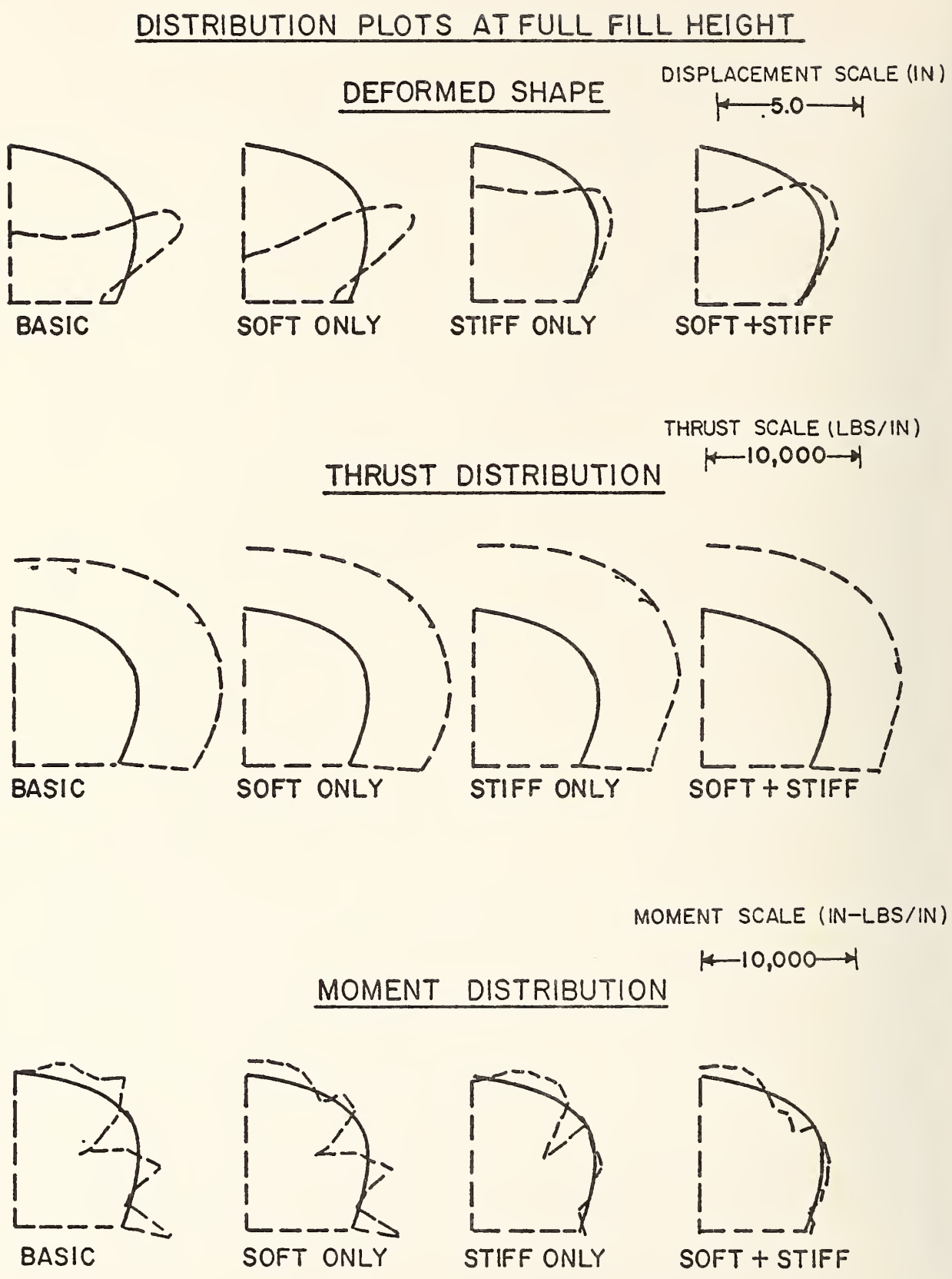

Figure 7.27 Distribution Plots for Soft and Stiff Inclusions

CHAPTER 8

PARAMETER STUDIES OF NEW CONCEPTS APPLIED TO TRADITIONAL CULVERTS

8.1 STATEMENT OF PURPOSE

In this chapter, parameter studies of "traditional" culverts (as opposed to long-span culverts) are investigated. Two common culvert types are considered; corrugated steel and reinforced concrete. These culverts are assumed round with a nominal diameter of 6.5 ft. (2.0m) and are detailed in Table 8-1. For this study, the culverts are assumed deeply buried so that soil loading is represented by equivalent overburden pressure as discussed in CANDE Engineering Manual. Soil properties are assumed homogenous and elastic and are also identified in Table 8-1.

Keeping the above material properties constant, the following system parameters are systematically changed to ascertain their effect on relieving the structural distress on both types of culverts: bedding configuration, imperfect trench, backpacking, stabilized soil, V-notch trench, and fluid jacket. The results of each of these studies are presented below. In all cases, levels 2 and 3 of the CANDE program were used to obtain solutions.

8.2 EFFECT OF BEDDING MATERIAL

Here bedding is considered as any special material placed under and adjacent to the culvert extrados to provide a uniform platform to support the culvert. Three bedding parameters are considered independently; width, height, and modulus of bedding material. In all cases, the bottom of the bedding material is located at one-half radius below the culvert invert and Poisson's ratio is taken as 0.33.

Figure 8-1 shows the assumed variation in bedding height from 0.0 to 3/2 radii, while the bedding half-width is held

TABLE 8-1

CONSTANT PARAMETERS FOR TRADITIONAL CULVERT STUDY

Reinforced Concrete Pipe	Corrugated Steel Pipe	Soil System and Loading
Inside dia. = 60.0 in.	Diameter = 66.0 in	Young's Mod., E_s = 2667 psi
Wall thickness = 6.0 in.	Corrugation = 3x1 in.	Poisson's ratio, v_s = 0.33
	Steel gage = 12	
Inner cage area = 0.061 in^2/in	Linear properties*	Overburden pressure = 10.0 psi
Outer cage area = 0.041 in^2/in		No soil weight or incremental construction
Nonlinear option: concrete cracking*		

*Standard material properties supplied by CANDE program are used for steel and concrete.

constant at 7/6 radii, and the bedding modulus is held constant at 10 times the soil modulus. Also shown in Figure 8-1 are key response ratios obtained from the finite element solutions for both corrugated steel and reinforced concrete culverts. Response ratios are formed by dividing key structural responses from the system with bedding by the corresponding system without bedding (i.e., natural soil replaces bedding).

For the corrugated steel culvert, key response ratios are maximum wall thrust and diametrical deflection (solid lines), while the key response ratios for reinforced concrete are maximum steel reinforcement stress and maximum concrete compressive stress (dashed lines). In all cases, a response ratio less than 1.0 implies the bedding parameter is beneficial in relieving pipe distress, whereas a response ratio greater than 1.0 implies an increase in pipe distress. Examination of Figure 8-1 reveals that bedding is not beneficial for stress relief for either type of pipe, however, displacements of the corrugated steel pipe are reduced as the bedding height is increased.

In a similar manner, Figure 8-2 shows the bedding configuration for varying the bedding width while holding the height constant at 2/3 radii. Again, it is observed that increased amounts of bedding are not beneficial for stress relief. Further, it is observed, bedding widths beyond 1.2 radii have minimal effect on the structural responses of both culvert types.

Lastly, the influence of bedding modulus is examined by varying the bedding modulus from 0.1 to 1000 times the soil modulus with the constant bedding dimensions shown in Figure 7-3. When the moduli ratio is below 1.0 (soft bedding) significant relief of structural responses is observed and is attributed to positive soil arching, i.e., the soil load is diverted around the culvert. Stiff beddings on the other hand, tend to increase stresses in both types of pipe, however, the displacements in the corrugated steel pipe are reduced.

The observation that soft materials tend to relieve structural distress in culverts has been known since the early part of this century and provides the stimulus for several of the concepts to be investigated later in this chapter. However, before dismissing stiff beddings out-of-hand, it must be recognized stiff beddings are beneficial with respect to longitudinal bending, alignment, and joint control.

8.3 EFFECT OF IMPERFECT TRENCH PARAMETERS

The purpose of an imperfect trench is to promote positive soil arching by introducing soft materials into a portion of the trench directly above the pipe crown. In practice, these soft inclusions are formed from loosely packed soil and/or organic materials. Manufactured soft materials are discussed in Appendix A.

In a manner similar to the previous bedding study, three imperfect trench parameters are considered; width, height, and modulus of imperfect trench material. In all cases, the bottom of the imperfect trench material is located 1/5 radii above the crown for both types of pipe, and Poisson's ratio is taken as 0.33.

Figure 8-4 shows the assumed variation in imperfect-trench height from 0.0 to 2.0 radii, while the trench half-width is held constant at 7/6 radii, and the trench modulus is held constant at 1/5 of the soil modulus.

Structural response ratios (as previously defined) shown in Figure 8-4 demonstrate that structural distress is significantly relieved as the height of the imperfect trench increases. However, for trench depths greater than 1.2 radii a point of diminishing returns is reached.

Figure 8-5 depicts an imperfect trench of constant height (6/5 radii), and a variable width ranging from 0.0 to 2.0 radii. Again, structural distress is significantly reduced up to a width of 1.2 radii after which a point of diminishing returns is reached.

Lastly, as shown in Figure 8-6, the modulus of the imperfect trench matial is varied from 0.1 to 1.0 times the modulus of the soil while maintaining constant trench dimensions. Structural distress is reduced as the trench modulus is reduced, however, practical considerations limit achieving a trench modulus ratio much below 0.1.

In overview, it is observed that the imperfect trench technique, if properly employed, can reduce peak concrete pipe responses by 50% and peak corrugated metal pipe responses by 20% for the system considered. Optimum imperfect trench size is 1.2 radii deep and 1.2 radii wide from the centerline. Larger sizes yield diminishing returns.

8.4 EFFECT OF BACKPACKING PARAMETERS

Backpacking is a relatively new construction technique and has not yet been accepted into regulatory design manuals. Like the imperfect trench or soft bedding, backpacking promotes positive arching by introducing an anular wrap of soft material around the pipe much like an external coating of insulation. Soft materials used for backpacking are usually manufactured materials, such as, plastic foam. Appendix A provides a complete discussion on potential soft materials that could be used for backpacking along with a description of their mechanical properties.

The backpacking material need not be a complete anular wrap around the pipe, but rather can be strategically placed around the culvert to optimize soil arching. This study investigates optimal placement of backpacking by symmetrically increasing the top and bottom angle of wrap in contact with the pipe. Thus, when the top and bottom angle of wrap is 90^{o}, the entire pipe is encased in a backpacking ring.

Three separate cases of backpacking modulus (stiffness) are considered representing the practical range of available soft

materials presented in Appendix A. Specifically, modulus ratios of backpacking-to-soil are 0.1, 0.2, and 0.5. In all cases, the thickness of the backpacking ring segments is 6.0 in. (15.2cm). Variations in ring thickness may be presumed to behave inversely to the backpacking modulus.

Figures 8-7, 8-8, and 8-9 show the key structural response ratios for the three values of backpacking modulus. In Figure 8-7 (softest case), it is observed the angle of wrap has a dramatic effect in reducing the distress in both types of pipe. For the concrete pipe the optimum angle of wrap is 54^{o} to 60^{o}, simultaneously reducing maximum concrete compressive stress and steel reinforcement stress by response ratios of 0.51 and 0.36, respectively.

On the other hand, the corrugated metal pipe is optimum with regard to vertical displacement (flattening) at a wrap angle of 36^{o}, and optimum with regard to thrust reduction at full wrap, 90^{o}. At approximately 60^{o} of wrap, an intersection point is observed wherein both displacement and thrust response ratios are 0.70, suggesting a "balanced" optimum.

Figures 8-8 and 8-9 illustrate the same trends, however, the reduction in pipe distress is not as significant because of the increased backpacking modulus. From these results it appears the backpacking modulus should be less than one-fourth of the soil modulus to significantly reduce pipe distress.

8.5 EFFECT OF SOIL STABILIZATION

The purpose of soil stabilization (as discussed in the previous chapter for long spans) is to enhance the stiffness characteristics of the soil in the immediate vicinity of the pipe. Unlike soft backpacking, the stiffened soil provides a lateral resistance to limit pipe deformations. Appendix A discusses materials, methods, and relative costs of stabilizing soils.

For this study, the effect of stabilized soil on reducing

pipe distress (reinforced concrete and corrugated steel pipe) is examined as function of percent encasement around the pipe. As shown in the insert of Figure 8-10, percent encasement is defined by the amount of stabilized soil that replaces "regular" backfill soil in a rectangular region surrounding the pipe. The rectangular region extends one radius laterally beyond the springline and one-half radius above the crown and below the invert. Thus, 100% encasement implies the entire rectangular region contains stablized soil, and 0% encasement implies no stabilized soil (i.e., reference condition). Intermediate encasement percentages are formed by symmetrically increasing the amount of stabilized soil in layers above and below the springline. Motivation for this arrangement of stabilized soil placement is based on the assumption that stiffened soils may be more beneficial at the sides of the pipe than at the crown and invert.

Figures 8-10, 8-11, and 8-12 show the effect of stabilized soil encasement for three modulus values of stabilized soil, 4, 20, and 100 times the soil modulus. These values represent a practical spectrum of enhancing soil stiffness from the stabilization techniques presented in Appendix A. In all cases, Poisson's ratio of the stabilized material is 0.2.

Inspection of these figures reveals that dramatic reductions in concrete pipe distress (both concrete compressive and steel reinforcement stress) is optimum when the percentage of encasement is 80 to 90%. Concrete structural responses are reduced by factors of approximately 0.5, 0.15, and 0.10 for the three cases of stabilized soil stiffness, respectively. Since the cost of stabilized soil increases with its stiffness characteristics, modulus values in the range of 10-to-20 times the soil modulus appear to be optimum with regard to cost effectiveness.

For the corrugated steel pipe, maximum crown displacement is dramatically reduced in a manner similar to the concrete pipe

(i.e., optimum encasement between 80 to 90% for all cases of stabilized soil stiffness). On the other hand, the percent encasement to reduce maximum thrust is highly dependent on the stabilized soil stiffness. In the first case, (Figure 8-10) maximum thrust is increased over the reference condition as percent encasement increases. However, for higher stiffness (Figures 8-11 and 8-12), maximum thrust is reduced by factors of 0.81 and 0.55, respectively, at percent encasements in the range of 50 to 70%.

In view of the above results, it is concluded that soil stabilization can be highly beneficial in reducing pipe distress; however, caution must be used for corrugated metal pipes to ensure the stabilized soil is sufficiently stiff to reduce thrust, say at least 20 times as stiff as the soil.

8.6 EFFECT OF V-NOTCH UNDER PIPE

From the previous studies on soft bedding and backpacking, it was observed that soft areas under the pipe relieve pipe distress by enhancing positive arching. The V-notch concept utilizes this principle by creating a V-shaped void beneath the pipe. Procedurally, structural quality backfill soil is compacted into a flat bedding foundation, then a V-shaped notch is carved in the foundation to cradle the pipe. The advantage of this concept is that no special bedding material is required only the labor cost of forming the V-notch by dragging a V-shaped template through the foundation material.

In this study, the effectiveness of the V-notch concept for reducing pipe distress is examined as a function of the V-notch angle. As shown in the insert of Figure 8-13, a V-notch angle of 180^{o} represents no notch, and hence, no void beneath the pipe. As the V-notch angle decreases the contact area between pipe and soil also decreases producing a greater void.

It is observed in Figure 8-13, that pipe distress is relieved as the V-notch angle decreases for both the reinforced concrete and corrugated metal pipe. However, the thrust stress in the corrugated metal pipe is not reduced as dramatically as the other structural responses. At an angle of 72^{o}, the concrete pipe distress is reduced by a factor of 0.50 whereas thrust in the corrugated metal is only reduced by the factor 0.85. V-notch angles smaller than 72^{o} are not practical unless special care is taken to preserve slope stability of the notch.

8.7 FLUID-LIKE JACKET FOR REINFORCED CONCRETE

In this section, a new concept is presented to reduce distress in reinforced conctete pipes by encasing the concrete pipe in fluid jacket to promote hydrostatic stress distribution. Unfortunately, an analytical simulation of this concept was not successful because of the inability to model fluid behavior with the particular finite element formulation used in this study. Thus, the ensuing discussion is only a qualitative discussion of the fluid jacket concept.

The structural capacity of buried concrete pipe is primarily dictated by the amount of bending stress in the pipe wall. That is, bending stress produces flexural cracking, yielding of steel reinforcement, and slabbing failure. Moreover, the interaction of shear and moments results in diagonal shear cracking.

If it were possible to alter the soil load distribution on the pipe so that only hydrostatic pressures existed (i.e., uniform normal pressure), then the pipe would predominantly carry ring compressive stress with little or no bending stress. Since concrete is ideally suited to carry compressive stress, the structural capacity is significantly enhanced under hydrostatic loading because the full thickness of conctete is available to resist crushing. Indeed, the need of reinforcing steel is

eliminated or significantly reduced.

Theoretically, a state of near hydrostatic loading can be achieved for any circular concrete pipe installation, by manufacturing the pipe with a fluid-like material surrounding the pipe periphery and encapsulated by a flexible membrane. Since the fluid-like material has no shear resistance, only uniform hydrostatic pressures are exerted on the concrete pipe regardless of the distortion of the flexible membrane during backfilling. Since a circular shape contains maximum area, the flexible liner cannot distort significantly out-of-round without compressing the fluid (nearly incompressible) and/or contracting the stiff pipe. Thus, the flexible liner should not come in load-contact with the pipe.

Economical fabrication of a concrete pipe with fluid jacket poses a challenging design problem. However, the potential benefits warrant serious consideration by innovators in the concrete pipe industry. Conceptually, the system could be fabricated by encircling the pipe with a flexible plastic liner slightly larger than the outer-diameter of a un-reinforced (or lightly reinforced) concrete pipe and filling the intervening space with grease, bentonite slurry, or some other fluid-like material. Special consideration is required for sealing the liner ends such as metal bands or embedding the liner in the concrete wall.

As a side remark, it should be observed that the fluid jacket concept is entirely different than the soft backpacking concept. The purpose of backpacking is to reduce the magnitude of load via the principle of soil arching. Backpacking does not redistribute the load in a hydrostatic fashion as is optimum for concrete.

Analytical attempts to evaluate the fluid-jacket concept were unsuccessful because of the inability to properly model the fluid material. Specifically, the fluid was modeled with a high bulk modulus and a zero shear modulus which resulted in numerical difficulties. Numerical difficulties were reduced by increasing

the shear modulus, however, the resulting stress distribution in the fluid deviated significantly from hydrostatic conditions. A proper fluid element requires formulating a new element and is outside the scope of this study.

Although a rigorous analytical evaluation of the concept was not obtained, it is possible to approximately evaluate the reduction in the pipe distress if it is assumed the fluid is at hydrostatic pressure equivalent to the overburden pressure of soil. Under this assumption, the concrete pipe with fluid jacket only experiences one-tenth of the maximum compressive stress that occurs in reference concrete pipe with bending stresses. Thus, the fluid jacket concept warrants further consideration and research.

8.8 Figures 8-1 through 8-13

		Page
Fig. 8-1	Influence of bedding height.	211
Fig. 8-2	Influence of Bedding width.	212
Fig. 8-3	Influence of bedding stiffness.	213
Fig. 8-4	Influence of imperfect trench height.	214
Fig. 8-5	Influence of imperfect trench width.	215
Fig. 8-6	Influence of imperfect trench stiffness.	216
Fig. 8-7	Influence of backpacking (1/10 Esoil).	217
Fig. 8-8	Influence of backpacking (1/5 Esoil).	218
Fig. 8-9	Influence of backpacking (1/2 Esoil).	219
Fig. 8-10	Influence of stabilized soil (4 Esoil).	220
Fig. 8-11	Influence of stabilized soil (20 Esoil).	221
Fig. 8-12	Influence of stabilized soil (100 Esoil).	222
Fig. 8-13	Influence of v-notch angle.	223

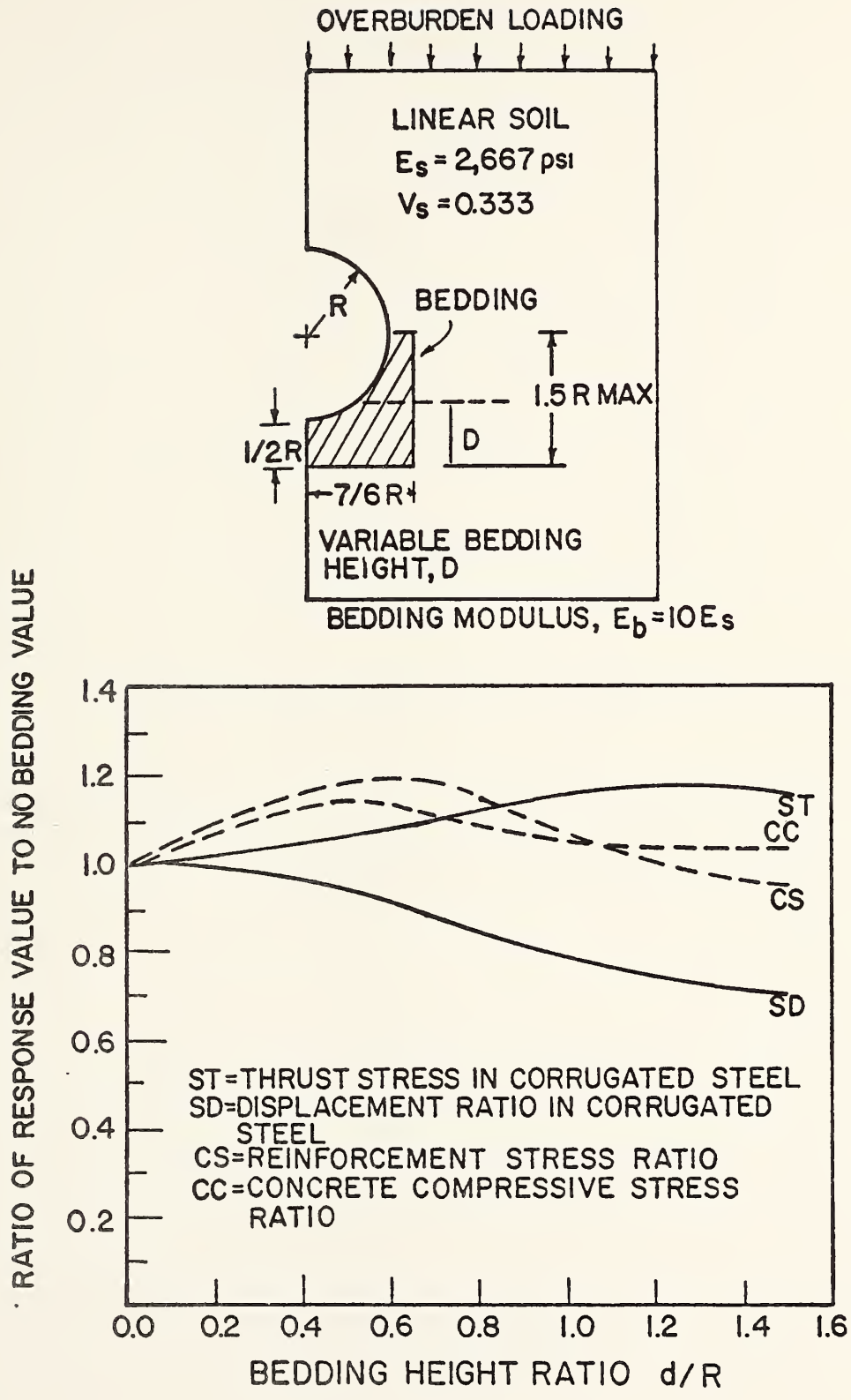

Figure 8.1 Influence of Bedding Height

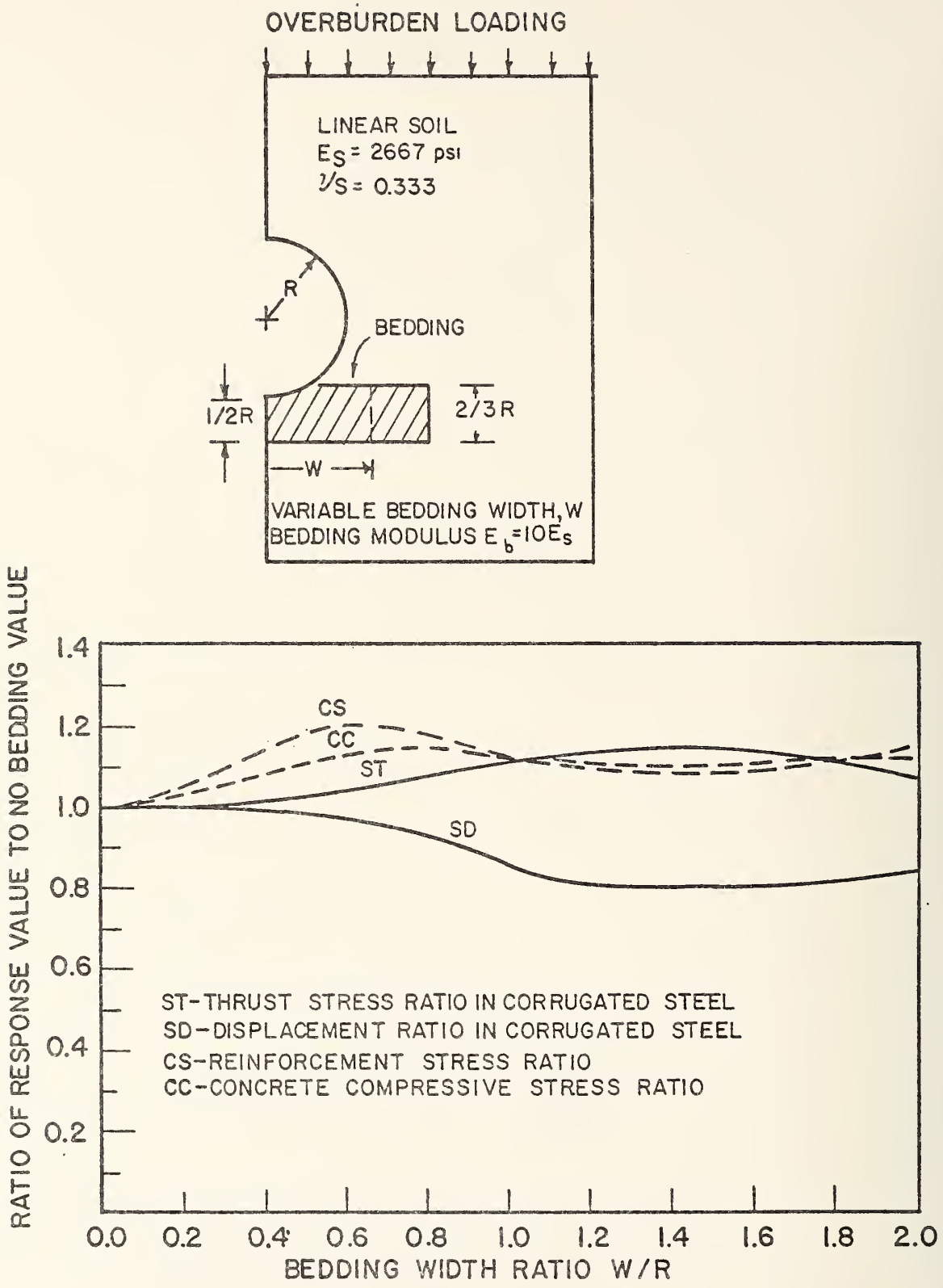

Figure 8.2 Influence of Bedding Width

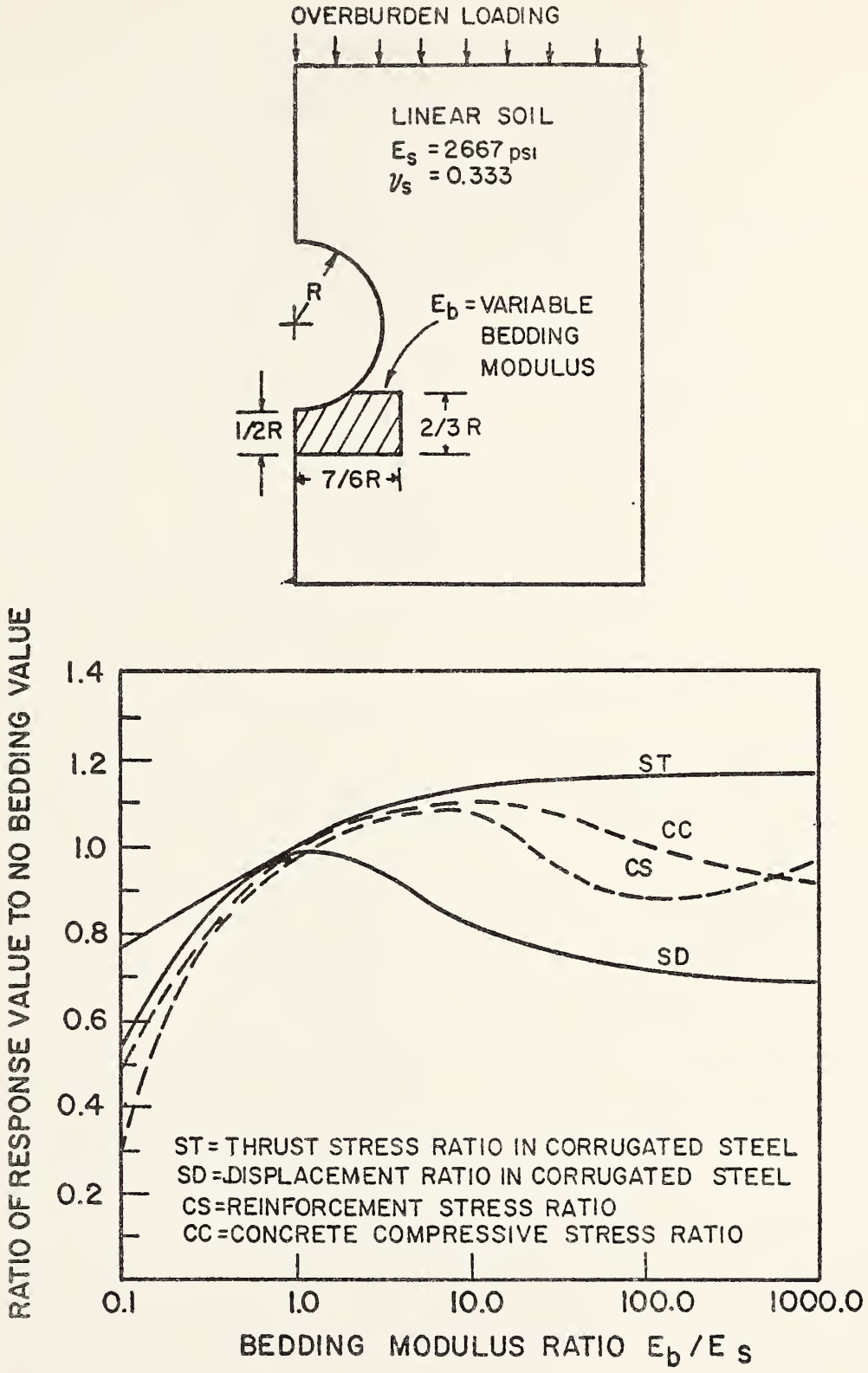

Figure 8.3 Influence of Bedding Stiffness

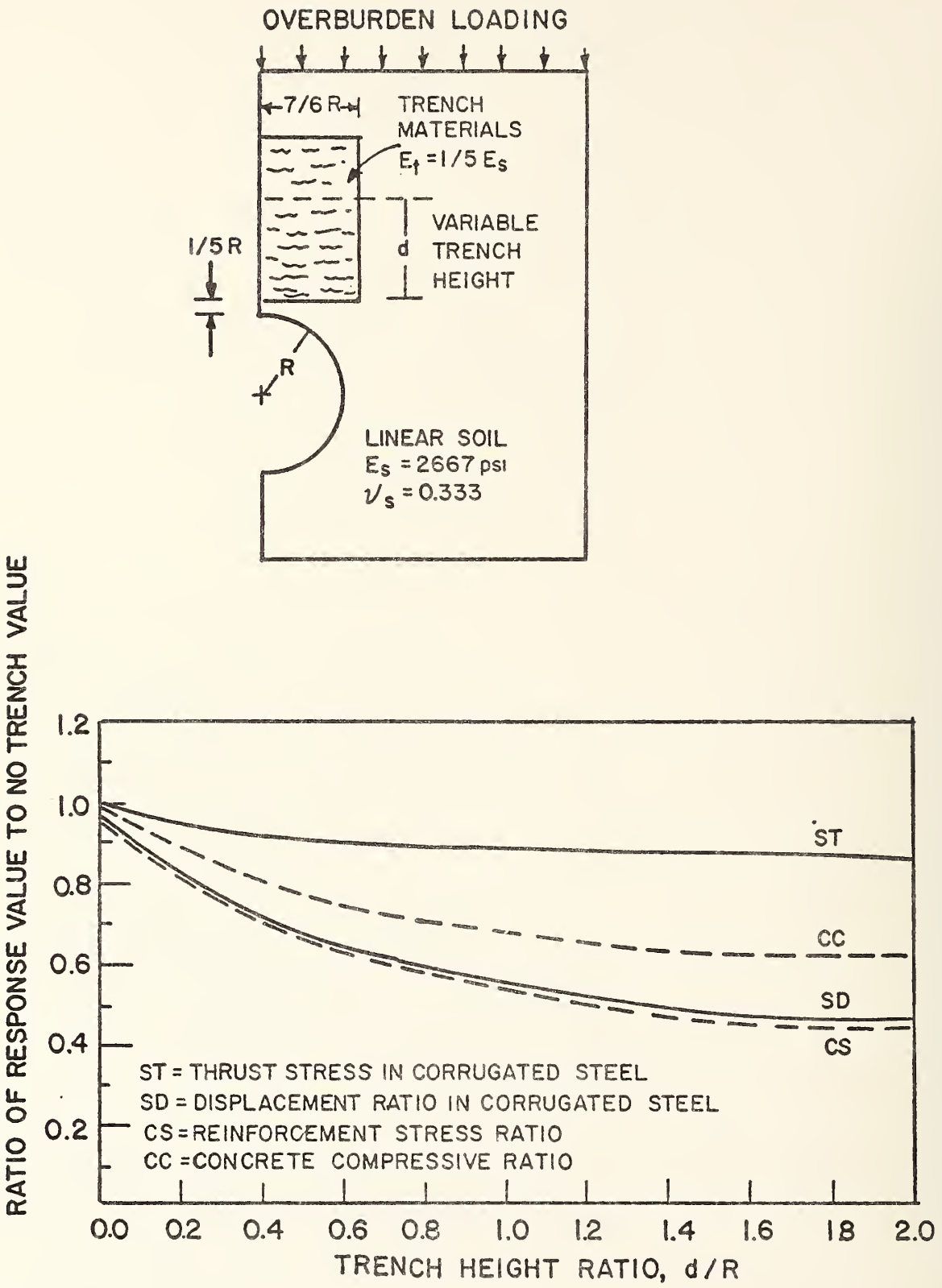

Figure 8.4 Influence of Imperfect Trench Height

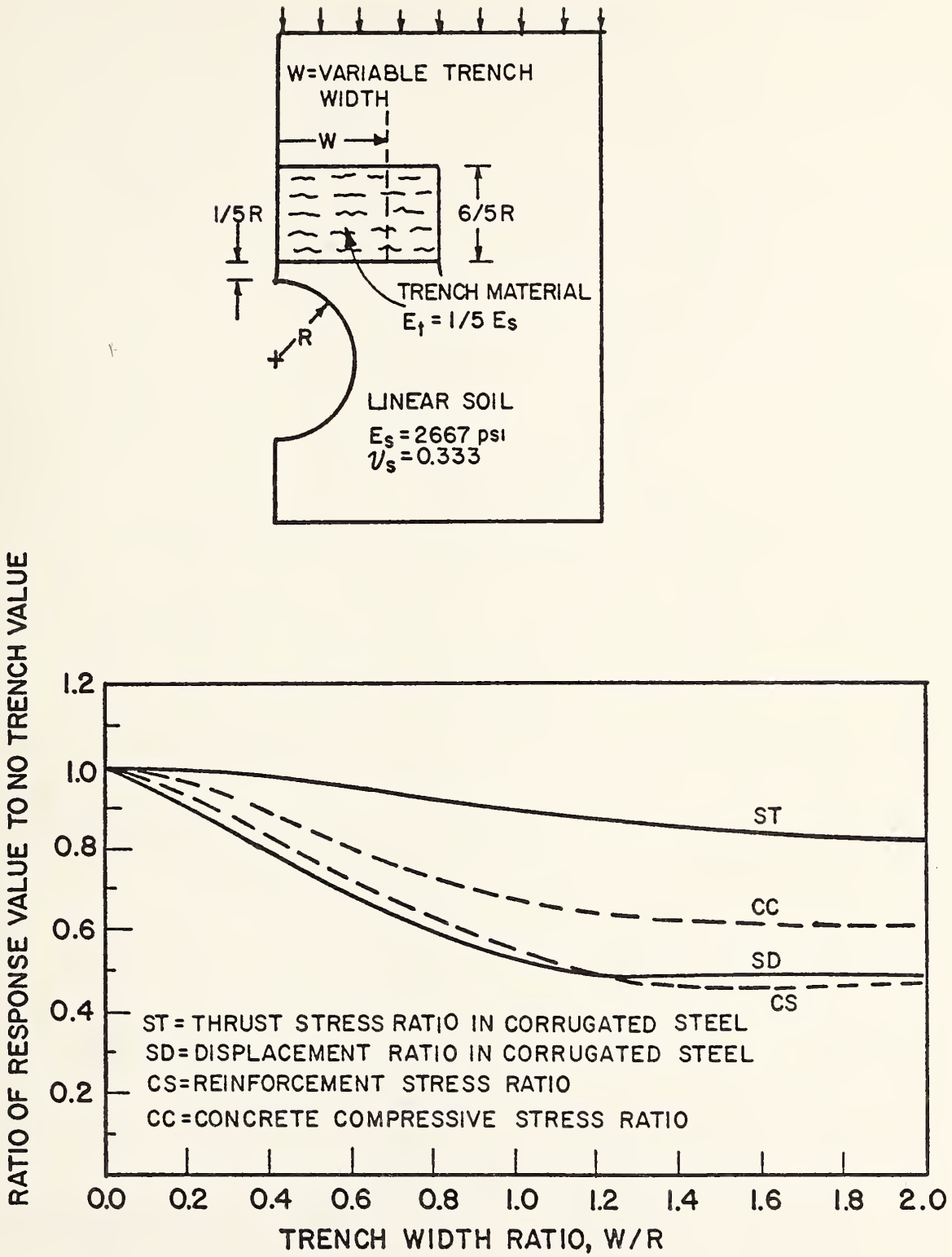

Figure 8.5 Influence of Imperfect Trench Width

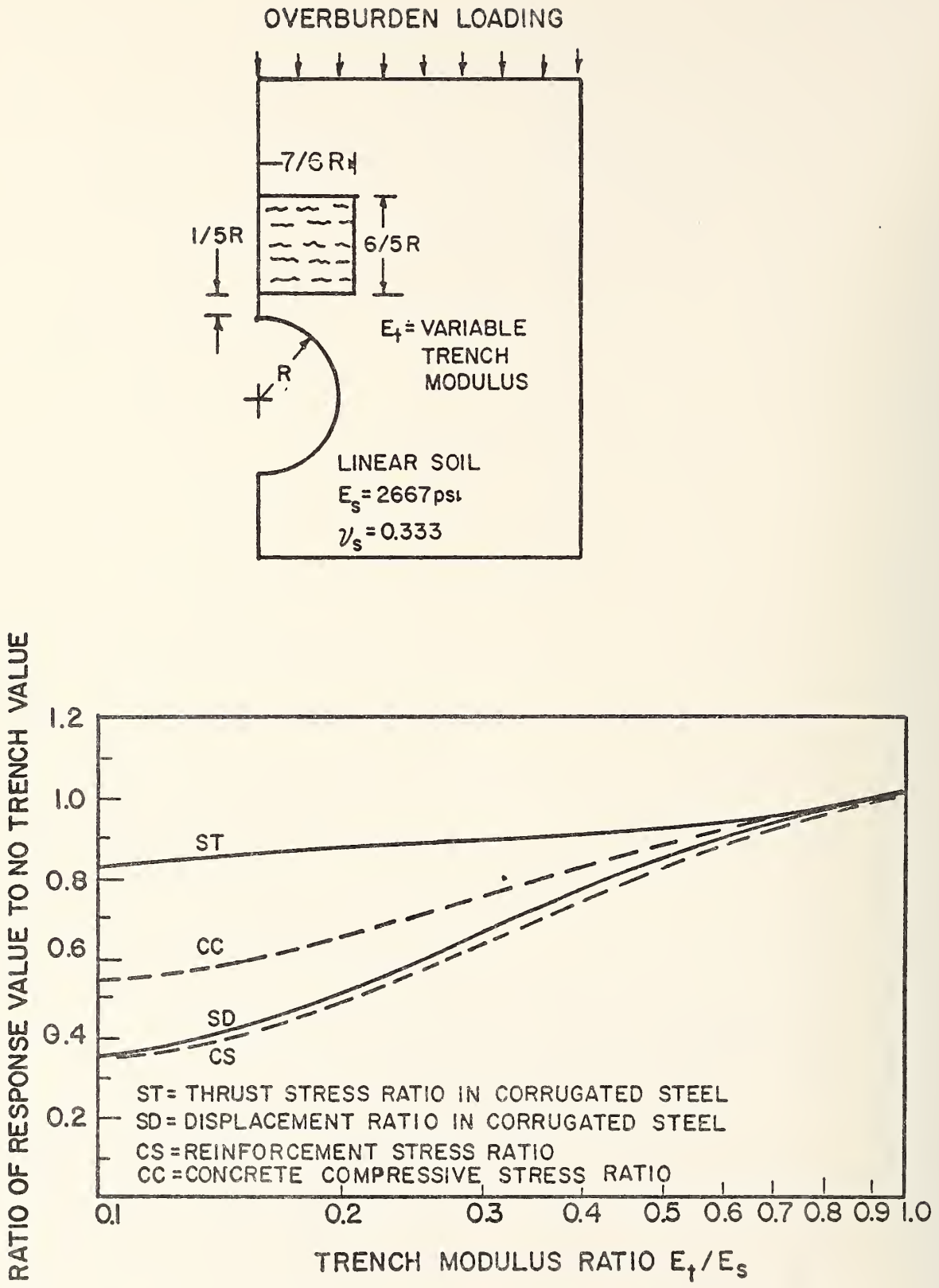

Figure 8.6 Influence of Imperfect Trench Stiffness.

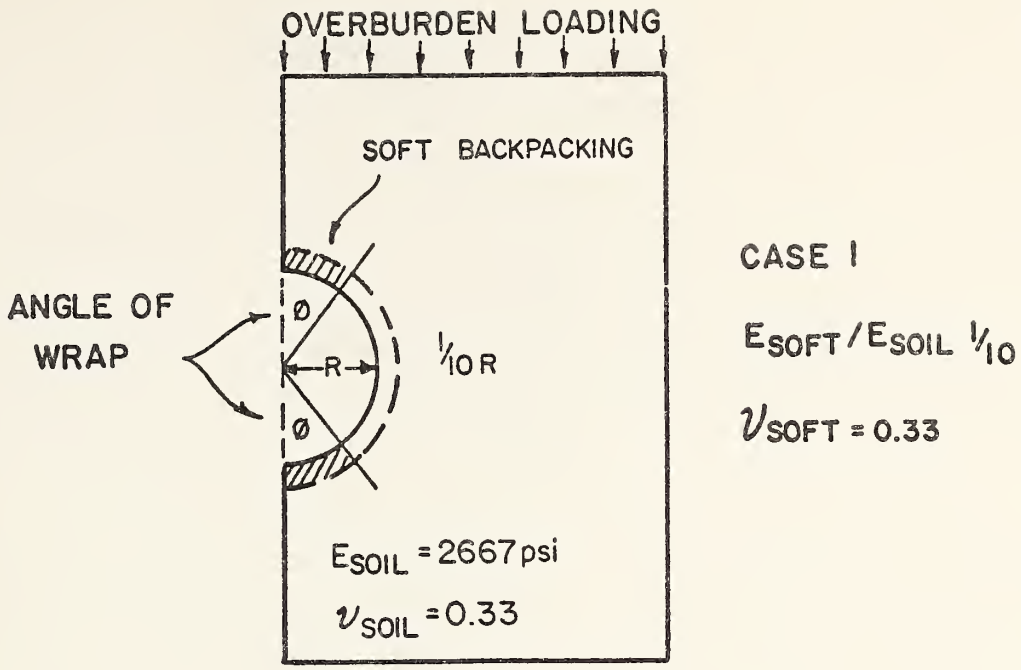

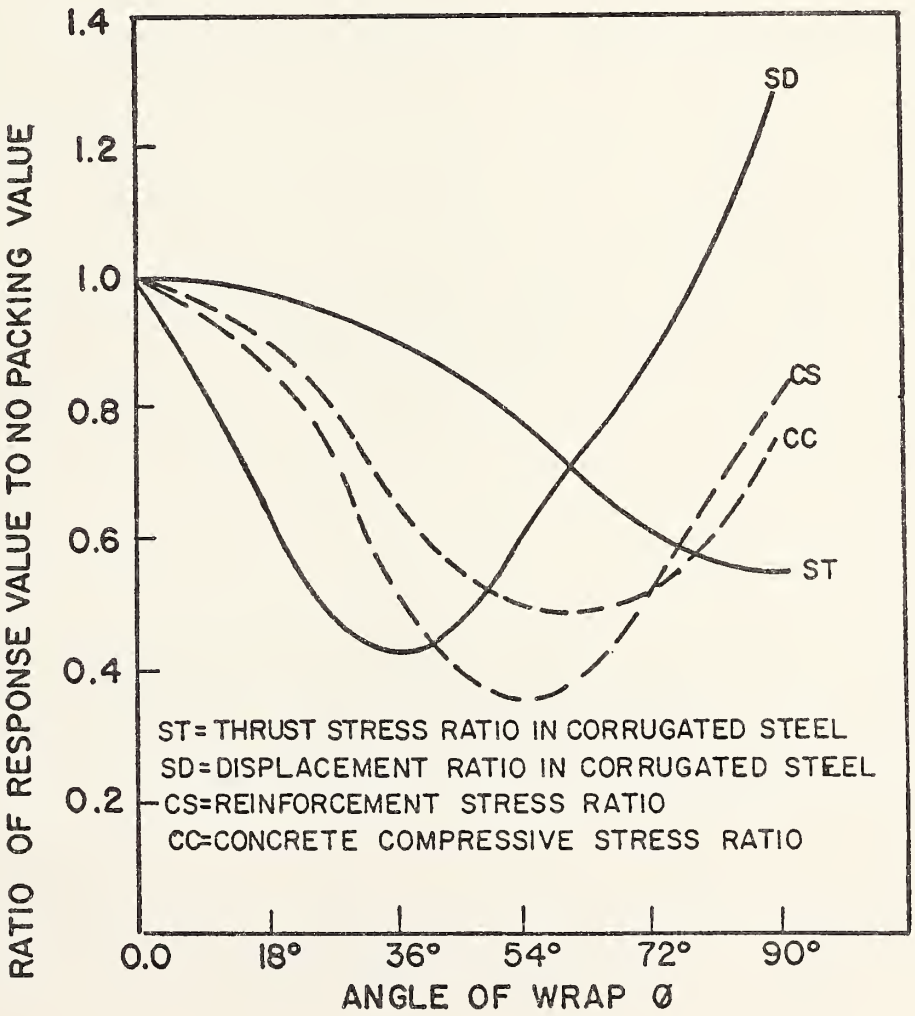

Figure 8.7 Influence of Backpacking (1/10 Esoil)

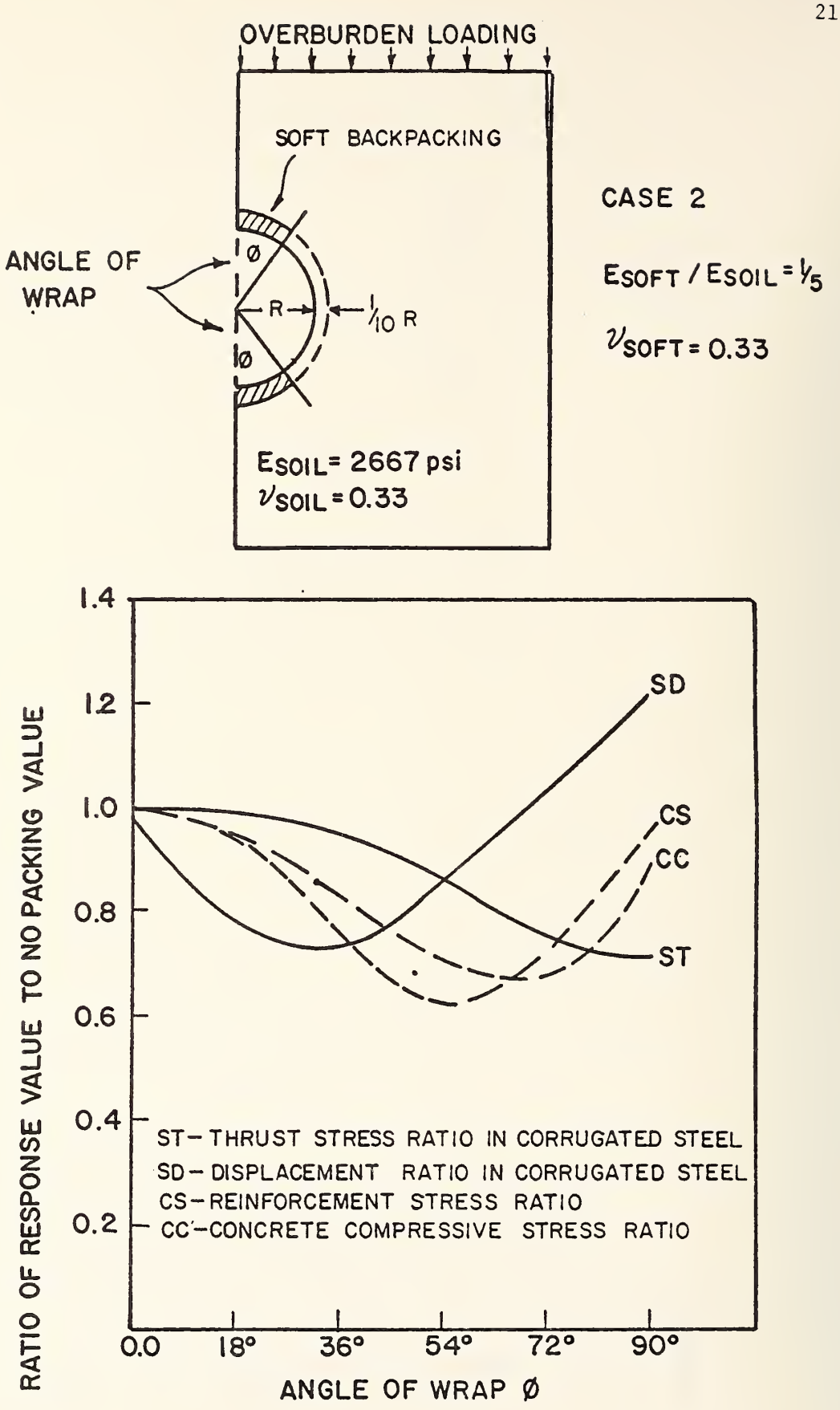

Figure 8.8 Influence of Backpacking (1/5 Esoil)

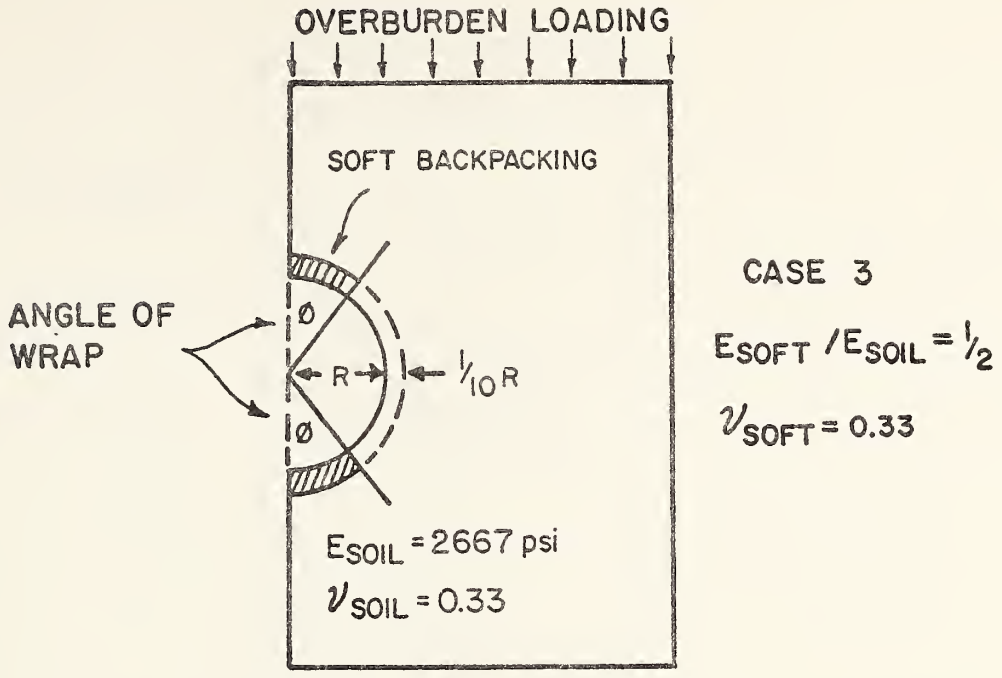

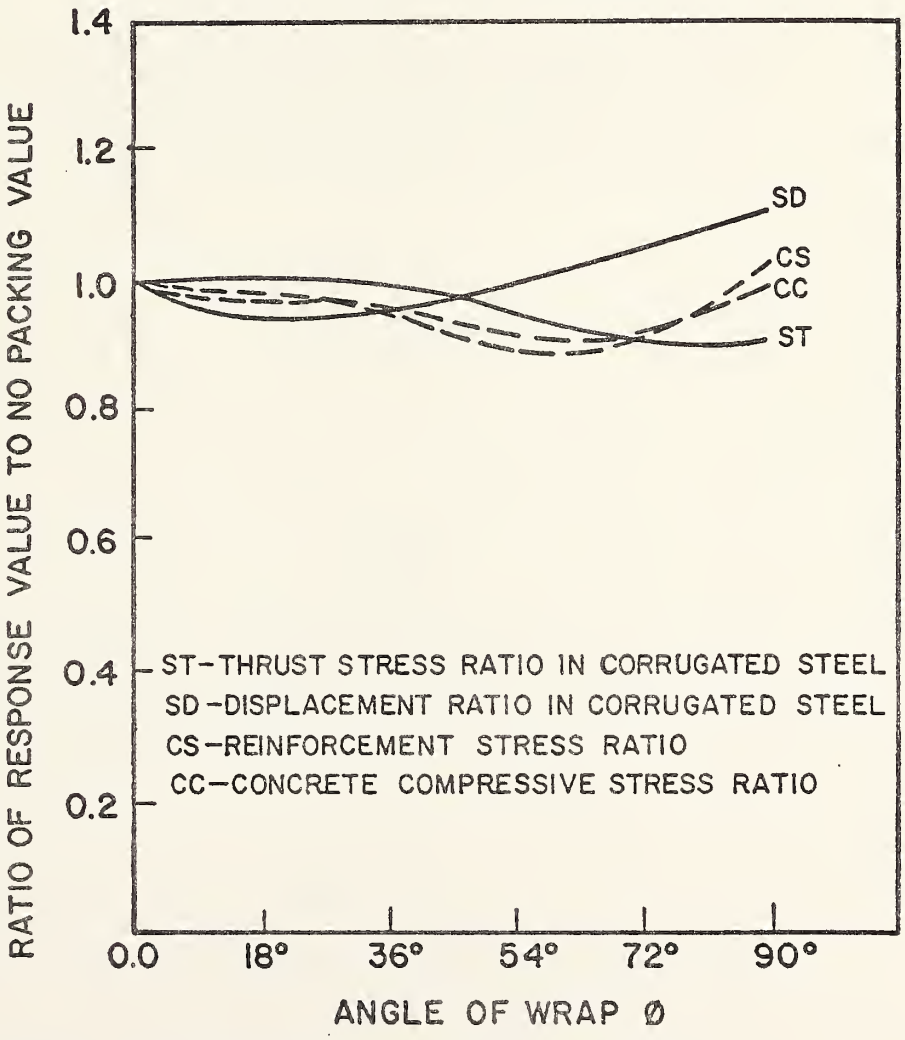

Figure 8.9 Influence of Backpacking (1/2 Esoil)

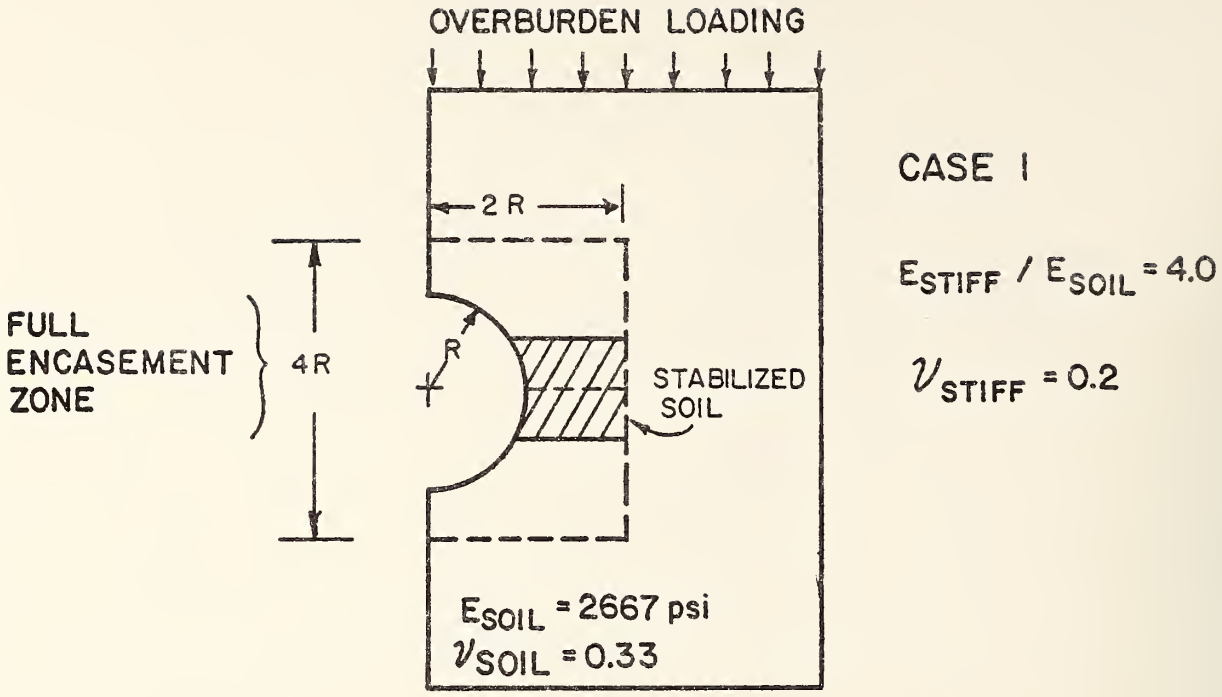

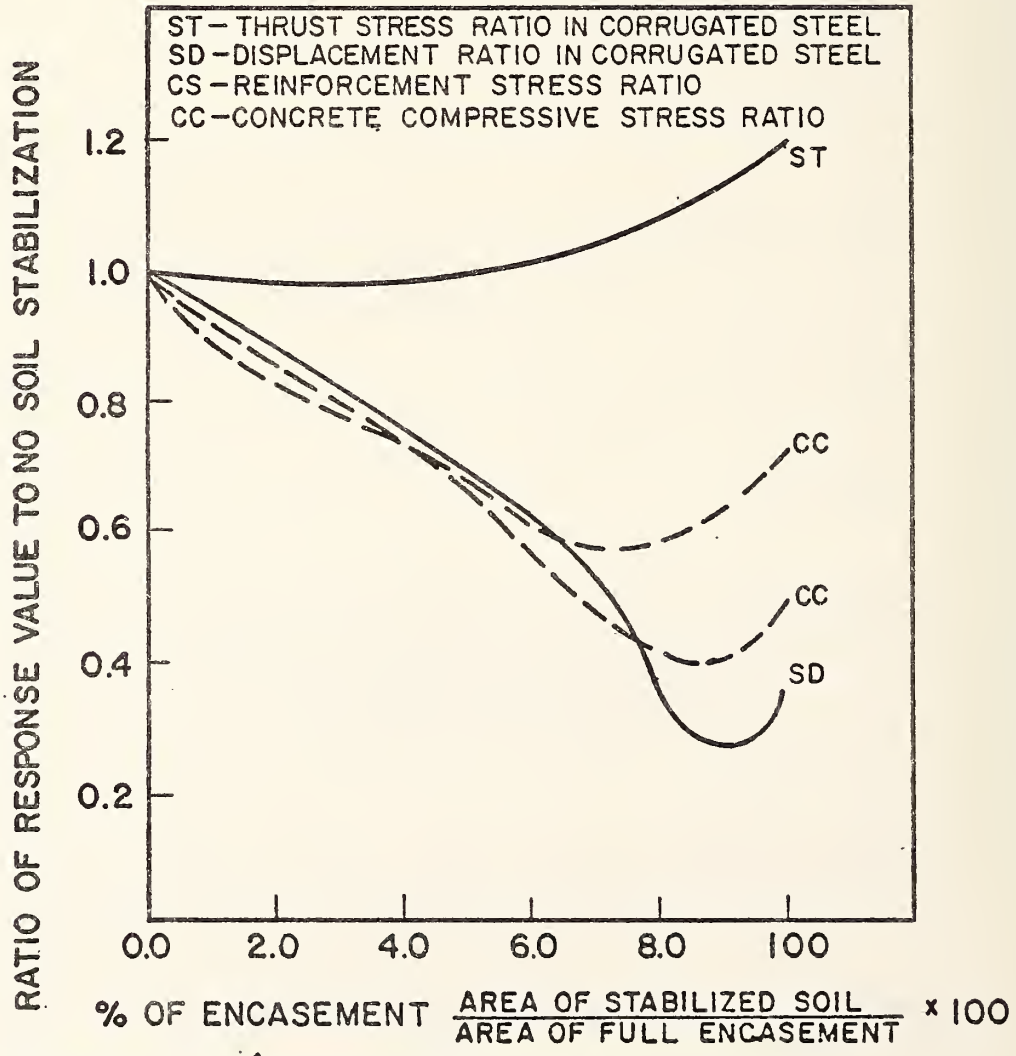

Figure 8.10 Influence of Stabilized Soil (4 Esoil)

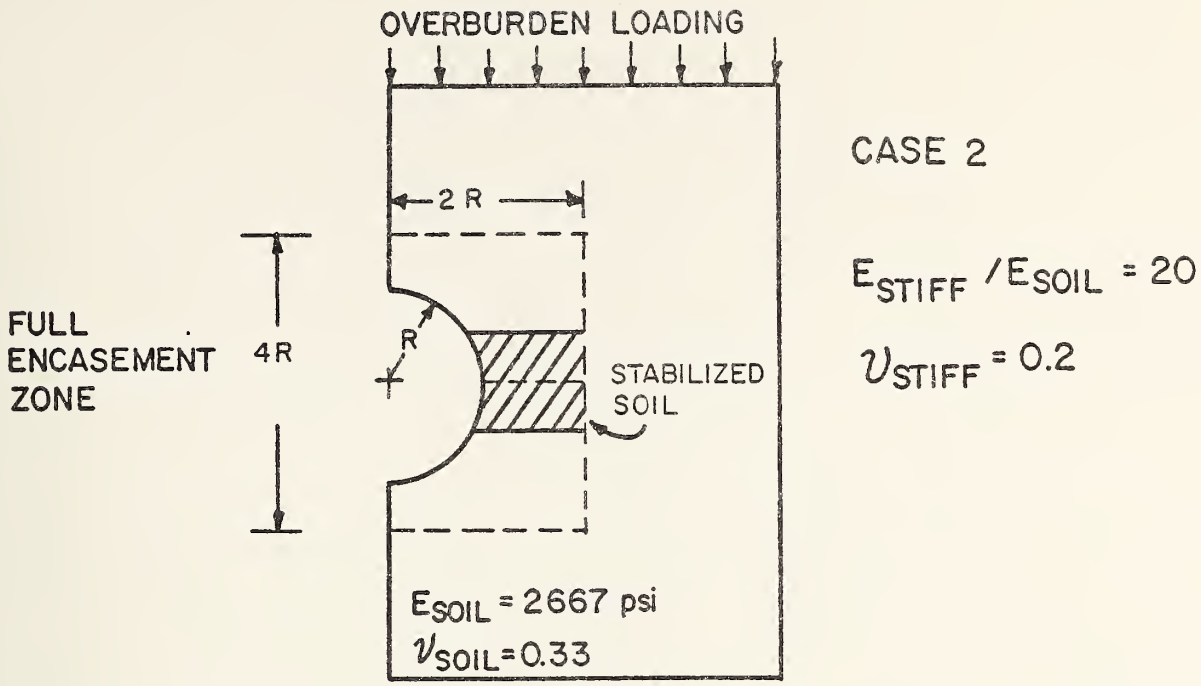

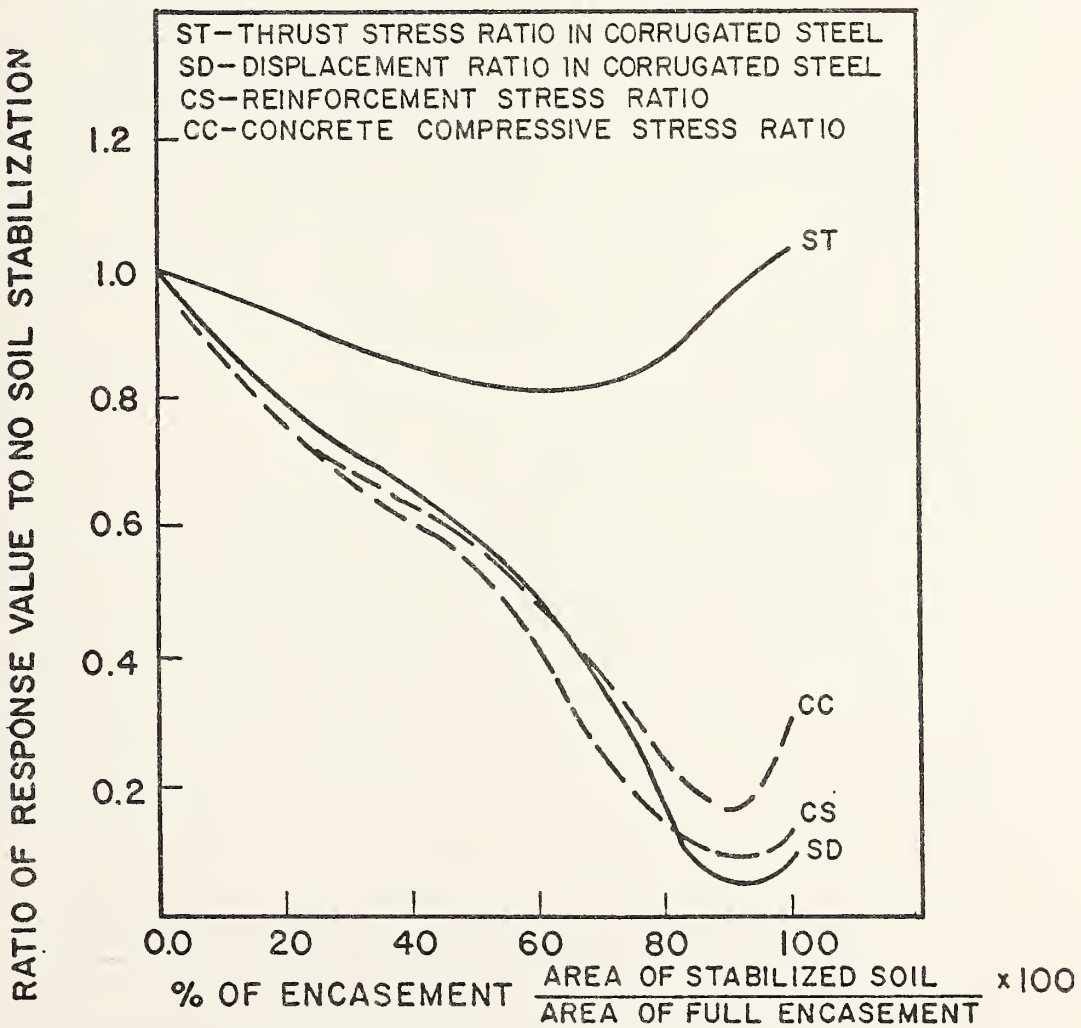

Figure 8.11 Influence of Stabilized Soil (20 Esoil)

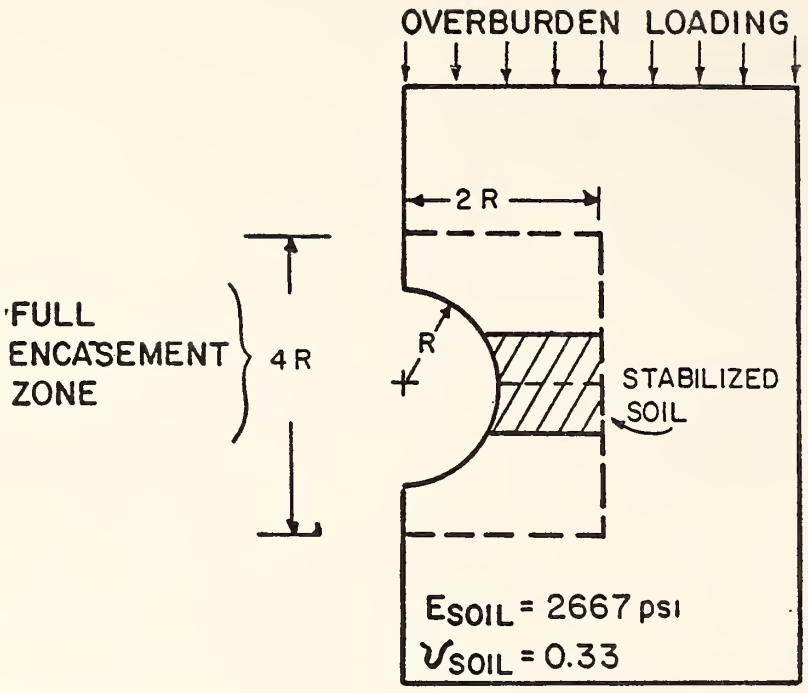

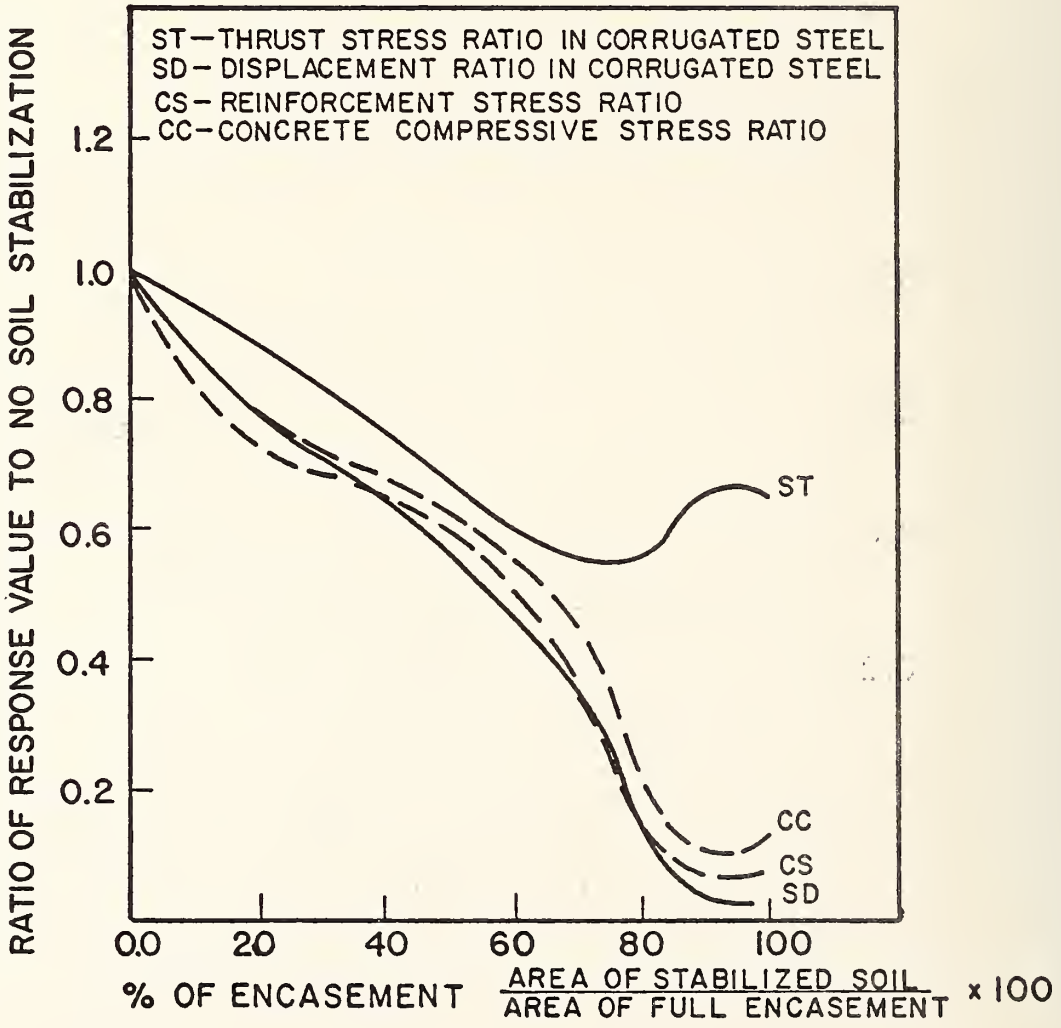

Figure 8.12 Influence of Stabilized Soil (100 Esoil)

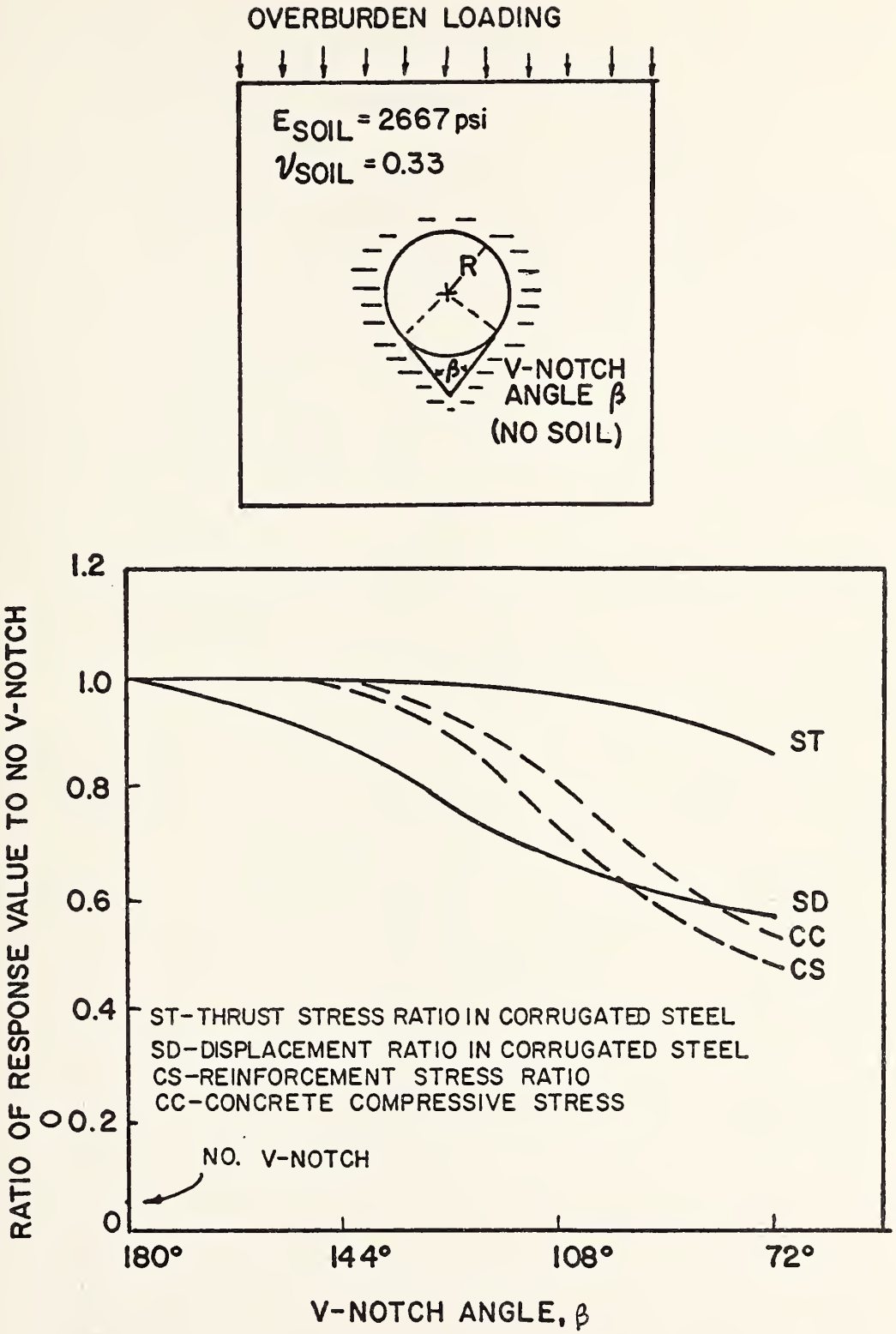

Figure 8.13 Influence of V-Notch Angle

CHAPTER 9

SUMMARY AND RECOMMENDATIONS

This report presented a comprehensive study on long-span systems including; experimental data, analytical modeling techniques, analysis of conventional long-span parameters, and analysis of new concepts to improve the structural performance of long spans. New concepts included improvements to the soil system (reinforced earth, stabilized soils, and soft inclusions) as well as improvements to the structure. Appendices A and B provide background information on these new concepts along with economic considerations. In addition to the above long-span studies, analytical evaluation of new concepts were also investigated for traditional flexible and rigid culverts.

Major findings and conclusions are summarized below followed by recommendations for future investigations.

9.1 SUMMARY OF FINDINGS FOR LONG SPANS

Experimental Data: Available experimental data is very limited and incomplete. However, based on the existing data, the following experimental observations appear valid.

During the construction process of compacting soil in lifts along the sides of the structure and then over the crown, the observed experimental trends are:

1. Crown movement is at its maximum peaking position when the fill soil is level with crown. Subsequent layers of soil promote downward movement but at a slower rate.
2. High and low profile arches exhibit similar trends for crown movement. Horizontal ellipses appear to peak less but flatten at a significantly higher rate than arches.
3. Thrust stresses in the structure are maximum in the region between footing and springline. Thrust stress at the crown is consistantly less than springline

thrust by about 25%. At full fill height, springline thrust force is slightly greater than the column weight of soil above the crown.

4. Vertical soil pressure in the vicinity of the crown is significantly less than free field overburden pressure. In the vicinity of the springline, verticle soil pressure is somewhat greater than free field pressure.

For shallow covered long spans loaded with traveling vehicles tranversing the span, the experimentally observed crown movements are:

1. As the load approaches the long span, the crown initially moves upward (peaking). As the load approaches the central portion, the crown begins to flatten and is maximum when the load is at the centerline. During this process maximum peaking is only 30% as large as maximum flattening.

2. Increasing fill soil cover height greatly reduces the magnitude of crown movement due to live loads, e.g., a cover height of 0.2 top-rise units reduces crown deflection by 60% compared to cover height of 0.1 top-rise units.

Analytical Modeling: Analytical modeling of the soil-structure interaction for long-spans is at best a difficult task and requires modern numerical methods such as the finite element method for predicting structural behavior. The CANDE computer program is well suited for this task and predicts structural responses in conformance with the observed experimental trends providing proper analytical modeling techniques are employed. Listed below are findings and observations with regard to various analytical modeling assumptions:

1. Soil Loading: In order to predict maximum crown peaking and the deformed shape of the structure, incremental soil lifts must be employed along with temporary surface pressures on each lift simulating compaction loads. Soil lifts

heights on the order of 1/5 of the structure rise with temporary surface pressures of 34 kPa (5psi) are reasonable approximations. In general, loading conditions on either side of the vertical centerline may be assumed symmetrical. However, analytical results demonstrate that staggard placement of soil lifts on either side of the structure and terminating in a uniform cover above the crown result in significantly nonsymmetrical deformations and moments "locked" in the structure. Thrusts, however, regain near symmetrical distribution at the uniform cover height.

2. Live Loading: Vehicular loads transvering shallowly buried installations may be approximated as "point" loads for each axle with the understanding that the point load is actually "strip" load (plane strain) whose magnitude may be approximated as wheel load divided by axle length. For linear systems structural influence lines may be easily established by a single point load whose position is changed on each load step. Thus a variety of vehicles may be considered by superposition. Analytical predictions of crown displacement due to traveling truck loads are in good agreement with experimental observations using this technique.

3. Large Deformations: For the basic long-span model defined in this study, large deformation solutions (both large strains and rotations) differed only slightly from small deformation solutions. Crown displacements exhibited the maximum discrepancy and were 8% greater for the large deformation solution. All other structural responses were in closer agreement. Discrepancies between large and small deformation solutions are due to large rotations, not large strains. Apparently, large deformation solutions (which inherently includes buckling) are not required for

long-span systems comparable to the system in this study. However, for larger structures with weaker soils, large deformations may be significant. Moreover, if ultimate capacity is desired, large deformation solutions or at least geometric stability solutions are necessary.

4. Soil-Structure Interface: The assumed frictional traction between structure and soil has a pronounced influence on on structural deformations. Maximum crown peaking is more than doubled when the interface is assumed frictionless as compared to a completely bonded assumption. Solutions with intermediate values of interface friction predict structural responses in better conformance with observed experimental behavior than the completely bonded assumption. To wit, maximum peaking is increased while maximum flattening is decreased, and maximum thrust stress is slightly reduced.

5. Material Nonlinearity: Nonlinear material models for soil (overburden-dependent) and structure (elastic-plastic) did not significantly alter responses of the structure displacements and thrusts as compared to linear material solutions. This does not infer soil stiffness is insignificant (on the contrary it is very significant), rather the inference is that the net effect of changing soil stiffness with overburden pressure produces structural responses that do not differ significantly from solutions using "average" elastic properties. However, if different soil modeling techniques (e.g., hyperbolic or plasticity models) are employed, this conclusion may not be valid.

Conventional Long-Span Parameters: Analytical parameter studies of conventional long-span parameters were undertaken to assess their relative merits for enhancing the long span's structural performance. The following findings are noted:

1. Soil Stiffness: The overall stiffness of the soil system (Young's modulus) is the most significant parameter with regard to controlling deformations and moments in the structure. Structural deformations are inversley proportional to soil stiffness. Evidently, the characterization of soil is crucial for controlling the deformed shape of the structure. On the other hand, thrust in the structure is practically insensitive to soil stiffness.

2. Liner Thickness: Within the range of standard corrugated metal thicknesses (gages 1 through 10) commonly used in long-span systems, the structural deformations are insensitive to liner gage because the soil stiffness dominates the system. Thrust force in the structure is also insensitive to liner gage, so that thrust stress is reduced in direct proportion to liner thickness. Since deformed shape and curvature remains nearly constant with variations in liner gage, moments increase in proportion to increased bending stiffness (moment of inertia) due to increased wall thickness. However, the section modulus of bending also increases in nearly the same proportion so that bending stresses remain nearly constant. Thus, the net effect of increased liner thickness reduces thrust stress with no change in bending stress or deformations.

3. Footing Width: For arch-type structures, variations of footing width over the range 0.6 to 1.2m (2.0 to 4.0 ft) does not significantly alter any of the structural responses. Of course, this is assuming the soil has sufficient bearing capacity.

4. Liner Shape: High and low profile arches exhibit similar structural responses except the high profile is slightly more flexible. In contrast, a horizontal ellipse, whose top half is identical to the arches, exhibits much less crown peaking but much more flattening under deep fills

than the corresponding arches. These findings were also observed in the experimental data. Apparently, the horizontal ellipse is well suited to resist lateral loading but not excessive vertical loading.

5. Liner Scale: Increasing the liner dimensions (span, rise, etc.) while maintaining constant cover height and liner thickness results in displacements and thrusts which increase in almost the same proportion as the scale factor.

6. Special Features: Special features investigated include; thrust beam, soil bin, and rib stiffners. At full fill height, the structures with special features experienced the same thrust forces and nearly the same amount of crown flattening as the basic model without special features. The rib-stiffened structure exhibited 15% less flattening, the thrust beam 1% less, and the soil bin 9% more flattening. During the initial stages of construction, the crown stiffened structures (soil bin and rib stiffeners...which are more expensive installations) exhibited significant reductions in crown peaking as compared to the thrust beam structure and basic structure. However, at least one attribute of the thrust beam structure not simulated in the analysis is the potentially improved soil compaction near the lateral face of the thrust beam.

7. Concrete Relieving Slab: For shallowly buried installations, concrete relieving slabs placed flush with the fill height surface significantly reduce live load effects on the structures. Displacements and thrusts due to live loads are reduced on the order of 50% for a 0.3m thick relieving slab extending over the structure span. Moments are reduced by even a greater percentage. Moreover, the bending curvature of the relieving slab at the point in contact with the live load is greatly reduced (18 times); thereby reducing bending stress and fatigue damage in pavement coverings.

New Concept for Long Spans: In order to improve the structural capacity and/or to increase the size of long-span systems, new concepts were proposed and analytically evaluated. With regard to the soil system, new concepts investigated are; reinforced earth, selective soil stabilization, and soft inclusions. Appendices A and B provide economic considerations and background information on these concepts. Suggested improvements to the structural liner include regulation of thrust by controlled joint slippage.

Summarized below are the relative merits of these new concepts:

1. Reinforced Earth. Small to moderate amounts of reinforced earth (0.05% to 0.10% by volume) laid in horizontal rows can reduce crown peaking by 90% or more. The rate of crown flattening is also significantly reduced but is dependent on the nonlinear behavior of the metal strips experiencing compressive strains in some regions of the reinforced earth zone. Like deformations, bending moments are significantly reduced, however, maximum thrust is not appreciably changed by the incorporation of reinforced earth.

   The optimum location of reinforced earth is between the footing and crown. Earth reinforcement above the crown has little effect.

   Whether or not the reinforcing strips are connected to the structural liner, the improvement in structural performance is nearly the same. However connected reinforcement may be better for ultimate capacity and deformation control.

   Assuming metal strip lengths of one span length, the lightly reinforced earth model required 44% less additional metal than the conventional rib stiffeners, but yet provided a much greater improvement in reducing deformations and bending stresses.

2. Stabilized Soil. The introduction of stabilized soil adjacent to the sides of the structure between the footing and 88% of the distance to the crown can reduce crown peaking and subsequent flattening by 50% or more. However maximum thrust increases

by 3 to 5%. Stabilized soil stiffnesses on the order of 10 times the soil stiffness appear optimum for cost-effectiveness (i.e., higher stiffnesses yield diminishing returns at higher costs, see Appendix A). Also, zone widths of ¼ span length appear to be optimum.

3. Soft Inclusions: Soft material placed in contact with the upper portion of the structure (extending over 84% of the span length) was incorporated into the long-span model in an attempt to reduce thrust by means of positive soil arching. However for all practical soft moduli values and height variations of the soft inclusion, the desired result of reducing thrust did not occur to any significant degree (i.e., 6% reduction maximum). Worse still, moments and displacements tended to increase as the soft inclusion zone was heightened and/or made softer. Thus, this concept does not appear fruitful for long-span installations similar to this study, (note, however, the concept has merit for traditional round culverts).

4. Improvements to Structure: Two seemingly opposed methods of modifying the strucutre to improve overall performance are: (1) a general increase in bending stiffness, and (2) controlled reduction of ring compression stiffness. For the former method, deformations can be controlled to some degree by substantial additions of structural material (e.g., metal and concrete) such as the special features previously discussed. Increased bending stiffness also provides greater restraint for soil compaction during initial backfilling, thereby further reducing deformations due to increased soil stiffness. However, the primary disadvantage of stiffened structures (outside of the additional costs) is that the structure "draws" additional thrust load (negative arching), compromising the improvement.

Thrust forces can be controlled by reducing ring compression stiffness via the slotted bolt-hole concept. That is, slotted seam connections maintain continuity until the thrust force exceeds the joint frictional resistance. Thereafter joint slippage circumferentially shortens the structure promoting positive soil arching. Although a realistic analytical model of joint slippage is yet to be developed and evaluated, this concept appears well founded.

9.2 SUMMARY OF FINDINGS FOR TRADITIONAL CULVERTS

New and old concepts for traditional culverts were analyzed to evaluate their relative merits for improving the performance and/or capacity in deeply buried installations. Two common culvert types were examined; corrugated steel and reinforced concrete, both with a nominal diameter of 2.0 meters. Techniques and concepts investigated are: bedding configuration, imperfect trench, backpacking, stabilized soil, v-notch trench, and fluid jacket. Summarized below are the major findings.

1. Bedding Configuration: Systematic variations in bedding height, width, and stiffness indicate that the structural performance is adversely affected for bedding stiffnesses greater than soil stiffness (except for displacements in the metal pipe). Soft beddings substantially reduce culvert stresses and deformations. However, it is recognized stiff beddings are beneficial with regard to alignment and unequal settlement in the longitudinal direction.
2. Imperfect Trench: Soft inclusion zones above the culverts (imperfect trench) were systematically varied in height, width, and stiffness. For both culvert types structural distress are significantly reduced, however, more so for the concrete pipe than the steel pipe. Optimum imperfect trench dimensions are 1.2 radii high and 2.4 radii wide with a modulus one-tenth of the soil.
3. Backpacking Wrap: A concentric ring of soft material selectively placed around the pipe periphery was investigated to determine

the optimum degree of wrap along the top and bottom of pipe for a practical range of soft material stiffness. Significant reductions in pipe distress (both concrete and steel) are achieved for an optimum wrap angle of 60% on either side of crown and invert for soft materials with less than one-fifth of soil stiffness.

4. Stabilized Soil: A rectangular zone of stabilized soil was incorporated along the sides of the pipe culverts and systematically increased in size until the stabilized soil completely encased the culverts, implying 100% encasement. Significant stress reductions (50 to 90%) were observed for 80% encasement of the concrete pipe for stabilized soil stiffness ranging from 4 to 100 times the fill soil stiffness. However for the steel pipe, thrust stresses were increased when stabilized soil stiffness was 4 times soil stiffness. At higher stiffness ratios the thrust stress was significantly reduced at 80% encasement.

5. V-Notch Bedding: A v-notch void beneath the pipe was modelled for v-notch angles ranging from 180° (no void) to 72°. In all cases, pipe distress was reduced as the v-notch angle decreased, however more so for the concrete pipe than the metal pipe. Based on practical considerations of the soil, v-notch angles less than 72° may not be achievable.

6. Fluid Jacket: Analytical attempts to simulate a fluid-like material encapsulating a concrete pipe were not successful and requires further analytical development. Nonetheless, the concept of the fluid jacket to promote uniform hydrostatic pressure on concrete pipe may have considerable merit for deeply buried systems.

9.3 RECOMMENDATIONS

Based on the results of this study, it appears the two most cost-effective techniques for increasing the load capacity and/or size

of long-span structures are reinforced earth and slotted seam connections. Small to moderate amounts of reinforced earth can control deformations and moments as well as provide increased resistance to buckling. Slotted seam connections can relieve thrust by frictional slippage thereby promoting positive soil arching to carry additional overburden loading.

To this end, controlled laboratory tests of scale models should be undertaken to investigate each technique individually and then combined. Concurrently, analytical models (e.g. CANDE program) should be tested and evaluated with the experimental data, thereby providing mutual information exchange between experiment and analysis. That is, analytical results can guide the experiments and visa-versa to determine optimum parameters, such as, slot widths and bolt torque, and reinforcement strip size, length, and location.

Based on information from laboratory experiments and analysis, a full scale field experiment can be designed and constructed with full instrumentation. Preferably, the full scale system should be nonfunctional so that it can be tested to failure, thereby providing a full range of experimental data to evaluate the analytical model.

Once the analytical model is validated and a data base established, design charts and guidelines can be established for these long-span systems.

For conventional round pipe culverts, new concepts that warrant in-depth investigations (experimental and analytical) are soft backpacking, v-notch trench, and fluid jacket concept.

APPENDIX A

MATERIALS FOR NEW STRUCTURAL CONCEPTS FOR CULVERTS

This appendix contains data on various materials for potential use in new structural concepts for culverts. The two primary categories in which these materials would fall are stiff materials for backfill stabilization, soft materials to promote soil arching, the former tends to increase soil strength and limit culvert deformations; the latter materials absorb strain energy and reduce thrust in the culvert. The intent is to provide data that will be useful for parameter studies herein as well as future studies.

Within each primary category generic materials are discussed in an approximately parallel manner. Thus, a general description of the material is followed by a discussion of present and potential utilization methods. Stress-strain curves and other engineering properties are presented along with in-place cost data to the extent it is available.

A predominant amount of the information was gathered from publications in the open literature from highway research efforts and from private communications.

I. STIFF MATERIALS FOR BACKFILL STABILIZATION

Materials in this category are generally stiffer and stronger than untreated backfill. They are intended to stiffen the combined soil-structure system and to increase the load carrying capacity by improving stress distributions within culverts. They are generally formed by adding a stabilizing material and possibly water to soil. The most promising additives are lime, lime-fly ash and portland cement. These and others will be discussed in this section.

Lime-Soil. Lime-soil stabilization is generally achieved by adding small amounts of hydrated lime to soil and compacting the

mixture. Lime contents are generally in the range of 3 to 7 percent by weight. This treatment tends to improve plasticity, workability and strength of soils. However, the magnitude and character of these improvements depends on in-situ soil properties such as the organic carbon content, pH, carbonate content and clay content. The extent to which these and other factors contribute to the stabilization process is discussed in Reference A-1. Once the soil characteristics are known the lime-soil properties can be estimated.

Lime-soil stabilization is achieved by mechanically mixing hydrated lime with select types of soil. Mixing can be done in a central plant, or lime may be spread over scarified soil and mixed in place using a rotary mixer mounted on the rear of a suitable tractor. Plant mixing provides better control over proportioning and moisture content but in-place mixing is more economical for mass placing such as highway subgrades. Plant mixing would probably be preferred for culvert installations. The mixture is generally compacted to 95-100% of AASHTO T-99 for roadway applications, so the following material property data are from soils compacted to that level.

Reference A-2 contains a summary of the engineering properties (Young's modulus and Poisson's ratio) of lime-soil mixtures and are presented as functions of unconfined compressive strength and flexural strength. Thus, if the strength properties can be measured or estimated for any specific soil, the engineering properties can be estimated. The data were based on soil tests from Illinois, but it seems reasonable to assume that engineering properties could be extrapolated to mixtures containing soils from other locals but having similar strength properties.

Figure A-1 is a generalized stress-strain curve for lime-soil mixtures. The curve remains linear up to about 70 percent of the maximum deviator stress. The modulus of elasticity in compression is described by the equation:

$$E = A + B f_u$$

where

E = modulus of elasticity, k Pa, (psi)

f_u = unconfined compressive strength, k Pa, (psi)

A = constant, 68800 k Pa, (9980 psi)

B = dimensionless constant, 124.

This equation was empirically derived from test data in which soils were subjected to 100 k Pa (15 psi) confining pressure. The average ultimate strain for the samples tested in Reference A-1 was approximately 1 percent. The ultimate strain appeared to be independent of strength properties of curing time.

Poisson's ratio for lime-soil mixtures is a function of the stress level. In general, the ratio increases for increasing stress levels. Figure A-2 shows a plot of the relationship for a typical mixture.

Lime-Fly Ash

The addition of both lime and fly ash to soil produces relatively strong stabilized mixtures. Lime to fly ash ratios of 1:3 and 1:4 are common, and these mixtures are added to soil in amounts of 12 to 30 percent by weight. The strengths of these mixtures is derived from the pozzolonic reaction of the two components which tends to cement the soil matrix together. As a result of this property, lime-fly ash (LFA) stabilization may be applied to a broader range of soil types than lime alone, because LFA stabilization is less dependent on the soil reactivity. Table A-1 shows some typical ranges for compressive strength of LFA with several soil types.

LFA mixtures are produced in virtually the same manner as lime-soil mixtures except that more material is added to the soil. The most efficient method is to combine all materials at a central batching plant, blend them with an appropriate amount of water and transport the material to the construction site.

Table A-1. Ranges of Compressive Strength for the Lime-Fly Ash-Stabilized Material (3)

Materials	28 Day Immersed Compressive Strength	
	kPa	(psi)
Gravels	2800-9000	(400-1300)
Sands	2100-4800	(300- 700)
Silts	2100-4800	(300- 700)
Clays	1400-3400	(200- 500)
Crushed Stones and Slag	10,000-14,000	(1400-2000)

LFA is best compacted by rubber-tired or vibratory compactors.

The primary limitation on LFA usage is the availability of fly ash. Very little fly ash is produced or used in states west of the Mississippi. Western states produce less than 15% of the total fly ash in United States, and their proportion of the total usage is about the same (A-3). Since fly ash is a major constituent of LFA, usage in western areas would probably be restricted to large projects where significant cost savings or other benefits may result.

Since most applications of LFA mixtures are in flexible pavements, the most readily available elastic property is Young's modulus determined from flexure tests. This is an effective modulus which is determined from the slope of the moment-curvature diagram for beam test specimens. It ranges between 10,000 and 17,000 Mpa (1.5×10^6 and 2.5×10^6 psi), and tends to be slightly lower than the compression modulus. These values are for mixtures which have been cured for at least 30 days. Indirect data on the compressive modulus were presented in Reference A-4 where the authors determined the "pulse velocity" as a function of the unconfined compressive strength of several different LFA and soil mixtures. The data show that the pulse velocity, and thus the compressive modulus, increases with increasing compressive strength. If the velocity values are converted to compressive moduli using assumed values of mass density and Poisson's ratio the modulus appears to be directly proportional to the unconfined compressive strength.

Poisson's ratio for LFA mixtures is a function of the applied stress. However, it is relatively constant at 0.08 for stress levels less than 60 percent of ultimate. It increases to approximately 0.3 near failure loads. Figure A-3 is a plot of Poisson's ratio versus stress level for a typical LFA mixture. For most pavement analyses values between 0.10 and 0.15 are used.

Soil-Cement

The addition of Portland cement to soils in amounts between 2 and 18 percent by dry weight of soil is commonly used for soil stabilization. Strength and stiffness of these materials results from the binding properties of the cement; thus, the elastic properties are somewhat dependent on the water-cement ratio. Mixtures are generally compacted at the optimum moisture content so changes in water-cement ratio interact with the density and strength properties of the mixture. Some mixtures with relatively high water contents have been used for concrete pipe bedding. These mixtures are referred to as plastic soil cement and are intended to be fluid enough to flow around the base of the pipe to give intimate contact between the pipe and bedding. Water-cement ratios for these latter mixes tend to be high, and, consequently, strength and stiffness tend to be less than for equivalent cement contents for compacted soil cements. However, unless specific data are available, the elastic properties of plastic soil cement can be assumed equal to those of a compacted soil cement with the same compressive strength and similar soil properties. Properties presented in this section are for compacted mixtures described in Reference A-6.

In its most common application, pavement subbases, soil cement is mixed in-place and compacted soon after mixing. Spreader trucks distribute the cement over pulverized and prewetted soil. Continuous mixing equipment then scoops up the ingredients, mixes them and redeposits them, before pneumatic tire rollers or other equipment compacts the mixture.

In other applications a central mixing plant is used to combine all ingredients, and the mixture is trucked to the job site for compaction. This latter operation might be more practical for pipe bedding or backfilling applications. Cement contents range between 3 and 15 percent by weight, and water contents are near optimum for the given soil.

Plastic soil cement can be batch mixed at the site, delivered as transit mix, or pumped to the location (A-5). The primary advantage of this material is that it can flow into the bedding area beneath the spring line of a pipe and provide intimate contact of pipe and bedding without requiring expensive hand compaction. Cement contents are about the same as those for compacted soil-cement. However, water contents are much higher so the mixture can have the desired flow characteristics (A-7). Plastic soil-cements are not compacted or vibrated, but simply left to harden in place.

Within the usual range of cement and water contents the modulus of elasticity of soil-cement is linearly related to the unconfined compressive strength for a given soil. Figure A-4 illustrates this relationship for two soils tested in Reference A-6. The data indicate static moduli between 7,000 and 14,000 MPa (1,000 to 2,000 ksi) for cement contents between 4 and 14 percent by weight. The data also indicates that compressive strength is approximately linearly related to the cement content for compacted soil-cement in a given soil.

Values of Poisson's ratio varied between 0.08 and 0.24 with an average value of about 0.15. The ratios for clayey soils tend to be somewhat higher than for granular soils but the variability is so great that the average value would be a reasonable choice for most calculations.

Other Materials

Several other soil stabilizing agents are available in addition to the ones already described. Although extensive data are available on these materials, very little data pertain to the engineering stress-strain properties. Some of these materials will be discussed in general terms in this section.

Bituminous stabilization is a frequently used and relatively inexpensive stabilization method. In general, roadway applications, asphaltic cutbacks are used in amounts of 4 to 7 percent

by weight of dry soil. The asphalt binds the soil particles together, so unconfined compressive strengths on the order of 3,400 KPa (5000 psi) are possible. Bituminous stabilization tends to be most effective in non-lastic soils with few fines.

Portland cement pressure grouting is occasionally used to stabilize soils in-place. In this method perforated pipes are inserted into the soil, and a water-cement grout is pumped into the pipes. Ideally, the grout permeates the soil around the pipes and hardens to give a material much like soil cement. Difficulties arise if the soil is not uniformly permeable because the grout tends to flow only into the more easily accessible soil voids. The volume through which the grout is effective is difficult to estimate in these cases. Elastic properties of soils stabilized in this manner are also difficult to estimate.

In-place stabilization by chemical injection is also used occasionally. Soluble silicates, chrome-lignin, analine-furfural and a variety of organic monomers are used as chemical grouts. These compounds are generally injected into the soil, and once in-place they react to form cementicious compounds that bind the soil particles together. The concept of chemical grouting is basically the same as that of portland cement grouting. The two are generally discussed separately because chemical grouting may cost as much as 50 times as much as portland cement grouting.

Relative Cost

Relative costs of different types of soil stabilization are difficult to quantify. Cost is generally a function of the properties of the soil that is to be stabilized, and the desired properties of the stabilized soil. Usually the amount of additive and compactive effort required to produce desired properties must be determined by a trial and error process for each soil. The only fair method of comparison would be to determine costs of methods to obtain a given set of properties for a given soil. A further complicating factor is the variation in cost of

stabilizing mixtures throughout the country. Material price data from Engineering News-Record indicate that the ratio of maximum to minimum cost of lime across the country is approximately 1.6 (A-8). The equivalent ratio for cement is 1.5, and the ratio for asphalt is 1.3 (A-9). Fly ash is even more variable, because the cost is highly dependent on delivery expenses. Fly ash cost may vary by a factor of two or more. Placement and mixing costs would also vary for different localities, but the costs for different stabilization methods should be equivalent for a given locale. Placing of plastic soil cement may be somewhat less expensive than some of the other methods, because it does not require careful control of compaction around culverts. This possible savings could be offset by equipment or other costs.

Table A-2 is an attempt to bracket the cost of some typical stabilization methods. Mixing and placing costs are not included in these values. The data represent a typical range of material costs for 1977 as taken from Reference A-8 and A-9. Columns indicating minimum and maximum quantities represent the ranges of amounts of additives per unit weight of soil. Values of minimum and maximum price represent the lowest and highest prices for additives used. This table is not intended to be used as a basis for comparing different stabilization methods; rather, it is intended to indicate the range of costs which can be expected if soil stabilization is to be used around culverts.

II. SOFT MATERIALS TO PROMOTE ARCHING

Soft materials as discussed in this report have low compressive moduli and low compressive strength. In traditional culvert practice such materials have been used in the imperfect trench placement method. Commonly used materials are straw, hay, cornstalks, leaves, brush, wood shavings, and loose soil. Despite their low cost and relative effectiveness very little quantifyable data is known about their stress-strain properties. Thus, any

Table A-2. Cost Ranges for Stabilized Soils in Dollars (March 1977) per Cubic Metre

Stabilization Method	Minimum Quantity		Maximum Quantity	
	Min. Price	Max. Price	Min. Price	Max. Price
Lime	3.65	5.96	8.20	13.39
Lime-FlyAsh (1:3)	4.92	8.68	10.59	18.69
Lime-FlyAsh (1:4)	4.32	7.79	9.38	16.79
Cement	1.20	1.79	9.33	13.96
Bituminous	4.28	5.75	7.27	9.80

Costs are based on the minimum and maximum prices of additive required. Minimum and maximum quantities of additives are based on general usage as described in the text. Mixing and compacting costs were assumed equal for all additives and are not included in the figures. Soil density was assumed to be 1600 kg/m^3 (100 lb/ft^3). Multiply above values by 0.7646 to obtain price per cubic yard.

use of these materials for purposes other than standard imperfect trench installations would be outside of the emperical data base. Long term stability of these materials is also questionable because of their organic nature. Therefore, a survey was conducted of potential soft materials for which engineering property data are available. The results of this survey are presented.

Soft materials can be separated into two categories based on their stress-strain relationships. First, are plastic-elastic materials which have a relatively low elastic modulus until they approach a "locking" strain, where modulus becomes very high. Plastic-elastic materials are generally low density granular solids. Second are elastic-plastic materials which have a moderate to high initial modulus, but yield at a relatively low stress level. The yield plateau is relatively flat until a locking strain is reached. Rigid foam materials generally fall into the elastic-plastic category. Figure A-5 illustrates the forms of stress-strain curves for the two different categories of soft materials. Either category has potential use for promoting soil arching depending on the engineering properties of the fill soil.

Plastic-Elastic Materials

Natural and manufactured aggregates are the most readily available material in this category. Foamed rubber and open-celled plastic foams also have these properties, but their costs tend to be relatively high. Materials discussed in this section are relatively inexpensive and widely available throughout the United States. The stress-strain properties are described by an initial modulus which becomes stiffer under one dimensional loading due to strain locking. Data on Poisson's ratio is not available for most materials. Typical stress-strain curves for natural and processed natural aggregates are shown in Figure A-6 (A-10). The materials will be discussed in order of decreasing stiffness.

Expanded shale and expanded clay are relatively stiff natural aggregates that are frequently used in the production of light weight concrete. They are produced by heating certain types of clay or shale in rotary kilns. The heating causes gas to form and expand within individual globules, and the material dries and hardens around these gas voids. The resulting particles are porous and lightweight. Typical values for the initial compressive moduli for expanded shale and expanded clay are 19,300 kPa (2,800 psi) and 8,300 kPa (1,200 psi), respectively. The locking stage begins at about 10 percent strain for expanded shale and at about 20 percent for expanded clay.

Volcanic cinders are derived from naturally occuring deposits in which gas-filled voids were created during volcanic action. Larger rocks are crushed until a granular product results with individual grains having irregular, angular shapes. A typical value for the initial compressive modulus is 7,000 kPa (1,000 psi). Locking begins at about 30 percent strain.

Expanded perlite is produced from a volcanic siliceous rock that is found primarily in the Rocky Mountain area (A-11). The ore is subjected to preliminary drying and crushing before it is heated in rotary kilns in a process similar to that used on expanded shale and clay. Good quality expanded perlite has a bulk specific gravity between 0.12 and 0.16. It is widely used as an aggregate for lightweight insulating concrete. As a bulk granular material it has a compressive modulus of about 2,800 kPa (400 psi). Locking begins at about 50 percent strain. The primary difficulty with expanded perlite is that it tends to absorb large quantities of water. Absorption of 10 to 50 percent by weight has been reported (A-12). Test data are not available on the effects of water content on its stress-strain behavior.

Expanded vermiculite is a micaceous mineral that has been dried, crushed and heated in special furnaces. The expansion process is similar to that which has been described for the

previously mentioned natural aggregates. Individual particles have a flat laminar structure. Primary use of the material is for aggregate in thermal or acoustic insulating concrete. A typical value for the bulk specific gravity is 0.13. The primary advantage of vermiculite for backpacking is its relatively low compression modulus. It has a modulus of elasticity in compression of 1,000 kPa (150 psi) and locking does not begin until strains are 60% or more. Expanded vermiculite tends to absorb large quantities of water, and its behavior and stiffness in a saturated state are not known.

Expanded polystyrene beads, expanded polystyrene scraps and polyvinyl scraps are artificially produced plastic aggregates that may be cost competitive with natural aggregates. The beads are produced by polymerizing styrene with a blowing agent in an aqueous solution. The granules produced in this process are then heated to produce expanded beads. The bulk specific gravity of polystyrene beads is nominally 0.03, and individual beads are between 1 and 5 mm (0.05 to 0.2 in.) diameter. Waste material from the manufacturer of expanded polystyrene may also be used as a soft material. Bulk specific gravity is about one-half that of the primary product, and the grain size ranges between 0.5 to 10 mm (0.03 to 0.4 in.). Expanded polyvinylchloride scrap is a similar by-product that can be pulverized and used as a soft aggregate. The bulk specific gravity is on the order of 0.01.

The initial modulus of elasticity in compression for expanded polystyrene beads is approximately 900 kPa (130 psi). Data from Reference A-10 indicates the material behaves almost linearly up to 60 percent strain. Expanded polystyrene scrap has a much lower modulus -- 76 kPa (11 psi), and remains linear out to about 40 percent strain. Expanded polyvinyl scrap has a modulus of only 9.0 kPa (1.3 psi) and begins to start locking at about 40 percent strain. However, the secant modulus in compression of 80 percent strain is only 21 kPa (3.0 psi), and the

material is probably too soft for most culvert applications. Figure A-7 shows stress-strain curves for all three artificial aggregates.

Elastic-Plastic Materials

Rigid foams and low density portland cement concretes are the most common elastic-plastic materials. Rigid cell foamed plastics are the largest single group of materials in this category; unfortunately, they are also among the most expensive materials. Foamed aluminum and aluminum honeycombs also have these properties, but are also very expensive. Paper honeycombs have potentially useful properties, but their long-term durability in soil is questionable. Materials in this category that appear most promising for culvert applications are cellular concrete, foamed sulfur, rigid expanded polyurethane and rigid expanded polystyrene. Typical stress-strain curves for these materials are shown in Figure A-8. Their properties are discussed below.

Cellular concrete is produced from a portland cement paste or mortar in which a preformed foam has been mixed (A-13, A-14). The foam has the properties that air bubbles remain stable during the mixing and placing operations, so the hardened concrete has a cellular structure. Individual bubbles are on the order of a few millimeters in diameter. The specific gravity of cellular concrete varies between 0.4 and 0.8, depending on the amount of foam added. It is typically used for thermal and acoustic insulation.

The lower density formulations have the greater potential applications to culvert applications because they have lower crushing strength plateaux. The yield stress can vary between 700 kPa (100 psi) and 4,900 kPa (700 psi), and it is approximately linearly related to the density for a given set of cement paste properties. The stress-strain curve shown in Figure A-8 is for a cellular concrete with a specific gravity of 0.64; it has an initial elastic modulus of 87,000 kPa (12, 600 psi) and

a yield stress of 900 kPa (130 psi).

Foamed sulfur is a formulation of elemental sulfur, stabilizers and a blowing agent (A-15). Sulfur is first heated to approximately 160°C (320°F). Stabilizers and blowing agents are added, and the mixture is agitated for 10 minutes or less. Two additional additives are then placed in the mix and the vessel is closed and pressurized with air to 550 kPa (80 psi) and agitated for an additional 2 to 5 minutes. The resulting foam is then discharged into molds where it cools and solidifies. Although the material is not in general use, it has been considered for thermal insulation and culvert applications.

Foamed sulfur can be produced in a range of densities, and like cellular concrete, the yield stress increases with density. Specific gravities range from 0.2 to 0.8, and yield stresses vary from 280 kPa (40 psi) to approximately 1,000 kPa (150 psi). The stress-strain curve shown in Figure A-8 is for a foam with a specific gravity to 0.75. Locking generally occurs at strains greater than 70 percent for foams with specific gravities less than about 0.3, but locking generally begins at about 50 percent for denser formulations.

Several rigid plastic foams have elastic-plastic properties which make them suitable for culvert applications. These foams are characterized by a closed, non-interconnecting cellular structure with relatively brittle walls. They are stable and do not absorb significant amounts of water. Rigid plastic foams are available in a wide range of densities and strengths. The primary disadvantage of these materials is their high cost compared to the previously discussed foams.

Rigid polyurethane and polystyrene foams are two formulations that could be competitive for culvert applications. Rigid polyurethane foam is placed by combining two or more constituents in a spray nozzle and foaming the material in-place. It is also available in preformed boards and blocks. The latter process

permits better control of dimensions and mechanical properties. Rigid polystyrene can also be produced by two different processes: by dispersion of a gas in a melted plastic resin and by heating an expandable polystyrane resin. The former produces a homogenous foam, and the latter produces matrix of fused individual expanded beads. Neither process is suitable for foaming in-place.

Rigid polyurethene foams are available in a range of specific gravities. Those with specific gravities between 0.02 and 0.11 tend to have strength properties that have potential for culvert applications. Crushing yield stresses are between 100 and 2,000 kPa (15 and 300 psi). A typical stress-strain curve for a rigid polyurethane foam with a specific gravity of 0.03 is shown in Figure A-8.

Rigid polystyrene foams are available with specific gravities between 0.02 and 0.10 for culvert applications. Crushing yield strengths for these formulations are between 70 and 2,000 kPa (10 and 300 psi). Stress-strain curves for these foams are similar to those for rigid polyurethane. Figure A-8 shows a curve for a rigid polystyrene foam with a specific gravity of 0.02.

Relative Cost

Relative costs for soft materials are more difficult to determine than those for stabilized materials. Costs of processed natural aggregates vary by a factor of two or more across the country. There is no obvious trend in this cost variation. The costs of foamed and expanded plastics also vary widely, because within each category there are several specific formulations that can provide a similar range of material properties. Relative cost data should thus be viewed with these variations in mind.

Relative costs of soft materials investigated are shown in Table A-3. Data were obtained from Engineering News-Record material price reports, national manufacturers' associations, manufacturers, and various suppliers and producers. The figures represent average costs for a unit volume of material. Costs

Table A-3. Relative Cost Per Unit Volume for Soft Materials

Plastic-Elastic Materials	
Volcanic Cinders	1.0
Expanded Clay/Shale	0.6
Expanded Vermiculite	0.9
Expanded Perlite	0.5
Expanded Polystyrene	1.5
Polyvinylchloride	-
Elastic-Plastic Materials	
Foamed Sulfur	3.1
Cellular Concrete	0.6
Polyurethane Foam	1.3
Expanded Polystyrene Boards	1.9

*As of 1977, the above relative costs are equivalent to dollars per cubic foot.

for both groups of materials are normalized with respect to the same base. No datum is given for polyvinyl chloride scraps, because the cost would be highly dependent on local availability and alternative uses of the material is different areas. Although it is a scrap or by-product, its cost would tend to escalate if it were in wide demand.

As with the stabilized materials, the cost data in Table A-3 should not be used to dictate the choice of materials. Engineering properties, durability and ground water effects must also be considered. The list includes a wide range of strengths and stress-strain behavior categories. Some of the materials are less durable than others when buried in soil, and some must be protected from water intrusion. Specific placement conditions and configurations could also alter cost and performance characteristics.

Figures A-1 through A-8

		Page
Fig. A-1	Generalized stress-strain curve for cured lime-soil mixtures (A-2).	254
Fig. A-2	Influence of stress level on Poisson's Ratio (A-2).	255
Fig. A-3	Effect of stress level on Poisson's Ratio for a lime-fly ash-gravel mixture (A-3).	256
Fig. A-4	Relationship of compressive strength to modulus of elasticity for typical soil-cement mixes (A-6).	257
Fig. A-5	Ideal stress-strain curves for backpacking materials.	258
Fig. A-6	Typical stress-strain curves for plastic-elastic natural aggregates.	259
Fig. A-7	Stress-strain curves for plastic-elastic artificial aggregates (A.10).	260
Fig. A-8	Typical stress-strain curves for elastic-plastic materials.	261

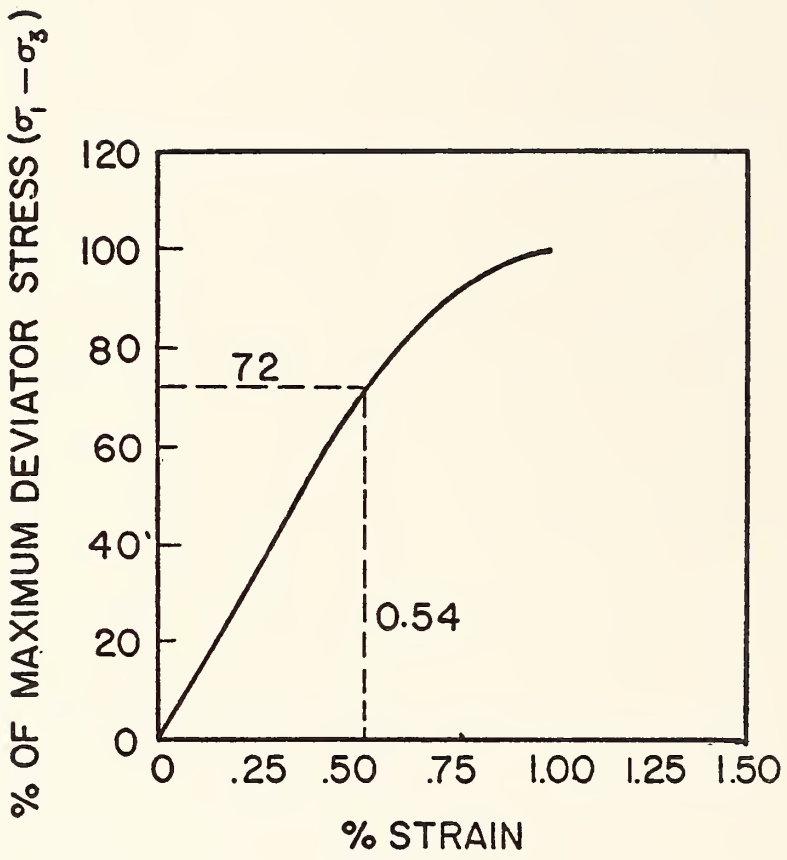

Figure A.1 Generalized Stress-Strain Curve for Cured Lime-Soil Mixtures (A.2).

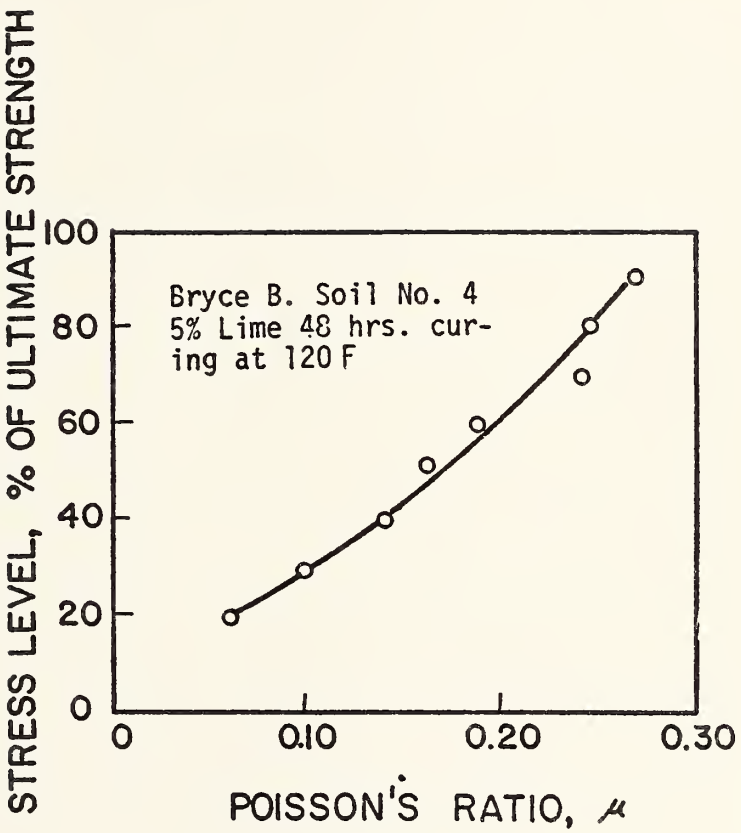

Figure A.2 Influence of Stress Level on Poisson's Ratio (A.2).

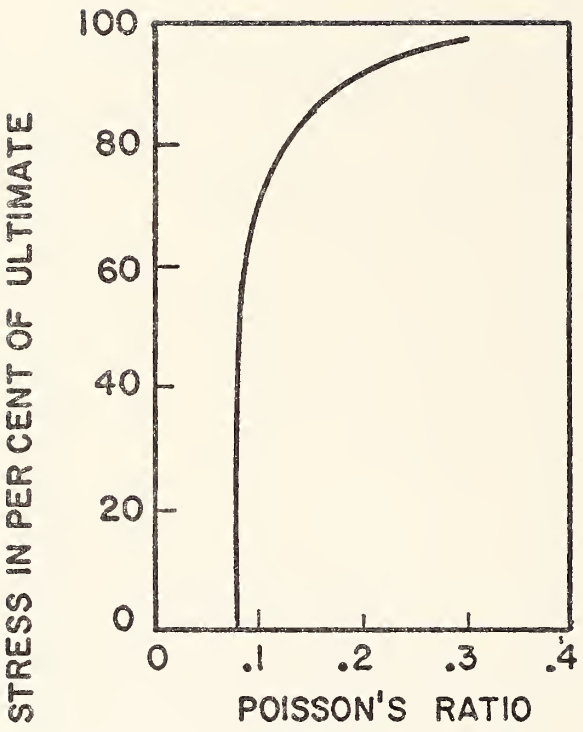

Figure A.3 Effect of Stress Level on Poisson's Ratio for a Lime-Fly Ash-Gravel Mixture (A.3).

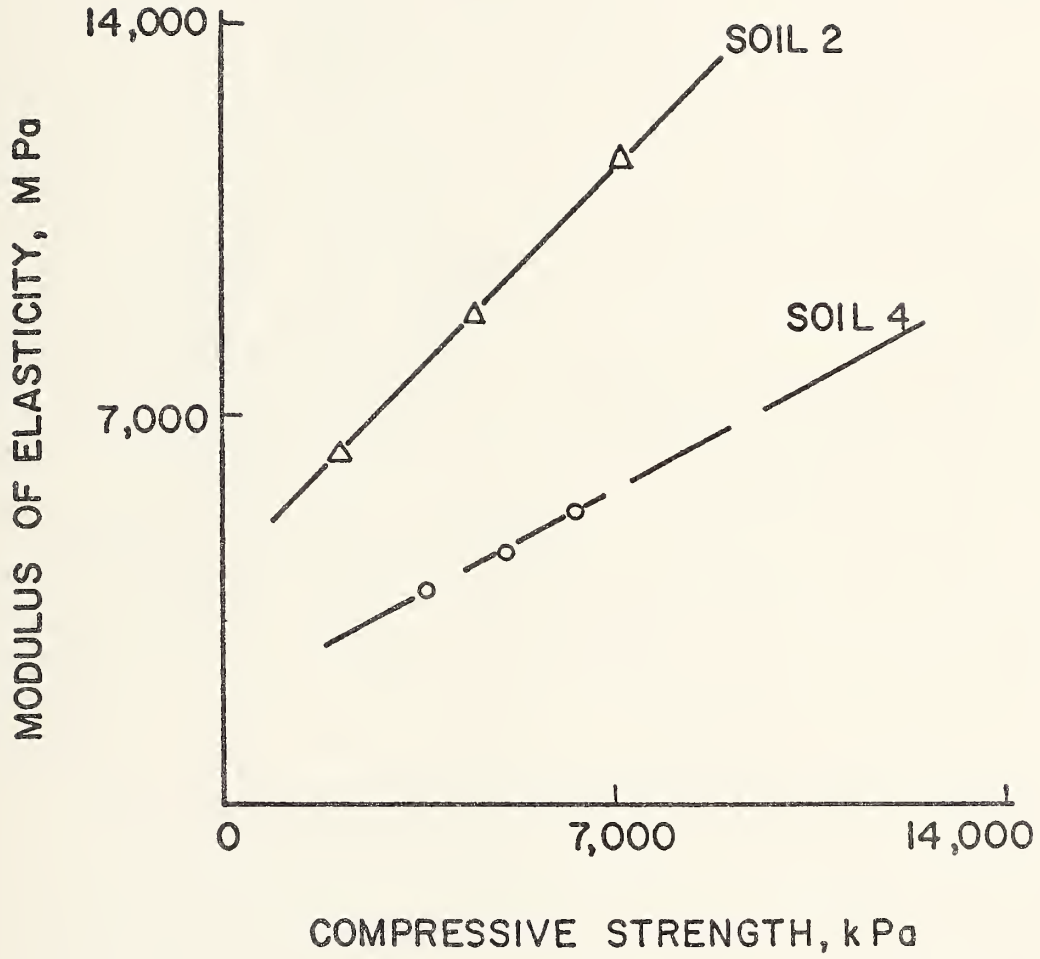

Figure A.4 Relationship of Compressive Strength to Modulus of Elasticity for Typical Soil-Cement Mixes (A.6).

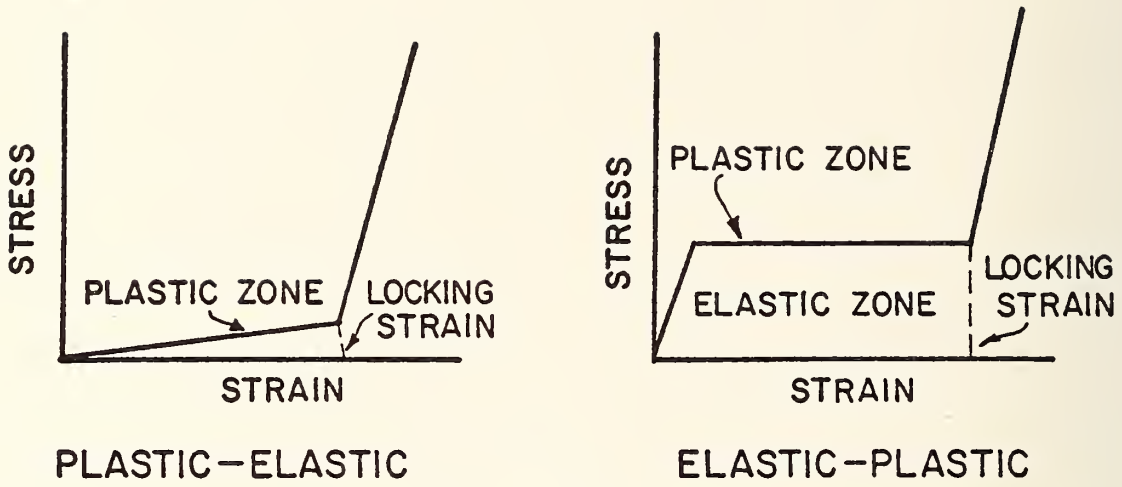

Figure A.5 Ideal Stress-Strain Curves for Backpacking Materials

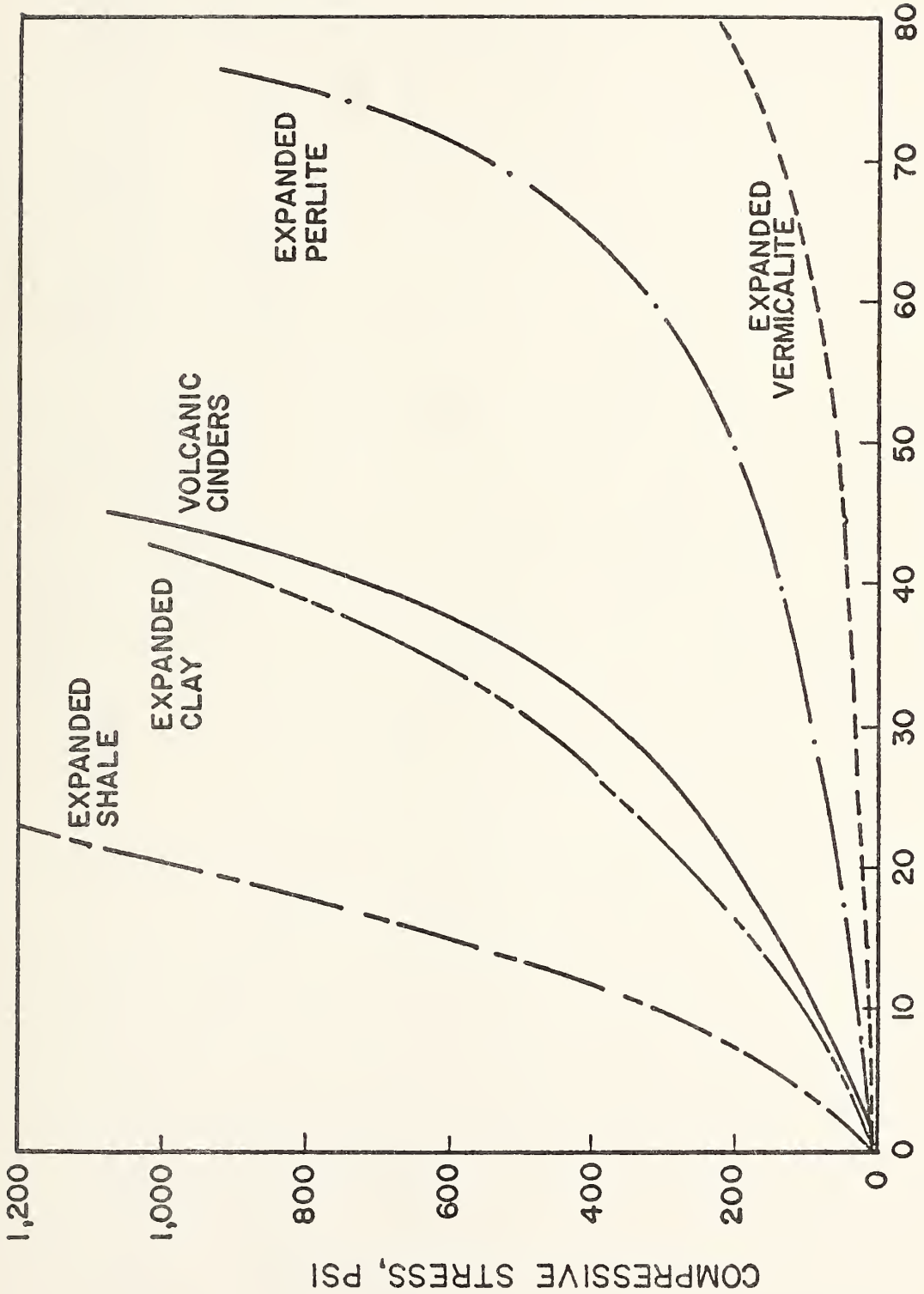

Figure A.6 Typical Stress-Strain Curves for Plastic-Elastic Natural Aggregates

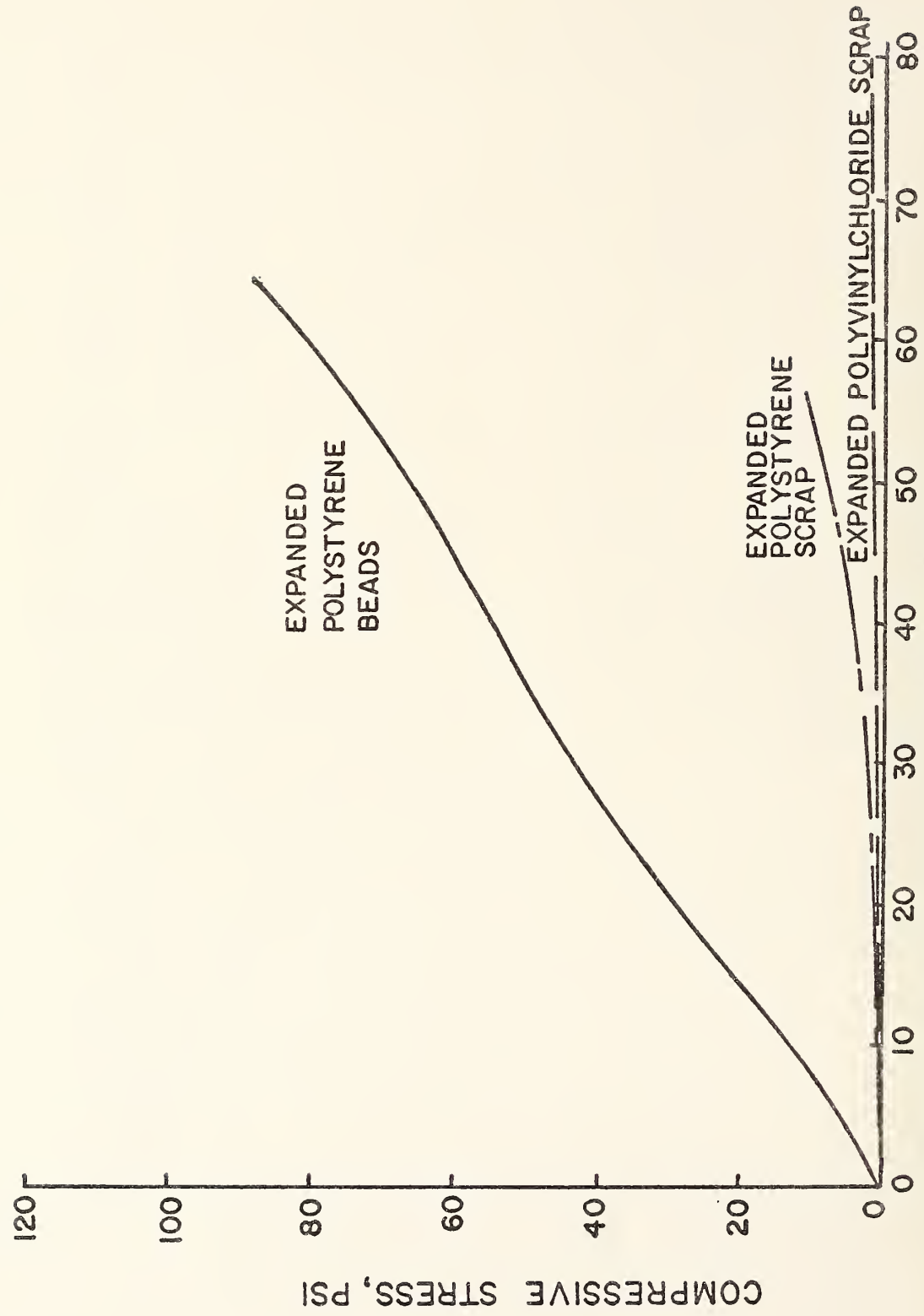

Figure A.7 Stress-Strain Curves for Plastic-Elastic Artificial Aggregates (A.10).

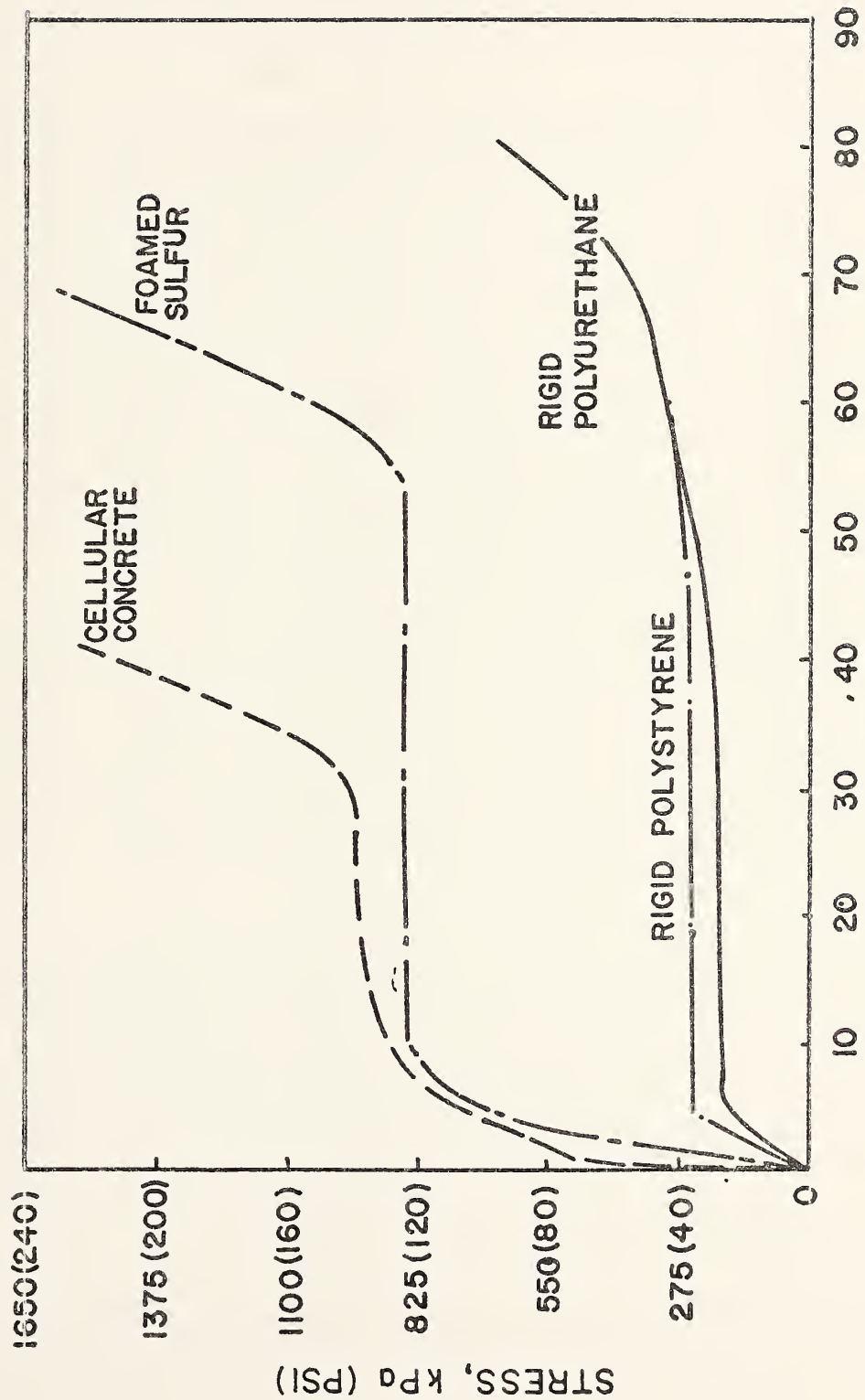

Figure A.8 Typical Stress-Strain Curves for Elastic-Plastic Materials

APPENDIX B

REINFORCED EARTH

INTRODUCTION

Concept of Reinforced Earth: The modern concept of reinforced earth was systematically presented by the French engineer Henri Vidal in 1966 (B-1).

Basically, the concept involves the introduction of small amounts of reinforcing materials like metal strips, bars or fabric in the soil to improve its tensile stiffness and strength in one direction. The tensile stresses in the reinforcing material is developed by frictional shear forces between the soil grain particles and the reinforcing strips. The resulting composite material behaves approximately like an orthotropic continuum whose stiff direction is dependent on the tensile stiffness of the reinforcement.

Current Application: Reference (B-2) gives a summary of the current applications which include retaining walls, platforms on sloping ground, quay walls, foundation slabs, and bridge abutements. These applications concentrate primarily in highway work. In November 1974, the FHWA approved Reinforced Earth as an acceptable standard highway construction practice suitable as an alternate to other methods for resisting earth forces (B-3).

Possibilities for Long Span System: The following features of reinforced earth may be a favorable indication for the possible use of reinforced earth concept in the long-span system.

1. Simple experiments by Lee, Adam and Vagneron (B-4) illustrated that small amount of wood-strip reinforcing in sand increased its strength (or stiffness) by more than four times (See Fig. B-1).

2. There is no practical height or length limitations as far as reinforced earth is concerned. This design

feasibility may make feasible the design of the span of culverts longer than presently conceivable.

A practical way of placing the reinforcements in a long-span system is shown in Fig. B-2 and investigated in the main body of this report.

CHARACTERISTICS OF REINFORCEMENT

Material Properties: The type of material used as reinforcement are usually galvanized steel or aluminum and/or fabric. Mild steel and stainless steel are less frequently used.

The galvanized steel strips used in a demonstration projects conducted by the California Division of Highways (B-6) have the following properties which are presumably typical.

Yielding Strength: F_y = 225 kPa (37 ksi)

Ultimate Strength: F_u = 345 kPa (50 ksi)

Young's Modulus: E = 197,000 kPa (28,500 ksi)

Poisson's Ratio: ν = 0.28

The U.S. Army Engineers (B-2) used galvanized steel strips and nylon fabric membrane strips as reinforcements in a demonstration project. The properties of these materials are shown in Figs. B-3 and B-4.

A typical load-deformation curve from a short term biaxial test of a woven polyester fabric is shown in Fig. B-5, (B-7).

Economics: The price of the galvanized steel strips (1978) imported from France is $750 per ton including delivery, patent rights, packing, custom duty and required service in design and supervision of construction (B-6).

Fabric costs are highly dependent on type and quality of fabric. Woven plastic fabric costs approximately $0.12 per square foot and non-woven from $0.06 to $0.25 and more dependent on type of fabric. USDA Forest Service provides excellent guidelines on use and cost of fabrics for construction (B-5).

CURRENT DESIGN PROCEDURE

General: The current design procedure is semi-empirical in nature based primarily on Rankine's Earth Pressure Theory. Lee, et al., (B-4) proposed a simple design procedure for the design of the reinforcements. Two failure modes were considered; namely, tie breaking and tie pull-out. A laboratory study of some 60 small retaining walls were carried out to justify the design procedure. Broms (B-7) also suggested similar design equations for the design of fabric reinforced retaining structures including creep behavior.

The determination of the maximum allowable vertical and horizontal spacing of the reinforcements is still uncertain.

Thus, the basic approach in current design procedure is to assume a set of dimensions and them compute the factor of safety against the various modes of failure. The following design equations for retaining walls appear to be satisfactory, assuming no slippage of reinforcement (B-4).

Design of Reinforcement Against Tie Breaking: A factor of safety against tie rupture is given by the force ratio fo yield force-to-actual force on the tie. For retaining walls this may be estimated by (B-4):

$$FS_{break} = \frac{P_{yield}}{P_{tie}} = \frac{\sigma_y wt}{K_A \gamma HSX}$$

S = horizontal spacing of strips

X = vertical spacing of strips

w = width of strip

t = thickness of strip

γ = unit weight of soil

H = height of wall

K_A = Rankine active earth pressure coefficient

σ_y = yield stress of strip

Design of Reinforcement Against Tie Pull-Out: A factor of safety against tie pull-out is given by the force ratio of maximum frictional resistance prior to slippage divided by actual force on tie end. For retaining walls this may be estimated by (B-4):

$$FS_{pull\text{-}out} = \frac{P_{friction}}{P_{tie}} = \frac{2\ell w \tan\phi_u}{K_A S X}$$

Where:

ℓ = length of strip behind the failure surface

ϕ_μ = the angle of frictional sliding resistance between the soil and the strip

Typical Ranges of the Design Parameters: The following ranges of reinforcement parameters represent typical values.

Spacing of Reinforcements:

Horizontal Spacing	0.46 to 1.5m (1.5 to 5.0 ft)
Vertical Spacing	0.30 to 0.70m (1.0 to 2.25 ft)

Size of Strip:

Width of strip	5.0 to 10.0cm (2.0 to 4.0 in)
Thickness of strip	0.06 to 0.60cm (0.025 to 0.25 in)

Length of Strip:

Length	7.0 to 14.0m (23 to 46 ft)

Corrosion: The design criteria to account for corrosion of the buried reinforcing elements are not well established. Herbert Uhlig (B-9) states that the major factors that govern corrosivity in a given soil are porosity, electrical conductivity, content of dissolved salts including depolarizers or inhibitors, moisture content and acidity or alkalinity.

The California Transport Laboratory (B-6) developed a chart for estimating the rate of metal loss due to corrosion and to establish the required thickness (corrosion allowance) of steel reinforcement for the design life. The combined influence of resistivity and pH value is used to estimate soil corrosivity.

CONSTRUCTION PRACTICES

The construction of reinforced earth structures is rapid and simple. No special skill and special construction equipment are needed.

Basically, the construction process is repetitive. For retaining walls, the first step is to secure the wall (or skin) element in its proper place. Then the earthfill is spread and compacted followed by the laying of the first row of reinforcements, The reinforcements are bolted onto the wall elements and are laid perpendicular to it. As subsequent wall elements are added on, the entire process is repeated. Stage construction is possible because the structure is internally stable as each layer of wall-backfill-reinforcement is added on.

The following types of backfill material are specified by the Reinforced Earth Company: sandy or silty gravels and silty or clayey sands. Cohesive soils with high water table are generally not recommended to avoid dealing with questionable pore-water pressure and the cohesive bond effects.

In fact, recent research (B-10) in soil-reinforcement interface friction in fine-grained soils concluded that (i) no more than 15% of all the backfill (by weight) may be smaller than 15μ, (ii) the internal friction angle of saturated and consolidated soil must be greater than 25°.

From corrosion resistant point of view, the soils selected as fill materials should ideally be of uniform composition having a high resistivity, high redox potential, low moisture content and of neutral pH value. An effective drainage system would be desirable to avoid microbial attack on deterioration of non-metallic reinforcing element (B-11).

EXPERIMENTAL STUDIES

Laboratory Models: Much of the past research has been directed primarily at one category of structure - the Vidal type of reinforced earth wall (B-12). However, some of the experimental findings on

reinforced earth slabs have also been reported. Summarized below are some key findings for both class of structures.

For reinforced earth slabs (footings) key laboratory experimental findings are:

1. The load settlement and ultimate bearing capacities of footings on reinforced earth are 2-4 times better than that of unreinforced earth (B-13).

2. A minimum critical number of layers of reinforcing is required to obtain significant load settlement and bearing capacity improvement. For the tests conducted, four or more layers were required (B-13).

3. Two failure modes are observed namely tie breaking and tie pull out. Tie pull out failure is generally associated with lightly reinforced slabs whereas tie breaking failure is generally associated with heavily reinforced slabs (B-13).

4. The classical slip surface bearing capacity theory no longer holds for R.E. slabs.

For reinforced earth retaining walls key experimental findings are:

1. The design procedure based upon Rankine's or Coulumb'-theory was found to be suitable for design (B-4).

2. The centrifugal models (B-14) support the proposition of Schlosser and Long (B-15) that reinforced earth retaining walls can be designed to avoid collapse by treating them as multi-anchor walls.

3. If the deformation of the wall is of flexible nature, the distribution of the horizontal earth pressure in the limit state differs from the linear distribution by the Rankine method (B-16).

4. Location of failure surfaces in reinforced soil vary in wide ranges, even appearing behind the ends of the strips (B-16).

5. After a "load-unload" cycle, residual stresses remain in ties. These stresses appear to be time-dependent (B-17).

6. Temporary loading to failure of a reinforced earth wall designed to fail by slippage rather than rupture of the ties causes deformation rather than catastrophic collapse (B-17).

7. The results obtained by Wolfe and et al., (B-18), indicate that for reinforced earth walls with low strain natural frequencies above the frequencies of greatest intensity of shaking, the vertical component of seismic motion may be disregarded in terms of practical seismic stability design.

Full-Scale Model: Al-Hussaini and Perry (2) investigated the field behavior of two full-scale reinforced earth retaining walls. One was reinforced with fabric and the other was reinforced with galvanized steel. The conclusions are summarized as follows:

1. Deformation of fabric reinforcements can cause excessive tilting of wall elements. Steel strip reinforcement performed better.

2. The measured lateral earth pressure, using pressure cells along the wall prior to failure under a substantial surcharge loading was maximum at the middle third of the wall and varied from 1.0 to 1.2 times the earth pressure predicted by the Rankine theory for the active case.

3. The curve connecting the points where maximum tensile stress occurred in the reinforcing ties did not coincide with the theoretical Rankine failure surface. Field observations of the reinforced earth bridge abutment (B-19) indicate that the potential failure surface is vertical at the upper part of the structure.

Chang (B-6) collected some field data for the reinforced earthfill constructed on California State Highway 39, Los Angeles County. The measured data agree reasonably well with the steel stresses calculated from the theoretical design equations. The distribution patterns of the analyzed steel stresses (by finite element analysis) generally agree with the field but with some discrepancies in magnitude.

ANALYTICAL MODELS

There are basically two approaches in the analysis of the reinforced earth. One is to treat the reinforced earth an an orthotropic material (unit cell), while the other is to treat it as a heterogenious material, i.e., every reinforcing member is descretely represented within the soil mass. A number of attempts also have been made to model the strip slipping. Elaboration of these models are provided below.

Orthotropic Model: The model was proposed by Romstad, Herrmann, and Shen (B-20) wherein reinforced earth is treated as composite material. Composite properties depend upon the properties of the individual component materials (soil and reinforcement) and the geometric arrangement of the reinforcement. The determination of these composite properties was based upon the concept of the "unit cell". For a material that has a regular reinforcing pattern, one can, in general, isolate a small unit of the material which exhibits the composite characteristics of the material; this fundamental building block is called the "unit cell". The resulting matrix of orthotropic properties is ideally suited for use in displacement finite element formulations. A derivation of the orthotropic matrix for plane strain is presented at the end of this appendix.

The advantage of this model is that is is more economical than the alternative approach of discrete analysis. Moreover, the model captures the essential response characteristics such as peak strip forces and soil stresses at service load level (B-20).

Because of the above advantages the orthotropic model was adopted in this study for analyzing long-span systems with reinforced earth.

Discrete Model: In constrast to the orthotropic model, the discrete model (B-20, B-21, B-22) involves the discrete representation of each and every reinforcing member within the soil mass. This can be accomplished by representing the soil with continuum elements overlain with beam (or rod) elements whose properties and location

match the reinforcing strips. The advantage of a discrete representation is that detailed information is directly about the interaction of the soil and the reinforcing members. The chief disadvantage (at times rendering the approach impractical) is excessive computational cost for those configurations containing large numbers (possibly hundreds) of reinforcing members.

Slip Models: Two models have proposed to represent reinforcement slippage in the soil. A slip model developed by Naylor (B-8) is intended to reproduce the following essential characteristics, (i) the longitudinal stiffness of strip, (ii) the transfer of shear stress by bond between the strips and the soil, (iii) the transfer of shear through the soil in the vertical plane containing the strips. To do this, Naylor defines a "conceptual" shear zone aligned in a vertical plane through a column of strips, and introduces an internal degree of freedom representing relative movement along the shear zone.

Another slip model developed by Herrmann and Yassin (B-22) involves the introduction of bond links or springs between the reinforcement and the soil. A pair of nodes are placed at the same initial geometric location, one attached to the reinforcement and the other to the soil and are linked with a pair of non-linear springs normal and tangential to the reinforcement. An attempt is then made to select the non-linear stiffness characteristics of the tangential bond springs to reproduce the force slip relationship observed in "pull-out" tests.

DEVELOPMENT OF ORTHOTROPIC MODEL FOR REINFORCED EARTH

Based on the unit cell concept previously discussed, an orthotropic elastic material matrix for plane strain is developed as follows. Referring to the unit cell in Figure B-6, a cartesian coordinate system is defined such that the x-axis is parallel to the lines of strip reinforcement, and the y-axis is perpendicular the horizontal strip rows.

In this reference system strains in the strip and soil are assumed as follows:

$$\varepsilon_x = \varepsilon_x^{strip} = \varepsilon_x^{soil}$$

$$\varepsilon_y = \varepsilon_y^{soil} \quad (\varepsilon_y^{strip} = 0)$$

$$\gamma_{xy} = \gamma_{xy}^{soil} \quad (\gamma_{xy}^{strip} = 0)$$

Isotropic stress-strain relations for soil in plane strain are:

$$\begin{bmatrix} \sigma_x \\ \sigma_y \\ \tau_{xy} \end{bmatrix}^{soil} = E_{soil} \begin{bmatrix} \beta & K_o\beta & 0 \\ K_o\beta & \beta & 0 \\ 0 & 0 & \frac{1}{2(1+\nu)} \end{bmatrix} \begin{bmatrix} \varepsilon_x \\ \varepsilon_y \\ \gamma_{xy} \end{bmatrix}^{soil} \qquad \text{(B-2)}$$

Where:

$\beta = (1-\nu)/(1+\nu)(1-2\nu)$

$K_o = \nu/(1-\nu)$

E_{soil} = Young's modulus of soil

ν = Poisson's ratio of soil

Axial stress-strain relationship for reinforcement strips is:

$$\sigma_X^{strip} = E_{strip}\, \varepsilon_X^{strip} \qquad \text{(B-3)}$$

where E_{strip} is Young's modulus of strip. All other strains and stresses in strip are assumed negligible.

Now to obtain a composite stress-strain relationship, <u>force</u> equilibrium in the x-direction is enforced to equate the average composite stress σ_X over the X-face with the force contributions of soil and strip (see Figure B-6):

$$A\sigma_x = A_{soil}\sigma_x^{soil} + A_{strip}\sigma_x^{strip} \qquad (B\text{-}4)$$

Where:

A = Area of unit cell = bd

A_{strip} = Area of strip = wt

A_{soil} = Area of soil = bd-wt = bd

Replacing σ_x^{soil} and σ_x^{strip} with Equations B-2 and B-3, and making use of Equation B-1, the composite stress-strain relationship for σ_x (Equation B-4) is:

$$\sigma_x = E_{soil}((\beta+\alpha)\varepsilon_x + \beta K_o \varepsilon_y) \qquad (B\text{-}5)$$

Where:

$$\alpha = \frac{E_{strip}}{E_{soil}} \quad \frac{A_{strip}}{A}$$

and:

$$\frac{A_{soil}}{A} \cong 1$$

Since only axial strain and stress (ε_x^{strip} and σ^{strip}) are nonzero in the strip, the final composite orthotropic relationship for the unit cell is:

$$\begin{bmatrix} \sigma_x \\ \sigma_y \\ T_{xy} \end{bmatrix} = E_{soil} \begin{bmatrix} \beta+\alpha & K_o\beta & 0 \\ K_o\beta & \beta & 0 \\ 0 & 0 & \frac{1}{2(1+\nu)} \end{bmatrix} \begin{bmatrix} \varepsilon_x \\ \varepsilon_y \\ \gamma_{xy} \end{bmatrix} \qquad (B\text{-}6)$$

Note the composite orthotropic matrix only differs from the isotropic soil matrix (Equation B-2) by the term α in the first matrix position.

If the material strips are not aligned with the global coordinate system, standard coordinate transformations for stress and strain are required.

SUMMARY AND CONCLUSIONS

A survey has been made on reinforced earth with the intent of supplying the background information necessary for the application of reinforced earth concept to the long span system. The survey included; the basic concept of reinforced earth, current applications, characteristics of reinforcements, reinforcement costs, current design procedures, construction practices, experimental studies, and various analytical models.

As there is no precedent in the application of reinforced earth concept in the long span culverts, the economic advantage, design flexibility and ease of construction associated with retaining walls and foundation slabs may or may not be true in the long span system. Hence, a preliminary study to investigate the benefit/cost ratio and the behavior of the long span culvert in relation to reinforced earth may be desirable.

Figures B-1 through B-6

		Page
Fig. B-1	Effect of adding reinforcing.	275
Fig. B-2	Long-span system with reinforcing strips.	275
Fig. B-3	Stress-strain relationship for the membrane strips (B.2).	276
Fig. B-4	Average stress-strain relationship for galvanized steel strips (B.2).	277
Fig. B-5	Stress-strain relationship for woven polyester fabric (B.7).	278
Fig. B-6	Unit cell concepts.	279

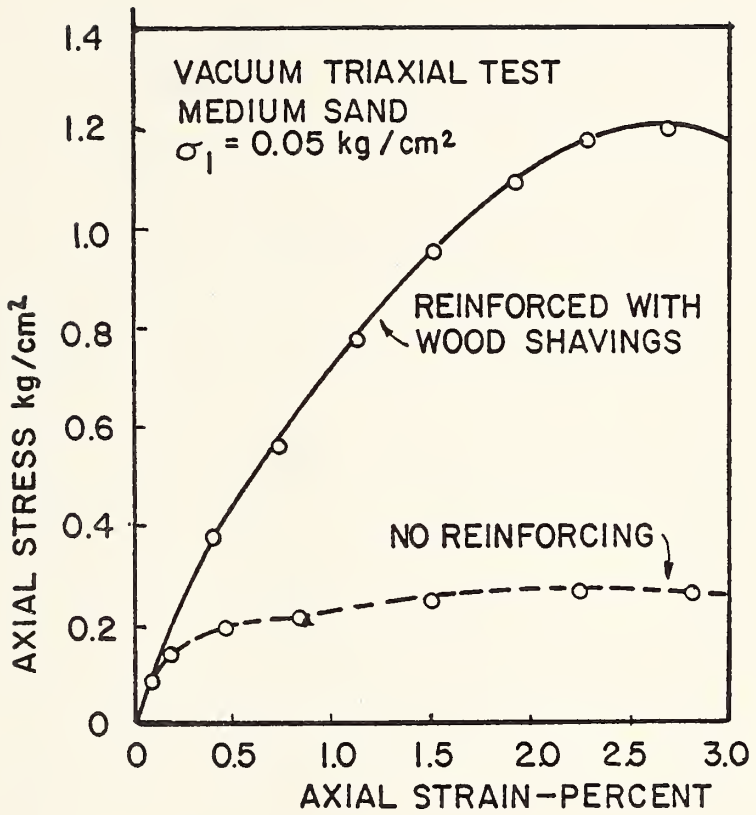

Figure B.1 Effect of Adding Reinforcing to Sand (B-4)

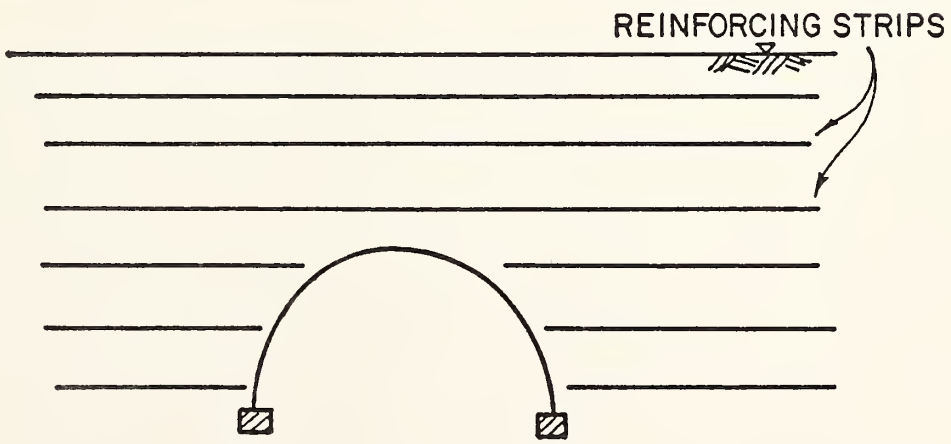

Figure B.2 Long-Span System with Reinforcing Strips

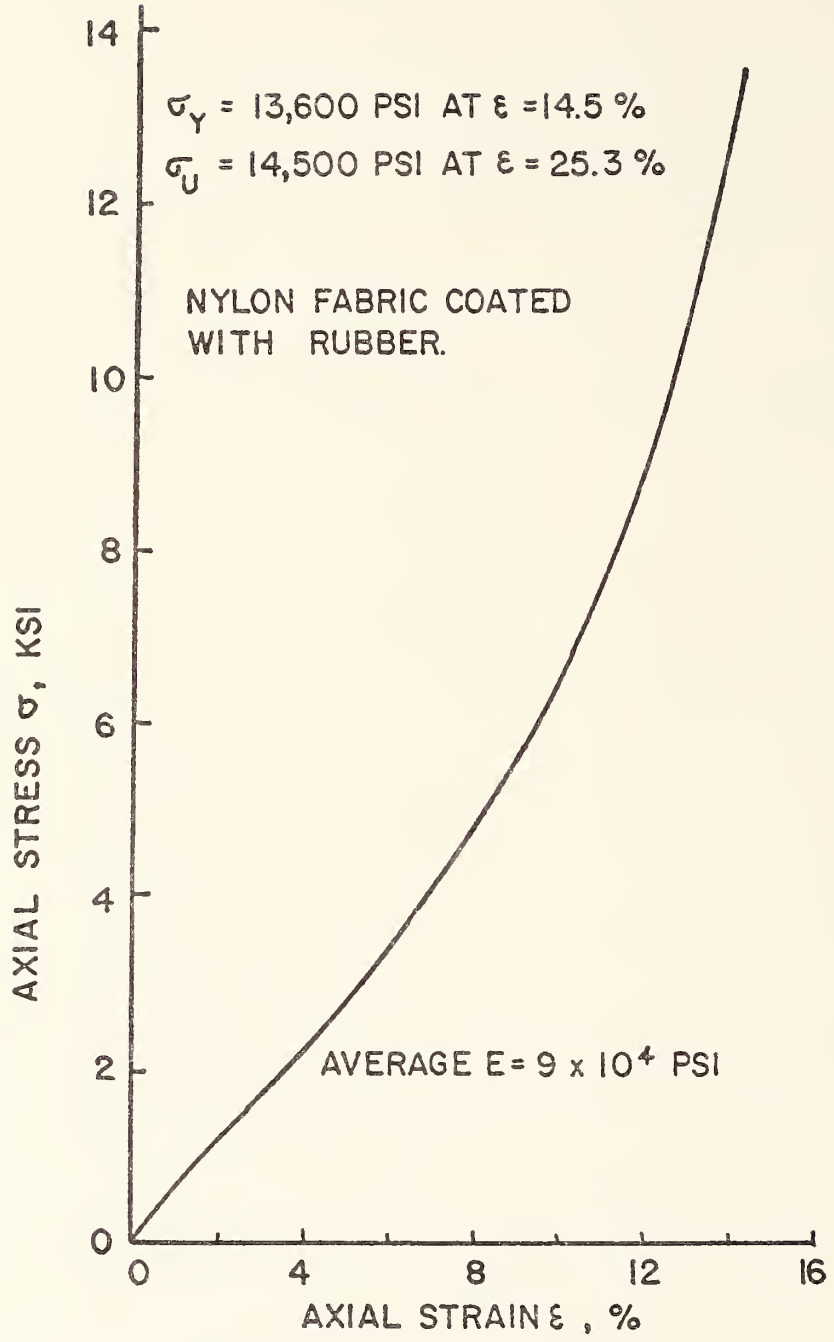

Figure B.3 Stress-Strain Relationship for the Membrane Strips (B.2).

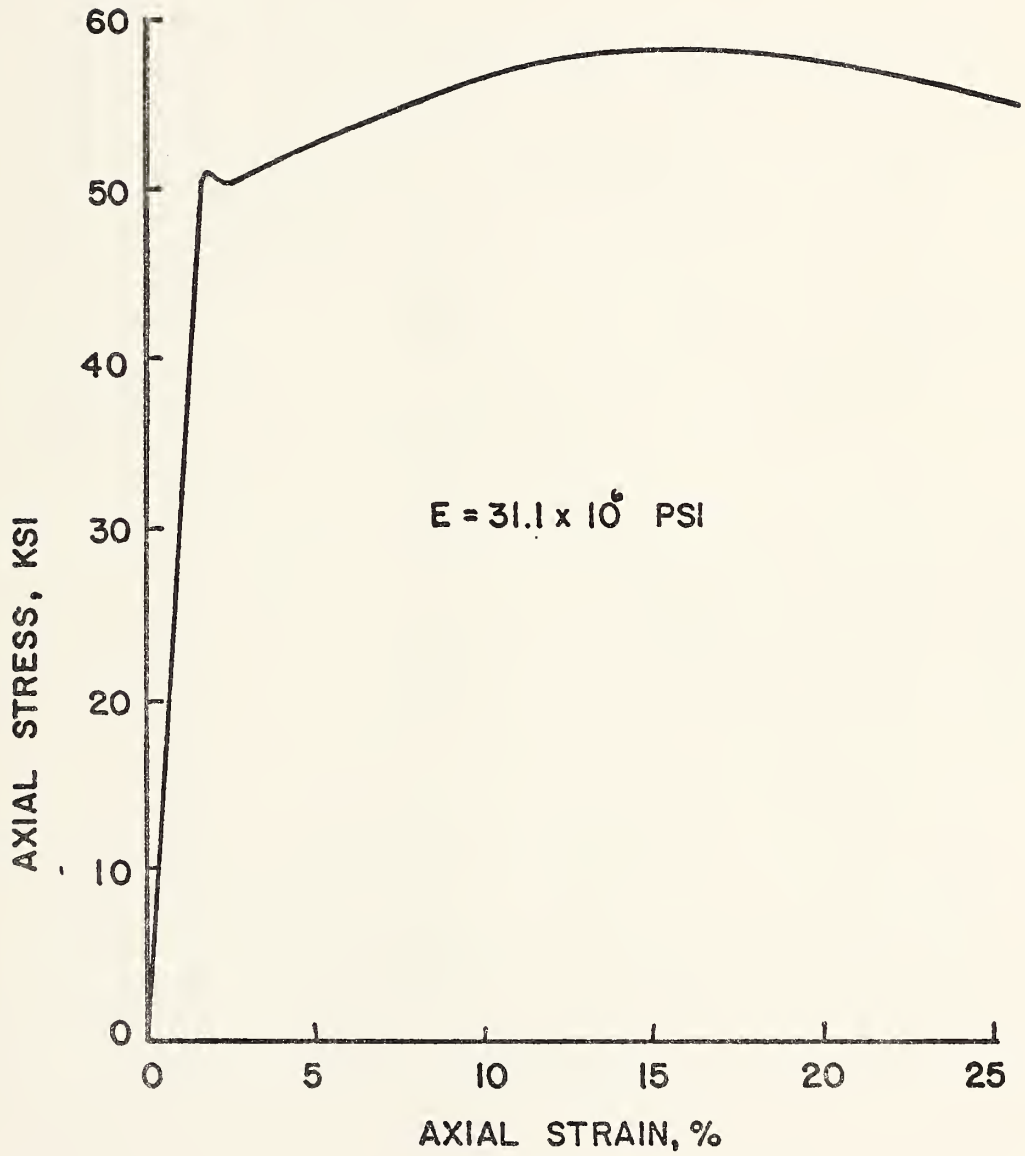

Figure B.4 Average Stress-Strain Relationship for Galvanized Steel Strips (B.2)

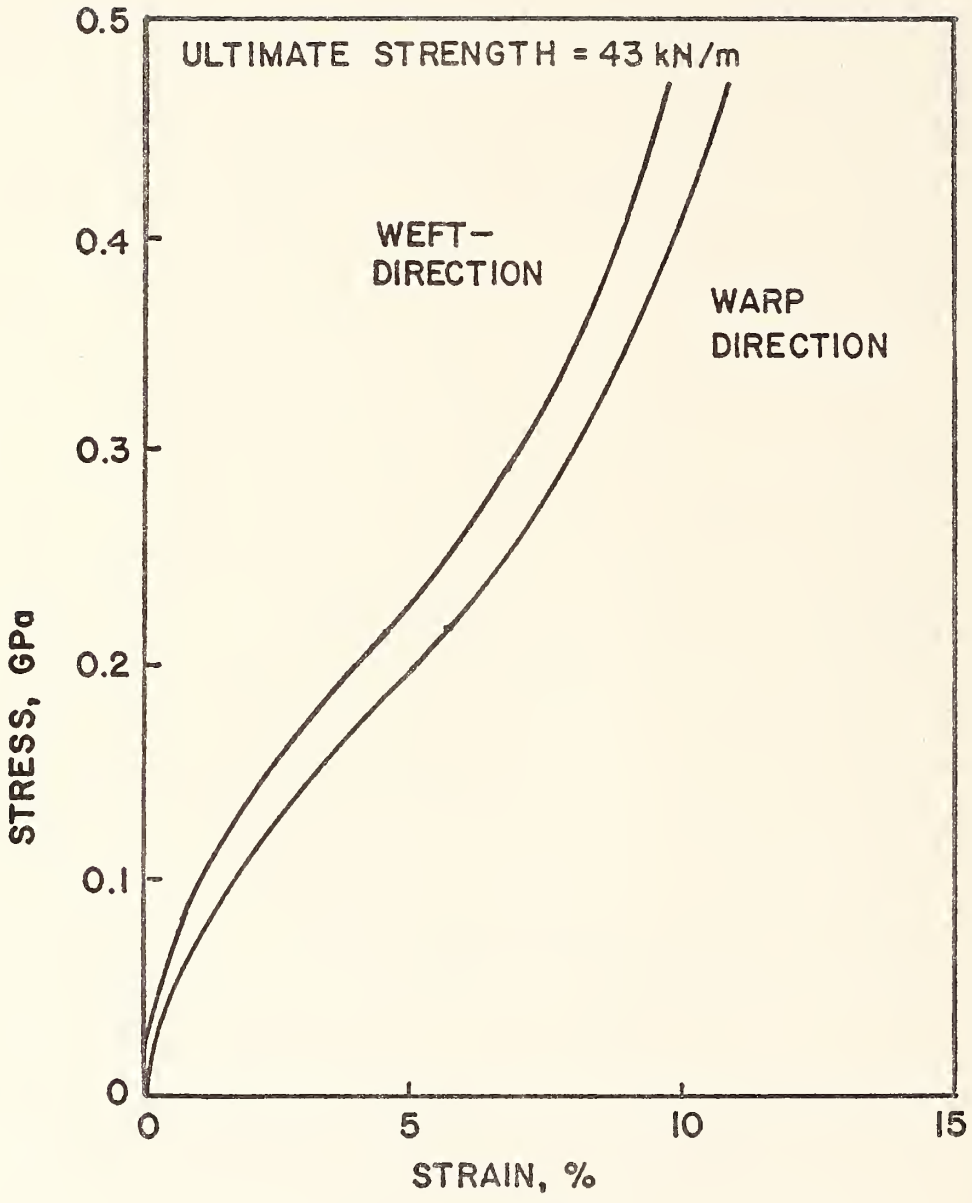

Figure B.5 Stress-Strain Relationship for Woven Polyester Fabric (B.7).

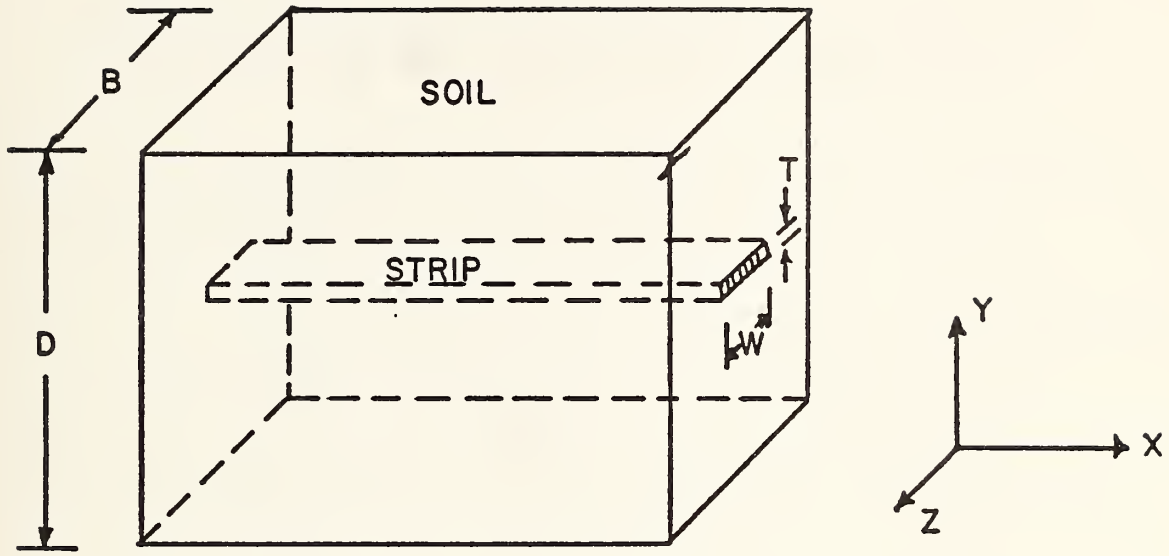

UNIT CELL

B-LATERAL STRIP SPACING
D-VERTICAL STRIP SPACING
T-STRIP THICKNESS
W-STRIP WIDTH

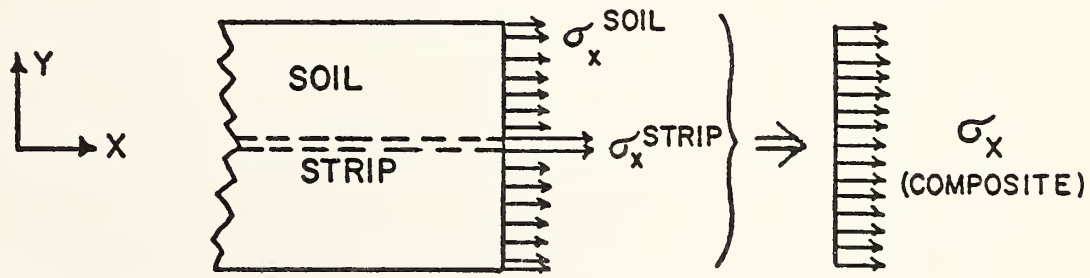

Figure B-6 Unit Cell Concepts

REFERENCES:

1-1. Selig, E. T., J. F. Abel, F. H. Kulhawy, and W. E. Falby, "Review of the Design and Construction of Long-Span, Corrugated-Metal, Buried Culverts", FHWA/RD-77-131, Federal Highway Administration Washington, D.C., August 1977.

1-2. Katona, M. G. and J. M. Smith, "A Modern Approach for Structural Design of Pipe Culverts," Second International Conference on Computers in Engineering and Building Design (CAD76) IPC Science and Technology Press Limited Guildford, Surrey, England, 1976.

1-3. Krizek, R. J., et al., "Structural Analysis and Design of Pipe Culverts", National Cooperative Highway Research Program. Report No. 116, NAS/NAE, Washington, D.C. 1971.

1-4. Brown, C. B., D. R. Green and S. Pawsey, "Flexible Culverts Under High Fills", Proc. ASCE, Vol. 94, No. ST4, April 1968.

1-5. Abel, J. F. and R. Mark, "Soil Stresses Around Flexible Elliptical Pipes", Proc. ASCE, Vol. 99, No. SM7, July 1973, pp. 509-526.

1-6. Duncan, J. M. "Finite Element Analysis of Buried Flexible Metal Culvert Structures", Laurits Bjerrum Memorial Volume, March 1975.

1-7. Leonards, G. A., "Performance of Pipe Culverts Buried in Soil", on going research project at Purdue University, Department of Civil Engineering, West Lafayette, Indiana.

1-8. Selig, E. T., J. F. Abel, F. H. Kulhawy and W. E. Falby, "Long-Span Buried Structure Design and Construction", Journal of Geotechnical Engineering Division, ASCE, Vol. 104, No. GT7, July pp. 953-996.

1-9. Katona, M. G., "On the Analysis of Long Span Culverts by the Finite Element Method", to be published by Transportation Research Board.

1-10. Duncan, J. M. "Behavior and Design of Long-Span Metal Culvert Structures", to be published in Journal of the Geotechnical Engineering Division, ASCE.

1-11. Chang, C. S., J. M. Espinoza, and E. T. Selig, "Computer Analysis of Newton Creek Culvert", Journal of the Geotechnical Engineering Division, ASCE, to be published.

1-12. Abel, J. G., G. A. Nasir and R. Mark, "Stresses and Deflections in Soil-Structure Systems formed by Long-Span Elliptic Pipe", report on Armco Steel Corp., Princeton University, July 1977.

1-13. Katona, M. G., et al., "CANDE User Manual" : Reports to the Federal Highway Administration, HRS-14, Washington, D.C. 1976.

1-14. Katona, M. G., "CANDE: A Versatile Soil-Structure Design and Analysis Computer Program," Journal of Advances in Engineering Software, 1978, Vol. 1, pp. 3-9.

2-1. Selig, E. T., Abel, J. F., Kulhway, F. H., and Falby, W. E., "Long-Span Buried Structure Design and Construction", Vol. 104, No. GT7, July 1978, pp. 953-966.

2-2. Selig, E. T., Abel, J. F., Kulhawy, F. H., and Falby, W. E., "Review of the Design and Construction of Long-Span Corrugated-Metal, Buried Conduits", FHWA/RD-77-131, Federal Highway Administration, Washington, D.C., August 1977.

2-3. Selig, E. T., Lockhart, C. W., and Lautensleger, R. W., "Measured Performance of Newton Creek Culvert", Journal of the Geotechnical Engineering Division, ASCE, to be published.

2-4. Chang, C. S., Espinoza, J. M., and Selig, E. T., "Computer Analysis of Newton Creek Culvert", Journal of the Geotechnical Engineering Division, ASCE, to be published.

2-5. Lockhart, C. W., "Performance of a Large, Corrugated-Metal, Buried Culvert in Bucks County, Pennsylvania", Master of Science Degree Project Report, State University of New York at Buffalo, New York, June 1975.

2-6. Espinoza, J. M., "Finite Element Analysis of a Long Span Corrugated Steel, Buried Culvert in Bucks County, Pennsylvania", Thesis submitted to the State University of New York at Buffalo in partial fulfillment of the requirements for the degree of Master of Science in Civil Engineering, 1978, pp. 165.

2-7. Condiotti, S. F., Donnelly, D. E., and LaForce, R. G., "Performance of a Multiplate Steel Arch Near Penrose, Colorado, CDOH-P&R-R-77-1, Colorado Division of Highways, Denver, Colorado, January 1977.

2-8. Bacher, A. E., and Banke, A. N., "Final Report - Stenner Creek Culvert", 05-SLO-101-28.61/28.8, 05-221734, Federal Highway Administration, California Division, Sacramento, California, October 1977.

2-9. Wong, K. S., and Duncan, J. M., "Summary of Field Instrumentation Study on a 35-ft. Span Aluminum Culvert in Greenbrier County, West Virginia", Report to Kaiser Aluminum and Chemical Sales Corp, Oakland, California, June 3, 1976.

2-10. Blower, H. E., Hickman, J. W., and Standley, R. L., a personal communication to Department of Civil Engineering, University of Notre Dame from Armco Inc., Metal Products Division, Lafayette, California, 1978.

2-11. Lefebure, G., Laliberte, M., Lefebvre, L. M., Lafleur, J., and Fisher, C. L., "Measurement of Soil Arching Above a Large Diamater Flexible Culvert", Canadian Geotechnical Journal, Vol. 13, No. 1, 1976, pp. 58-71.

2-12. Duncan, J. M., "A Study of the Performance and Safety of the Kaiser-Aetna Culvert", a report to the Highway Products Division, Kaiser Aluminum.

2-13. Selig, E. T., and Calabrese, S. J., "Performance of a Large Corrugated Steel Culvert", Transportation Research Record 548, 1975, pp. 62-76.

2-14. Lautensleger, R. W., personnal communication to the Department of Civil Engineering from Armco Incorporated Research and Technology, Middletown, Ohio, 1978.

2-15. Selig, E. T., "Instrumentation of Large Buried Culverts", Performance Monitoring for Geotechnical Construction, ASTM STP 584, American Society for Testing and Materials, 1975, pp. 159-181.

2-16. Demmin, J., "Field Verification of Ring Compression Conduit Design", Highway Research Record 116, 1966, pp. 36-86.

2-17. Handbook of Steel Drainage and Highway Construction Products, AISC, Washington, D.C., 1971, 2nd Ed.

5-1 Bathe, K.J., "ADINA: A Finite Element Program for Automatic Dynamic Incremental Nonlinear Analysis," Report 82448-1, Acoustics and Vibration Laboratory, Department of Mechanical Engineering, Massachusetts Institute of Technology, Cambridge, Massachusetts, 1975.

5-2 Christian, J.T. and Chandrakant S. Kesai, Numerical Methods in Geotechnical Engineering, McGraw-Hill, 1977.

5-3 Duncan, J.M. and Chin-Yung Chang, "Nonlinear Analysis of Stress and Strain in Soils," Journal of the Soil Mechanics and Foundation Division, ASCE, Vol. 96, No. SM5, Sept. 1970, pp. 1629-1653.

5-4 Hardin, B.O., "Constitutive Relationships for Air Field Subgrade and Base Course Materials," Technical Report UKY 32-71-CE5, University of Kentucky, College of Engineering, Soil Mechanics Series No. 4, Lexington, KY, 1970.

5-5 Konder, R.L., "Hyperbolic Stress-strain Response: Cohesive Soils, J. Soil Mech. Found. Div. ASCE, Vol. 89, No. SM1, Jan. 1963, pp. 115-143.

5-6 Corotis, B., M.H. Farzin, and R.J. Krizek, "Nonlinear Stress-strain Formulation for Soils," Jour. Geo. Eng. Div., ASCE, Vol. 100, No. GT9, Sept. 1974, pp. 993-1008.

7-1. Lefebure, G., et al., "Measurement of Soil Arching Above a Large Diameter Flexible Culvert," Canadian Geotechnical Journal, Vol. 13, No. 1, 1976, pp. 58-71.

7-2. Standley, R., personal communication from Armco Incorporated Research and Technology, Middletown, Ohio, 1978.

7-3. Chang, C.S., J.M. Espinoza, and Ernest T. Selig, "Computer Analysis of Newton Creek Culvert" to be published by ASCE, Geotechnical Engineering Division, 1979.

A-1 M.R. Thompson. "Lime reactivity of Illinois soils," Journal of Soil Mechanics and Foundations Division, ASCE, vol. 92, no. SMS, Sept. 1966, pp 67-92.

A-2 Univ. of Illinois Engineering Experiment Station, Highway Engineering Series No. 30: Engineering properties of lime-soil mixtures, by M.R. Thompson. Urbana, IL, May 1969.

A-3 National Cooperative Highway Research Program. Synthesis of Highway Practice 37: Lime-fly ash-stabilized bases and subbases. Transportation Research Board 1976.

A-4 Highway Research Board Bulletin 69: Properties of lime-fly ash-soil composition employed in road construction, by L.J. Minnick and W.F. Meyers, 1953, pp 1-28.

A-5 Portland Cement Association Research and Development, Bulletin RD038.01W, Load factors for concrete pipes bedded in cement-treated soil, by P.J. Nussbaum, Lilian Cadiena, Skokie, IL 1975.

A-6 E.J. Felt, M.S. Abrams. "Strength and elastic properties of compacted soil-cement mixtures." Second Pacific Area National Meeting at Los Angeles, CA, Sept. 17, 1956. ASTM Special Technical Publication No. 206, Soils, Philadelphia, PA, 1957.

A-7 C.A. Lowitz, G. DeGroot. "Soil-cement pipe bedding: Canadian River Aqueduct," ASCE Jour. Construction Division, vol. 94, no. CO1, Proc. Paper 5723, Jan. 1968, pp. 17-33.

A-8 "Material Prices," Engineering News-Record, vol. 198, no. 13, March 31, 1977, p. 34.

A-9 "Material Prices," Engineering News-Record, vol. 198, no. 10, March 10, 1977, p. 34.

A-10 U.S. Army Engineers Waterways Experiment Station Technical Report 6-763: Shock absorbing materials, Report 1, Backpacking materials for deeply buried protective structures, by G.C. Hoff. Vicksburg, MS, March 1967.

A-11 J.J. Brouk. "Perlite insulating concrete," American Concrete Institute Jour., Proc. vol. 50, June 1954, pp. 857-867, Title No. 50-50.

A-12 G.W. Washa. "Properties of lightweight aggregates and lightweight concretes," American Concrete Institute, Jour., Proc., vol. 53, Oct. 1956, pp. 375-383, Title No. 53-20.

A-13 A. Short, W. Kinniburgh. Lightweight concrete. rev. ed., London, CR, Books, Ltd., 1968, pp. 224-241.

A-14 American Concrete Institute Special Publication SP 29: Light weight concrete. Detroit, 1971.

A-15 U.S. Army Cold Regions Research & Engineering Laboratory Technical Report 206: Preparation of low density sulfur foam, by J.M. Dale and A.C. Ludwig. Hanover, N.H., Sept. 1967.

B-1. Vidal, H., "La Terre Armée, Anneles de ℓ'Institut Technique du Batiment et des Travaux Publics, July-August, 1966, pp. 888-938.

B-2. Al-Hussaini, M. M., and Perry, E. B., "Effects of Horizontal Reinforcement on Stability of Earth Masses", Technical Report S-76-11, September 1976.

B-3. Linberg, H. A. "Reinforced Earth-Termination of an Experimental Feature of Construction", FHWA Notice N5080.26, 22 Nov. 1974, Feceral Highway Administration, U.S. Department of Transportation, Arlington, VA.

B-4. Lee, K. L., Adams, B. D., and Vagneron, J. J., "Reinforced Earth Retaining Walls", Journal of the Soil Mechanics and Foundation Division, ASCE, October 1973, pp. 745-764.

B-5. Steward, John E., "Guidelines for Use of Fabrics in Construction and Maintenance of Low-Volume Roads", USDA, Forest Service, Portland, Oregon, June 1977.

B-6. Chang, J. C., "Earthwork Reinforcement Techniques", Research Report CA-DOT-TL-2115-9-74-37, October 1974, California Department of Transportation, Division of Highways, Sacramento, CA.

B-7. Broms, B. B., "Design of Fabric Reinforced Retaining Structures" Preprint 3128, ASCE Spring Convention and Exhibit, Pittsburgh, Pennsylvania, Arpil 24-28, 1978.

B-8. Naylor, D. J., "A Study of R. E. Walls Allowing Strip Slip", Preprint 3129, ASCE Spring Convention and Exhibit, Pittsburgh, Pennsylvania, April 24-28, 1978.

B-9. Uhlig, Herbert H., "Corrosion and Corrosion Control", John Wiley and Sons, Inc., New York, July 1962, pp. 421-437.

B-10. Schlosser, F. and Victor, E., "Friction in Reinforced Earth", Preprint 3274, ASCE Spring Convention and Exhibit, Pittsburgh, Pennsylvania, April 24-28, 1978.

B-11. King, R. A., "A Review of Soil Corrosiveness with Particular Reference to Reinforced Earth", Digest of Report, Research Lab Dept. of Environment, Department of Transportation.

B-12. Lee, Kenneth L., "Mechanisms, Analysis and Design of Reinforced Earth, State of the Art Report", Preprint 3231, ASCE Srping Convention and Exhibit, Pittsburgh, Pennsylvania, April 24-28, 1978.

B-13. Binguet, J. and Lee, K. L., "Bearing Capacity Tests on Reinforced Earth Slabs", ASCE Journal of the Geotechnical Engineering Division, December 1975, pp. 1241-1255.

B-14. Bolton, M. D., et al., "Reinforced Earth Walls: A Centrifugal Model Study", Preprint 3188, ASCE Spring Convention and Exhibit, Pittsburgh, Pennsylvania, April 24-28, 1978.

B-15. Schlosser, F. and Long, N. T., "Recent Results in French Research on Reinforced Earth", ASCE Journal of the Construction Division, September 1974, pp. 223-237.

B-16. Hoshiya, M., "Strength of Reinforced Earth Retaining Walls", Preprint 3120, ASCE Spring Convention and Exhibit, Pittsburgh, Pennsylvania, April 24-28,

B-17. Hausman, M. R. and Lee, K. L., "Rigid Wall Model with Soil Reinforcement", Preprint 3121, ASCE Spring Convention and Exhibit, Pittsburgh, Pennsylvania, April 24-28, 1978.

B-18. Wolfe, W. E. and et al., "The Effect of Vertical Motion on the Seismic Stability of Reinforced Earth Walls," Preprint 3133 ASCE Spring Convention and Exhibit, Pittsburgh, Penn., April 24-28, 1978.

B-19. Juan, T. and et al., "Full Scale Experiments on a Reinforced Earth Bridge Abatement in Lille", Preprint 3275, ASCE Spring Convention and Exhibit, Pittsburgh, Pennsylvania, April 24-28, 1978.

B-20. Ramstad, K. M., Herrmann, L. R. and Shen, C. K., "Integrated Study of Reinforced Earth-I: "Theoretical Formulation", ASCE Journal of the Geotechnical Engineering Division, May 1976, pp. 457-471.

B-21. Al-Hussain, M. M., and Johnson, L. D., "Numerical Analysis of a Reinforced Earth Wall", Preprint 3132, ASCE Srping Convention and Exhibit, Pittsburgh, Pennsylvania, April 24-28, 1978.

B-22. Herrmann, L. R. and Al Yassin, Z., "Numerical Analysis of a Reinforced Soil System", Preprint 3125, ASCE Spring Convention and Exhibit, Pittsburgh, Pennsylvania, April 24-28, 1978.

*U.S. GOVERNMENT PRINTING OFFICE: 1980 634-871/700 1-3

TE 662 .A3
79-115

Structural
concepts
culverts

Form DOT F 172
FORMERLY FORM DO

FEDERALLY COORDINATED PROGRAM OF HIGHWAY RESEARCH AND DEVELOPMENT (FCP)

The Offices of Research and Development of the Federal Highway Administration are responsible for a broad program of research with resources including its own staff, contract programs, and a Federal-Aid program which is conducted by or through the State highway departments and which also finances the National Cooperative Highway Research Program managed by the Transportation Research Board. The Federally Coordinated Program of Highway Research and Development (FCP) is a carefully selected group of projects aimed at urgent, national problems, which concentrates these resources on these problems to obtain timely solutions. Virtually all of the available funds and staff resources are a part of the FCP, together with as much of the Federal-aid research funds of the States and the NCHRP resources as the States agree to devote to these projects.*

FCP Category Descriptions

1. Improved Highway Design and Operation for Safety

Safety R&D addresses problems connected with the responsibilities of the Federal Highway Administration under the Highway Safety Act and includes investigation of appropriate design standards, roadside hardware, signing, and physical and scientific data for the formulation of improved safety regulations.

2. Reduction of Traffic Congestion and Improved Operational Efficiency

Traffic R&D is concerned with increasing the operational efficiency of existing highways by advancing technology, by improving designs for existing as well as new facilities, and by keeping the demand-capacity relationship in better balance through traffic management techniques such as bus and carpool preferential treatment, motorist information, and rerouting of traffic.

3. Environmental Considerations in Highway Design, Location, Construction, and Operation

Environmental R&D is directed toward identifying and evaluating highway elements which affect the quality* of the human environment. The ultimate goals are reduction of adverse highway and traffic impacts, and protection and enhancement of the environment.

4. Improved Materials Utilization and Durability

Materials R&D is concerned with expanding the knowledge of materials properties and technology to fully utilize available naturally occurring materials, to develop extender or substitute materials for materials in short supply, and to devise procedures for converting industrial and other wastes into useful highway products. These activities are all directed toward the common goals of lowering the cost of highway construction and extending the period of maintenance-free operation.

5. Improved Design to Reduce Costs, Extend Life Expectancy, and Insure Structural Safety

Structural R&D is concerned with furthering the latest technological advances in structural designs, fabrication processes, and construction techniques, to provide safe, efficient highways at reasonable cost.

6. Prototype Development and Implementation of Research

This category is concerned with developing and transferring research and technology into practice, or, as it has been commonly identified, "technology transfer."

7. Improved Technology for Highway Maintenance

Maintenance R&D objectives include the development and application of new technology to improve management, to augment the utilization of resources, and to increase operational efficiency and safety in the maintenance of highway facilities.

---

* The complete 7-volume official statement of the FCP is available from the National Technical Information Service (NTIS), Springfield, Virginia 22161 (Order No. PB 242057, price $45 postpaid). Single copies of the introductory volume are obtainable without charge from Program Analysis (HRD-2), Offices of Research and Development, Federal Highway Administration, Washington, D.C. 20590.

DOT LIBRARY
00056472